JAEA-Data/Code
2022-009
DOI:10.11484/jaea-data-code-2022-009

JAEA-Data/Code

Nuclear Data Processing Code FRENDY Version 2

Kenichi TADA, Akio YAMAMOTO, Satoshi KUNIEDA and Yasunobu NAGAYA

Nuclear Science and Reactor Engineering Division
Nuclear Science and Engineering Center
Nuclear Science Research Institute
Sector of Nuclear Science Research

February 2023

Japan Atomic Energy Agency

日本原子力研究開発機構

国立研究開発法人日本原子力研究開発機構　JAEA イノベーションハブ　研究成果利活用課
〒 319-1195　茨城県那珂郡東海村大字白方 2 番地 4
電話 029-282-6387, Fax 029-282-5920, E-mail:ird-support@jaea.go.jp

JAEA-Data/Code 2022-009

Nuclear Data Processing Code FRENDY Version 2

Kenichi TADA, Akio YAMAMOTO*, Satoshi KUNIEDA and Yasunobu NAGAYA

Nuclear Science and Reactor Engineering Division
Nuclear Science and Engineering Center
Nuclear Science Research Institute
Sector of Nuclear Science Research
Japan Atomic Energy Agency
Tokai-mura, Naka-gun, Ibaraki-ken

(Received November 7, 2022)

The nuclear data processing code has an important role to connect evaluated nuclear data libraries and neutronics calculation codes. Japan Atomic Energy Agency (JAEA) has developed the nuclear data processing code FRENDY since 2013 to generate cross section files from evaluated nuclear data libraries, such as JENDL, ENDF/B, JEFF, and TENDL.

The first version of FRENDY was released in 2019. FRENDY version 1 generates ACE files which are used for continuous energy Monte Carlo codes such as PHITS, Serpent, and MCNP. FRENDY version 2 generates multi-group neutron cross-section files from ACE files. The other major improvements are as follows: (1) uncertainty quantification for the probability tables of the unresolved resonance cross-section; (2) perturbation of the ACE file for the uncertainty quantification using a continuous Monte Carlo code; (3) modification of the ENDF-6 formatted nuclear data file.

This report describes an overview of the nuclear data processing methods and input instructions for FRENDY.

Keywords: FRENDY, JENDL, Nuclear Data Processing, User's Manual

* Nagoya University

JAEA-Data/Code 2022-009

核データ処理コード FRENDY 第 2 版

日本原子力研究開発機構
原子力科学研究部門 原子力科学研究所 原子力基礎工学研究センター
核工学・炉工学ディビジョン

多田　健一、山本　章夫*、国枝　賢、長家　康展

（2022 年 11 月 7 日受理）

核データ処理コードは評価済み核データライブラリと核計算コードを繋げる重要な役割を担っている。日本原子力研究開発機構は JENDL や ENDF/B、JEFF、TENDL などの評価済み核データライブラリーを処理するため、2013 年より核データ処理コード FRENDY の開発を行っている。

FRENDY 第 1 版は 2019 年にリリースされた。FRENDY 第 1 版では、PHITS や Serpent、MCNP などの連続エネルギーモンテカルロ計算コードで用いられる ACE ファイルの生成が可能である。FRENDY 第 2 版では、多群の中性子断面積を ACE ファイルから生成可能になった。また、そのほかの主な改良点は、(1) 非分離共鳴領域の断面積の自己遮蔽効果を取り扱う確率テーブルの統計的不確かさの定量化、(2) 連続エネルギーモンテカルロ計算コードを用いた不確かさ解析のための ACE ファイルの摂動、(3) ENDF-6 形式の核データファイルの編集、の三点である。

本報告書では FRENDY で用いられている核データ処理手法と FRENDY の入力について説明する。

原子力科学研究所：〒319-1195 茨城県那珂郡東海村大字白方 2 番地 4
* 名古屋大学

Contents

目　次

List of Tables

List of Figures

1 Introduction

1.1 Background

The Japan Atomic Energy Agency (JAEA) has developed the evaluated nuclear data library JENDL[1] and many neutronics calculation codes including a general purpose Monte Carlo code MVP,[2] a versatile reactor analysis code system MARBLE2,[3] and a particle and heavy-ion transport code system PHITS.[4] Though JAEA developed some nuclear data processing codes a few decades ago,[5,6] these codes cannot treat the current nuclear data format. JAEA uses the foreign processing codes, *i.e.*, NJOY[7,8] and PREPRO,[9] and an in-house nuclear data processing code to prepare cross-section data libraries for these neutronics calculation codes. It is very difficult for the neutronics calculation code users to create cross-section data libraries for these neutronics calculation codes. They must wait for the release of the new or revised cross-section data library.

The nuclear data processing code must be modified if a nuclear data representation, *e.g.*, a resonance format, cannot be treated by the code. The foreign processing codes are developed to process their own evaluated nuclear data libraries. If a new nuclear data representation is adopted in ENDF[10] or JEFF,[11] a high priority is assigned to modify NJOY and PREPRO. However, if the new nuclear data representation was used only by other evaluated nuclear data library, the priority of modification would be low and these codes might be modified by ourselves.

Recently, the introduction of the Generalized Nuclear Data Structure (GNDS) has been considered[12] as a new nuclear data format. The current processing codes cannot treat the GNDS format without extremely large revision of the processing codes since the format uses eXtensible Markup Language (XML) and it is quite different from the current nuclear data format, *i.e.*, the ENDF-6 format.[13]

To overcome such problems, JAEA has developed a nuclear data processing code FRENDY (FRom Evaluated Nuclear Data librarY to any application).[14] The first version of FRENDY, *i.e.*, FRENDY version 1, treats the ENDF-6 format and generates A Compact ENDF (ACE) files which are used for continuous energy Monte Carlo codes including PHITS, Serpent[15], and MCNP.[16] New functions have been developed after the release of FRENDY version 1. The major developed functions are as follows:

- Multi-group neutron cross-section file generation function[17],
- Uncertainty quantification for probability tables of the cross-section in the unresolved resonance region,
- Perturbation of the ACE file for the uncertainty quantification using a continuous energy Monte Carlo code,[18]
- Modification of the ENDF-6 formatted nuclear data file.

This report describes an overview of the nuclear data processing methods used in FRENDY and input instructions of FRENDY.

1.2 Overview of FRENDY

FRENDY is developed with consideration of maintainability, modularity, portability, and flexibility. FRENDY is written in the object-oriented language C++ to achieve these requirements. The maintainability and modularity are better than the conventional codes written in FORTRAN since all classes in FRENDY were encapsulated. Each class is designed to be compact and independent for portability and flexibility. FRENDY is developed not only to process the evaluated nuclear data file but also to implement the FRENDY functions to other calculation codes. The users can easily employ many functions *e.g.*, read, write, and process the evaluated nuclear data file, in their codes.

The version control system Git[19] is used to ensure traceability and quality assurance. The version control system enables us to easily create and manage the sources. The Boost test library[20] is used for the test programs, which are prepared to verify capabilities of FRENDY. The programs would be helpful to learn each capability and avoid installation problems. Moreover, if a developer wants to modify some class in FRENDY, the test programs assure the original capabilities.

The system structure of FRENDY is shown in Fig. 1.2.1. The modules with solid-lined shapes have been already implemented, while the ones with dashed-lined shapes have not been developed yet. Though the current version of FRENDY only treats the ENDF-6formatted file, FRENDY is designed not only for the ENDF-6 format but also for other nuclear data formats. FRENDY converts the nuclear data from each nuclear data format to NuclearDataObject. FRENDY can process the other nuclear data formats if parser, writer, and converter modules for a new format are implemented. Each module can be easily improved, extended, and modified to satisfy user's needs since each module is encapsulated and is unaffected by other modules. FRENDY keeps all data on NuclearDataObject and uses NuclearDataObject for the data transfer between different processing modules, *e.g.*, the resonance reconstruction and Doppler broadening, to reduce the effect of rounding errors and overhead by file access. NJOY uses an intermediate file, which is called the Point-wise Evaluated Nuclear Data Format (PENDF) file or Group-wise Evaluated Nuclear Data Format (GENDF) file, for the data transfer. Because the memory capacity of old computers was limited, the intermediate file was required to reduce the memory size. This limitation is not so meaningful from the viewpoint of current computational resources.

FRENDY has parser and writer modules to handle the ACE file. These modules are useful for the generation and modification of the ACE file. There are some cases where users want to modify a cross-section data library by themselves to estimate the impact of the perturbation of a cross-section

on neutronics calculation results. The modification of the pointer data in the ACE file is difficult for the neutronics calculation code users who do not know well about the ACE format. The ACE file uses random access with pointers to the various parts of the data. If the number of energy grid points is modified, modification of the pointer data is also required. FRENDY automatically adjusts the pointer data by the writer module. Users can modify the ACE file if they prepare a main (control) program with the parser and writer modules in FRENDY.

FRENDY generates a multi-group neutron cross-section file from an ACE file. The ACE file can be generated with FRENDY or other nuclear data processing codes: the existing ACE file in the past is also acceptable. The impact of the difference in the nuclear data processing on the neutronics calculation can be removed if users use the same ACE files for Monte Carlo and deterministic codes.

The dot-lined modules in Fig. 1.2.1 have not been implemented yet in the current version of FRENDY. These modules will be implemented in the future.

FRENDY can accept the input files and the PENDF file used in NJOY. NJOY is widely used in many laboratories and companies to generate the cross-section data library for their neutronics calculation codes. The NJOY users can easily use FRENDY without modification of their processing environment, *e.g.*, running shell scripts, input files, and post-processing programs.

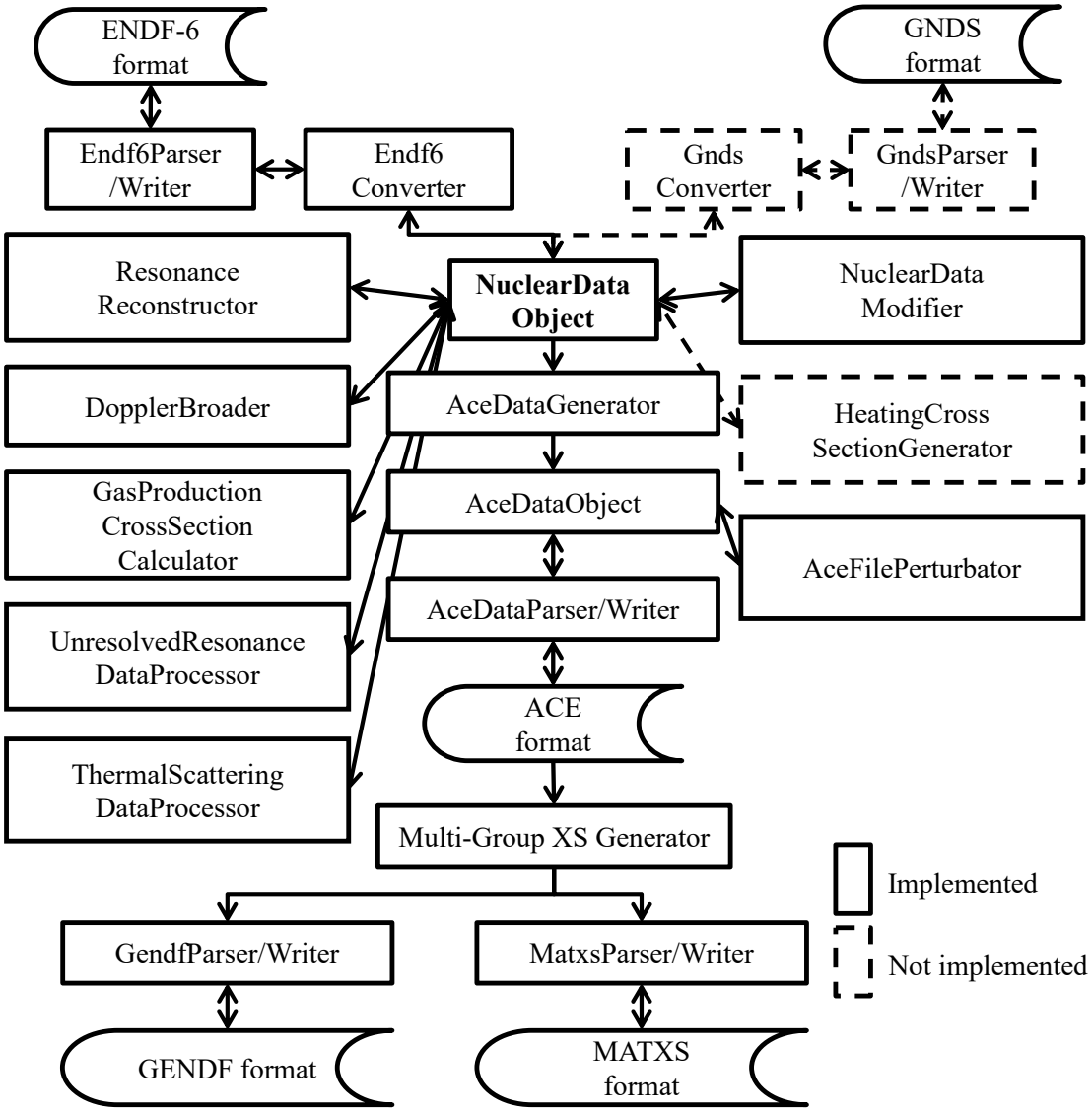

Figure 1.2.1 The system structure of FRENDY

2 Resonance Reconstruction

2.1 Tasks of Resonance Reconstruction

2.1.1 Unionization of Energy Grid

Generally, the evaluated nuclear data file contains cross sections for many reactions, such as total, elastic scattering, first chance fission, second chance fission, and radiative capture cross-sections. The energy grid of cross-sections is not necessarily the same for the different reactions in the evaluated nuclear data file. Considering the post process for the Doppler broadening and the cross-section data library generation, the energy grid should be unified for all the reactions.

As shown in Fig. 2.1.1, the cross-section data given in the evaluated nuclear data file is divided into three energy regions, *i.e.*, resolved resonance, unresolved resonance, and smooth regions. In the ENDF-6 format,[13] File 2 contains resonance parameters that are used to reconstruct point-wise cross-sections (exceptional cases may be found for the typical light-nuclei where only File 3 is used to give the excitation functions[1]). In many cases, the evaluated nuclear data file contains the resonance parameters for the total, elastic scattering, fission, and radiative capture reaction. The cross-sections of other reactions and cross-sections in the smooth region are given in File 3, together with background cross-sections which are used to supplement the cross-sections in the resonance region.

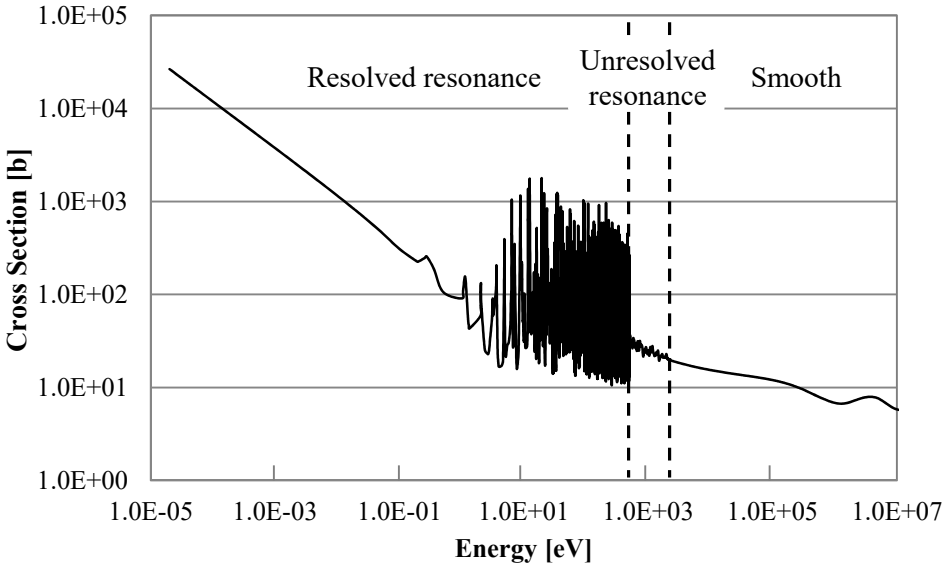

Figure 2.1.1 Example of resolved, unresolved, and smooth regions

2.1.2 Linearization of All Cross-Sections Given in File 3

The interpolation scheme is not necessarily the same for the different reactions and energy regions to describe smooth cross-section curves with a minimized number of energy grid points. For example, the radiative capture cross-section obeys the 1/v law in the low energy region where it could be described with a few energy grid points by the log-log interpolation rather than the linear-linear interpolation. In contrast, the elastic scattering cross-sections are constant due to potential scattering at the low-energy region. In such a case, the linear-linear interpolation is appropriate. Different interpolation schemes are usually used for each reaction to reduce the data size of the evaluated nuclear data file, which is inconvenient for neutronics calculation codes. Therefore, unification of the interpolation scheme is desirable for easy handling by neutronics calculation codes.

2.1.3 Reconstruction of Resolved and Unresolved Resonance Cross-Section

A significant number of energy grid points are required to describe a resonance cross-section curve, especially for heavier nuclei due to many resonance peaks. The evaluated nuclear data file provides the parameters of the cross-section formulae, *e.g.*, the Single- and Multi-Level Breit-Wigner,[21] Adler-Adler,[22,23] Reich-Moore[24,25], and R-matrix limited.[13] The explanation of these formulae is described in Section 2.3.

As shown in Fig. 2.1.2, the resonance region is divided into two regions, *i.e.*, the resolved and unresolved resonance regions.[26] The resonance peaks correspond to the excited levels of a compound nucleus. As the excitation energy increases, the level spacing becomes so narrow that each excitation level cannot be separated. The region where each excited level can be resolved is called a “resolved” resonance region, whereas the region where each excited level cannot be resolved is called an “unresolved” resonance region. At the higher energy, the resonance cannot be observed. This region is called a “smooth region”.

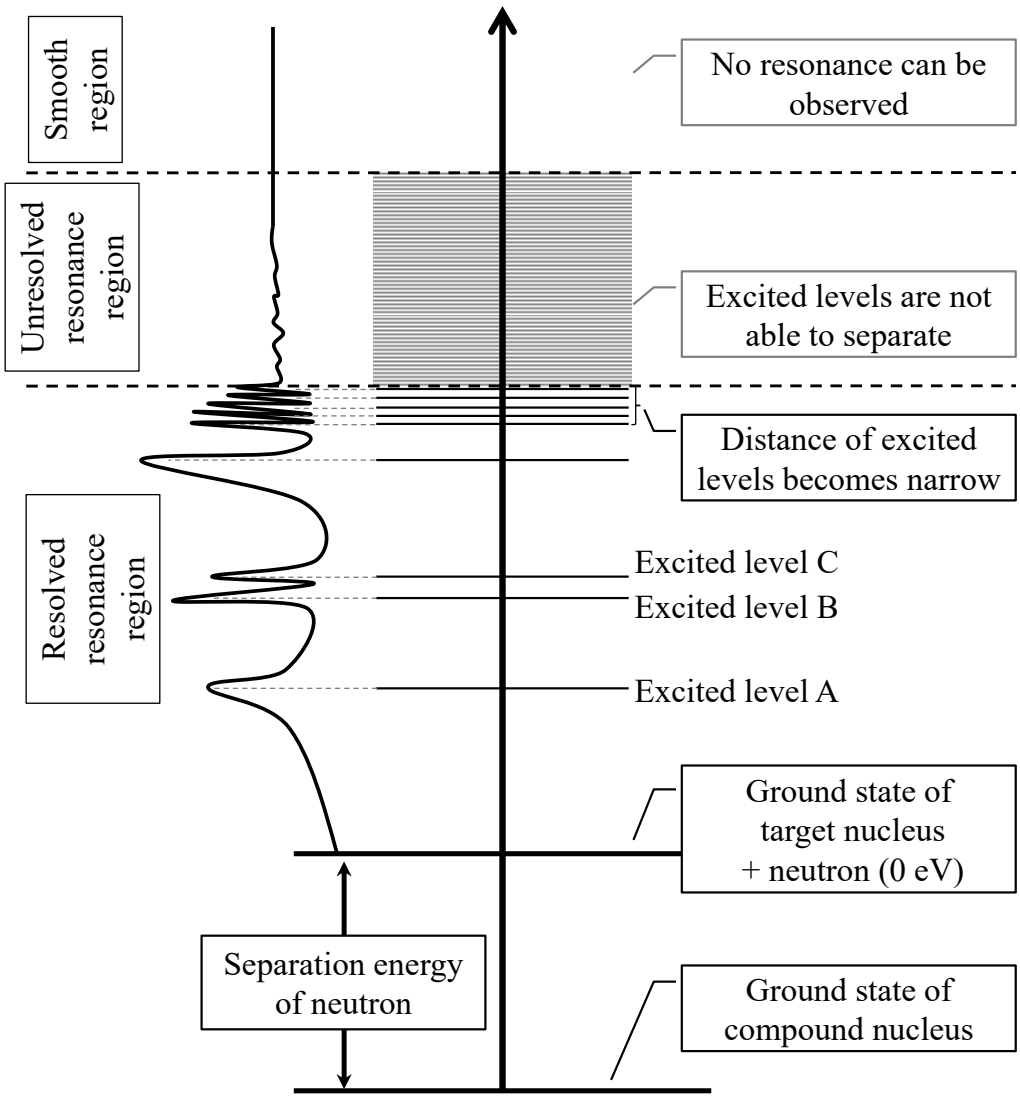

Figure 2.1.2 Difference of resolved and unresolved resonance regions

2.2 Calculation Flow of Linearization and Resonance Reconstruction

A calculation flow of the cross-section linearization and resonance reconstruction is shown in Fig. 2.2.1. The evaluated nuclear data file uses the table data for all cross-sections without resonance cross-section and the parameter of the cross-section formulae in the resonance region to describe the cross-section of these regions. Therefore, the linearization process is divided into two processes, *i.e.*, the linearization of all cross-sections given in File 3 and that of the resolved and unresolved resonance cross-sections given in File 2. The evaluated nuclear data file might contain background cross-sections in the resolved and unresolved resonance regions in File 3. The background cross-sections are also linearized in the former process.

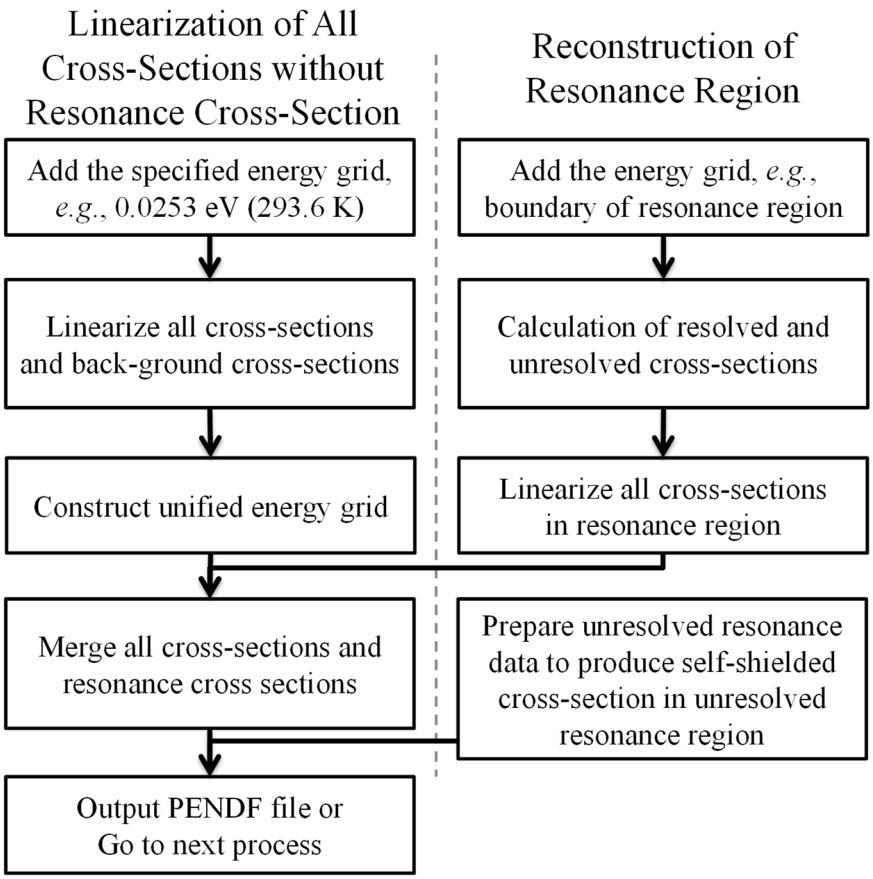

Figure 2.2.1 Calculation flow of linearization and resonance reconstruction

2.2.1 Algorithm of Linearization

An algorithm of the linearization is shown in Fig. 2.2.2. The linearization flow is as follows:

1. If the distance of energy grid points is large, a middle energy grid point is added.
2. Calculate the cross-sections $\sigma_{i+1/2}$ and $\sigma'_{i+1/2}$ at the middle point $x_{i+1/2}$.
3. If $\sigma'_{i+1/2}$ does not satisfy Eqs. (2.2.2) and (2.2.3), the middle energy grid point is added.
4. If $\sigma'_{i+1/2}$ satisfies Eqs. (2.2.2) and (2.2.3), go to next energy grid point (i=i+1).

Here, σ is a cross-section in the original interpolation, σ' a cross-section interpolated by the linear-linear interpolation, i an index of energy grid point, and x an incident particle energy. They are shown in Fig. 2.2.3. FRENDY uses three criteria for linearizing the cross-section, *i.e.*, the distance of energy grid points (dif_1), the relative difference of $\sigma_{i+1/2}$ and $\sigma'_{i+1/2}$ (dif_2), and integral difference of $\sigma_{i+1/2}$ and $\sigma'_{i+1/2}$ (dif_3), where

$$dif_1 = \frac{x_{i+1}}{x_i} > 1.0 + \sqrt{5.3 \times err}, \tag{2.2.1}$$

$$dif_2 = \frac{\left|\sigma'_{i+1/2} - \sigma_{i+1/2}\right|}{\sigma_{i+1/2}} \leq err, \tag{2.2.2}$$

$$dif_3 = \left(\frac{x_{i+1} - x_i}{2}\right)\left|\sigma'_{i+1/2} - \sigma_{i+1/2}\right| \leq err_{int} \times x_{i+\frac{1}{2}}, \tag{2.2.3}$$

err and err_{int} are the tolerance value and maximum integral error for linearization. These values are input for nuclear data processing codes.

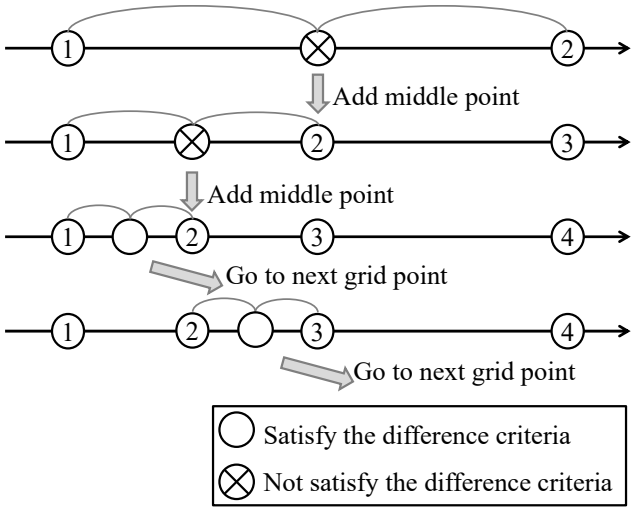

Figure 2.2.2 Example of the linearization flow

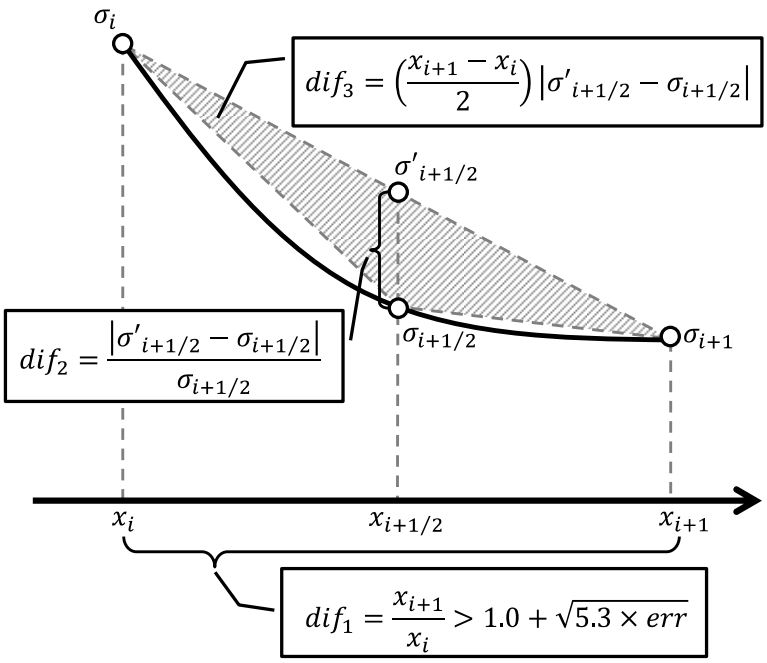

Figure 2.2.3 Example of the middle point addition and the relation of σ and σ', and x

2.2.2 Linearization of All Cross-Sections without Resonance Cross-Section

FRENDY adds the specified energy grid points to all the reaction types before linearization. FRENDY automatically adds energy grid points, *i.e.*, $1.0 \times 10^{\pm n}$, $2.0 \times 10^{\pm n}$, and $5.0 \times 10^{\pm n}$ eV, where, n is an integer. Cross-sections are measured at 293.6 K in most cases. At 293.6 K, the most probable neutron energy E is

$$E = k_B T = \frac{1.3806488 \times 10^{-23}[\mathrm{J/K}]}{1.6021766 \times 10^{-19}[\mathrm{J/eV}]} \times 293.6[\mathrm{K}] = 0.0253[\mathrm{eV}], \tag{2.2.4}$$

where k_B is the Boltzmann constant. The most probable neutron energy E = 0.0253 eV is automatically added to the grid points. FRENDY is also able to add the arbitrary energy grid points specified in the input file by users.

Similar to NJOY, FRENDY version 1 modified the discontinuity points. When the discontinuity is found, FRENDY version 1 deleted the energy grid point E_0, and added the energy grid points $E_0 \pm \Delta E$ to obtain a continuous curve of the cross-section. FRENDY version 2 does not modify the discontinuity points to treat the cross-sections as given in the evaluated nuclear data. As described in Section 2.1.1, the linearization process is required for the Doppler broadening. The cross-section integrated by energy at the discontinuity points is zero since the width of energy is zero. Therefore, this discontinuity point has no impact on the Doppler broadening.

The energy grid points in each reaction are unionized as shown in Fig. 2.2.4. In the unionized energy grid, a cross-section is calculated by interpolation when the corresponding energy grid is not found in the original energy grid. If the relative difference of the energy grid point is less than 1.0×10^{-10} eV, FRENDY assumes that both energy grid points are identical.

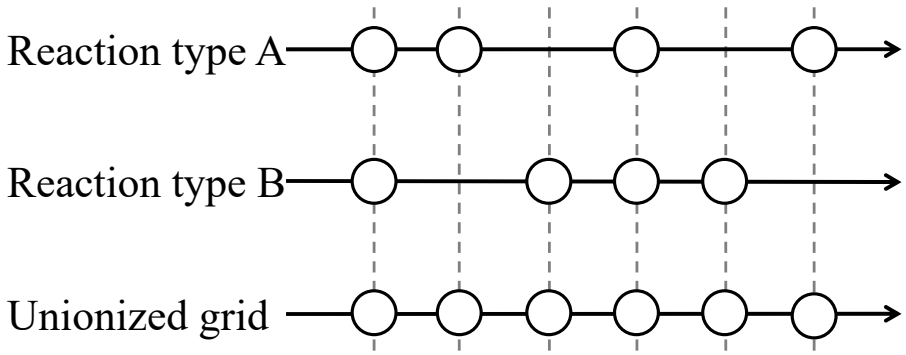

Figure 2.2.4 Example of the unionization of the energy grid

2.2.3 Resonance Reconstruction and Linearization in Resonance Region

FRENDY uses the energy grid points obtained in Section 2.2.2 as initial grid points. FRENDY adds energy grid points before linearization, *i.e.*, $1.0 \times 10^{\pm n}$, $2.0 \times 10^{\pm n}$, $5.0 \times 10^{\pm n}$, and 0.0253 eV, in the resolved resonance region, and also adds 13 energy grid points per decade, *i.e.*,

$1.0 \times 10^{\pm n}$, $1.25 \times 10^{\pm n}$, $1.5 \times 10^{\pm n}$, $1.7 \times 10^{\pm n}$, $2.0 \times 10^{\pm n}$, $2.5 \times 10^{\pm n}$, $3.0 \times 10^{\pm n}$, $3.5 \times 10^{\pm n}$, $4.0 \times 10^{\pm n}$, $5.0 \times 10^{\pm n}$, $6.0 \times 10^{\pm n}$, $7.2 \times 10^{\pm n}$, and $8.5 \times 10^{\pm n}$ eV, in the unresolved resonance region.

In the unresolved resonance region, the ENDF-6 format contains the interpolation scheme to represent the cross section[13]. NJOY calculates the unresolved resonance cross-section using the cross-section formulae on the fixed energy grid points and the other energy grid points between the fixed energy grid points are calculated by the log-log interpolation. FRENDY does not use interpolation and calculates the unresolved resonance cross-sections on all energy grid points using the cross-section formulae to rigorously reproduce the unresolved resonance cross-sections.

The resonance cross-sections are also linearized using the similar method which is described in Section 2.2.1. If $\sigma'_{r,i+1/2}$ does not satisfy Eq. (2.2.5), a middle energy grid point is added so that

$$E \times \left[dif_{1,r}\right]_{max} < err \ \cup \ \left(dif_{1,r} \leq err_{max} \ \cap \ dif_{2,r} \leq err_{int} \times x_{i+\frac{1}{2}}\right)_{r \in All}, \tag{2.2.5}$$

where r is the type of a reaction and err and err_{int} are the tolerance value and maximum integral error for linearization, and

$$dif_{1,r} = \frac{\left|\sigma'_{r,i+1/2} - \sigma_{r,i+1/2}\right|}{\sigma_{r,i+1/2}}, \tag{2.2.6}$$

$$dif_{2,r} = \frac{1}{2}(x_{i+1} - x_i)\left|\sigma'_{r,i+1/2} - \sigma_{r,i+1/2}\right|. \tag{2.2.7}$$

In the ENDF-6 format file (MT 151 section of File 2 except for LRF=3 and 7), the resonance parameters for the total, elastic scattering, fission, and radiative capture cross-sections are stored. The symbol $\left[dif_{1,r}\right]_{max}$ indicates the maximum relative difference in each reaction.

2.2.4 Merge and Output Cross Sections

The linearized cross-sections in the smooth and resonance regions are merged. FRENDY checks the consistency of the cross-sections and corrects the total and total inelastic scattering cross-sections when the cross-sections are merged. The total (MT 1) and total inelastic scattering cross-sections (MT 4) obtained by the evaluated nuclear data file may be different from the sum of each component cross-section. Thus, FRENDY makes the total and total inelastic scattering cross-sections from the sum of each component cross-section.

Though the reconstruction of the resonance cross-sections is appropriately carried out, the resonance cross-sections occasionally become negative due to a limitation of resonance formulae. In such a case, FRENDY sets the cross-section as 1.0×10^{-15} b.

As described in Section 1.2, FRENDY can treat and write the PENDF file. The PENDF file contains the self-shielded cross-sections in the unresolved resonance region in the MT 152 section of File 2.

2.3 Cross-Section Formulas in Resolved Resonance Region

This section describes the cross-section formulas in the resolved resonance region.[8,13] The derivations of the cross-section formulas are written in References 27 and 28.

The ENDF-6 format adopts the Single- and Multi-Level Breit-Wigner, Adler-Adler, Reich-Moore, and R-matrix limited. FRENDY can treat all resonance formulas in the ENDF-6 format. FRENDY uses the AMUR code[29] to calculate the R-matrix limited.

2.3.1 Single-Level Breit-Wigner Resonance Formula

The Single-Level Breit-Wigner (SLBW) resonance formula is as follows:

$$\sigma_{n,n}(E) = \sigma_p + \frac{4\pi}{k^2}\sum_J g_J \sum_l \sum_r \frac{\Gamma_{n,r}(E)}{\Gamma_r}\left\{\begin{array}{c}\left[\cos 2\phi_l - \left(1 - \frac{\Gamma_{n,r}(E)}{\Gamma_r}\right)\right]\psi(x) \\ +[\sin 2\phi_l]\chi(x)\end{array}\right\}, \tag{2.3.1}$$

$$\sigma_f(E) = \frac{4\pi}{k^2}\sum_J g_J \sum_r \frac{\Gamma_{n,r}(E)\Gamma_{f,r}}{{\Gamma_r}^2}\psi(x), \tag{2.3.2}$$

$$\sigma_\gamma(E) = \frac{4\pi}{k^2}\sum_J g_J \sum_r \frac{\Gamma_{n,r}(E)\Gamma_{\gamma,r}}{{\Gamma_r}^2}\psi(x), \tag{2.3.3}$$

$$\sigma_t(E) = \sigma_{n,n}(E) + \sigma_f(E) + \sigma_\gamma(E), \tag{2.3.4}$$

$$\sigma_p = \frac{4\pi}{k^2}\sum_l (2l+1)\sin^2\phi_l, \tag{2.3.5}$$

where $\sigma_{n,n}$ is the elastic scattering cross-section, σ_p the potential scattering cross-section, σ_f the fission cross-section, σ_γ the radiative capture cross-section, E the incident neutron energy [eV], g_J the spin statistical factor, k the neutron wave number, Γ the total width, Γ_n the neutron width, Γ_f the total width, Γ_γ the capture width, ϕ_l the phase shift, and

$$k = \frac{2\pi}{h}\sqrt{2m_n E}\frac{A}{A+1} = (2.196771\times 10^{-3})\frac{A}{A+1}\sqrt{E}, \tag{2.3.6}$$

$$g_J = \frac{2J+1}{2(2I+1)} = \frac{2J+1}{4I+2}, \tag{2.3.7}$$

$$\Gamma_{n,r}(E) = \frac{P_l(E)\Gamma_{n,r}}{P_l(|E_r|)}, \tag{2.3.8}$$

$$\psi(x) = \frac{1}{1+x^2}, \tag{2.3.9}$$

$$\chi(x) = \frac{x}{1+x^2}, \tag{2.3.10}$$

$$x = \frac{2(\mathrm{E} - E_r')}{\Gamma_r}, \tag{2.3.11}$$

$$E_r' = E_r + \frac{S_l(|E_r|) - S_l(E)}{2P_l(|E_r|)}\Gamma_{n,r}(|E_r|). \tag{2.3.12}$$

Here h is Planck's constant, m_n the mass of the neutron, A the ratio of the mass of the isotope to that of the neutron, I the target spin, P_l the penetration factor, S_l the shift factor, and E_r the resonance energy [eV]. The phase shift ϕ_l is given by[13,27,30,31)]

$$\phi_l = \phi_{l-1} - \tan^{-1}\left(\frac{P_{l-1}}{l - S_{l-1}}\right), \tag{2.3.13}$$

$$\phi = \hat{\rho}, \tag{2.3.14}$$

$$\phi_1 = \hat{\rho} - \tan^{-1}\hat{\rho}, \tag{2.3.15}$$

$$\phi_2 = \hat{\rho} - \tan^{-1}\frac{3\hat{\rho}}{3 - \hat{\rho}^2}, \tag{2.3.16}$$

$$\phi_3 = \hat{\rho} - \tan^{-1}\frac{\hat{\rho}(15 - \hat{\rho}^2)}{15 - 6\hat{\rho}^2}, \tag{2.3.17}$$

$$\phi_4 = \hat{\rho} - \tan^{-1}\frac{\hat{\rho}(105 - 10\hat{\rho}^2)}{105 - 45\hat{\rho}^2 + \hat{\rho}^4}. \tag{2.3.18}$$

The penetration factor P_l is given by[13,27,30,31)]

$$P_l = \frac{\rho^2 P_{l-1}}{(l - S_{l-1})^2 + {P_{l-1}}^2}, \tag{2.3.19}$$

$$P_0 = \rho, \tag{2.3.20}$$

$$P_1 = \frac{\rho^3}{\rho^2 + 1}, \tag{2.3.21}$$

$$P_2 = \frac{\rho^5}{\rho^4 + 3\rho^2 + 9}, \tag{2.3.22}$$

$$P_3 = \frac{\rho^7}{\rho^6 + 6\rho^4 + 45\rho^2 + 225}, \tag{2.3.23}$$

$$P_4 = \frac{\rho^9}{\rho^8 + 10\rho^6 + 135\rho^4 + 1575\rho^2 + 11025}. \tag{2.3.24}$$

The shift factor S_l is given by[13,27,30,31)]

$$S_l = \frac{\rho^2(l - S_{l-1})}{(l - S_{l-1})^2 + {P_{l-1}}^2} - l, \tag{2.3.25}$$

$$S_0 = 0, \tag{2.3.26}$$

$$S_1 = -\frac{1}{\rho^2 + 1}, \tag{2.3.27}$$

$$S_2 = -\frac{3\rho^2 + 18}{\rho^4 + 3\rho^2 + 9}, \tag{2.3.28}$$

$$S_3 = -\frac{6\rho^4 + 90\rho^2 + 675}{\rho^6 + 6\rho^4 + 45\rho^2 + 225}, \tag{2.3.29}$$

$$S_4 = -\frac{10\rho^6 + 270\rho^4 + 4725\rho^2 + 44100}{\rho^8 + 10\rho^6 + 135\rho^4 + 1575\rho^2 + 11025}, \tag{2.3.30}$$

where

$$\rho = ka, \tag{2.3.31}$$

$$\hat{\rho} = k\hat{a}. \tag{2.3.32}$$

Here a and $\hat{a}$ are the channel radii in units of 10^{-12} cm. In the ENDF-6 format, the meaning of a and $\hat{a}$ varies with the value of *NRO* and *NAPS* in the MT 151 section of File 2 as follows:

$$a = \begin{cases} 0.123A^{\frac{1}{3}} + 0.08 & (NAPS = 0) \\ \hat{a} & (NAPS = 1) \\ AP & (NAPS = 2) \end{cases}, \tag{2.3.33}$$

$$\hat{a} = \begin{cases} AP & (NRO = 0) \\ AP(E) & (NRO = 1) \end{cases}. \tag{2.3.34}$$

The quantities *AP* and *AP(E)* are given in File 2 if required.

The SLBW resonance formulas can represent the Doppler broadened cross-section using the ψ-χ method[32]. In the ψ-χ method, the cross-section at *T* K is calculated as follows[8,28,31]:

$$\sigma_{n,n}(E) = \sigma_p + \frac{4\pi}{k^2}\sum_J g_J \sum_l \sum_r \frac{\Gamma_{n,r}(E)}{\Gamma_r}\left\{\begin{matrix}\left[\cos 2\phi_l - \left(1 - \frac{\Gamma_{n,r}(E)}{\Gamma_r}\right)\right]\psi(\theta,x) \\ +[\sin 2\phi_l]\chi(\theta,x)\end{matrix}\right\}, \tag{2.3.35}$$

$$\sigma_f(E) = \frac{4\pi}{k^2}\sum_J g_J \sum_r \frac{\Gamma_{n,r}(E)\Gamma_{f,r}}{{\Gamma_r}^2}\psi(\theta,x), \tag{2.3.36}$$

$$\sigma_\gamma(E) = \frac{4\pi}{k^2}\sum_J g_J \sum_r \frac{\Gamma_{n,r}(E)\Gamma_{\gamma,r}}{{\Gamma_r}^2}\psi(\theta,x), \tag{2.3.37}$$

where

$$\psi(\theta,x) = \frac{\sqrt{\pi}}{2}\theta \times \mathrm{Re}\left[W\left(\frac{\theta x}{2}, \frac{\theta}{2}\right)\right], \tag{2.3.38}$$

$$\chi(\theta,x) = \frac{\sqrt{\pi}}{2}\theta \times \mathrm{Im}\left[W\left(\frac{\theta x}{2}, \frac{\theta}{2}\right)\right], \tag{2.3.39}$$

$$\theta = \frac{\Gamma}{\sqrt{\frac{4k_B TE}{A}}}. \tag{2.3.40}$$

The symbol $W(x,y)$ is the complex error function. The complex error function is defined by

$$W(x,y) = W(z) = e^{-z^2}\mathrm{erfc}(-iz) = \frac{2e^{-z^2}}{\sqrt{\pi}}\int_{-iz}^{\infty} e^{-t^2}\,\mathrm{d}t = \frac{i}{\pi}\int_{-\infty}^{\infty}\frac{e^{-t^2}}{z-t}\,\mathrm{d}t, \tag{2.3.41}$$

$$z = x + iy, \tag{2.3.42}$$

where $\mathrm{erfc}(z)$ is the complementary error function.

2.3.2 Multi-Level Breit-Wigner Resonance Formula

The Multi-Level Breit-Wigner (MLBW) resonance formula is the same as the SLBW resonance formula, except for the elastic scattering cross-section. The elastic scattering cross-section is as follows:

$$\sigma_{n,n}(E) = \frac{4\pi}{k^2}\sum_{l}\sum_{J} g_J \left\{ \begin{array}{c} \left(1 - \cos 2\phi_l - \sum_r \frac{\Gamma_{n,r}(E)}{\Gamma_r}\frac{2}{1+{x_r}^2}\right)^2 \\ + \left(\sin 2\phi_l + \sum_r \frac{\Gamma_{n,r}(E)}{\Gamma_r}\frac{2x_r}{1+{x_r}^2}\right)^2 + 2D_l(1-\cos 2\phi_l) \end{array} \right\}, \tag{2.3.43}$$

where

$$D_l = (2l+1) - \sum_{J=\left||I-l|-\frac{1}{2}\right|}^{I+l+\frac{1}{2}} g_J. \tag{2.3.44}$$

2.3.3 Adler-Adler Resonance Formula

The Adler-Adler resonance formula is as follows:

$$\sigma_t(E) = \sigma_p + \frac{\pi\sqrt{E}}{k^2}\left\{ \begin{array}{c} \sum_r \frac{1}{v_{t,r}}\left[\begin{array}{l} \left(G_{t,r}\cos 2\phi_0 + H_{t,r}\sin 2\phi_0\right)\times\psi\left(x_{t,r}\right) \\ +\left(H_{t,r}\cos 2\phi_0 - G_{t,r}\sin 2\phi_0\right)\times\chi\left(x_{t,r}\right) \end{array} \right] \\ +A_{t,1} + \frac{A_{t,2}}{E} + \frac{A_{t,3}}{E^2} + \frac{A_{t,4}}{E^3} + B_{t,1}E + B_{t,2}E^2 \end{array} \right\}, \tag{2.3.45}$$

$$\sigma_f(E) = \frac{\pi\sqrt{E}}{k^2}\sum_r \left\{ \begin{array}{c} \sum_r \frac{1}{v_r}\left(G_{f,r}\psi\left(x_{f,r}\right) + H_{f,r}\chi\left(x_{f,r}\right)\right) \\ +A_{f,1} + \frac{A_{f,2}}{E} + \frac{A_{f,3}}{E^2} + \frac{A_{f,4}}{E^3} + B_{f,1}E + B_{f,2}E^2 \end{array} \right\}, \tag{2.3.46}$$

$$\sigma_\gamma(E) = \frac{\pi\sqrt{E}}{k^2}\sum_r \left\{ \begin{array}{c} \sum_r \frac{1}{v_r}\left(G_{\gamma,r}\psi\left(x_{\gamma,r}\right) + H_{\gamma,r}\chi\left(x_{\gamma,r}\right)\right) \\ +A_{\gamma,1} + \frac{A_{\gamma,2}}{E} + \frac{A_{\gamma,3}}{E^2} + \frac{A_{\gamma,4}}{E^3} + B_{\gamma,1}E + B_{\gamma,2}E^2 \end{array} \right\}, \tag{2.3.47}$$

$$\sigma_{n,n}(E) = \sigma_t(E) - \sigma_\gamma(E) - \sigma_f(E), \tag{2.3.48}$$

$$\sigma_p = \frac{4\pi}{k^2}\sin^2\phi_0, \tag{2.3.49}$$

where

$$\psi(x_{c,r}) = \frac{1}{{x_{c,r}}^2 + 1}, \tag{2.3.50}$$

$$\chi(x_{c,r}) = \frac{x_{c,r}}{{x_{c,r}}^2 + 1}, \tag{2.3.51}$$

$$x_{c,r} = \frac{\mu_{c,r} - E}{\nu_{c,r}}. \tag{2.3.52}$$

Here $\nu_{c,r}$ is the resonance half-width $\Gamma_{c,r}/2$ for the reaction type c, $G_{c,r}$ the symmetrical parameter for the reaction type c, $H_{c,r}$ the asymmetrical parameter for reaction type c, and $A_{c,i}$ and $B_{c,j}$ the background constants for the reaction type c, and $\mu_{c,r}$ the resonance energy for the reaction type c. These values are obtained from the evaluated nuclear data file.

2.3.4 Reich-Moore Resonance Formula

The Reich-Moore resonance formula is as follows:

$$\sigma_t(E) = \frac{2\pi}{k^2}\sum_l\sum_J g_J\left\{\left(1 - \mathrm{Re}\left[U_{n,n}^{l,J}\right]\right) + 2d_{l,J}(1 - \cos 2\phi_l)\right\}, \tag{2.3.53}$$

$$\sigma_{n,n}(E) = \frac{\pi}{k^2}\sum_l\sum_J g_J\left\{\left|1 - U_{n,n}^{l,J}\right|^2 + 2d_{l,J}(1 - \cos 2\phi_l)\right\}, \tag{2.3.54}$$

$$\sigma_f(E) = \frac{4\pi}{k^2}\sum_l\sum_J g_J\sum_c\left|L_{n,c}^{l,J}\right|^2, \tag{2.3.55}$$

$$\sigma_\gamma(E) = \sigma_t(E) - \sigma_{n,n}(E) - \sigma_f(E). \tag{2.3.56}$$

Here $U_{n,n}^{l,J}$ is an element of the collision matrix and $L_{n,c}^{l,J}$ is an element of the R-matrix $\boldsymbol{R}^{l,J}$ which are given by

$$U_{n,n}^{l,J} = \mathrm{e}^{2i\phi_l}\left(2L_{n,n}^{l,J} - 1\right), \tag{2.3.57}$$

$$L_{n,c}^{l,J} = (\boldsymbol{R}^{l,J})_{n,c}^{-1}, \tag{2.3.58}$$

$$R_{n,c}^{l,J} = \delta_{n,c} - \frac{i}{2}\sum_r \frac{{\Gamma_{n,r}}^{\frac{1}{2}}{\Gamma_{c,r}}^{\frac{1}{2}}}{E_r - E - \frac{i}{2}\Gamma_{\gamma,r}}. \tag{2.3.59}$$

The term d_{lJ} is used to account for the possibility of an additional contribution to the potential scattering cross-section from the second channel spin. It is unity when there is a second J value equal to J, and zero otherwise[8,13].

It is difficult to calculate the inverse matrix $(\boldsymbol{R}^{l,J})_{n,c}^{-1}$ directly since the R-matrix is the complex matrix. In the ENDF-6 format, the maximum number of channels is 3, *i.e.*, 1 channel for elastic scattering and 2 channels for fission. Therefore, the maximum matrix size of the R-matrix $\boldsymbol{R}^{l,J}$ in Eq. (2.3.59) is 3×3. The inverse of the 3×3 complex matrix can be analytically calculated without using the iteration method. FRENDY directly calculates the inverse of 3×3 complex matrix as follows:

$$\boldsymbol{R}^{-1} = \frac{1}{\det\boldsymbol{R}}\begin{pmatrix} R_{2,2}R_{3,3} - R_{2,3}R_{3,2} & R_{1,3}R_{3,2} - R_{1,2}R_{3,3} & R_{1,2}R_{2,3} - R_{1,3}R_{2,2} \\ R_{2,3}R_{3,1} - R_{2,1}R_{3,3} & R_{1,1}R_{3,3} - R_{1,3}R_{3,1} & R_{1,3}R_{2,1} - R_{1,1}R_{2,3} \\ R_{2,1}R_{3,2} - R_{2,2}R_{3,1} & R_{1,2}R_{3,1} - R_{1,1}R_{3,2} & R_{1,1}R_{2,2} - R_{1,2}R_{2,1} \end{pmatrix}, \tag{2.3.60}$$

where

$$\boldsymbol{R} = \begin{pmatrix} R_{1,1} & R_{1,2} & R_{1,3} \\ R_{2,1} & R_{2,2} & R_{2,3} \\ R_{3,1} & R_{3,2} & R_{3,3} \end{pmatrix}, \tag{2.3.61}$$

$$\det\boldsymbol{R} = \begin{matrix} R_{1,1}R_{2,2}R_{3,3} + R_{2,1}R_{3,2}R_{1,3} + R_{3,1}R_{1,2}R_{2,3} \\ -R_{1,1}R_{3,2}R_{2,3} - R_{3,1}R_{2,2}R_{1,3} - R_{2,1}R_{1,2}R_{3,3} \end{matrix}. \tag{2.3.62}$$

2.4 Cross-Section Formulas in Unresolved Resonance Region

In the ENDF-6 format, only the Single-Level Breit-Wigner representation is available for the unresolved resonance region.[13)]

Each resonance parameter cannot be determined in the unresolved resonance region. The average value and the distribution are used to represent the unresolved resonance cross-sections. Porter and Thomas revealed that the reaction width distribution is described by the chi-square distribution[33)]:

$$P_\mu(x) = \frac{\mu}{2}\frac{1}{\Gamma\left(\frac{\mu}{2}\right)}\left(\frac{\mu x}{2}\right)^{\frac{\mu}{2}-1} e^{-\frac{\mu x}{2}}, \tag{2.4.1}$$

where $P_\mu(x)$ is the chi-square distribution for μ degrees of freedom, x the ratio of $\Gamma(E)$ to $\bar{\Gamma}$:

$$x = \frac{\Gamma(E)}{\bar{\Gamma}}. \tag{2.4.2}$$

$\Gamma(E)$ is the reaction width at energy E, and $\bar{\Gamma}$ the average reaction width. It should be noted that $\Gamma(\mu/2)$ in Eq. (2.4.1) is the gamma function. The unresolved resonance cross-sections are obtained using the chi-square distribution and the average reaction width which are obtained from the evaluated nuclear data file.

Infinitely dilute cross-sections in the unresolved resonance region are defined based on the SLBW approximation as follows:[8,13)]

$$\sigma_t = \sigma_{n,n} + \sigma_\gamma + \sigma_f, \tag{2.4.3}$$

$$\sigma_\gamma = \frac{2\pi^2}{k^2}\sum_l \frac{g_J}{\bar{D}}\left\langle\frac{\Gamma_n\Gamma_\gamma}{\Gamma}\right\rangle, \tag{2.4.4}$$

$$\sigma_f = \frac{2\pi^2}{k^2}\sum_l \frac{g_J}{\bar{D}}\left\langle\frac{\Gamma_n\Gamma_f}{\Gamma}\right\rangle, \tag{2.4.5}$$

$$\sigma_{n,n} = \sigma_p + \frac{2\pi^2}{k^2}\sum_l \frac{g_J}{\bar{D}}\left(\left\langle\frac{\Gamma_n\Gamma_n}{\Gamma}\right\rangle - 2\bar{\Gamma_n}\sin^2\varphi_l\right), \tag{2.4.6}$$

where

$$\left\langle \frac{\Gamma_{n,l}\Gamma_{f,l}}{\Gamma} \right\rangle = \int_0^\infty P_\mu(x_{n,l})\,\mathrm{d}x_{n,l} \int_0^\infty P_\nu(x_{f,l})\,\mathrm{d}x_f \int_0^\infty P_\lambda(x_{c,l})\,\mathrm{d}x_c \frac{\Gamma_{n,l}\Gamma_{f,l}}{\Gamma_{n,l}+\Gamma_{f,l}+\Gamma_{\gamma,l}+\Gamma_{c,l}}$$
$$= \int_0^\infty P_\mu(x_{n,l})\,\mathrm{d}x_n \int_0^\infty P_\nu(x_{f,l})\,\mathrm{d}x_f \int_0^\infty P_\lambda(x_{c,l})\,\mathrm{d}x_c \frac{\overline{\Gamma_{n,l}}x_{n,l}\overline{\Gamma_{f,l}}x_{f,l}}{\overline{\Gamma_{n,l}}x_{n,l}+\overline{\Gamma_{f,l}}x_{f,l}+\overline{\Gamma_{\gamma,l}}+\overline{\Gamma_{c,l}}x_{c,l}}, \quad (2.4.7)$$

$\overline{D}$ is the average level spacing, $\overline{\Gamma_{n,l}}$ average neutron width, $\overline{\Gamma_{f,l}}$ average fission width, $\overline{\Gamma_{\gamma,l}}$ average radiation width, and $\overline{\Gamma_{c,l}}$ average competitive reaction width. It should be noted that Eq. (2.4.7) assumes that the radiation width is constant.

In the ENDF-6 format, the average reduced neutron width at the angular momentum quantum number l is given instead of the average neutron width. The average neutron width is written by the average reduced neutron width as

$$\overline{\Gamma_{n,l}} = \overline{\Gamma_{n,l}}^0 \sqrt{E}\mu_{n,l}V_l(E), \quad (2.4.8)$$

where $\overline{\Gamma_{n,l}}^0$ is the average reduced neutron width, $\mu_{n,l}$ the number of degrees of freedom in the neutron width, and $V_l(E)$ penetrabilities for the unresolved region. Penetabilities $V_l(E)$ are given by[8,13)]

$$V_0 = 1, \quad (2.4.9)$$

$$V_1 = \frac{\rho^2}{\rho^2+1}, \quad (2.4.10)$$

$$V_2 = \frac{\rho^4}{\rho^4+3\rho^2+\rho}. \quad (2.4.11)$$

As shown in Eq. (2.4.7), integrals of the form

$$\langle f(x,y)\rangle = \int_0^\infty P_\mu(x)\,\mathrm{d}x \int_0^\infty P_\nu(y)\,f(x,y)\mathrm{d}y, \quad (2.4.12)$$

are required[32)] to calculate the unresolved resonance cross-sections. Equation (2.4.12) is evaluated using the method proposed by Hwang[34)] as

$$\langle f(x,y)\rangle = \sum_{j=1}^{10}\sum_{k=1}^{10} A_j^\mu A_k^\nu \times f\left(x_j^\mu, y_k^\nu\right), \quad (2.4.13)$$

where A_j^μ is the quadrature weight and x_j^μ is the abscissa. The A_j^μ and x_j^μ have been calculated for μ=1, 2, 3, and 4. The ten-point quadrature is used for both the neutron and the fission width distributions. For odd μ

$$A_j^\mu = \frac{2w_j{}^s z_j{}^{\mu-1}}{\Gamma\left(\frac{\mu}{2}\right)}, \quad (2.4.14)$$

$$x_j^\mu = \frac{2z_j{}^2}{\mu}, \quad (2.4.15)$$

while for even μ

$$A_j^{\mu} = \frac{\mu {w_j}^L \left(\frac{\mu x_j}{2}\right)^{\frac{\mu}{2}-1} e^{\left(-\frac{\mu x_j}{2}\right)}}{\Gamma\left(\frac{\mu}{2}\right)\left(1+s_j\right)}, \tag{2.4.16}$$

$$x_j^{\mu} = \frac{\left(1-s_j\right)}{\left(1+s_j\right)}. \tag{2.4.17}$$

${w_j}^s$ and z_j in Eqs. (2.4.14) and (2.4.15) are respectively the ordinates and the weights of the half-range Gauss-Hermite quadrature derived by Steen, et al.[35] On the other hand, ${w_j}^L$ and s_j in Eqs. (2.4.16) and (2.4.17) are the usual Gauss-Legendre ordinates and the weights, respectively. The same relationship holds for A_k^{ν} and y_k^{ν}. The A_j^{μ} and x_j^{μ} for μ=1, 2, 3, and 4 and j=1, 2, …, 10 are shown in Tables 2.4.1 and 2.4.2.[31,34]

Substituting Eq. (2.4.13) into Eq. (2.4.7), the latter equation is

$$\left\langle\frac{\Gamma_{n,l}\Gamma_{f,l}}{\Gamma}\right\rangle = \sum_i^{10} A_i^{\mu_{n,l}} \sum_j^{10} A_j^{\nu_{f,l}} \sum_k^{10} A_k^{\lambda_{c,l}} \frac{\overline{\Gamma_{n,l}} x_i^{\mu_{n,l}} \overline{\Gamma_{f,l}} x_j^{\nu_{f,l}}}{\overline{\Gamma_{n,l}} x_i^{\mu_{n,l}} + \overline{\Gamma_{f,l}} x_j^{\nu_{f,l}} + \overline{\Gamma_{\gamma,l}} + \overline{\Gamma_{c,l}} x_k^{\lambda_{c,l}}} \tag{2.4.18}$$

$$= \overline{\Gamma_{n,l}\Gamma_{f,l}} R_{f,l},$$

where

$$R_{f,l} = \sum_i^{10} A_i^{\mu_{n,l}} \sum_j^{10} A_j^{\nu_{f,l}} \sum_k^{10} A_k^{\lambda_{c,l}} \frac{x_i^{\mu_{n,l}} x_j^{\nu_{f,l}}}{\overline{\Gamma_{n,l}} x_i^{\mu_{n,l}} + \overline{\Gamma_{f,l}} x_j^{\nu_{f,l}} + \overline{\Gamma_{\gamma,l}} + \overline{\Gamma_{c,l}} x_k^{\lambda_{c,l}}}. \tag{2.4.19}$$

$\nu_{f,l}$ is the number of degrees of freedom in the fission width, and $\lambda_{c,l}$ the number of degrees of freedom in the competitive reaction width. Using Eq. (2.4.19), Eqs. (2.4.3) - (2.4.6) are rearranged as

$$\sigma_t = \sigma_{n,n} + \sigma_\gamma + \sigma_f, \tag{2.4.20}$$

$$\sigma_\gamma = \frac{2\pi^2}{k^2} \sum_l \frac{g_J}{\overline{D}} \Gamma_{n,l}\Gamma_{\gamma,l} R_{\gamma,l}, \tag{2.4.21}$$

$$\sigma_f = \frac{2\pi^2}{k^2} \sum_l \frac{g_J}{\overline{D}} \Gamma_{n,l}\Gamma_{f,l} R_{f,l}, \tag{2.4.22}$$

$$\sigma_{n,n} = \sigma_p + \frac{2\pi^2}{k^2} \sum_l \frac{g_J}{\overline{D}} \left({\Gamma_{n,l}}^2 R_{n,l} - 2\overline{\Gamma_n} \sin^2 \varphi_l\right), \tag{2.4.23}$$

where

$$R_{\gamma,l} = \sum_i^{10} A_i^{\mu_{n,l}} \sum_j^{10} A_j^{\nu_{f,l}} \sum_k^{10} A_k^{\lambda_{c,l}} \frac{x_i^{\mu_{n,l}}}{\overline{\Gamma_{n,l}} x_i^{\mu_{n,l}} + \overline{\Gamma_{f,l}} x_j^{\nu_{f,l}} + \overline{\Gamma_{\gamma,l}} + \overline{\Gamma_{c,l}} x_k^{\lambda_{c,l}}}, \tag{2.4.24}$$

$$R_{n,l} = \sum_i^{10} A_i^{\mu_{n,l}} \sum_j^{10} A_j^{\nu_{f,l}} \sum_k^{10} A_k^{\lambda_{c,l}} \frac{\left(x_i^{\mu_{n,l}}\right)^2}{\overline{\Gamma_{n,l}} x_i^{\mu_{n,l}} + \overline{\Gamma_{f,l}} x_j^{\nu_{f,l}} + \overline{\Gamma_{\gamma,l}} + \overline{\Gamma_{c,l}} x_k^{\lambda_{c,l}}}. \tag{2.4.25}$$

Infinitely dilute cross-sections in the unresolved resonance region are calculated using Eqs. (2.4.20) - (2.4.23).

Table 2.4.1 Ten Point Quadrature Weights and Abscissa for Statistical Integration (μ=1, 2)

	One Degree of Freedom (μ=1)		Two Degree of Freedom (μ=2)	
	Abscissa x_j	Weight A_j	Abscissa x_j	Weight A_j
1	3.0013465E-03	1.1120413E-01	1.3219203E-02	3.3773418E-02
2	7.8592886E-02	2.3546798E-01	7.2349624E-02	7.9932171E-02
3	4.3282415E-01	2.8440987E-01	1.9089473E-01	1.2835937E-01
4	1.3345267E+00	2.2419127E-01	3.9528842E-01	1.7652616E-01
5	3.0481846E+00	1.0967668E-01	7.4083443E-01	2.1347043E-01
j 6	5.8263198E+00	3.0493789E-02	1.3498293E+00	2.1154965E-01
7	9.9452656E+00	4.2930874E-03	2.5297983E+00	1.3365186E-01
8	1.5782128E+01	2.5827047E-04	5.2384894E+00	2.2630659E-02
9	2.3996824E+01	4.9031965E-06	1.3821772E+01	1.6313638E-05
10	3.6216208E+01	1.4079206E-08	7.5647525E+01	2.7453830E-31

Table 2.4.2 Ten Point Quadrature Weights and Abscissa for Statistical Integration (μ=3, 4)

	Three Degree of Freedom (μ=3)		Four Degree of Freedom (μ=4)	
	Abscissa x_j	Weight A_j	Abscissa x_j	Weight A_j
1	1.0004488E-03	3.3376214E-04	1.3219203E-02	1.7623788E-03
2	2.6197629E-02	1.8506108E-02	7.2349624E-02	2.1517749E-02
3	1.4427472E-01	1.2309946E-01	1.9089473E-01	8.0979849E-02
4	4.4484223E-01	2.9918923E-01	3.9528842E-01	1.8797998E-01
5	1.0160615E+00	3.3431475E-01	7.4083443E-01	3.0156335E-01
j 6	1.9421066E+00	1.7766657E-01	1.3498293E+00	2.9616091E-01
7	3.3150885E+00	4.2695894E-02	2.5297983E+00	1.0775649E-01
8	5.2607092E+00	4.0760575E-03	5.2384894E+00	2.5171914E-03
9	7.9989414E+00	1.1766115E-04	1.3821772E+01	8.9630388E-10
10	1.2072069E+01	5.0989546E-07	7.5647525E+01	0.0000000E+00

3 Doppler Broadening

3.1 Task of Doppler Broadening

The task of the Doppler broadening is to calculate the cross-sections at T_B K when cross-sections are given at T_A K (where $T_A < T_B$)[36]. Most of the evaluated nuclear data files contain the cross-sections at 0 K. The Doppler broadening is required when the cross-sections at T K are required.

At 0 K, a target nucleus is at rest in the laboratory system and the relative velocity between an incident particle and the nucleus is uniquely determined. At an arbitrary temperature of T K, the nucleus vibrates with an average energy $3k_BT/2$, where k_B is the Boltzmann constant. In a such case, the relative velocity between the incident particle and nucleus varies with the velocity of the nucleus, v, in the laboratory system. For example, when the velocity of the incident particle is v_n, the energy range of the incident channel E is

$$\frac{1}{2}(m{v_n}^2 - Mv^2) \leq E \leq \frac{1}{2}(m{v_n}^2 + Mv^2), \tag{3.1.1}$$

where m and M are the masses of the incident particle and nucleus, respectively.

An example of Doppler broadened cross-sections is shown in Fig. 3.1.1. The resonance width becomes wider as the temperature increases, whereas a peak value of the Doppler broadened cross-section becomes lower as the nuclear temperature increases. It should be noted that the integral value of the cross-section remains unchanged even if the temperature is changed.

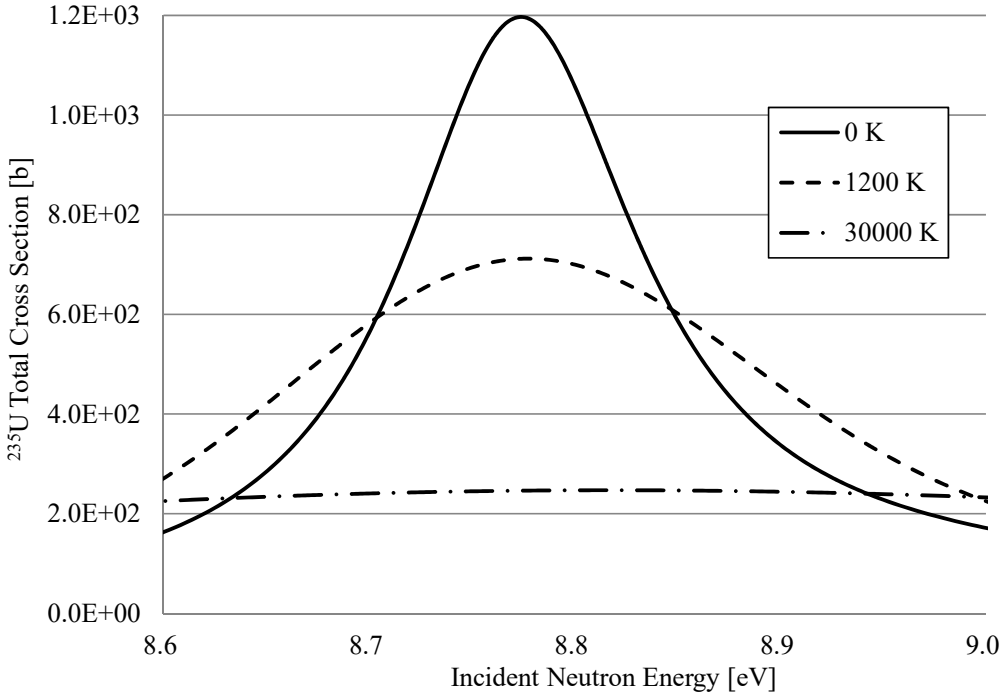

Figure 3.1.1 Example of Doppler broadened cross-sections

3.2 Calculation Flow of Doppler Broadening

A calculation flow of the Doppler broadening is shown in Fig. 3.2.1. First, coefficients used for the Doppler broadening are calculated to reduce the calculation time since these coefficients are independent of the incident particle energies. Next, FRENDY calculates the Doppler broadened cross-sections. Figure 3.2.2 shows an example of the difference of energy grid points at each temperature. Additional energy grid points are required from 8.40 to 8.50 eV to reduce the linearization error. The linearization flow of the Doppler broadening is similar to that of the resonance reconstruction described in Section 2.2.1. It should be noted that FRENDY sets an upper limit of the Doppler broadening as the upper limit of the resolved resonance region or 10^6 eV.

As the temperature becomes higher, the cross-sections may be linearized with fewer energy grid points as shown in Fig. 3.2.2. In such a case, NJOY eliminates redundant energy grid points. However, FRENDY does not eliminate the redundant energy grid points. The current computational platform accepts a large memory size and a large data size. The elimination of the energy grid points is not necessary from the viewpoint of utilizing the computational resources. Keeping the unionized base energy grid *i.e.*, keeping the original energy grid at 0 K, will be useful for the generation of the cross-section data library and the comparison of the cross-sections.

NJOY outputs thermal quantities when the temperature is equal to 293.6 K, *i.e.*, the most probable nucleus energy k_BT is equal to 0.0253 eV[7,8]. Though these quantities may not be used in the current reactor analysis, users might know them for their applications. FRENDY calculates the thermal quantities for the users. The thermal quantities consist of the fission and radiative capture cross-sections at the standard thermal value of 0.0253 eV, the integrals of these cross-sections against a Maxwellian distribution at 0.0253 eV, the *g*-factors, η, α, and K_1. Here the *g*-factor is the ratio between a Maxwellian integral and a corresponding thermal cross-section, η Maxwellian-weighted average of $(\bar{\nu}\sigma_f)/(\sigma_f+\sigma_c)$, α average of σ_f/σ_c, and K_1 average of $(\bar{\nu}-1)\sigma_f-\sigma_c$, where $\bar{\nu}$, σ_f, and σ_c are the average number of neutrons per fission, fission cross-section, radiation capture cross-section, respectively.

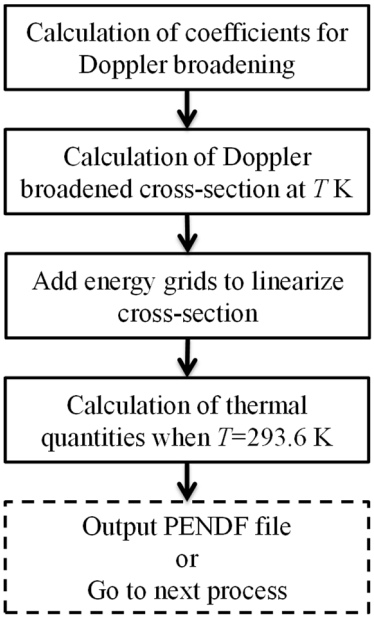

Figure 3.2.1 Calculation flow of the Doppler broadening

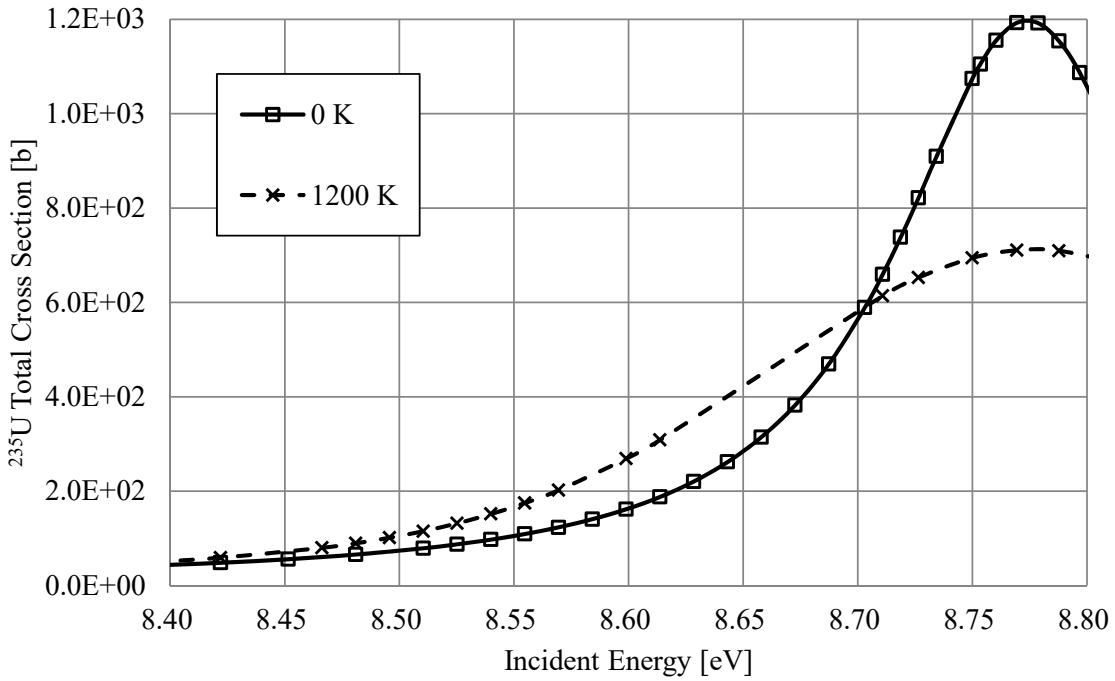

Figure 3.2.2 Example of the difference of energy grids in each temperature
(^{235}U(n, total) cross-section in JENDL-4.0)
It should be noted that the actual FRENDY calculation does not delete the energy grid points and keeps the original energy grid points.

3.3 Doppler Broadening Formula

3.3.1 Doppler Broadening Theory

3.3.1.1 Derivation of Doppler Broadening Formula

The neutron flux ϕ is written with the velocity vector of a neutron in the laboratory system $\boldsymbol{v}_n$ and the neutron density *n* as

$$\phi = n|\boldsymbol{v}_n|. \tag{3.3.1}$$

Considering the velocity distribution of the target nucleus at temperature *T* K in the laboratory system as $P(\boldsymbol{v}_t, T)$, the number of reactions between the neutron and target nucleus is

$$\int_0^\infty n|\boldsymbol{v}_r|\sigma(|\boldsymbol{v}_r|)\, N\, P(\boldsymbol{v}_t, T)\, \mathrm{d}\boldsymbol{v}_t. \tag{3.3.2}$$

Here $\boldsymbol{v}_t$ is the velocity vector of the target nucleus, *N* the number density of the target nucleus and $\boldsymbol{v}_r$ the relative velocity vector between the neutron and target nucleus

$$\boldsymbol{v}_r = \boldsymbol{v}_n - \boldsymbol{v}_t. \tag{3.3.3}$$

Here the effective cross-section $\sigma(|\boldsymbol{v}_n|, T)$ at *T* K is defined as follows:

$$\phi\, N\, \sigma(|\boldsymbol{v}_n|, T) = \int_{-\infty}^\infty n|\boldsymbol{v}_r|\sigma(|\boldsymbol{v}_r|)\, N\, P(\boldsymbol{v}_t, T)\, \mathrm{d}\boldsymbol{v}_t, \tag{3.3.4}$$

$$\sigma(|\boldsymbol{v}_n|, T) \equiv \frac{1}{|\boldsymbol{v}_n|}\int_{-\infty}^\infty |\boldsymbol{v}_r|\sigma(|\boldsymbol{v}_r|)P(\boldsymbol{v}_t, T)\, \mathrm{d}\boldsymbol{v}_t. \tag{3.3.5}$$

Let us approximate the velocity distribution of the target nucleus $\boldsymbol{P}(\boldsymbol{v}_t, T)$ as the Maxwell-Boltzmann distribution as follows:

$$P(\boldsymbol{v}_t, T) = \left(\frac{M}{2\pi k_B T}\right)^{\frac{3}{2}} e^{-\frac{M}{2k_B T}|\boldsymbol{v}_t|^2}. \tag{3.3.6}$$

Substituting Eq. (3.3.6) into Eq. (3.3.5), the effective cross-section is expressed by

$$\sigma(v_n, T) = \frac{1}{v_n}\int_{-\infty}^\infty v_r\sigma(v_r)\left(\frac{M}{2\pi k_B T}\right)^{\frac{3}{2}} e^{-\frac{M}{2k_B T}|\boldsymbol{v}_t|^2}\, \mathrm{d}\boldsymbol{v}_t, \tag{3.3.7}$$

where

$$v_n = |\boldsymbol{v}_n|, \tag{3.3.8}$$

$$v_r = |\boldsymbol{v}_r|. \tag{3.3.9}$$

The relation between the velocity vector of the neutron $\boldsymbol{v}_n$ and that of the target nucleus $\boldsymbol{v}_t$ is shown in Fig. 3.3.1. $\boldsymbol{v}_t$ is written by *xy*- and *z*-components of the target nucleus velocity vectors $\boldsymbol{v}_{t,xy}$ and $\boldsymbol{v}_{t,z}$ as

$$\boldsymbol{v}_t = \boldsymbol{v}_{t,xy} + \boldsymbol{v}_{t,z} = \left(v_{t,xy}\cos\varphi\,, v_{t,xy}\sin\varphi\,, v_{t,z}\right), \tag{3.3.10}$$

where $v_{t,xy}\cos\varphi$ and $v_{t,xy}\sin\varphi$ are the *x*- and *y*-components of the target nucleus velocity. Using Eq. (3.3.10), Eq. (3.3.7) becomes

$$\sigma(v_n, T) = \frac{1}{v_n}\int_{-\infty}^\infty v_r\sigma(v_r)\left(\frac{M}{2\pi k_B T}\right)^{\frac{3}{2}} e^{-\frac{M}{2k_B T}\left({v_r}^2 - {v_n}^2 + 2v_n v_{t,z}\right)}\, \mathrm{d}\boldsymbol{v} \tag{3.3.11}$$

$$= \left(\frac{\beta}{\pi}\right)^{\frac{3}{2}} \frac{1}{v_n} \int_{-\infty}^{\infty} \int_{0}^{\infty} v_{t,xy} v_r \sigma(v_r) e^{-\beta\left({v_r}^2 - {v_n}^2 + 2v_n v_{t,z}\right)} \mathrm{d}v_{t,xy} \mathrm{d}v_{t,z} \int_{0}^{2\pi} \mathrm{d}\varphi$$

$$= \frac{2\beta^{\frac{3}{2}}}{\pi^{\frac{1}{2}} v_n} \int_{0}^{\infty} v_{t,xy} v_r \sigma(v_r) e^{-\beta\left({v_r}^2 - {v_n}^2\right)} \int_{-\infty}^{\infty} e^{-2\beta v_n v_{t,z}} \mathrm{d}v_{t,z}\, \mathrm{d}v_{t,xy}.$$

Here the following relations are used:

$$\beta = \frac{M}{2k_B T}, \tag{3.3.12}$$

$$v_{t,z} = \left|\boldsymbol{v}_{t,z}\right|, \tag{3.3.13}$$

$$v_{t,xy} = \left|\boldsymbol{v}_{t,xy}\right|, \tag{3.3.14}$$

$$\begin{aligned} {v_r}^2 = |\boldsymbol{v}_n - \boldsymbol{v}_t|^2 = \left|\boldsymbol{v}_n - \boldsymbol{v}_{t,z}\right|^2 + \left|\boldsymbol{v}_{t,xy}\right|^2 = {v_n}^2 - 2v_n v_{t,z} + {v_{t,z}}^2 + {v_{t,xy}}^2 \\ = {v_n}^2 + {v_t}^2 - 2v_n v_{t,z}, \end{aligned} \tag{3.3.15}$$

$$\int_{-\infty}^{\infty} \mathrm{d}\boldsymbol{v} = \int_{0}^{\infty} v_{t,xy} \mathrm{d}v_{t,xy} \int_{-\infty}^{\infty} \mathrm{d}v_{t,xy} \int_{0}^{2\pi} \mathrm{d}\varphi. \tag{3.3.16}$$

Using Eq. (3.3.15), the following relation is obtained:

$$\begin{aligned} \frac{\mathrm{d}v_r}{\mathrm{d}v_{t,xy}} &= \frac{\mathrm{d}}{\mathrm{d}v_{t,xy}} \sqrt{{v_n}^2 - 2v_n v_{t,z} + {v_{t,z}}^2 + {v_{t,xy}}^2} \\ &= \frac{1}{2}\left({v_n}^2 - 2v_n v_{t,z} + {v_{t,z}}^2 + {v_{t,xy}}^2\right)^{-\frac{1}{2}} \times 2v_{t,xy} = \frac{v_{t,xy}}{v_r}. \end{aligned} \tag{3.3.17}$$

Substituting Eq. (3.3.17) into Eq. (3.3.11), the effective cross-section is calculated from

$$\sigma(v_n, T) = \frac{2\beta^{\frac{3}{2}}}{\pi^{\frac{1}{2}} v_n} \int_{0}^{\infty} {v_r}^2 \sigma(v_r) e^{-\beta\left({v_r}^2 - {v_n}^2\right)} \int_{-\infty}^{\infty} e^{-2\beta v_n v_{t,z}} \mathrm{d}v_{t,z}\, \mathrm{d}v_r. \tag{3.3.18}$$

As shown in Fig. 3.3.1, the range of v_z is

$$v_n - v_r \le v_z \le v_n + v_r. \tag{3.3.19}$$

Using the range of v_z, the integral range in Eq. (3.3.18) is

$$\begin{aligned} \sigma(v_n, T) &= \frac{2\beta^{\frac{3}{2}}}{\pi^{\frac{1}{2}} v_n} \int_{0}^{\infty} {v_r}^2 \sigma(v_r) e^{-\beta\left({v_r}^2 - {v_n}^2\right)} \int_{v_n - v_r}^{v_n + v_r} e^{-2\beta v_n v_{t,z}} \mathrm{d}v_{t,z} \mathrm{d}v_r \\ &= \frac{\beta^{\frac{1}{2}}}{\pi^{\frac{1}{2}} {v_n}^2} \int_{0}^{\infty} {v_r}^2 \sigma(v_r) e^{-\beta\left({v_r}^2 - {v_n}^2\right)} \left\{e^{-2\beta v_n (v_n - v_r)} - e^{-2\beta v_n (v_n + v_r)}\right\} \mathrm{d}v_r \\ &= \frac{\beta^{\frac{1}{2}}}{\pi^{\frac{1}{2}} {v_n}^2} \int_{0}^{\infty} {v_r}^2 \sigma(v_r) \left\{e^{-\beta(v_r - v_n)^2} - e^{-\beta(v_r + v_n)^2}\right\} \mathrm{d}v_r \end{aligned} \tag{3.3.20}$$

$$= \sqrt{\frac{\beta}{\pi}} \frac{1}{{v_n}^2} \int_0^\infty {v_r}^2 \sigma(v_r) \left\{ e^{-\left(\sqrt{\beta} v_r - \sqrt{\beta} v_n\right)^2} - e^{-\left(\sqrt{\beta} v_r + \sqrt{\beta} v_n\right)^2} \right\} \mathrm{d}v_r.$$

The Doppler broadened cross-section is finally expressed by Eq. (3.3.20). Eq. (3.3.20) is given by a simple form as follows:

$$\sigma(v_n, T) = \sigma^*(v_n, T) - \sigma^*(-v_n, T), \tag{3.3.21}$$

where

$$\sigma^*(v_n, T) = \sqrt{\frac{\beta}{\pi}} \frac{1}{{v_n}^2} \int_0^\infty {v_r}^2 \sigma(v_r) e^{-\left(\sqrt{\beta} v_r - \sqrt{\beta} v_n\right)^2} \mathrm{d}v_r. \tag{3.3.22}$$

Though the integral range in Eq. (3.3.22) is from zero to infinity, it is practically limited from v_{min} to v_{max}. Using v_{min} and v_{max}, Eq. (3.3.22) is

$$\sigma^*(v_n, T) = \sqrt{\frac{\beta}{\pi}} \frac{1}{{v_n}^2} \int_{v_{min}}^{v_{max}} {v_r}^2 \sigma(v_r) e^{-\left(\sqrt{\beta} v_r - \sqrt{\beta} v_n\right)^2} \mathrm{d}v_r. \tag{3.3.23}$$

The number of energy grid points from v_{min} to v_{max} is very large. For example, ^{238}U has more than one million energy grid points. In such a case, a long computing time is required to calculate Eq. (3.3.23).

In the equations described above, the distribution of the relative speed v_r is considered. As shown in Eqs. (3.3.3) and (3.3.15), the relative speed is given by the sum of the target nucleus and incident particle velocities. Because the neutron speed in Eq. (3.3.23) is constant, only the target nucleus speed distribution affects the relative speed distribution. As shown in Eq. (3.3.6), the target nucleus speed distribution is approximated by the Maxwell-Boltzmann distribution. The relation of $\sqrt{\beta} v_t$ and the Maxwell-Boltzmann distribution $P(v_t, T)$ is shown in Fig. 3.3.2 and Table 3.3.1. It should be noted that $P(v_t, T)$ in Fig. 3.3.2 and Table 3.3.1 is normalized by a maximal value of $P(v_t, T)$. As shown in Fig. 3.3.2 and Table 3.3.1, $P(v_t, T)$ is extremely reduced with increasing $\sqrt{\beta} v_t$.

The target nucleus speed range of FRENDY is set as follows[7,8]:

$$\sqrt{\beta} v_t \leq 4.0. \tag{3.3.24}$$

As shown in Table 3.3.1, $\mathrm{P}(v_t, T)$ is 1.1×10^{-7} when $\sqrt{\beta} v_t = 4.0$. This speed range would not cause any problems practically. Using Eq. (3.3.24), the integral range in Eq. (3.3.23) is

$$v_n - \frac{4}{\sqrt{\beta}} \leq v_r \leq v_n + \frac{4}{\sqrt{\beta}}. \tag{3.3.25}$$

The integral range for $\sigma^*(-v_n, T)$ is also given by Eq. (3.3.24)

$$0 \leq v_r \leq \frac{4}{\sqrt{\beta}}. \tag{3.3.26}$$

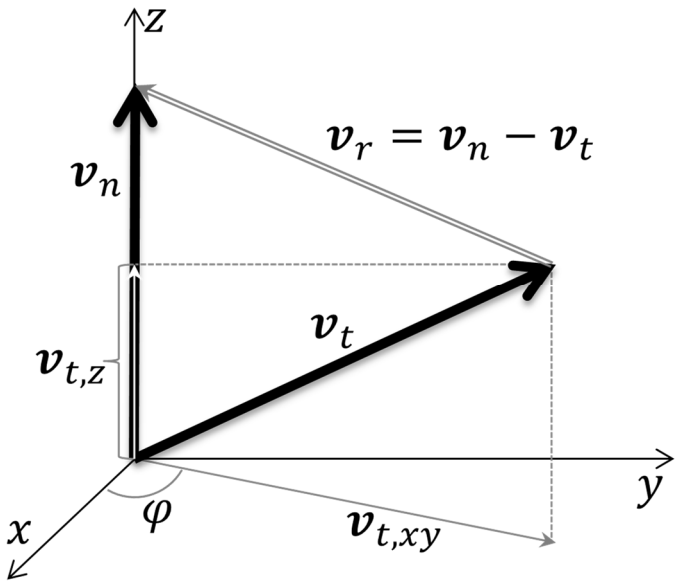

Figure 3.3.1 The relation between the neutron velocity vector v_n and the target nucleus velocity vector v_t

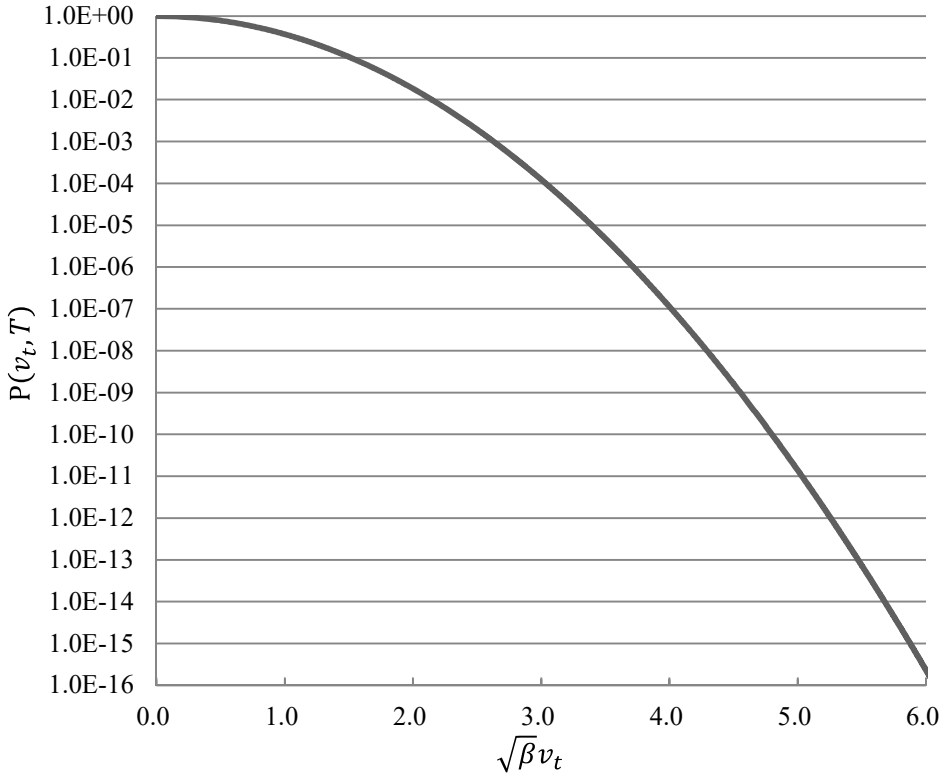

Figure 3.3.2 The relation of $\sqrt{\beta}v_t$ and the Maxwell-Boltzmann distribution $P(v_t, T)$ ($P(v_t, T)$ is normalized by a maximal value of $P(v_t, T)$)

Table 3.3.1 The relation of $\sqrt{\beta}v_t$ and the Maxwell-Boltzmann distribution $P(v_t,T)$ ($P(v_t,T)$ is normalized by a maximal value of $P(v_t,T)$)

$\sqrt{\beta}v_t$	$P(v_t,T)$	$\sqrt{\beta}v_t$	$P(v_t,T)$
0.0	1.00E+00	4.0	1.12E-07
0.5	7.79E-01	4.5	1.61E-09
1.0	3.68E-01	5.0	1.38E-11
1.5	1.05E-01	5.5	7.29E-14
2.0	1.83E-02	6.0	2.31E-16
2.5	1.93E-03	6.5	4.46E-19
3.0	1.23E-04	7.0	5.24E-22
3.5	4.79E-06	7.5	3.72E-25

To rewrite Eq. (3.3.23) with a simpler form, *x* and *y* are defined as follows:

$$x = \sqrt{\beta}v_r = \sqrt{\frac{M}{2k_BT}}\sqrt{\frac{2E_r}{m}} = \sqrt{\frac{A}{k_BT}E_r} = \sqrt{\alpha E_r}, \tag{3.3.27}$$

$$y = \sqrt{\beta}v_n = \sqrt{\frac{M}{2k_BT}}\sqrt{\frac{2E_n}{m}} = \sqrt{\frac{A}{k_BT}E_n} = \sqrt{\alpha E_n}. \tag{3.3.28}$$

Here E_r is the relative energy of the neutron given by $\frac{1}{2}m{v_r}^2$, E_n the neutron energy in the laboratory system, *A* the ratio of the mass of the nucleus to that of a neutron and

$$\alpha = \frac{A}{k_BT} = \frac{2}{m}\beta. \tag{3.3.29}$$

Substituting Eqs. (3.3.25) - (3.3.29) into Eq. (3.3.23), the latter equation leads to

$$\sigma^*(y,T) = \frac{1}{\sqrt{\pi}}\frac{1}{y^2}\int_{y-4}^{y+4} x^2\sigma(x)e^{-(x-y)^2}\mathrm{d}x. \tag{3.3.30}$$

where

$$\mathrm{d}v_r = \frac{1}{\sqrt{\beta}}\mathrm{d}x. \tag{3.3.31}$$

To calculate Eq. (3.3.30), $\sigma(x)$ is linearized as[37)]

$$\begin{aligned}\sigma(x) &= \frac{E-E_i}{E_{i+1}-E_i}\sigma(E_{i+1}) + \frac{E_{i+1}-E}{E_{i+1}-E_i}\sigma(E_i)\\ &= \frac{x^2-x_i^2}{x_{i+1}^2-x_i^2}\sigma\left(x_{i+1}^2\right) + \frac{x_{i+1}^2-x^2}{x_{i+1}^2-x_i^2}\sigma\left(x_i^2\right)\\ &= A_i + B_i x^2,\end{aligned} \tag{3.3.32}$$

where

$$A_i = \frac{x_{i+1}^2 \sigma\left(x_i^2\right) - E_i \sigma\left(x_{i+1}^2\right)}{x_{i+1}^2 - x_i^2} \tag{3.3.33}$$

$$B_i = \frac{\sigma\left(x_{i+1}^2\right) - \sigma\left(x_i^2\right)}{x_{i+1}^2 - x_i^2}. \tag{3.3.34}$$

Substituting Eq. (3.3.32) into Eq. (3.3.30), the latter equation turns out to be

$$\sigma^*(y,T) = \frac{1}{\sqrt{\pi}} \frac{1}{y^2} \sum_{i=0}^{N} \int_{x_i}^{x_{i+1}} \{A_i x^2 + B_i x^4\} e^{-(x-y)^2} \mathrm{d}x. \tag{3.3.35}$$

To calculate Eq. (3.3.35), z is defined as

$$z = x - y. \tag{3.3.36}$$

Using Eq. (3.3.36), Eq. (3.3.35) is given by

$$\sigma^*(y,T) = \frac{1}{\sqrt{\pi}} \frac{1}{y^2} \sum_{i=0}^{N} \int_{x_i - y}^{x_{i+1} - y} C_i(z) e^{-z^2} \mathrm{d}z, \tag{3.3.37}$$

where

$$C_i(z) = B_i z^4 + 4B_i y z^3 + (A_i + 6B_i y^2) z^2 + (2A_i y + 4B_i y^3) z + (A_i y^2 + B_i y^4). \tag{3.3.38}$$

To calculate Eq. (3.3.37), $G_n(a,b)$ is introduced as

$$G_n(a,b) = \frac{1}{\sqrt{\pi}} \int_a^b z^n e^{-z^2} \, \mathrm{d}z. \tag{3.3.39}$$

Here, Eq. (3.3.39) is rewritten as

$$G_n(a,b) = \frac{1}{2}\left(D_n(b) - D_n(a)\right), \tag{3.3.40}$$

where

$$D_n(a) = \frac{2}{\sqrt{\pi}} \int_0^a z^n e^{-z^2} \, \mathrm{d}z. \tag{3.3.41}$$

Equation (3.3.41) satisfies the following recursive relations[38]:

$$D_0(a) = \mathrm{erf}(a), \tag{3.3.42}$$

$$D_1(a) = \frac{1}{\sqrt{\pi}}\left(1 - e^{-a^2}\right), \tag{3.3.43}$$

$$D_n(a) = \frac{n-1}{2} F_{n-2}(a) - \frac{1}{\sqrt{\pi}} a^{n-1} e^{-a^2} + \frac{1}{\sqrt{\pi}} \delta_{n,1}. \tag{3.3.44}$$

Here $\delta_{n,1}$ is the Kronecker delta and $\mathrm{erf}(a)$ the error function. The error function is defined by

$$\mathrm{erf}(a) = \frac{1}{\sqrt{\pi}} \int_0^a e^{-z^2} \, \mathrm{d}z. \tag{3.3.45}$$

Using Eq. (3.3.39), Eq. (3.3.35) is written by

$$\sigma^*(y,T) = \frac{1}{\frac{1}{\pi^2}y^2}\sum_{i=0}^{N} C_i, \tag{3.3.46}$$

where

$$C_i = B_i G_4 + 4B_i y G_3 + (A_i + 6B_i y^2)G_2 + (2A_i y + 4B_i y^3)G_1 + (A_i y^2 + B_i y^4)G_0, \tag{3.3.47}$$

$$G_n = G_n(x_i - y, x_{i+1} - y). \tag{3.3.48}$$

3.3.1.2 Treatment of cross-section at 0 *eV*

Treatment of cross-section is required from 0 eV to the lowest energy (E_L) given in an evaluated nuclear data file. Normally, a cross-section at 0 eV is not included in the evaluated nuclear data file. The cross-section at 0 eV is required to calculate the Doppler broadened cross-section in low energy region.

NJOY and SIGMA1 approximate that the cross-section obeys the 1/v law. Eq. (3.3.30) is given by

$$\begin{aligned}\sigma^*(v) &= \frac{1}{\sqrt{\pi}y^2}\int_0^{x_1}\frac{\sigma_1 x_1}{x}x^2 e^{-(x-y)^2}\,dx = \frac{\sigma_1 x_1}{\sqrt{\pi}y^2}\int_0^{x_1-y}(z-y)e^{-z^2}\,dz \\ &= -\frac{\sigma_1 x_1}{\sqrt{\pi}}\left(\frac{H_1(0,x_1-y)}{y^2} + \frac{H_0(0,x_1-y)}{y^2}\right).\end{aligned} \tag{3.3.49}$$

$$H_n(a,b) = \frac{1}{\sqrt{\pi}}\int_a^b z^n e^{-z^2}\,dz \tag{3.3.50}$$

Here σ_1 and x_1 are the cross-section and the x value at E_L, respectively. Equation (3.3.49) is valid below E_L as far as since the cross-section obeys the 1/v law. However, the cross-sections which do not exhibit the 1/v behavior, *e.g.*, the elastic scattering cross-section, are not expressed, appropriately.

FRENDY determines the cross-sections at 0 eV by the linear extrapolation with the cross-sections at the lowest and next-to-the-lowest energy grid points. Our study[39] has revealed that the difference of the cross-sections of the linear extrapolation is so small, even if the capture cross-section, which obeys the 1/v law, is concerned. Therefore, the linear extrapolation is appropriate for the treatment of the cross-section at 0 eV.

3.3.2 Speed-Up of Doppler Broadening

The Doppler broadening process requires a relatively long computational time for the calculation of the error function of Eq. (3.3.45). As shown in Eq. (3.3.46), $G_n(a,b)$ is dependent only on the x value, *i.e.*, the relative neutron energy E_r. The $G_n(a,b)$ values for each cross-section at energy grid point E are identical since the energy grids of many cross-sections are unionized by the previous process. FRENDY calculates all cross-sections at energy grid point E simultaneously to reduce the number of the error function calculation.

Consequently, the actual calculation formula is as follows:

$$\sigma_c^*(y,T) = \frac{1}{\frac{1}{\pi^2}y^2}\sum_{i=0}^{N} C_{i,c}, \tag{3.3.51}$$

where

$$C_{i,c} = \begin{matrix} B_{i,c}G_4 + 4B_{i,c}yG_3 + \left(A_{i,c} + 6B_{i,c}y^2\right)G_2 \\ +\left(2A_{i,c}y + 4B_{i,c}y^3\right)G_1 + \left(A_{i,c}y^2 + B_{i,c}y^4\right)G_0 \end{matrix}, \tag{3.3.52}$$

$$A_{i,c} = \frac{E_{i+1}\sigma_c(E_i) - E_i\sigma_c(E_{i+1})}{x_{i+1}^2 - x_i^2}, \tag{3.3.53}$$

$$B_{i,c} = \frac{\sigma_c(E_{i+1}) - \sigma_c(E_i)}{x_{i+1}^2 - x_i^2}. \tag{3.3.54}$$

Many reactions have a threshold and their cross-sections are zero below the threshold. FRENDY eliminates the energy grid points below the threshold because these energy grid points are not used in nuclear data processing and neutronics calculations. Therefore, the number of energy grids becomes lower when the reaction has higher threshold energy. The Doppler broadening below the threshold is not required since the Doppler broadened cross-sections are also zero below the threshold. To skip the Doppler broadening below the threshold, FRENDY divides all reactions into six groups, *i.e*, the number of energy grid points is less than 100, 500, 1000, 5000, 10000, and more than 10000, and the Doppler broadening is carried out in each group.

3.4 Calculation of Thermal Quantities

The evaluated thermal quantities are as follows:

- Fission cross-section at 0.0253 eV $\sigma_{f,th}$
- Average neutron production at 0.0253 eV $\bar{\nu}_{th}$
- Capture cross-section at 0.0253 eV $\sigma_{c,th}$
- Integral of fission cross-section against a Maxwell-Boltzmann distribution in the thermal region $I_{f,th}$
- Integral of radiative capture cross-section against a Maxwell-Boltzmann distribution in the thermal region $I_{c,th}$
- *g*-factor of the fission reaction g_f
- *g*-factor of radiative capture reaction g_c
- Average value of α at thermal region α
- Average value of η at thermal region η
- Average value of K_1 at thermal region K_1
- Integral of fission cross-section against a Maxwell-Boltzmann distribution in the resonance region $I_{f,reso}$

・Integral of radiative capture cross-section against a Maxwell-Boltzmann distribution in the resonance region $I_{c,reso}$

$\sigma_{f,th}$, $\bar{\nu}_{th}$ and $\sigma_{c,th}$ are values at 0.0253 eV. Other values are defined as follows[8,40]:

$$I_{r,th} = \int_{E\in th} \sigma_r(E) \frac{E}{(k_B T)^2} e^{-\frac{E}{k_B T}} \mathrm{d}E, \tag{3.4.1}$$

$$g_r = \frac{2}{\sqrt{\pi}} \frac{1}{\sqrt{k_B T}\sigma_{r,th}} \int_{E\in th} \sqrt{E}\sigma_r(E) \sqrt{\frac{E}{(k_B T)^3}} e^{-\frac{E}{k_B T}} \mathrm{d}E = \frac{2}{\sqrt{\pi}} \frac{\mathrm{I}_{r,th}}{\sigma_{r,th}}, \tag{3.4.2}$$

$$\alpha = \int_{E\in th} \frac{\sigma_c(E)}{\sigma_f(E)} \frac{E}{(k_B T)^2} e^{-\frac{E}{k_B T}} \mathrm{d}E, \tag{3.4.3}$$

$$\eta = \int_{E\in th} \frac{\sigma_f(E)}{\sigma_f(E)+\sigma_c(E)} \frac{E}{(k_B T)^2} e^{-\frac{E}{k_B T}} \mathrm{d}E, \tag{3.4.4}$$

$$K_1 = \int_{E\in th} \{(\nu(E)-1)\sigma_f(E) - \sigma_c(E)\} \frac{E}{(k_B T)^2} e^{-\frac{E}{k_B T}} \mathrm{d}E, \tag{3.4.5}$$

$$I_{r,reso} = \int_{E\in reso} \sigma_r(E) \frac{E}{(k_B T)^2} e^{-\frac{E}{k_B T}} \mathrm{d}E, \tag{3.4.6}$$

where *r* indicates the reaction, *i.e.*, *r=f* for the fission reaction and *r=c* for the radiative capture reaction. The integral range in Eqs. (3.4.1) - (3.4.6) is from the lowest energy grid point to 1.0 eV for the thermal region and from 0.5 eV to the highest energy grid point for the resonance region, respectively. The trapezoidal integration is used to calculate the integration in Eqs. (3.4.1) - (3.4.6)

$$I_{r,th} = \sum_{E_{min}}^{E_i<1.0} \frac{E_i - E_{i-1}}{2(k_B T)^2} \left(\sigma_r(E_i) E_i e^{-\frac{E_i}{k_B T}} - \sigma_r(E_{i-1}) E_{i-1} e^{-\frac{E_{i-1}}{k_B T}} \right), \tag{3.4.7}$$

$$\alpha = \sum_{E_{min}}^{E_i<1.0} \frac{E_i - E_{i-1}}{2(k_B T)^2} \left(\frac{\sigma_c(E_i)}{\sigma_f(E_i)} E_i e^{-\frac{E_i}{k_B T}} - \frac{\sigma_c(E_{i-1})}{\sigma_f(E_{i-1})} E_{i-1} e^{-\frac{E_{i-1}}{k_B T}} \right), \tag{3.4.8}$$

$$\eta = \sum_{E_{min}}^{E_i<1.0} \frac{E_i - E_{i-1}}{2(k_B T)^2} \left(\frac{\sigma_c(E_i)}{\sigma_f(E_i)+\sigma_c(E_i)} E_i e^{-\frac{E_i}{k_B T}} - \frac{\sigma_c(E_{i-1})}{\sigma_f(E_{i-1})+\sigma_c(E_{i-1})} E_{i-1} e^{-\frac{E_{i-1}}{k_B T}} \right), \tag{3.4.9}$$

$$K_1 = \sum_{E_{min}}^{E_i<1.0} \frac{E_i - E_{i-1}}{2(k_B T)^2} \begin{pmatrix} \{(\nu(E_i)-1)\sigma_f(E_i) + \sigma_c(E_i)\} E_i e^{-\frac{E_i}{k_B T}} \\ -\{(\nu(E_{i-1})-1)\sigma_f(E_{i-1}) + \sigma_c(E_{i-1})\} E_{i-1} e^{-\frac{E_{i-1}}{k_B T}} \end{pmatrix}, \tag{3.4.10}$$

$$I_{r,reso} = \sum_{E_i=0.5}^{E_{max}} \frac{E_i - E_{i-1}}{2(k_B T)^2} \left(\sigma_r(E_i) E_i e^{-\frac{E_i}{k_B T}} - \sigma_r(E_{i-1}) E_{i-1} e^{-\frac{E_{i-1}}{k_B T}} \right). \tag{3.4.11}$$

4 Thermal Scattering Cross-section Calculation

4.1 Thermal Scattering Law Data

At high energies, the wavelengths of neutrons are small, and it is reasonable to treat scattering as classical collisions between particles. At thermal energies, the wavelengths of neutrons are similar to the size of molecules and the spacing of crystalline lattice and the theory of classical collisions cannot be adopted, directly[36]. In such energy regions, consideration of thermal scattering caused by crystalline and chemical binding is important for many materials, *e.g.*, H_2O, ZrH, and graphite, to improve the prediction accuracy of neutron calculations. The evaluated nuclear data file gives the Thermal Scattering Law (TSL) data to consider the scattering by crystalline and chemical binding. In the ENDF-6 format[13], the following scattering cross-sections are defined:

- coherent elastic scattering for crystalline materials,
- incoherent elastic scattering for partially ordered materials,
- incoherent inelastic scattering for non-crystalline materials.

The evaluated nuclear data file contains only parameters to calculate the thermal scattering cross-sections. Reconstruction and linearization of the thermal scattering cross-sections, secondary neutron energy, and scattering angle are required.

4.2 Calculation Flow of Thermal Scattering Cross-Sections

A calculation flow of the thermal scattering cross-sections is shown in Fig. 4.2.1. The thermal scattering cross-sections, secondary neutron energy, and scattering angle are calculated when the evaluated nuclear data file contains the parameters of these cross-sections. FRENDY also calculates the incoherent inelastic thermal scattering cross-sections with the free monatomic gas model[8] when the evaluated nuclear data file does not contain the parameters or users want to calculate them.

As shown in Fig. 4.2.1, FRENDY skips the calculation of the incoherent elastic scattering cross-section using the Debye-Waller factor when the Bragg edge data is included in the evaluated nuclear data file. The ENDF-6 format cannot contain the parameters of both the coherent and incoherent elastic scattering cross-sections in the evaluated nuclear data file. If a new nuclear data format contains both parameters, the calculation flow can be changed and FRENDY will be able to calculate both the coherent and incoherent elastic scattering cross-sections.

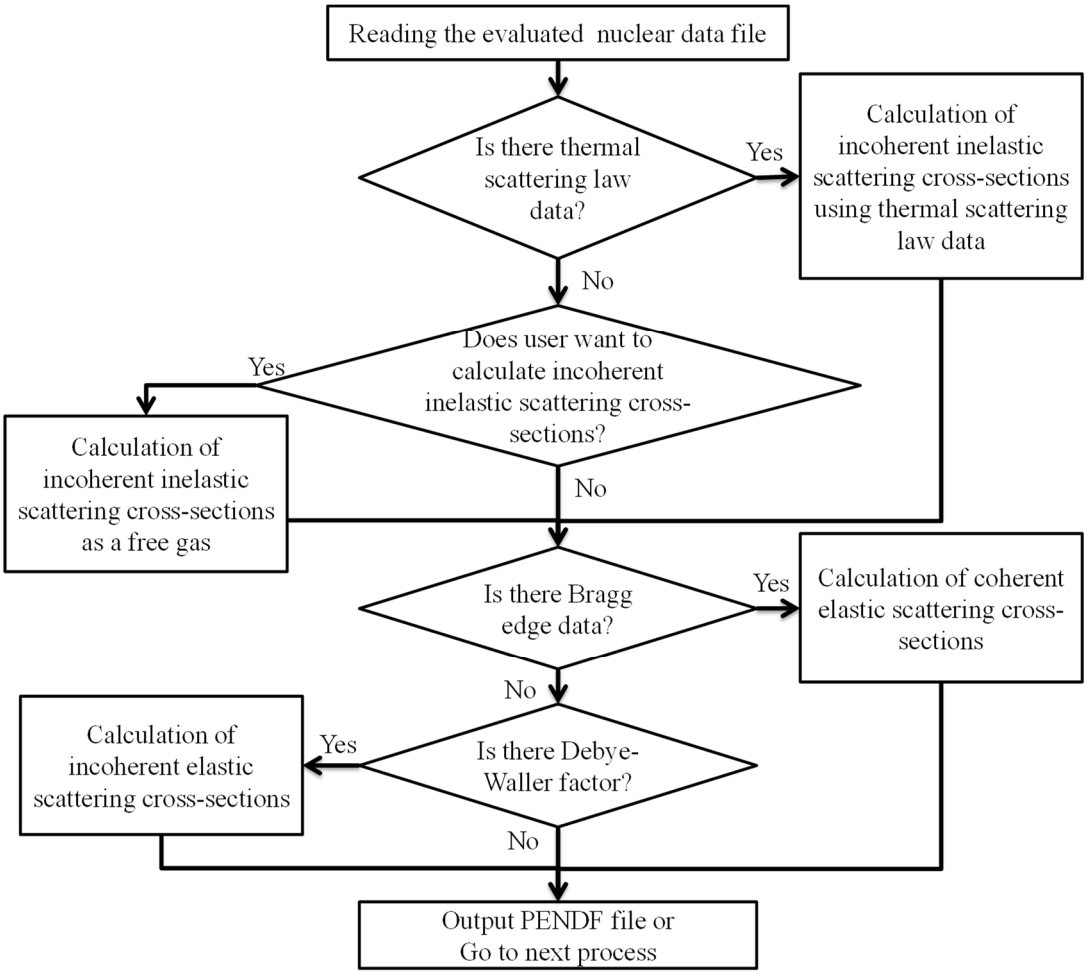

Figure 4.2.1 Calculation flow of the thermal scattering cross-sections

4.2.1 Coherent Elastic Scattering

The coherent elastic scattering is observed in crystalline materials such as graphite. As shown in Fig. 4.2.2, the crystalline atoms cause neutrons to scatter into many specific directions and it is called “Bragg diffraction”.

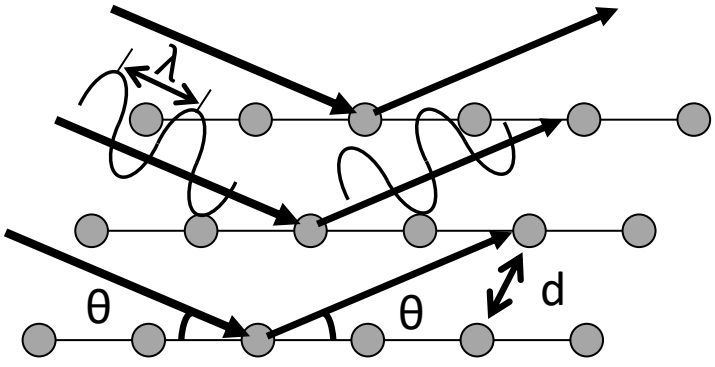

Figure 4.2.2 Example of Bragg diffraction

The Bragg diffraction is observed in the specified energy. In the Bragg's law, the interference is strongest when the wavelength λ is satisfied with Eq. (4.2.1)[41)]

$$2d \sin\theta = n\lambda = \frac{h}{\sqrt{2mE_i}}, \tag{4.2.1}$$

where d is the distance between atomic layers in a crystal, θ the scattering angle, n a positive integer, h Planck's constant, and E_i the energy of the i-th Bragg edge.

Figure 4.2.3 shows the coherent elastic scattering cross-section for graphite at 296 K taken from JENDL-4.0[1)]. As shown in Fig. 4.2.3, the very strong peaks which are known as Bragg edges are observed in the coherent elastic scattering cross-section. It should be noted that the cross-section is zero below the first Bragg edge.

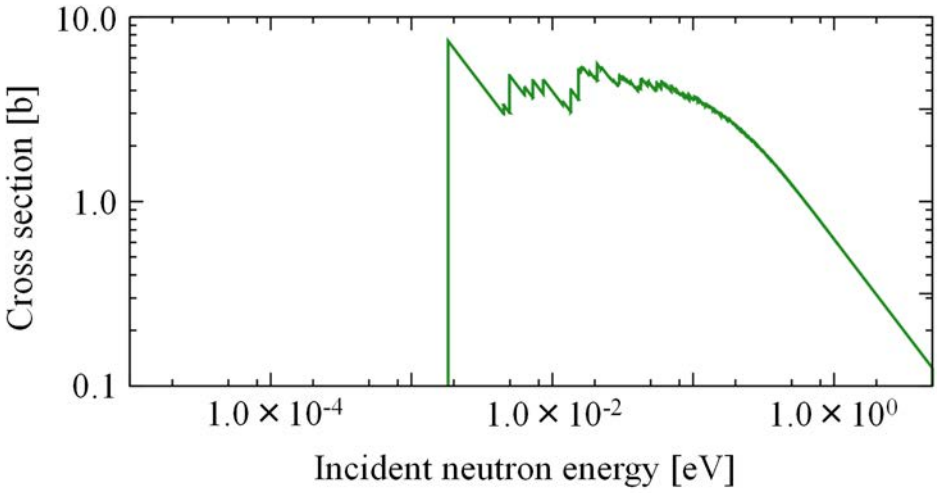

Figure 4.2.3 Example of coherent elastic scattering cross-section for a crystalline material (Graphite, 296 K, JENDL-4.0)

The evaluated nuclear data file provides the number of the Bragg edges, the energy of the Bragg edges, and the crystallographic structure factor. The coherent elastic scattering cross-section σ^{coh} is represented as follows:[42)]

$$\sigma^{coh}(E, E', \mu) = \frac{1}{E}\sum_{i}^{E_i<E} \sigma_c f_i e^{-2WE_i} \delta(\mu - \mu_i)\delta(E - E'), \tag{4.2.2}$$

where

$$\mu_i = 1 - \frac{2E_i}{E}, \tag{4.2.3}$$

$$E_i = \frac{\hbar^2 \tau_i^2}{8m}, \tag{4.2.4}$$

$$f_i = \frac{\pi^2 \hbar^2}{2mNV} \sum_{\tau_i} |F(\tau_i)|, \tag{4.2.5}$$

$$\hbar = \frac{h}{2\pi}. \tag{4.2.6}$$

In the above equations, E is the incident neutron energy, E' the secondary neutron energy, μ the scattering cosine in the laboratory system, σ_c the characteristics coherent scattering cross-section, W the Debye-Waller factor, E_i the energy of the Bragg edge, $\delta(x)$ the delta function, τ_i the vectors of one particular "shell" of the reciprocal lattice, m the neutron mass, N the number of atoms in the unit shell, V the volume in the unit shell, and $F(\tau_i)$ the crystallographic structure factors. The evaluated nuclear data file contains s_i which is proportional to the structure factor. Using s_i, Eq. (4.2.2) is

$$\sigma^{coh}(E, E', \mu) = \frac{1}{E} \sum_{i}^{E_i<E} s_i \delta(\mu - \mu_i) \delta(E - E'). \tag{4.2.7}$$

The coherent elastic scattering cross-section is linearized in this module using a similar method that is used in the resonance reconstruction. As described in Eq. (4.2.7), the secondary neutron energy is equal to the incident neutron energy, and the scattering cosine is fixed. The linearization of the secondary energy and scattering angle is not required for the coherent elastic scattering.

For the incident neutron energy, FRENDY adds a middle energy grid point when the following conditions are satisfied:

$$\sigma^{inc}\left(E_{i+\frac{1}{2}}, E', \mu\right) - \frac{\sigma^{inc}(E_{i+1}, E', \mu) + \sigma^{inc}(E_i, E', \mu)}{2} \geq err \times \sigma^{inc}\left(E_{i+\frac{1}{2}}, E', \mu\right), \tag{4.2.8}$$

$$\sigma^{inc}\left(E_{i+\frac{1}{2}}, E', \mu\right) - \frac{\sigma^{inc}(E_{i+1}, E', \mu) + \sigma^{inc}(E_i, E', \mu)}{2} \geq 1.0 \times 10^{-6}, \tag{4.2.9}$$

where err is the tolerance value for the linearization. FRENDY terminates the linearization when the energy interval satisfies the following criterion:

$$E_{i+1} - E_i \geq E_{i+\frac{1}{2}} \times 3.0 \times 10^{-5}. \tag{4.2.10}$$

4.2.2 Incoherent Elastic Scattering

The incoherent elastic scattering is observed in partially ordered materials such as ZrH and polyethylene. The incoherent elastic scattering is isotropic and contains no structural information since the intensity of this type of scattering is independent of the scattering angle.[43] The incoherent inelastic scattering cross-section $\sigma^{iel}(E, E', \mu)$ is given by

$$\sigma^{iel}(E, E', \mu) = \frac{\sigma_b}{2} e^{-2WE(1-\mu)} \delta(E - E'), \tag{4.2.11}$$

where σ_b is the characteristic bound scattering cross-section[42].

The angle-integrated cross-section $\sigma^{iel}(E)$, which is divided into equally probable cosine bins, and the cumulative distribution are output in the PENDF file. Because the incoherent elastic scattering is isotropic, the integrated cross-section $\sigma^{iel}(E)$ is calculated by

$$\sigma^{iel}(E) = \int_{-1}^{1} \frac{\sigma_b}{2} e^{-2WE(1-\mu)}\, d\mu = \frac{\sigma_b}{2}\left\{\frac{1-e^{-4WE}}{2WE}\right\}. \tag{4.2.12}$$

The equally probable angle $\bar{\mu}_i$ is also calculated by

$$\bar{\mu}_i = \frac{n_{bin}}{2WE}\frac{e^{-2WE(1-\mu_i)}(2WE\mu_i - 1) - e^{-2WE(1-\mu_{i-1})}(2WE\mu_{i-1} - 1)}{1-e^{-4WE}}, \tag{4.2.13}$$

where n_{bin} is the number of cosine bins and μ_i is the upper limit of cosine bin which is given by

$$\mu_i = 1 + \frac{1}{2WE}\ln\left(\frac{1-e^{-4WE}}{n_{bin}} + e^{-2WE(1-\mu_{i-1})}\right), \tag{4.2.14}$$

$$\mu_0 = -1. \tag{4.2.15}$$

Figure 4.2.4 shows the incoherent elastic scattering cross-section for H in ZrH at 296 K taken from JENDL-4.0. Compared to the other reactions, the incoherent elastic scattering cross-section can be represented with a slowly varying function. Therefore, the linearization of the incoherent elastic scattering cross-section is not performed and the energy grid of the total cross-section is used for the incident neutron energy grid.

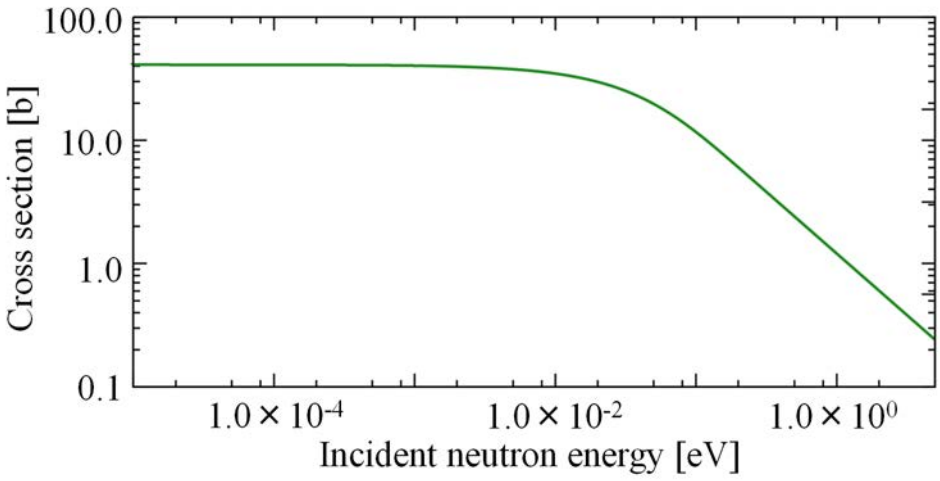

Figure 4.2.4 Example of incoherent elastic scattering cross-section (H in ZrH, 296 K, JENDL-4.0)

4.2.3 Incoherent Inelastic Scattering

The incoherent inelastic scattering is observed in non-crystalline materials such as H_2O and ZrH[36]. The thermal scattering law data is used to consider the effect of the chemical binding of a molecule on neutron scattering. Using the thermal scattering law data $S(\alpha,\beta)$, the double differential

scattering cross-section $\frac{\mathrm{d}^2\sigma^{inc}(E,E',\mu)}{\mathrm{d}E\mathrm{d}\Omega}$ is written as follows[44]:

$$\frac{\mathrm{d}^2\sigma^{inc}(E,E',\mu)}{\mathrm{d}E\mathrm{d}\Omega} = \frac{\sigma_b}{4\pi k_B T}\sqrt{\frac{E'}{E}}S(\alpha,\beta), \tag{4.2.16}$$

where

$$\alpha = \frac{E' + E - 2\mu\sqrt{EE'}}{Ak_BT}, \tag{4.2.17}$$

$$\beta = \frac{E' - E}{k_BT}, \tag{4.2.18}$$

α the dimensionless momentum transfer, β the dimensionless energy transfer, A the ratio of the target mass to the neutron mass, and k_B the Boltzmann constant.

The evaluated nuclear data file provides the thermal scattering law data of *n*-th type atom because molecule consists of many elements. FRENDY uses the following equations to calculate the inelastic incoherent scattering cross-section at *T* K in each energy grid point[13]:

$$\sigma^{inc}(E,E',\mu) = \sum_{n=0}^{N_s}\frac{M_n\sigma_{bn}}{2k_BT}\sqrt{\frac{E'}{E}}e^{-\frac{\beta}{2}}S_n(\alpha_n,\beta), \tag{4.2.19}$$

$$\sigma_{bn} = \sigma_{fn}\left(\frac{A_n+1}{A_n}\right)^2, \tag{4.2.20}$$

$$\sigma_{fn} = 4\pi{\alpha_n}^2, \tag{4.2.21}$$

$$\alpha_n = \frac{E' + E - 2\mu\sqrt{EE'}}{A_nk_BT}, \tag{4.2.22}$$

where N_s is the number of non-principal scattering atom types, M_n the number of *n*-th type atoms in the molecule or unit cell, σ_{bn} the characteristic bound incoherent scattering cross-section, and σ_{fn} the characteristic free atom scattering cross-section.

The thermal scattering law data describes the thermal neutron scattering cross-section of the atom for which the chemical binding is considered[42]. For a free gas of scatterers with no internal structure, the thermal scattering law data $S_n(\alpha_n,\beta)$ is

$$S_n(\alpha_n,\beta) = \frac{1}{\sqrt{4\pi\alpha_n}}\exp\left\{-\frac{{\alpha_n}^2+\beta^2}{4\alpha_n}\right\}. \tag{4.2.23}$$

When the evaluated nuclear data file does not include the thermal scattering law data or users want to calculate the incoherent inelastic scattering cross-section as a free gas, FRENDY assumes that the nucleus is a free particle with no internal structure and the thermal scattering law data is calculated using Eq. (4.2.23).

When α or β value is outside the range of the table, the differential scattering cross-section can

be computed using the short collision time (SCT) approximation[42]:

$$\sigma^{inc,SCT}(E,E',\mu)=\sum_{n=0}^{N_s}\frac{\sigma_{bn}}{2k_BT}\sqrt{\frac{E'}{E}\frac{T}{T_{eff}}}\frac{1}{\sqrt{4\pi\alpha_n}}\exp\left\{-\frac{(\alpha_n-|\beta|)^2}{4\alpha_n}\frac{T}{T_{eff}}-\frac{\beta+|\beta|}{2}\right\}, \quad (4.2.24)$$

where T_{eff} is the effective temperature for the SCT approximation which is given in the evaluated nuclear data file.

Figures 4.2.5 and 4.2.6 show the incoherent inelastic scattering cross-section for H in H_2O and H in ZrH at 296 K taken from JENDL-4.0. The THERMR module of NJOY[7,8] uses the fixed incident neutron energy grid, which consists of 117 energy grid points from 1.0×10^{-5} to 10 eV, to calculate the incoherent inelastic scattering cross-section and secondary energy and angular distributions. The incoherent inelastic scattering cross-section at the other energy grid points are interpolated using the fifth order Lagrange interpolation and secondary energy and angular distributions are not calculated to reduce calculation time and data size. As shown in Fig. 4.2.5, the incoherent inelastic scattering cross-section for many materials can be represented with a slowly varying function. In such a case, the fixed incident neutron energy grid is appropriate. However, the fixed incident neutron energy grid is inappropriate for some materials, *e.g.*, H in ZrH. The incoherent inelastic scattering cross-section of these materials oscillates at the higher energy region as shown in Fig. 4.2.6. The adoption of the finer energy grid is required to adequately reproduce the incoherent inelastic scattering cross-section distribution in such materials[45].

FRENDY calculates the incoherent inelastic scattering cross-section in all energy grid points of the total cross-section to appropriately treat such materials when the thermal scattering law data is given. FRENDY uses the fixed energy grid points to calculate the incoherent inelastic scattering cross-section when the thermal scattering law data is not given. Similar to NJOY, the fixed incident neutron energy grid, which consists of 117 energy grid points from 1.0×10^{-5} to 10 eV, is used to calculate the incoherent inelastic scattering, and other energy grid points are interpolated using the fifth order Lagrange interpolation. This is because the number of energy grid points of heavy nuclides is very large. The incoherent inelastic scattering cross-section for a free gas is not so important for neutronics calculation and it can be represented with a slowly varying function of the incident neutron energy. A large amount of data size is required to show the secondary energy and angular distributions. The secondary energy and angular distributions are output only in the fixed incident neutron energy grid points to reduce calculation time and data size.

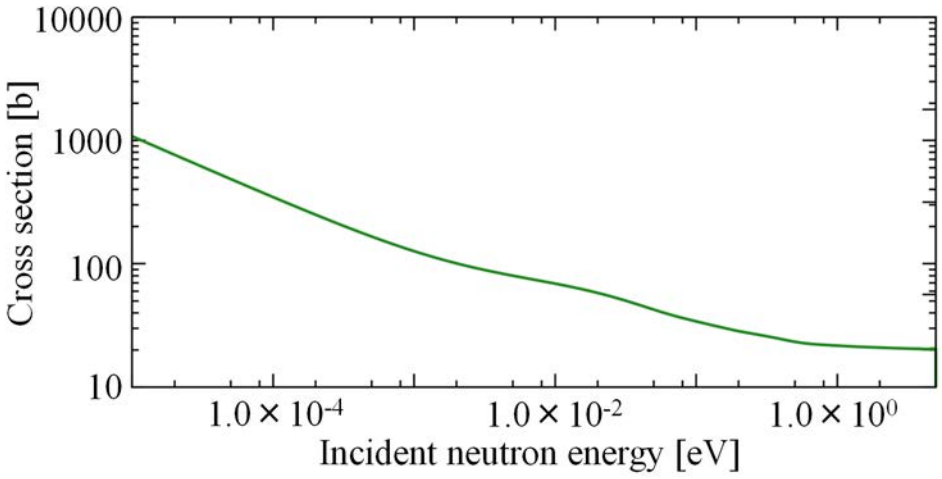

Figure 4.2.5 Example of incoherent inelastic scattering cross-section
(H in H_2O, 296 K, JENDL-4.0)

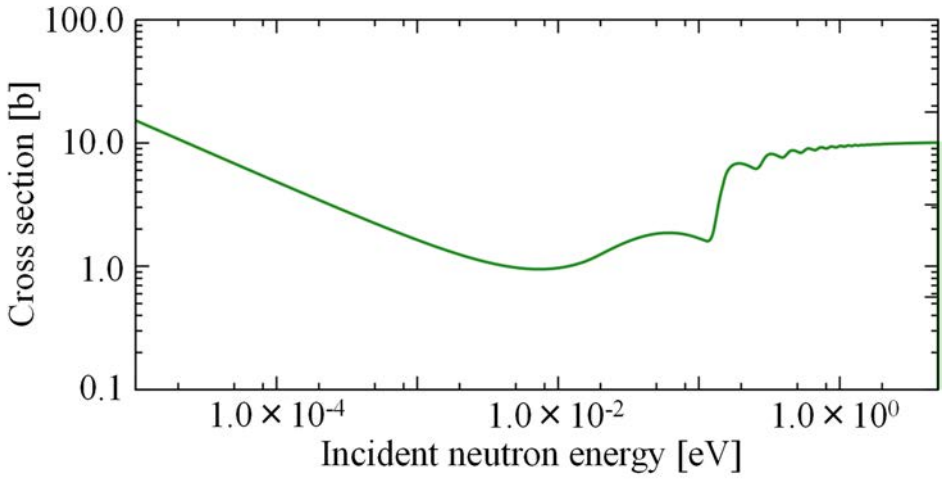

Figure 4.2.6 Example of incoherent inelastic scattering cross-section
(H in ZrH, 296 K, JENDL-4.0)

Linearization of the secondary energy and angular distributions for the incoherent inelastic scattering is required. For the secondary energy, FRENDY adds a middle energy grid point when the following condition is satisfied:

$$\left|\sigma^{inc}\left(E,E'_{i+\frac{1}{2}}\right)-\frac{\sigma^{inc}(E,E'_{i+1})+\sigma^{inc}(E,E'_{i})}{2}\right| \geq err\times\left|\sigma^{inc}\left(E,E'_{i+\frac{1}{2}}\right)+1.0\times10^{-3}\right|, \tag{4.2.25}$$

where err is the tolerance value for the linearization and

$$\sigma^{inc}(E,E') = \int_{-1}^{1} \sigma^{inc}(E,E',\mu)\,\mathrm{d}\mu. \tag{4.2.26}$$

When the integrated incoherent inelastic scattering cross-section satisfies the following equation, the linearization at this energy grid point is finished and moves to the next energy grid point

$$\frac{1}{2}({E'}_{i+1} - {E'}_{i})\left(\sigma^{inc}(E,{E'}_{i+1}) + \sigma^{inc}(E,{E'}_{i})\right) < 1.0 \times 10^{-6}. \tag{4.2.27}$$

For the angular distribution, FRENDY adds a middle angular point when either of the following conditions is satisfied:

$$\begin{aligned}\left|\sigma^{inc}\left(E,E',\mu_{i+\frac{1}{2}}\right) - \frac{\sigma^{inc}(E,E',\mu_i) + \sigma^{inc}(E,E',\mu_{i+1})}{2}\right| \\ > err \times \left|\sigma^{inc}\left(E,E',\mu_{i+\frac{1}{2}}\right)\right|,\end{aligned} \tag{4.2.28}$$

$$\left|\sigma^{inc}(E,E',\mu_i) - \sigma^{inc}(E,E',\mu_{i+1})\right| \geq \left|\frac{\sigma^{inc}(E,E',\mu_i) + \sigma^{inc}(E,E',\mu_{i+1})}{2}\right|. \tag{4.2.29}$$

The linearization is finished and moves to the next angular point when the distance of the angular points is so small, *i.e.*, it satisfies the following equation:

$$\mu_i - \mu_{i+1} < 1.0 \times 10^{-5}. \tag{4.2.30}$$

The integrated cross-section $\sigma^{inc}(E)$, which is divided into equally probable cosine bins, and the cumulative distribution are written in the PENDF file. Because the incoherent inelastic scattering cross-sections are linearized, $\sigma^{inc}(E)$ is easily calculated with the trapezoidal integration as follows:

$$\begin{aligned}\sigma^{inc}(E) &= \int_0^{\infty} \sigma^{inc}(E,E')\mathrm{d}E' \\ &= \sum_i \frac{\sigma^{inc}(E,{E'}_i) + \sigma^{inc}(E,{E'}_{i-1})}{2} \times ({E'}_i - {E'}_{i-1}),\end{aligned} \tag{4.2.31}$$

where

$$\begin{aligned}\sigma^{inc}(E,E') &= \int_{-1}^{1} \sigma^{inc}(E,E',\mu)\mathrm{d}\mu \\ &= \sum_j \frac{\sigma^{inc}\left(E,E'\mu_j\right) + \sigma^{inc}\left(E,E'\mu_{j-1}\right)}{2} \times \left(\mu_j - \mu_{j-1}\right).\end{aligned} \tag{4.2.32}$$

To calculate the cumulative distribution, FRENDY searches for the *j*-th cosine bin μ_j that satisfies the following equation:

$$\int_{\mu_{j-1}}^{\mu_j} \sigma^{inc}(E,E',\mu)\,\mathrm{d}\mu = \frac{\sigma^{inc}(E,E')}{n_{bin}}, \tag{4.2.33}$$

where n_{bin} is the number of bins. The cumulative $\sigma^{inc}_{PENDF}\left(E,E',\mu_j\right)$ value, which is calculated by the following equation, is written in the PENDF file

$$\sigma_{PENDF}^{inc}(E,E',\mu_j) = \int_1^{\mu_j} \mu \times \sigma^{inc}(E,E',\mu)\,\mathrm{d}\mu$$

$$= \sum_i \frac{1}{3}\left(\sigma^{inc}(E,E',\mu_{i+1}) - \sigma^{inc}(E,E',\mu_i)\right)\left({\mu_{i+1}}^2 + \mu_{i+1}\mu_i + {\mu_i}^2\right) + \frac{1}{2}\left(\mu_{i+1}\sigma^{inc}(E,E',\mu_i) - \mu_i\sigma^{inc}(E,E',\mu_{i+1})\right)(\mu_{i+1} + \mu_i) \tag{4.2.34}$$

$$= \sum_i \int_{\mu_i}^{\mu_{i+1}} \mu(a\mu + b)\,d\mu,$$

where

$$a = \frac{\sigma^{inc}(E,E',\mu_{i+1}) - \sigma^{inc}(E,E',\mu_i)}{\mu_{i+1} - \mu_i}, \tag{4.2.35}$$

$$b = \frac{\mu_i\sigma^{inc}(E,E',\mu_{i+1}) - \mu_{i+1}\sigma^{inc}(E,E',\mu_i)}{\mu_{i+1} - \mu_i}. \tag{4.2.36}$$

5 Probability Table Generation

5.1 Treatment of Self-Shielding Effect in Unresolved Resonance Region

In the unresolved resonance region, each resonance cannot be separated and the evaluated nuclear data file provides mean values of resonance spacing and resonance partial width.[13] The self-shielding effect in the unresolved resonance region also has a large impact on the fast reactor.[46] The probability table method is widely used to appropriately treat the self-shielding effect in the unresolved resonance region for continuous energy Monte Carlo codes.[42,47] In this method, a table provides the probability distribution of the cross-section in a given energy grid point which corresponds to the resonance structure. Consideration of the self-shielding effect in the unresolved resonance region is also used for the multi-group transport calculation. The Bondarenko-style self-shielded cross-section[48] is used to treat this effect and it is generated using the probability table. Though some nuclear data processing codes generate the Bondarenko-style self-shielded cross-section by the deterministic method, *e.g.*, the UNRESR module in NJOY.[7,8] According to the manual of NJOY, the Bondarenko-style self-shielded cross-section generated by the probability table is more appropriate than that by the deterministic method.[42] The self-shielding factor generated by the deterministic method sometimes shows inappropriate values, *e.g.*, negative or larger than 1.0. Therefore, FRENDY uses only the probability method to calculate it.

5.2 Calculation Flow of Probability Table Generation

The evaluated nuclear data file provides only mean values of the resonance parameters in the unresolved resonance region. In the unresolved resonance region, the ladder method[42] is used to generate a lot of pseudo resonance structures using random numbers based on the averaged resonance parameters. A resonance structure generated by random numbers is called a “ladder” and an example is shown in Fig. 5.2.1. The pseudo resonance structure is generated as follows:

(1) Determination of the *i*-th resonance energy $E_{r,i}$ by multiplying the average level spacing $\overline{D}$ by the random number R_W conforming to the Wigner distribution function,
(2) Determination of the resonance width $\Gamma_{r,i}$ by multiplying the average resonance width $\overline{\Gamma_r}$ by the chi-squared random numbers with k degrees of freedom $R_{\chi^2}(k)$,
(3) Determination of the energy grid point E_j at which the cross-section is calculated using the uniform random number R_u,
(4) Calculation of the cross-section $\sigma_{r,j}(E_j, T)$ of the energy grid point E_j at T K with the ψ-χ method[49], and
(5) Calculation of the probability $P_{\mathrm{n}}(T)$ of $\sigma_{n-1} \leq \sigma_{t,j}(E_j, T) < \sigma_n$,

where r is a reaction type, σ_n the upper limit cross-section of the n-th probability bin, and $\sigma_{t,j}(E_j, T)$ the total cross-section of the energy grid point E_j at T K.

To calculate probability table $P_{\mathrm{n}}(T)$, we generate a lot of ladders. The evaluated nuclear data library contains the energy-dependent average resonance parameters. Therefore, the probability table is calculated in each energy point which corresponds to the energy-dependent parameters. Generally, the number of sampling energy grid point E_j is 10,000 and the number of ladders is 20-100. When the number of energy points is 30, the cross-section should be calculated 6-30 million times. Since the number of the energy grid points of the linearized cross-section is less than a few million, the calculation of probability tables in all energy points requires a long calculation time.

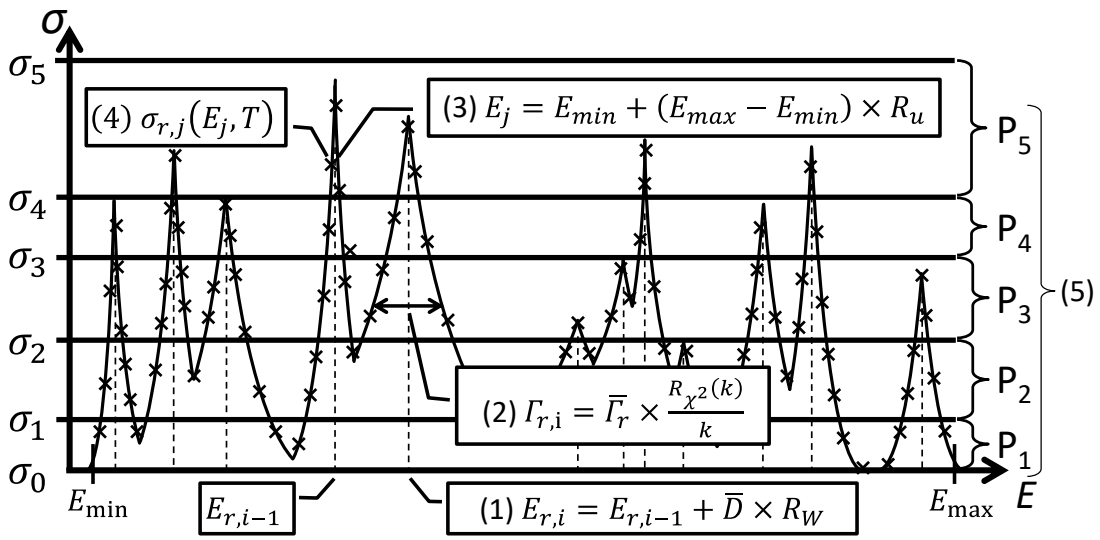

Figure 5.2.1 Example of pseudo resonance structure generation for the ladder method

5.2.1 Determination of Resonance Energy

The average level spacing $\overline{D}$ is the mean value of the distribution of resonance spacing and it obeys the Wigner distribution. The resonance spacing is determined by multiplying the average level spacing $\overline{D}$ by the random number R_W conforming to the Wigner distribution function. R_W is calculated using the inverse transform sampling. The Wigner distribution function $P_w(y)$ is given as follows:

$$P_w(y) = \frac{\pi}{2} y e^{-\frac{\pi}{4}y^2}. \tag{5.2.1}$$

The cumulative distribution function $F_w(\zeta)$ of the Wigner distribution is

$$F_w(\zeta) = \int_0^{\zeta} P_w(y)\,\mathrm{d}y = 1 - e^{-\frac{\pi}{4}\zeta^2}. \tag{5.2.2}$$

The inverse function of $F_w(\zeta)$ is

$$\zeta = \pm\sqrt{\frac{4}{\pi}\ln\left(\frac{1}{1-F_w(\zeta)}\right)}. \tag{5.2.3}$$

Using Eq. (5.2.3), R_W is calculated using the uniform random number R_u as follows:

$$R_W = \frac{2}{\sqrt{\pi}}\sqrt{\ln\left(\frac{1}{1-R_u}\right)} = \frac{2}{\sqrt{\pi}}\sqrt{\ln\left(\frac{1}{R_u}\right)}. \tag{5.2.4}$$

5.2.2 Determination of Resonance Width

The resonance width Γ_r distributes according to the chi-squared distribution with a certain number of degrees of freedom[13]. The resonance width is determined by multiplying the average resonance width $\overline{\Gamma_r}$ by the chi-squared random numbers with k degrees of freedom $R_{\chi^2}(k)$. To calculate $R_{\chi^2}(k)$, the PURR module in NJOY and the U3R code[50] use discrete random numbers. Table 5.2.1 shows the chi-squared random numbers $R_{\chi^2}(k)$ in PURR. For example, if R_u is 0.03 and the number of degrees of freedom is 1, the chi-squared random number is 0.0013100 from Table 5.2.1. The discrete random numbers are inappropriate because the resonance structure depends on the chi-squared random numbers.

To appropriately calculate the chi-squared random numbers, FRENDY uses[51]

$$R_{\chi^2}(k) = \begin{cases} R_\Gamma\left(\frac{k}{2}, 2\right) & (k > 1) \\ (R_u)^2 R_\Gamma\left(\frac{3}{2}, 2\right) & (k = 1) \end{cases}, \tag{5.2.5}$$

where $R_\Gamma(\alpha, \beta)$ is the gamma random number, α a shape parameter, and β a scale parameter. Marsaglina's method[52] is used to calculate the gamma random number.

Table 5.2.1 Chi-squared random numbers $R_{\chi^2}(k)$ in PURR

R_u	$R_{\chi 2}(1)$	$R_{\chi 2}(2)$	$R_{\chi 2}(3)$	$R_{\chi 2}(4)$
0.00~0.05	0.0013100	0.0508548	0.2068320	0.4594620
0.05~0.10	0.0091950	0.1561670	0.4707190	0.8937350
0.10~0.15	0.0250905	0.2673350	0.6919330	1.2175300
0.15~0.20	0.0492540	0.3850500	0.9016740	1.5087200
0.20~0.25	0.0820892	0.5101310	1.1086800	1.7860500
0.25~0.30	0.1241690	0.6435640	1.3176500	2.0585400
0.30~0.35	0.1762680	0.7865430	1.5319300	2.3319400
0.35~0.40	0.2394170	0.9405410	1.7544400	2.6106900
0.40~0.45	0.3149770	1.1074000	1.9881200	2.8987800
0.45~0.50	0.4047490	1.2894700	2.2362100	3.2003200
0.50~0.55	0.5111450	1.4898100	2.5025700	3.5199500
0.55~0.60	0.6374610	1.7124900	2.7921300	3.8633100
0.60~0.65	0.7883150	1.9631400	3.1114300	4.2377600
0.65~0.70	0.9704190	2.2498400	3.4696700	4.6534500
0.70~0.75	1.1940000	2.5847300	3.8805300	5.1253300
0.75~0.80	1.4757300	2.9874400	4.3658600	5.6771200
0.80~0.85	1.8454700	3.4927800	4.9641700	6.3504400
0.85~0.90	2.3652200	4.1723800	5.7542300	7.2299600
0.90~0.95	3.2037100	5.2188800	6.9464600	8.5410000
0.95~1.00	5.5820100	7.9914600	10.0048000	11.8359000

5.2.3 Determination of Energy Grid Points

To calculate the probability $P_n(T)$ of $\sigma_{n-1} \leq \sigma_r(E,T) \leq \sigma_n$, FRENDY sets 10,000 energy grid points in each ladder and calculates only the Doppler broadened cross-section on these energy grid points. The energy grid point is determined by the uniform random number R_u as follows:

$$E_j = E_{min} + (E_{max} - E_{min}) \times R_u, \tag{5.2.6}$$

where E_j is j-th energy grid point, E_{min} the lower energy limit of a resonance range in the unresolved resonance region, and E_{max} the upper energy limit of the resonance range in the unresolved resonance region.

5.2.4 Calculation of Cross-Sections

In general, the kernel broadening method,[37] which is adopted in Doppler broadening of FRENDY, the BROADR module in NJOY, and SIGMA1 module in PREPRO,[9] is used to more accurately calculate the Doppler broadened cross-sections in the resolved resonance region than the other calculation methods. This method requires a long calculation time to calculate the Doppler broadened cross-sections. The ladder method generates a lot of resonance structures and calculates the Doppler broadened cross-sections. Thus, the kernel broadening method for the ladder method is not accepted in the unresolved resonance region from the viewpoint of calculation time.

In the ENDF-6 format, only the Single-Level Breit-Wigner (SLBW) representation is available for the unresolved resonance region.[13] The SLBW approximation allows the use of the ψ-χ method[49] which approximately calculates the Doppler broadened cross-sections in short calculation time.

In the ψ-χ method, the cross-sections at T K are calculated as follows:[42]

$$\sigma_\gamma(E,T) \cong \frac{\sigma_1 \Gamma_{\gamma r}}{\Gamma_r}\psi(\zeta,x), \tag{5.2.7}$$

$$\sigma_f(E,T) \cong \frac{\sigma_1 \Gamma_{fr}}{\Gamma_r}\psi(\zeta,x), \tag{5.2.8}$$

$$\sigma_s(E,T) = \sigma_1\left(\psi(\zeta,x)\left(\cos 2\phi_l - 1 + \frac{\Gamma_{nr}}{\Gamma_r}\right) + \chi(\zeta,x)\sin 2\phi_l\right) + \sigma_p, \tag{5.2.9}$$

where

$$\sigma_1 = \frac{4\pi}{k_r{}^2} g_J \frac{\Gamma_{nr}}{\Gamma_r}, \tag{5.2.10}$$

$$\psi(\zeta,x) = \frac{\zeta}{2\sqrt{\pi}}\int_{-\infty}^{\infty} \frac{1}{1+y^2} e^{-\frac{\zeta^2}{4}(x-y)^2}\,\mathrm{d}y, \tag{5.2.11}$$

$$\chi(\zeta,x) = \frac{\zeta}{2\sqrt{\pi}}\int_{-\infty}^{\infty} \frac{y}{1+y^2} e^{-\frac{\zeta^2}{4}(x-y)^2}\,\mathrm{d}y, \tag{5.2.12}$$

$$x = \frac{2}{\Gamma_r}(E - E_1), \tag{5.2.13}$$

$$y = \frac{2}{\Gamma_r}(E_r - E_1), \tag{5.2.14}$$

$$\zeta = \frac{\Gamma_r}{\sqrt{4Ek_BT\dfrac{m}{M}}}, \tag{5.2.15}$$

$$E_1 = E_r + \frac{S_l(|E_r|) - S_l(E)}{2\big(P_l(|E_r|)\big)}\frac{P_l(E)}{P_l(|E_r|)}\Gamma_{nr}, \tag{5.2.16}$$

σ_γ the radiative capture cross-section, σ_f the fission cross-section, σ_s the elastic scattering cross-section, σ_p the potential scattering cross-section, Γ_r the total width, $\Gamma_{\gamma r}$ the radiative

capture width, Γ_{fr} the fission width, Γ_{nr} the neutron widths, k_r a wave number, g_J a spin statistical factor, E an incident neutron energy, E_r a relative kinetic energy, ϕ_l a hard sphere phase shift, S_l a shift factor, P_l a penetration factor, m the mass of the neutron, M the mass of target nucleus, and k_B the Boltzmann constant.

Equations (5.2.11) and (5.2.12) are rewritten as

$$\begin{aligned}\psi(s,x) &= \frac{1}{\sqrt{\pi}}\int_{-\infty}^{\infty}\frac{1}{1+\left(x-\frac{2}{\zeta}s\right)^2}e^{-s^2}\,\mathrm{d}s \\ &= \frac{\zeta}{2\sqrt{\pi}}\int_{-\infty}^{\infty}\frac{\frac{\zeta}{2}}{s^2-\zeta s x+\frac{\zeta^2}{4}x^2+\frac{\zeta^2}{4}}e^{-s^2}\,\mathrm{d}s,\end{aligned} \tag{5.2.17}$$

$$\begin{aligned}\chi(s,x) &= \frac{1}{\sqrt{\pi}}\int_{-\infty}^{\infty}\frac{x-\frac{2}{\zeta}s}{1+\left(x-\frac{2}{\zeta}s\right)^2}e^{-s^2}\,\mathrm{d}s \\ &= \frac{\zeta}{2\sqrt{\pi}}\int_{-\infty}^{\infty}\frac{\frac{\zeta}{2}x-s}{s^2-\zeta s x+\frac{\zeta^2}{4}x^2+\frac{\zeta^2}{4}}e^{-s^2}\,\mathrm{d}s,\end{aligned} \tag{5.2.18}$$

where

$$s = \frac{\zeta}{2}(x-y), \tag{5.2.19}$$

$$y = x-\frac{2}{\zeta}s, \tag{5.2.20}$$

$$\frac{\mathrm{d}y}{\mathrm{d}s} = -\frac{2}{\zeta}. \tag{5.2.21}$$

We re-introduce the complex error function $w(z)$ mentioned in Eq. (2.3.41) as follows:

$$w(z) = e^{-z^2}\mathrm{erfc}(-iz) = e^{-z^2}\left(1-\mathrm{erf}(-iz)\right) = \frac{i}{\pi}\int_{-\infty}^{\infty}\frac{e^{-s^2}}{z-s}\mathrm{d}s. \tag{5.2.22}$$

Here $\mathrm{erfc}(\alpha)$ is the complementary error function of complex argument α, $\mathrm{erf}(\alpha)$ the error function of complex argument α, and

$$z = (x+i)\frac{\zeta}{2} = u+ih, \tag{5.2.23}$$

where

$$u = \frac{\zeta}{2}x, \tag{5.2.24}$$

$$h = \frac{\zeta}{2}. \tag{5.2.25}$$

Substituting Eq. (5.2.23) into Eq. (5.2.22), the latter equation is rearranged as

$$\begin{aligned} w(z) &= \frac{i}{\pi}\int_{-\infty}^{\infty}\frac{1}{s-(x+i)\frac{\zeta}{2}}e^{-s^2}\,\mathrm{d}s \\ &= \frac{i}{\pi}\int_{-\infty}^{\infty}\left(s-\frac{\zeta}{2}x+i\frac{\zeta}{2}\right)\frac{1}{s^2-\zeta sx+\frac{\zeta^2}{4}x^2+\frac{\zeta^2}{4}}e^{-s^2}\,\mathrm{d}s. \end{aligned} \tag{5.2.26}$$

From the above equation, we obtain

$$\mathrm{Re}[w(z)] = \frac{1}{\pi}\int_{-\infty}^{\infty}\frac{\frac{\zeta}{2}}{s^2-\zeta sx+\frac{\zeta^2}{4}x^2+\frac{\zeta^2}{4}}e^{-s^2}\,\mathrm{d}s, \tag{5.2.27}$$

and

$$\mathrm{Im}[w(z)] = \frac{1}{\pi}\int_{-\infty}^{\infty}\frac{\frac{\zeta}{2}x-s}{s^2-\zeta sx+\frac{\zeta^2}{4}x^2+\frac{\zeta^2}{4}}e^{-s^2}\,\mathrm{d}s. \tag{5.2.28}$$

Using Eqs. (5.2.27) and (5.2.28), Eqs. (5.2.17) and (5.2.18) are expressed as

$$\psi(s,x) = \frac{\zeta\sqrt{\pi}}{2}\mathrm{Re}[w(z)], \tag{5.2.29}$$

$$\chi(s,x) = \frac{\zeta\sqrt{\pi}}{2}\mathrm{Im}[w(z)]. \tag{5.2.30}$$

As shown in Eqs. (5.2.29) and (5.2.30), $\psi(s,x)$ and $\chi(s,x)$ are calculated using the real and imaginary parts of the complex error function $w(z)$.

To estimate the complex error function, some calculation methods are proposed.[53,54] We adopted the 4-pole Padé approximation[55-57] to reduce the calculation time while keeping enough accuracy. This is one of the most efficient methods to reduce the calculation time with the ψ-χ method.

The complex error function using the 4-pole Padé approximation is written as

$$\begin{aligned} w(u+ih) &\approx \frac{i}{\sqrt{\pi}}\frac{p_0+p_1(u+ih)+p_2(u+ih)^2+p_3(u+ih)^3}{1+q_1(u+ih)+q_2(u+ih)^2+q_3(u+ih)^3+q_4(u+ih)^4} \\ &= \frac{i}{\sqrt{\pi}}\frac{A_1u+A_2u^3+i(A_3+A_4u^2)}{B_1+B_2u^2+B_3u^4+i(B_4u+B_5u^3)}, \end{aligned} \tag{5.2.31}$$

where

$$A_1 = p_1-2p_2h-3p_3h^2, \tag{5.2.32}$$

$$A_2 = p_3, \tag{5.2.33}$$

$$A_3 = p_0+p_1h-p_2h^2-p_3h^3, \tag{5.2.34}$$

$$A_4 = p_2+3p_3h, \tag{5.2.35}$$

$$B_1 = 1-q_1h-q_2h^2+q_3h^3+q_4h^4, \tag{5.2.36}$$

$$B_2 = q_2-3q_3h-6q_4h^2, \tag{5.2.37}$$

$$B_3 = q_4, \tag{5.2.38}$$

$$B_4 = q_1 + 2q_2h - 3q_3h^2 - 4q_4h^3, \tag{5.2.39}$$

$$B_5 = q_3 + 4q_4h, \tag{5.2.40}$$

$$p_0 = i\sqrt{\pi}, \tag{5.2.41}$$

$$p_1 = \frac{-15\pi^2 + 88\pi - 128}{2(6\pi^2 - 29\pi + 32)}, \tag{5.2.42}$$

$$p_2 = -i\frac{-33\pi + 104}{6(6\pi^2 - 29\pi + 32)}\sqrt{\pi}, \tag{5.2.43}$$

$$p_3 = -\frac{9\pi^2 - 69\pi + 128}{3(6\pi^2 - 29\pi + 32)}, \tag{5.2.44}$$

$$q_1 = -i\frac{9\pi - 28}{2(6\pi^2 - 29\pi + 32)}\sqrt{\pi}, \tag{5.2.45}$$

$$q_2 = -\frac{-36\pi^2 + 195\pi - 256}{6(6\pi^2 - 29\pi + 32)}, \tag{5.2.46}$$

$$q_3 = i\frac{-33\pi + 104}{6(6\pi^2 - 29\pi + 32)}\sqrt{\pi}, \tag{5.2.47}$$

$$q_4 = \frac{9\pi^2 - 69\pi + 128}{3(6\pi^2 - 29\pi + 32)}. \tag{5.2.48}$$

5.2.5 Calculation of Probability

To calculate the probability of the *n*-th bin $P_n(T)$, we count the number of energy grid points that the total cross-section $\sigma_{t,j}(E_j, T)$ satisfies the following equation

$$\sigma_{n-1} \le \sigma_{t,j}(E_j, T) \le \sigma_n. \tag{5.2.49}$$

The PENDF file contains $P_n(T)$, average cross-section $\bar{\sigma}_r(T)$, and cross-section of the *n*-th bin $\sigma_{r,n}(T)$. $\bar{\sigma}_r(T)$ and $\sigma_{r,n}(T)$ are obtained by

$$\bar{\sigma}_r(T) = \frac{\sum_j \sigma_{r,j}(E_j, T)}{N_{ladder} \times N_{sample}}, \tag{5.2.50}$$

$$\sigma_{r,n}(T) = \frac{\bar{\sigma}_{r,n}(T)}{\bar{\sigma}_r(T)}, \tag{5.2.51}$$

where, $\bar{\sigma}_{x,n}$ is an average cross-section of $\sigma_{n-1} \le \sigma_{t,j}(E_j, T) < \sigma_n$, N_{ladder} the number of ladders, and N_{sample} the number of sampling energy grid points.

The Bondarenko-style self-shielded cross-section $\sigma_{b,r}(T)$ is also calculated using $\sigma_{r,n}(T)$ and $\bar{\sigma}_{t,n}(T)$ as follows:

$$\sigma_{b,r}(T) = \frac{\sum_n \frac{\sigma_0 \bar{\sigma}_{r,n}(T)}{\sigma_0 + \bar{\sigma}_{t,n}(T)}}{\sum_n \frac{\sigma_0}{\sigma_0 + \bar{\sigma}_{t,n}(T)}}, \tag{5.2.52}$$

where r is the reaction type, *i.e.*, the total, elastic scattering, fission, and radiative capture.

5.3 Investigation of Appropriate Number of Ladders

The ladder method generates a lot of pseudo resonance structures to produce a probability table. Investigation of the appropriate number of ladders, *i.e.*, the number of pseudo resonance structures, is important to reduce nuclear data processing time while keeping the accuracy of neutronics calculations.[57)]

To determine the appropriate number of ladders, we address major heavy nuclides, *i.e.*, ^{232}Th, ^{233}U, ^{234}U, ^{235}U, ^{238}U, ^{237}Np, ^{238}Pu, ^{239}Pu, ^{240}Pu, ^{241}Pu, ^{242}Pu, ^{241}Am, and ^{242}Cm, from JENDL-4.0[1)] as target nuclides. The number of probability bins is 20 and the number of ladders is 10, 50, 100, 200, 300, and 500. The number of ladders for the reference case is 1,000. The calculation time of ^{235}U and ^{238}U are 10 hours and 4 hours, respectively, using Intel Core i7-3960X processor (3.30 GHz) without parallel computation when the number of ladders is 1,000. From the viewpoint of calculation time, the larger number of ladders is not acceptable.

As described in Section 5.2, the probability table is calculated in each energy point which corresponds to the energy-dependent average resonance parameter. In this study, we compared the RMS value of all energy points and probability bins. The RMS value $RMS_{l,r}(T)$ is calculated as follows:

$$RMS_{l,r}(T) = \sqrt{\frac{\sum_g^G \sum_n^B \left\{P_{l_{ref},g,n}(T) \times \sigma_{l_{ref},r,g,n}(T) - P_{l,g,n}(T) \times \sigma_{l,r,g,n}(T)\right\}^2}{G \times B}}, \qquad (5.3.1)$$

where l is an index of the ladder number, x a reaction type, G the number of energy points, B the number of probability bin, and l_{ref} a reference number of ladders. Tables 5.3.1 - 5.3.3 show the RMS value of each ladder number. As shown in Tables 5.3.1 - 5.3.3, the RMS values are enough small when the number of ladders is 100. The generation time of the probability table for each nuclide (number of ladders: 100, number of temperatures: 1) was usually 1 to 2 hours. This generation time is acceptable from the viewpoint of the current computational performance.

Table 5.3.1 RMS value of probability table difference in each number of ladders (293.6 K) (1/3)

Nuclide	Ladder No.	Total	Scatter	Fission	Radiation
^{232}Th	10	0.20%	0.20%	0.18%	0.22%
	20	0.15%	0.15%	0.14%	0.16%
	30	0.12%	0.12%	0.11%	0.12%
	50	0.08%	0.08%	0.08%	0.09%
	100	0.06%	0.06%	0.06%	0.07%
	200	0.05%	0.05%	0.04%	0.05%
	300	0.04%	0.04%	0.03%	0.04%
	500	0.03%	0.03%	0.03%	0.03%
^{233}U	10	0.31%	0.31%	0.33%	0.35%
	20	0.24%	0.23%	0.26%	0.27%
	30	0.18%	0.18%	0.20%	0.22%
	50	0.16%	0.16%	0.17%	0.19%
	100	0.11%	0.10%	0.12%	0.12%
	200	0.08%	0.08%	0.08%	0.09%
	300	0.06%	0.06%	0.06%	0.07%
	500	0.05%	0.05%	0.05%	0.05%
^{234}U	10	0.23%	0.23%	0.33%	0.26%
	20	0.15%	0.15%	0.23%	0.17%
	30	0.14%	0.14%	0.21%	0.16%
	50	0.09%	0.09%	0.13%	0.11%
	100	0.07%	0.07%	0.09%	0.08%
	200	0.05%	0.05%	0.06%	0.05%
	300	0.04%	0.04%	0.05%	0.05%
	500	0.03%	0.03%	0.05%	0.04%
^{235}U	10	0.31%	0.30%	0.33%	0.34%
	20	0.23%	0.22%	0.24%	0.25%
	30	0.18%	0.18%	0.19%	0.20%
	50	0.14%	0.13%	0.15%	0.15%
	100	0.10%	0.10%	0.11%	0.11%
	200	0.07%	0.07%	0.08%	0.08%
	300	0.06%	0.06%	0.07%	0.07%
	500	0.05%	0.05%	0.05%	0.05%
^{236}U	10	0.22%	0.22%	0.20%	0.23%
	20	0.14%	0.14%	0.13%	0.15%
	30	0.11%	0.12%	0.11%	0.12%
	50	0.09%	0.09%	0.08%	0.09%
	100	0.07%	0.07%	0.06%	0.08%
	200	0.05%	0.05%	0.05%	0.05%
	300	0.04%	0.04%	0.04%	0.04%
	500	0.03%	0.03%	0.03%	0.03%

Table 5.3.1 RMS value of probability table difference in each number of ladders (293.6 K) (2/3)

Nuclide	Ladder No.	Total	Scatter	Fission	Radiation
^{238}U	10	0.23%	0.23%	0.22%	0.23%
	20	0.15%	0.15%	0.15%	0.17%
	30	0.12%	0.12%	0.12%	0.13%
	50	0.10%	0.10%	0.10%	0.11%
	100	0.08%	0.08%	0.07%	0.08%
	200	0.06%	0.06%	0.06%	0.06%
	300	0.04%	0.04%	0.04%	0.05%
	500	0.03%	0.03%	0.03%	0.03%
^{237}Np	10	0.31%	0.30%	0.36%	0.32%
	20	0.22%	0.22%	0.25%	0.24%
	30	0.18%	0.18%	0.20%	0.19%
	50	0.15%	0.14%	0.17%	0.15%
	100	0.11%	0.11%	0.11%	0.11%
	200	0.07%	0.07%	0.08%	0.07%
	300	0.07%	0.07%	0.07%	0.07%
	500	0.05%	0.05%	0.05%	0.05%
^{238}Pu	10	0.24%	0.24%	0.34%	0.27%
	20	0.16%	0.16%	0.25%	0.18%
	30	0.13%	0.13%	0.20%	0.15%
	50	0.11%	0.11%	0.16%	0.12%
	100	0.09%	0.09%	0.12%	0.10%
	200	0.05%	0.05%	0.07%	0.06%
	300	0.04%	0.05%	0.06%	0.05%
	500	0.04%	0.04%	0.05%	0.04%
^{239}Pu	10	0.26%	0.26%	0.30%	0.30%
	20	0.19%	0.18%	0.22%	0.22%
	30	0.14%	0.14%	0.16%	0.16%
	50	0.12%	0.12%	0.15%	0.14%
	100	0.08%	0.08%	0.09%	0.10%
	200	0.06%	0.06%	0.06%	0.07%
	300	0.05%	0.05%	0.05%	0.06%
	500	0.04%	0.04%	0.05%	0.05%
^{240}Pu	10	0.23%	0.23%	0.28%	0.24%
	20	0.16%	0.16%	0.22%	0.18%
	30	0.12%	0.12%	0.18%	0.14%
	50	0.10%	0.10%	0.13%	0.11%
	100	0.06%	0.06%	0.08%	0.07%
	200	0.05%	0.05%	0.06%	0.05%
	300	0.04%	0.04%	0.05%	0.04%
	500	0.03%	0.03%	0.04%	0.04%

Table 5.3.1 RMS value of probability table difference in each number of ladders (293.6 K) (3/3)

Nuclide	Ladder No.	Total	Scatter	Fission	Radiation
^{241}Pu	10	0.19%	0.18%	0.23%	0.24%
	20	0.14%	0.13%	0.16%	0.17%
	30	0.11%	0.10%	0.12%	0.13%
	50	0.09%	0.08%	0.10%	0.11%
	100	0.06%	0.06%	0.07%	0.08%
	200	0.05%	0.05%	0.05%	0.06%
	300	0.04%	0.04%	0.04%	0.05%
	500	0.03%	0.03%	0.04%	0.04%
^{242}Pu	10	0.21%	0.21%	0.33%	0.23%
	20	0.14%	0.14%	0.22%	0.15%
	30	0.12%	0.12%	0.19%	0.13%
	50	0.09%	0.09%	0.14%	0.11%
	100	0.06%	0.06%	0.10%	0.07%
	200	0.05%	0.05%	0.07%	0.05%
	300	0.04%	0.04%	0.05%	0.04%
	500	0.03%	0.03%	0.05%	0.04%
^{241}Am	10	0.30%	0.29%	0.36%	0.31%
	20	0.22%	0.21%	0.26%	0.23%
	30	0.17%	0.16%	0.20%	0.18%
	50	0.14%	0.14%	0.17%	0.15%
	100	0.10%	0.10%	0.11%	0.10%
	200	0.07%	0.07%	0.08%	0.08%
	300	0.06%	0.06%	0.07%	0.07%
	500	0.04%	0.04%	0.05%	0.05%
^{242}Cm	10	0.25%	0.25%	0.39%	0.28%
	20	0.19%	0.18%	0.28%	0.21%
	30	0.14%	0.14%	0.20%	0.16%
	50	0.11%	0.10%	0.17%	0.13%
	100	0.08%	0.08%	0.12%	0.09%
	200	0.06%	0.06%	0.07%	0.06%
	300	0.05%	0.05%	0.07%	0.05%
	500	0.04%	0.04%	0.05%	0.04%

Table 5.3.2 RMS value of probability table difference in each number of ladders (1000 K) (1/3)

Nuclide	Ladder No.	Total	Scatter	Fission	Radiation
^{232}Th	10	0.25%	0.25%	0.23%	0.26%
	20	0.15%	0.15%	0.14%	0.16%
	30	0.14%	0.14%	0.13%	0.15%
	50	0.10%	0.10%	0.10%	0.11%
	100	0.08%	0.08%	0.08%	0.08%
	200	0.06%	0.06%	0.05%	0.06%
	300	0.04%	0.04%	0.04%	0.05%
	500	0.03%	0.03%	0.03%	0.04%
^{233}U	10	0.41%	0.40%	0.42%	0.44%
	20	0.31%	0.31%	0.33%	0.34%
	30	0.23%	0.23%	0.25%	0.25%
	50	0.19%	0.19%	0.21%	0.22%
	100	0.14%	0.14%	0.15%	0.16%
	200	0.09%	0.09%	0.10%	0.11%
	300	0.08%	0.08%	0.09%	0.09%
	500	0.06%	0.06%	0.07%	0.07%
^{234}U	10	0.27%	0.27%	0.34%	0.28%
	20	0.18%	0.18%	0.24%	0.19%
	30	0.16%	0.16%	0.21%	0.18%
	50	0.11%	0.11%	0.15%	0.12%
	100	0.08%	0.08%	0.10%	0.09%
	200	0.05%	0.05%	0.06%	0.06%
	300	0.05%	0.05%	0.06%	0.05%
	500	0.04%	0.04%	0.05%	0.04%
^{235}U	10	0.42%	0.42%	0.44%	0.45%
	20	0.30%	0.30%	0.31%	0.32%
	30	0.25%	0.25%	0.27%	0.27%
	50	0.18%	0.18%	0.19%	0.19%
	100	0.13%	0.13%	0.14%	0.13%
	200	0.09%	0.09%	0.10%	0.09%
	300	0.08%	0.08%	0.08%	0.08%
	500	0.07%	0.06%	0.07%	0.07%
^{236}U	10	0.28%	0.28%	0.26%	0.30%
	20	0.17%	0.17%	0.16%	0.18%
	30	0.14%	0.14%	0.13%	0.14%
	50	0.10%	0.10%	0.10%	0.11%
	100	0.09%	0.09%	0.08%	0.09%
	200	0.06%	0.06%	0.06%	0.06%
	300	0.05%	0.05%	0.05%	0.05%
	500	0.04%	0.04%	0.03%	0.04%

Table 5.3.2 RMS value of probability table difference in each number of ladders (1000 K) (2/3)

Nuclide	Ladder No.	Total	Scatter	Fission	Radiation
^{238}U	10	0.28%	0.28%	0.27%	0.29%
	20	0.20%	0.20%	0.19%	0.20%
	30	0.15%	0.15%	0.15%	0.16%
	50	0.13%	0.13%	0.13%	0.14%
	100	0.09%	0.09%	0.09%	0.09%
	200	0.07%	0.07%	0.07%	0.07%
	300	0.05%	0.05%	0.05%	0.06%
	500	0.04%	0.04%	0.04%	0.04%
^{237}Np	10	0.40%	0.40%	0.43%	0.41%
	20	0.32%	0.32%	0.34%	0.33%
	30	0.25%	0.25%	0.26%	0.26%
	50	0.19%	0.18%	0.20%	0.19%
	100	0.14%	0.14%	0.14%	0.14%
	200	0.10%	0.10%	0.10%	0.10%
	300	0.08%	0.08%	0.09%	0.09%
	500	0.07%	0.07%	0.07%	0.07%
^{238}Pu	10	0.29%	0.29%	0.36%	0.31%
	20	0.19%	0.19%	0.26%	0.21%
	30	0.14%	0.14%	0.19%	0.16%
	50	0.13%	0.13%	0.16%	0.14%
	100	0.09%	0.09%	0.11%	0.10%
	200	0.06%	0.06%	0.07%	0.06%
	300	0.05%	0.05%	0.06%	0.05%
	500	0.04%	0.04%	0.05%	0.04%
^{239}Pu	10	0.32%	0.31%	0.36%	0.35%
	20	0.24%	0.24%	0.26%	0.27%
	30	0.19%	0.19%	0.20%	0.20%
	50	0.15%	0.15%	0.17%	0.16%
	100	0.10%	0.10%	0.11%	0.11%
	200	0.08%	0.07%	0.08%	0.08%
	300	0.06%	0.06%	0.07%	0.07%
	500	0.05%	0.05%	0.06%	0.06%
^{240}Pu	10	0.27%	0.27%	0.32%	0.27%
	20	0.18%	0.18%	0.23%	0.19%
	30	0.15%	0.15%	0.18%	0.16%
	50	0.12%	0.12%	0.14%	0.12%
	100	0.07%	0.07%	0.09%	0.08%
	200	0.06%	0.06%	0.07%	0.06%
	300	0.05%	0.05%	0.06%	0.05%
	500	0.04%	0.04%	0.05%	0.04%

Table 5.3.2 RMS value of probability table difference in each number of ladders (1000 K) (3/3)

Nuclide	Ladder No.	Total	Scatter	Fission	Radiation
^{241}Pu	10	0.22%	0.21%	0.25%	0.24%
	20	0.16%	0.15%	0.18%	0.18%
	30	0.13%	0.13%	0.14%	0.14%
	50	0.11%	0.11%	0.12%	0.13%
	100	0.07%	0.07%	0.08%	0.08%
	200	0.06%	0.06%	0.06%	0.06%
	300	0.05%	0.04%	0.05%	0.05%
	500	0.04%	0.04%	0.04%	0.04%
^{242}Pu	10	0.26%	0.26%	0.33%	0.26%
	20	0.17%	0.17%	0.24%	0.19%
	30	0.13%	0.13%	0.17%	0.15%
	50	0.10%	0.10%	0.14%	0.12%
	100	0.08%	0.08%	0.09%	0.09%
	200	0.05%	0.05%	0.07%	0.06%
	300	0.04%	0.04%	0.06%	0.05%
	500	0.04%	0.04%	0.05%	0.04%
^{241}Am	10	0.43%	0.42%	0.46%	0.43%
	20	0.29%	0.29%	0.32%	0.30%
	30	0.24%	0.24%	0.26%	0.24%
	50	0.18%	0.18%	0.21%	0.19%
	100	0.13%	0.13%	0.14%	0.13%
	200	0.10%	0.09%	0.10%	0.10%
	300	0.08%	0.08%	0.09%	0.08%
	500	0.07%	0.07%	0.07%	0.07%
^{242}Cm	10	0.30%	0.30%	0.40%	0.32%
	20	0.22%	0.21%	0.30%	0.24%
	30	0.17%	0.17%	0.23%	0.19%
	50	0.13%	0.12%	0.16%	0.14%
	100	0.09%	0.09%	0.12%	0.10%
	200	0.06%	0.06%	0.08%	0.07%
	300	0.06%	0.06%	0.07%	0.06%
	500	0.05%	0.04%	0.06%	0.05%

Table 5.3.3 RMS value of probability table difference in each number of ladders (2000 K) (1/3)

Nuclide	Ladder No.	Total	Scatter	Fission	Radiation
^{232}Th	10	0.28%	0.28%	0.26%	0.30%
	20	0.17%	0.18%	0.16%	0.18%
	30	0.16%	0.16%	0.15%	0.16%
	50	0.11%	0.11%	0.10%	0.11%
	100	0.09%	0.09%	0.09%	0.09%
	200	0.06%	0.06%	0.06%	0.07%
	300	0.05%	0.05%	0.05%	0.05%
	500	0.04%	0.04%	0.04%	0.04%
^{233}U	10	0.45%	0.44%	0.46%	0.48%
	20	0.36%	0.36%	0.37%	0.38%
	30	0.28%	0.28%	0.28%	0.29%
	50	0.23%	0.23%	0.24%	0.25%
	100	0.17%	0.16%	0.17%	0.18%
	200	0.11%	0.11%	0.11%	0.12%
	300	0.10%	0.09%	0.10%	0.10%
	500	0.08%	0.08%	0.08%	0.08%
^{234}U	10	0.32%	0.32%	0.37%	0.33%
	20	0.22%	0.22%	0.28%	0.23%
	30	0.17%	0.17%	0.22%	0.18%
	50	0.12%	0.12%	0.15%	0.13%
	100	0.09%	0.09%	0.10%	0.09%
	200	0.07%	0.07%	0.08%	0.07%
	300	0.05%	0.05%	0.06%	0.06%
	500	0.04%	0.04%	0.05%	0.05%
^{235}U	10	0.48%	0.48%	0.49%	0.51%
	20	0.36%	0.36%	0.37%	0.37%
	30	0.30%	0.30%	0.31%	0.31%
	50	0.24%	0.24%	0.24%	0.25%
	100	0.15%	0.15%	0.16%	0.16%
	200	0.12%	0.12%	0.12%	0.11%
	300	0.09%	0.09%	0.09%	0.10%
	500	0.08%	0.08%	0.08%	0.08%
^{236}U	10	0.32%	0.32%	0.31%	0.33%
	20	0.20%	0.20%	0.19%	0.21%
	30	0.16%	0.16%	0.15%	0.16%
	50	0.13%	0.13%	0.12%	0.13%
	100	0.10%	0.10%	0.10%	0.10%
	200	0.07%	0.07%	0.07%	0.07%
	300	0.06%	0.06%	0.05%	0.06%
	500	0.04%	0.04%	0.04%	0.04%

Table 5.3.3 RMS value of probability table difference in each number of ladders (2000 K) (2/3)

Nuclide	Ladder No.	Total	Scatter	Fission	Radiation
^{238}U	10	0.31%	0.31%	0.30%	0.32%
	20	0.22%	0.22%	0.22%	0.23%
	30	0.17%	0.17%	0.17%	0.18%
	50	0.15%	0.15%	0.15%	0.16%
	100	0.10%	0.10%	0.10%	0.10%
	200	0.09%	0.09%	0.08%	0.09%
	300	0.06%	0.06%	0.06%	0.06%
	500	0.05%	0.05%	0.05%	0.05%
^{237}Np	10	0.48%	0.48%	0.51%	0.49%
	20	0.38%	0.38%	0.40%	0.39%
	30	0.29%	0.29%	0.30%	0.29%
	50	0.23%	0.23%	0.24%	0.23%
	100	0.15%	0.15%	0.15%	0.15%
	200	0.12%	0.12%	0.13%	0.12%
	300	0.10%	0.10%	0.11%	0.10%
	500	0.08%	0.08%	0.08%	0.08%
^{238}Pu	10	0.32%	0.32%	0.38%	0.34%
	20	0.22%	0.22%	0.28%	0.23%
	30	0.15%	0.15%	0.20%	0.17%
	50	0.13%	0.13%	0.16%	0.14%
	100	0.10%	0.10%	0.12%	0.11%
	200	0.06%	0.06%	0.07%	0.07%
	300	0.06%	0.06%	0.06%	0.06%
	500	0.04%	0.04%	0.05%	0.05%
^{239}Pu	10	0.36%	0.36%	0.39%	0.39%
	20	0.27%	0.27%	0.30%	0.29%
	30	0.20%	0.20%	0.22%	0.22%
	50	0.18%	0.17%	0.20%	0.19%
	100	0.13%	0.13%	0.13%	0.14%
	200	0.08%	0.08%	0.09%	0.09%
	300	0.08%	0.08%	0.08%	0.08%
	500	0.06%	0.06%	0.07%	0.07%
^{240}Pu	10	0.31%	0.31%	0.35%	0.31%
	20	0.21%	0.21%	0.25%	0.22%
	30	0.17%	0.18%	0.20%	0.18%
	50	0.13%	0.13%	0.15%	0.13%
	100	0.08%	0.08%	0.09%	0.08%
	200	0.06%	0.06%	0.07%	0.07%
	300	0.06%	0.06%	0.06%	0.06%
	500	0.05%	0.05%	0.05%	0.05%

Table 5.3.3 RMS value of probability table difference in each number of ladders (2000 K) (3/3)

Nuclide	Ladder No.	Total	Scatter	Fission	Radiation
^{241}Pu	10	0.25%	0.25%	0.28%	0.27%
	20	0.18%	0.17%	0.20%	0.19%
	30	0.15%	0.14%	0.16%	0.16%
	50	0.12%	0.12%	0.13%	0.14%
	100	0.08%	0.08%	0.09%	0.09%
	200	0.06%	0.06%	0.06%	0.07%
	300	0.05%	0.05%	0.06%	0.06%
	500	0.04%	0.04%	0.04%	0.04%
^{242}Pu	10	0.29%	0.30%	0.35%	0.29%
	20	0.20%	0.20%	0.25%	0.21%
	30	0.15%	0.15%	0.20%	0.16%
	50	0.11%	0.11%	0.14%	0.12%
	100	0.09%	0.09%	0.11%	0.10%
	200	0.06%	0.06%	0.07%	0.06%
	300	0.05%	0.05%	0.06%	0.05%
	500	0.04%	0.04%	0.05%	0.04%
^{241}Am	10	0.50%	0.49%	0.52%	0.50%
	20	0.37%	0.36%	0.39%	0.37%
	30	0.29%	0.29%	0.31%	0.30%
	50	0.21%	0.21%	0.23%	0.22%
	100	0.16%	0.16%	0.17%	0.17%
	200	0.11%	0.11%	0.11%	0.11%
	300	0.10%	0.10%	0.10%	0.10%
	500	0.08%	0.08%	0.09%	0.08%
^{242}Cm	10	0.34%	0.34%	0.44%	0.36%
	20	0.25%	0.25%	0.32%	0.26%
	30	0.19%	0.19%	0.24%	0.21%
	50	0.15%	0.14%	0.18%	0.15%
	100	0.11%	0.11%	0.13%	0.11%
	200	0.07%	0.07%	0.08%	0.07%
	300	0.06%	0.06%	0.08%	0.06%
	500	0.05%	0.05%	0.06%	0.05%

5.4 Uncertainty Quantification for Probability Table

As described in Section 5.3, the optimal number of ladders depends on the resonance parameters. FRENDY version 1 requires the number of ladders as an input parameter to generate the probability table. The generation time of the probability table will be reduced if we can set the optimal number of ladders. FRENDY version 2 prepares the uncertainty quantification function for the probability table. FRENDY version 2 allows setting the tolerance of the probability table as an input parameter. Users can generate the probability table with the optimal number of ladders when they set this input parameter.

The probability table is used for the consideration of the self-shielding effect in the unresolved resonance region. The probability bin which has the larger cross-section is more important since the large cross-section, *i.e.*, the resonance peak, has a large impact on the self-shielding effect. FRENDY version 2 considers the product of the probability table $P(T)$ and the total cross-section $\bar{\sigma}_t(T)$ as the target of the statistical uncertainty of the probability table to consider the difference of the cross-section at each probability bin. Note that this method calculates the statistical uncertainty for each probability bin.

When the number of ladders is i, i numbers are given, *i.e.*, $P_{0,j}(T)\bar{\sigma}_{t,0,j}(T)$, $P_{1,j}(T)\bar{\sigma}_{t,i,j}(T)$, $P_{2,j}(T)\bar{\sigma}_{t,2,j}(T)$, $\cdots$, $P_{i,j}(T)\bar{\sigma}_{t,i,j}(T)$, where j is the bin number. The central limit theorem (CLT) method is used for uncertainty quantification. The maximum value of the statistical uncertainty of each probability bin is considered as the statistical uncertainty of ladder i. FRENDY calculates the statistical uncertainty of the probability table every 10 times to reduce the calculation time of the statistical uncertainty.

Table 5.4.1 and Fig. 5.4.1 show the uncertainty of the probability table in each ladder number. As shown in Fig. 5.4.1, the uncertainty of the probability table decreases in proportion to the square of the number of data. Tables 5.4.2 and 5.4.3 show the uncertainty of the probability table in each probability bin. As shown in these tables, the uncertainty of the higher and lower cross-section regions, where bin number is 18~20 and 1~3, is smaller than that of the other probability bins. These tables also show that the position of the largest uncertainty bin is not changed in each number of ladders and the uncertainty of the probability table in each probability bin also decreases in proportion to the square of the number of data. These results indicate that the convergence of the uncertainty in the higher and the lower cross-section regions is fast.

The default number of ladders in FRENDY is 100. As shown in Table 5.4.1, the uncertainty of the probability table, where the number of ladders is 100, is almost less than 5%. Using these results, the default value of the uncertainty of the probability table is 5%.

Table 5.4.1 Uncertainty of the probability table

		U233		U235		U238		Pu239		Pu240		Pu241		Am241	
	Ein	6.0E+02	3.0E+04	5.0E+02	3.0E+04	2.0E+03	1.5E+05	2.5E+03	3.0E+04	2.7E+03	9.0E+04	3.0E+02	3.0E+04	1.5E+02	4.0E+04
Number of ladders	50	7.29%	5.25%	6.46%	3.84%	2.69%	2.43%	3.90%	4.35%	5.73%	2.67%	9.14%	3.07%	8.85%	5.19%
	100	4.63%	3.60%	4.27%	2.72%	1.75%	1.70%	3.04%	3.41%	3.66%	1.86%	6.60%	2.00%	6.49%	3.24%
	200	3.12%	2.53%	2.79%	1.98%	1.22%	1.24%	2.03%	2.29%	2.37%	1.30%	4.54%	1.45%	4.53%	2.58%
	300	2.60%	1.98%	2.39%	1.60%	0.98%	0.98%	1.65%	1.89%	1.95%	1.03%	3.75%	1.18%	3.77%	2.08%
	500	2.00%	1.55%	1.90%	1.25%	0.75%	0.75%	1.24%	1.44%	1.49%	0.78%	3.06%	0.91%	3.02%	1.60%
	1,000	1.45%	1.05%	1.35%	0.87%	0.54%	0.55%	0.88%	0.97%	1.07%	0.54%	2.08%	0.62%	2.15%	1.13%
	2,000	1.04%	0.74%	0.99%	0.61%	0.37%	0.38%	0.61%	0.68%	0.75%	0.38%	1.42%	0.44%	1.50%	0.77%
	3,000	0.87%	0.61%	0.81%	0.50%	0.30%	0.31%	0.50%	0.55%	0.61%	0.31%	1.17%	0.36%	1.23%	0.64%
	5,000	0.67%	0.47%	0.63%	0.38%	0.23%	0.24%	0.38%	0.42%	0.47%	0.24%	0.89%	0.28%	0.96%	0.50%
	10,000	0.47%	0.33%	0.45%	0.27%	0.17%	0.17%	0.27%	0.30%	0.33%	0.17%	0.63%	0.20%	0.67%	0.35%

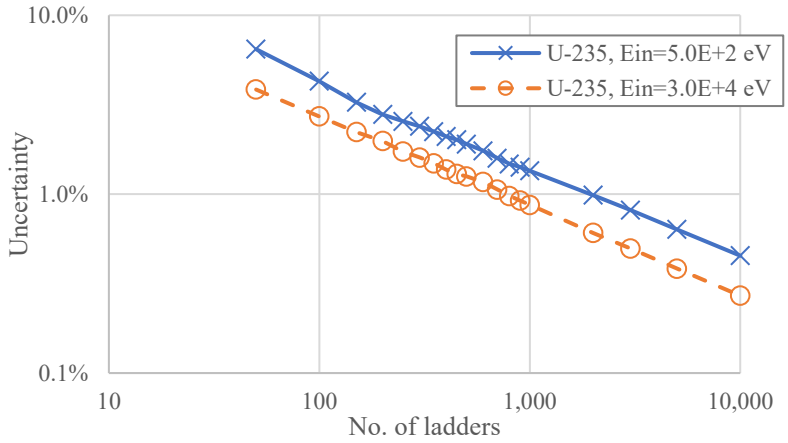

Figure 5.4.1 Uncertainty of the probability table in each number of ladders

Table 5.4.2 Uncertainty of probability table in each probability bin (U-235 from JENDL-4.0, Ein = 500 eV)

		50	100	150	200	250	300	400	500	600	700	800	900	1,000	2,000	3,000	5,000	10,000
probability bin No.	1	0.05%	0.05%	0.03%	0.04%	0.03%	0.03%	0.03%	0.02%	0.02%	0.02%	0.02%	0.02%	0.02%	0.01%	0.01%	0.01%	0.01%
	2	0.13%	0.11%	0.08%	0.07%	0.06%	0.05%	0.05%	0.04%	0.04%	0.04%	0.03%	0.03%	0.03%	0.02%	0.02%	0.01%	0.01%
	3	0.43%	0.29%	0.23%	0.20%	0.18%	0.17%	0.15%	0.14%	0.12%	0.11%	0.11%	0.10%	0.10%	0.07%	0.06%	0.05%	0.03%
	4	0.72%	0.48%	0.43%	0.37%	0.34%	0.31%	0.27%	0.24%	0.21%	0.20%	0.18%	0.18%	0.17%	0.12%	0.10%	0.08%	0.05%
	5	1.29%	0.84%	0.67%	0.60%	0.54%	0.48%	0.43%	0.38%	0.34%	0.31%	0.29%	0.27%	0.26%	0.19%	0.15%	0.12%	0.08%
	6	2.42%	1.61%	1.28%	1.13%	1.02%	0.91%	0.79%	0.71%	0.66%	0.62%	0.58%	0.53%	0.50%	0.36%	0.30%	0.23%	0.16%
	7	2.22%	1.53%	1.32%	1.15%	1.02%	0.93%	0.81%	0.71%	0.66%	0.63%	0.58%	0.55%	0.53%	0.37%	0.30%	0.24%	0.17%
	8	1.87%	1.36%	1.13%	0.98%	0.88%	0.79%	0.69%	0.62%	0.56%	0.52%	0.49%	0.46%	0.44%	0.31%	0.25%	0.20%	0.14%
	9	1.83%	1.31%	1.06%	0.90%	0.85%	0.77%	0.67%	0.60%	0.56%	0.52%	0.48%	0.46%	0.44%	0.32%	0.26%	0.20%	0.14%
	10	2.47%	1.60%	1.35%	1.14%	1.02%	0.91%	0.80%	0.73%	0.67%	0.62%	0.57%	0.54%	0.51%	0.36%	0.29%	0.23%	0.16%
	11	2.04%	1.53%	1.37%	1.29%	1.15%	1.06%	0.95%	0.85%	0.77%	0.72%	0.66%	0.62%	0.58%	0.41%	0.33%	0.26%	0.18%
	12	2.45%	1.72%	1.47%	1.27%	1.16%	1.05%	0.89%	0.80%	0.74%	0.70%	0.66%	0.62%	0.59%	0.41%	0.34%	0.26%	0.19%
	13	3.06%	2.33%	1.95%	1.67%	1.56%	1.39%	1.20%	1.06%	0.98%	0.90%	0.85%	0.80%	0.76%	0.54%	0.44%	0.34%	0.24%
	14	5.28%	3.45%	2.69%	2.33%	2.09%	1.88%	1.64%	1.46%	1.34%	1.24%	1.16%	1.09%	1.04%	0.74%	0.61%	0.47%	0.33%
	15	6.46%	4.27%	3.26%	2.79%	2.55%	2.39%	2.10%	1.90%	1.74%	1.59%	1.47%	1.41%	1.35%	0.99%	0.81%	0.63%	0.45%
	16	4.69%	3.31%	2.74%	2.45%	2.20%	2.04%	1.74%	1.58%	1.45%	1.36%	1.27%	1.20%	1.15%	0.82%	0.67%	0.51%	0.37%
	17	3.59%	2.77%	2.34%	2.05%	1.84%	1.68%	1.43%	1.27%	1.18%	1.11%	1.04%	0.98%	0.93%	0.66%	0.54%	0.41%	0.30%
	18	3.69%	2.72%	2.25%	1.91%	1.74%	1.59%	1.36%	1.20%	1.09%	1.00%	0.94%	0.90%	0.85%	0.60%	0.49%	0.38%	0.27%
	19	2.05%	1.23%	1.01%	0.87%	0.79%	0.71%	0.62%	0.54%	0.49%	0.47%	0.43%	0.40%	0.38%	0.26%	0.21%	0.16%	0.11%
	20	0.47%	0.23%	0.16%	0.12%	0.09%	0.08%	0.06%	0.05%	0.04%	0.04%	0.03%	0.04%	0.03%	0.03%	0.02%	0.01%	0.01%
	Max	6.46%	4.27%	3.26%	2.79%	2.55%	2.39%	2.10%	1.90%	1.74%	1.59%	1.47%	1.41%	1.35%	0.99%	0.81%	0.63%	0.45%

Table 5.4.3 Uncertainty of probability table in each probability bin (U-235 from JENDL-4.0, Ein = 30 keV)

probability bin No.	50	100	150	200	250	300	400	500	600	700	800	900	1,000	2,000	3,000	5,000	10,000
1	0.71%	0.55%	0.44%	0.37%	0.34%	0.31%	0.29%	0.26%	0.24%	0.22%	0.20%	0.19%	0.18%	0.13%	0.11%	0.08%	0.06%
2	0.14%	0.09%	0.07%	0.06%	0.05%	0.05%	0.04%	0.04%	0.04%	0.03%	0.03%	0.03%	0.03%	0.02%	0.02%	0.01%	0.01%
3	0.99%	0.74%	0.65%	0.54%	0.46%	0.42%	0.37%	0.33%	0.30%	0.28%	0.26%	0.24%	0.23%	0.16%	0.13%	0.10%	0.07%
4	1.92%	1.43%	1.17%	0.97%	0.89%	0.83%	0.72%	0.63%	0.58%	0.54%	0.50%	0.47%	0.46%	0.32%	0.26%	0.20%	0.14%
5	3.27%	2.63%	2.14%	1.81%	1.63%	1.45%	1.28%	1.14%	1.04%	0.95%	0.89%	0.84%	0.80%	0.56%	0.45%	0.35%	0.25%
6	3.53%	2.66%	2.22%	1.95%	1.73%	1.53%	1.30%	1.17%	1.07%	0.98%	0.91%	0.86%	0.82%	0.58%	0.47%	0.37%	0.26%
7	2.79%	2.03%	1.71%	1.58%	1.43%	1.30%	1.18%	1.07%	0.96%	0.90%	0.83%	0.79%	0.74%	0.53%	0.43%	0.33%	0.23%
8	3.77%	2.52%	2.06%	1.73%	1.51%	1.39%	1.22%	1.11%	1.01%	0.94%	0.87%	0.83%	0.79%	0.56%	0.46%	0.35%	0.25%
9	3.77%	2.72%	2.20%	1.98%	1.71%	1.60%	1.37%	1.25%	1.17%	1.06%	0.98%	0.92%	0.87%	0.60%	0.50%	0.38%	0.27%
10	3.19%	2.07%	1.91%	1.59%	1.40%	1.25%	1.07%	0.96%	0.88%	0.80%	0.76%	0.71%	0.68%	0.48%	0.40%	0.30%	0.22%
11	3.01%	2.20%	1.71%	1.43%	1.27%	1.20%	1.05%	0.95%	0.87%	0.80%	0.75%	0.70%	0.66%	0.46%	0.37%	0.29%	0.20%
12	3.16%	2.29%	2.00%	1.69%	1.49%	1.36%	1.19%	1.07%	0.98%	0.88%	0.83%	0.78%	0.74%	0.52%	0.43%	0.33%	0.23%
13	3.03%	2.27%	1.90%	1.63%	1.45%	1.34%	1.11%	0.97%	0.86%	0.78%	0.73%	0.70%	0.66%	0.46%	0.37%	0.29%	0.20%
14	3.11%	2.19%	1.78%	1.61%	1.42%	1.32%	1.13%	1.03%	0.95%	0.89%	0.84%	0.79%	0.75%	0.53%	0.43%	0.33%	0.23%
15	3.84%	2.54%	2.11%	1.79%	1.55%	1.46%	1.29%	1.21%	1.11%	1.02%	0.96%	0.90%	0.85%	0.61%	0.49%	0.38%	0.27%
16	2.47%	1.99%	1.75%	1.49%	1.28%	1.18%	1.02%	0.89%	0.83%	0.77%	0.72%	0.69%	0.66%	0.47%	0.38%	0.30%	0.21%
17	1.84%	1.32%	1.12%	0.98%	0.88%	0.81%	0.73%	0.65%	0.60%	0.55%	0.51%	0.48%	0.46%	0.33%	0.27%	0.21%	0.15%
18	1.60%	1.08%	0.86%	0.76%	0.67%	0.61%	0.53%	0.49%	0.44%	0.40%	0.37%	0.34%	0.32%	0.23%	0.19%	0.14%	0.10%
19	1.61%	1.00%	0.74%	0.63%	0.55%	0.51%	0.46%	0.40%	0.36%	0.32%	0.30%	0.28%	0.27%	0.19%	0.15%	0.12%	0.09%
20	2.73%	1.72%	1.40%	1.21%	1.11%	1.02%	0.93%	0.83%	0.75%	0.68%	0.63%	0.61%	0.57%	0.40%	0.33%	0.26%	0.18%
Max	3.84%	2.72%	2.22%	1.98%	1.73%	1.60%	1.37%	1.25%	1.17%	1.06%	0.98%	0.92%	0.87%	0.61%	0.50%	0.38%	0.27%

6 Gas Production Cross-Section Calculation

When the incident particle energy is large, the induced nuclear reactions yield such light particles as proton (^{1}H), deuteron (^{2}H), triton (^{3}H), ^{3}He, and alpha particle (^{4}He). These light particles accumulate as gases in a nuclear system. The estimation of the gas generation is important since gas generation affects the embrittlement of material and the internal gas pressure in a fuel pin.

Though the ENDF-6 format defines the total gas production cross-sections, *i.e.*, (z, Xp), (z, Xd), (z, Xt), (z, X^{3}He), and (z, Xα) in MT 203-207 sections of File 3, these production cross-sections are mainly used for derived libraries.[13] Here, z is the incident particle and X is the number of emitted light particles. FRENDY sums all the gas production reactions to calculate the total gas production cross-sections. For example, when a nucleus has only (n, p) and (n, 2p) reactions for gas production cross-section, the total proton production cross-section $\sigma_{(n,Xp)}(E)$ is calculated as follows:

$$\sigma_{(n,Xp)}(E) = \sigma_{(n,p)}(E) + 2 \times \sigma_{(n,2p)}(E), \tag{6.1}$$

where E is the incident particle energy.

FRENDY also considers the residual nucleus for the calculation of the total gas production cross-section. For example, ^{2}H(n, γ)^{3}H or ^{6}Li(n, α)^{3}H reactions yield tritium as the residual nucleus. In such cases, FRENDY adds tritium to the total gas production cross-section.

FRENDY overwrites the total gas production cross-sections even if the total gas production cross-sections are already defined in the evaluated nuclear data file.

7 ACE File Generation and Its Application

7.1 ACE File Generation

Continuous-energy Monte Carlo calculation codes do not use either the evaluated nuclear data file or the PENDF file which is the intermediate file of NJOY,[7,8] directly. The ACE (A Compact ENDF) file is one of the cross-section data library formats and it is employed in many continuous-energy Monte Carlo calculation codes including PHITS,[4] MCNP,[15] and Serpent.[16] Users can consult the MCNP manual[15] for the ACE format. The ACE format is designed to include all the details of the ENDF-6 representations for neutron and photon data.[42] The ACE format adopts the unionized energy grid and the cumulative probability distribution for the Monte Carlo calculation codes to handle the data conveniently. The unit of energy is changed from eV to MeV. The detail of the transformation is explained in Reference 42.

The ACE file generation module transforms the original nuclear data format, *e.g.*, the ENDF-6 format,[13] into the ACE format. The ACE file generation module transforms the original angular and energy distributions to the specific representation suitable for Monte Carlo sampling procedures.

The ACE format provides for several different "data classes[8]" as shown in Table 7.1.1. Each class is distinguished by the suffix. For example, "92235.50c" represents the continuous-energy neutron data. It should be noted that the current version of FRENDY does not generate photo-atomic and photo-nuclear data. Though the processing modules for the continuous-energy neutron data, the thermal scattering law data, and the dosimetry data are well verified, those for the other data, *i.e.*, the continuous-energy photon, deuteron, triton, ^{3}He, and alpha data, are not verified. Users must carefully check the processing results when they process these incident particle data.

As described in Section 1.2, FRENDY prepares the ACE data parser and writer modules to easily handle the ACE file. There are some cases where users want to modify the cross-section data library to estimate the impact of the modification of the cross-section data library on the neutronics calculation results. The modification of the ACE file is so difficult for users who do not know well about the ACE format. The ACE file uses random access with pointers to the various parts of the data. If the users want to modify the parameters of the ACE files, they also must modify the pointers. The users can easily modify the ACE file using the ACE data parser and writer modules of FRENDY since FRENDY automatically adjusts the pointers in the writer module.

Table 7.1.1 ACE data classes and suffixes

Suffix	ACE data class	Implementation of FRENDY
c	continuous-energy neutron data	Yes
t	thermal scattering law data	Yes
y	dosimetry data	Yes
p	photo-atomic data	No
u	photonuclear data	No
h	continuous-energy proton data	Yes but not verified
o	continuous-energy deuteron data	Yes but not verified
r	continuous-energy triton data	Yes but not verified
s	continuous-energy ^{3}He data	Yes but not verified
a	continuous-energy alpha data	Yes but not verified

7.2 ACE File Perturbation

The perturbation of the cross-section, number of neutrons per fission, fission spectrum, and so on are required for the sensitivity analysis. The perturbation of these data is also used for the uncertainty quantification of the nuclear characteristics due to the covariance of the nuclear data. FRENDY prepares the ACE file perturbation tool to easily perturb the cross-section, number of neutrons per fission, and fission spectrum.[18)]

The perturbation tool multiplies the perturbation factor f by cross-section, number of neutrons per fission, and fission spectrum at the arbitrary energy region as shown in Fig. 7.2.1. Note that this tool does not consider the continuity of the distribution. The energy boundary of the perturbation becomes discontinuity.

The ACE file contains many reaction-type data, *e.g.*, total, elastic, fission, and radiative capture reactions. The perturbation tool not only perturbs the target reaction data but also modifies the total reaction data. For example, the total (MT=1), the non-elastic neutron (MT=3), the absorption (MT=27), and the neutron disappearance reactions (MT=101) contain the radiative capture reaction (MT=102). The perturbation tool modifies the cross-sections of MT=1, 3, 27, and 101 when it perturbs the cross-section of MT=102. If users perturb the total reaction using the perturbation factor, consisting of reaction types, *e.g.*, MT=3, 27, 101, and 102 are also perturbed using the perturbation factor.

The energy integral of the fission spectrum must be 1.0. The perturbation tool normalizes the fission spectrum after the fission spectrum is perturbed. The perturbation tool modifies the other energy range so that the energy integral of the fission spectrum is 1.0 if users want to perturb the fission spectrum at the specified energy range.

FRENDY also prepares the ACE file editing tool. This editing tool outputs the one-dimensional data, *i.e.*, cross-section, number of neutrons per fission, and fission spectrum. Users can plot the one-dimensional data using plotting tools such as Excel, GNUPLOT, and Matplotlib. Users can easily compare the original ACE file and the perturbed ACE file using this editing tool.

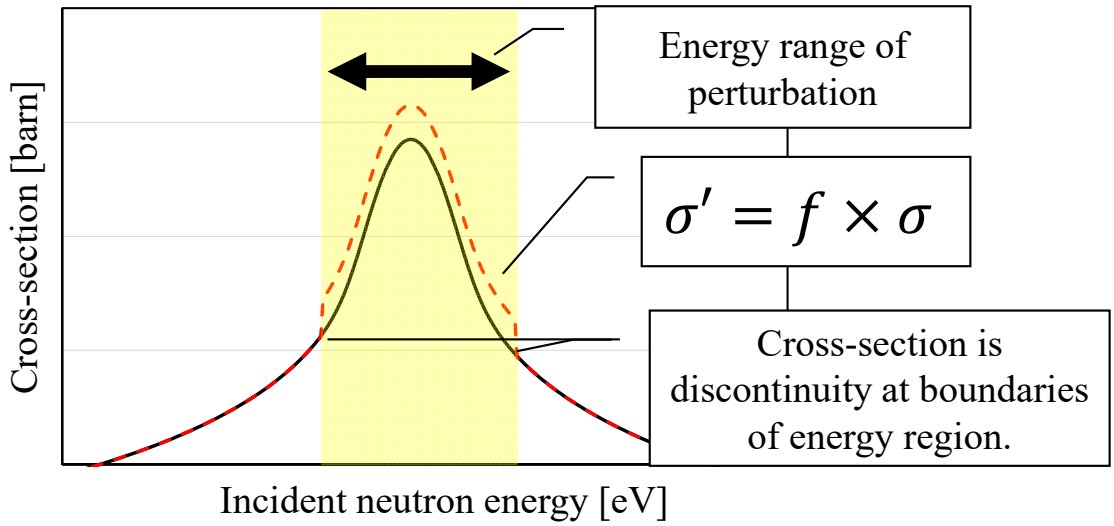

Figure 7.2.1 Overview of ACE perturbation tool

8 Multi-Group Neutron Cross-Section Generation

8.1 Multi-Group Neutron Cross-Section Generation of FRENDY

The continuous energy Monte Carlo calculation codes are widely used for neutronics calculations and radiation shielding calculations. The multi-group deterministic calculation is also important for the design of the nuclear reactor, calculation of the optimum loading pattern, transient analysis, and so on. The multi-group neutron cross-section generation code FRENDY/MG[17] was implemented in FRENDY to generate the multi-group cross-section file. This section explains the procedure of multi-group neutron cross-section generation in FRENDY.

FRENDY can generate GENDF, MATXS, and KRAM[58] formatted multi-group neutron cross-section files from ACE files. Similar to the ACE file generation, FRENDY can treat NJOY compatible input format. The input of the GROUPR and MATXSR modules of NJOY are available in FRENDY version 2. The other modules, *e.g.*, CCCR and WIMSR, are not available in FRENDY version 2. If users use the input file of GROUPR module, FRENDY automatically generates an ACE file before the generation of a multi-group neutron cross-section file.

FRENDY has new functions, *e.g.*, the automatic background cross-section set with the minimum number of background cross-sections[59] and the explicit consideration of the resonance interference effect of the compound of different isotopes. These new functions are only available for the FRENDY original input format.

8.2 Overview of Multi-Group Neutron Cross-Section Generation

FRENDYgenerates neutron multi-group microscopic cross-sections of various nuclides using the point-wise cross-sections in ACE format files. Major capabilities are summarized as follows:

- Process neutron cross-sections.
- Use only ACE files to provide cross-sections. No ENDF format file or other supplemental data is necessary.
- $1/E$, Fission + $1/E$ + Maxwell with temperature specification for fission and Maxwell, or user input spectrum can be used as a weighting function for the narrow resonance (NR) approximation.
- Self-shielded cross-sections in the unresolved resonance energy region are generated by using the probability tables in an ACE file.
- Self-shielded cross sections for all 1-dimensional (1d, *e.g.*, total, capture)/2-dimensional (2d, *e.g.*, scattering) cross-sections are generated (NJOY considers self-shielding only for total, capture, fission, and elastic scattering in the 1d cross-sections, for elastic scattering in the 2d cross-sections).

- Ultra-fine group slowing down calculation or the NR approximation can be used to generate a continuous energy neutron spectrum that is used to collapse cross-sections. The recurrent relation proposed by Kier is adopted in a slowing down calculation to reduce computation time.
- A compound of different isotopes can be specified to explicitly consider the resonance interference effect in a material, *e.g.*, ^{235}U, ^{238}U, and ^{16}O in UO_2.
- Arbitrary mass can be used for the background moderator nuclide in the slowing down calculation to compute the λ factor for the intermediate resonance (IR) approximation.
- Any number of background cross-sections can be used.
- Any order of anisotropic scattering cross-sections can be considered.
- Calculation of the current (P_1 flux) weighted total cross-section in addition to the conventional scalar flux (P_0 flux) weighted total cross-section.
- Any energy grid points can be used for an ultra-fine group slowing down calculation. Energy grid points specified in user input data (in mg_ufg_structure and mg_flux_calc_w_eh_el) for a slowing down calculation are automatically refined based on the energy grid points in an ACE file.
- Treat the angle/energy distribution law for LAW=3, 4, 7, 9, 11, 44, 61, 66 in an ACE file; treatments of all nuclides in major recent nuclear data files (JENDL-4, ENDF/B-VII.1, VIII.0, and JEFF-3.3) are possible.
- Treat an energy-dependent number of neutron emissions mainly in the high energy range (*e.g.*, C-natural, MT=5, ENDF/B-VII.1, corresponding to (n, *x*n) reaction where *x* indicates the number of emitted neutrons).
- Can treat the free gas model, the short time collision time (SCT) approximation, incoherent inelastic, incoherent elastic, coherent elastic in $S(\alpha,\beta)$ data. The types of $S(\alpha,\beta)$ that can be used are: H in H_2O, D in D_2O, Be, Be in BeO, O in BeO, Graphite, Benzene, H in ZrH, Zr in ZrH, O in UO_2, U in UO_2, Al, Fe, H in Polyethylene.
- In the computation of thermal scattering cross-sections, detailed energy discretization is used for numerical integration. While NJOY2016 utilizes fixed incident energy grid points (118 points) for thermal scattering cross section treatment, approximately 20,000 incident energy grids are used for numerical integration of thermal scattering cross sections in FRENDY.
- Fission spectrum and ν values for the prompt, delayed, and total (=prompt + delayed) neutrons can be generated. These for independent delayed neutron groups are explicitly calculated and edited.
- Treat arbitrary thermal cut-off energy (both for the incident and outgoing energies).
- Treat arbitrary multi-group energy structure.

8.3 Theory of Multi-Group Neutron Cross-Section Generation

8.3.1 Calculation of Multi-Group Constants

8.3.1.1 Overview

There are two different types of multi-group cross-sections, *i.e.*, one-dimensional (1D) and two-dimensional (2D) cross-sections. The 1D cross-sections include total, capture, fission, and so on. The 2D cross-sections correspond to those with energy transfer such as elastic scattering, inelastic scattering, fission, (n, 2n), and so on. The multi-group cross-sections are collapsed from pointwise cross-sections using appropriate pointwise (or ultra-fine group) flux or current.

8.3.1.2 One-dimensional cross-section

The 1D cross-sections are generated as follows:

$$\sigma_{g,x,l} = \frac{\int_{E\in E_g} \sigma_x(E)\phi_l(E)dE}{\int_{E\in E_g} \phi_l(E)dE}, \tag{8.1}$$

where g, x, l, $\sigma_x(E)$, $\phi_l(E)$, E_g, and E are energy group index, reaction type, Legendre order of angular flux moment, the pointwise cross-section of reaction x, l-th order angular flux moment, energy range for energy group g, and incident energy, respectively.

Only P_0 flux (0-th order of angular flux moment) is used except for the P_1 flux weighted total cross-section and anisotropic components of elastic and inelastic scattering cross-sections. For the total cross-section, the P_0 flux weighted total cross-section (P_0 total) and the P_1 flux weighted total cross-section (P_1 total) are edited since total cross sections are multiplied by neutron current, which corresponds to P_1 flux, in diffusion and transport equations. For l-th order anisotropic scattering cross-sections, l-th order flux moment (P_l flux) is used for energy collapsing.

8.3.1.3 Two-dimensional cross-section

The 2D cross-sections are generated as follows:

$$\sigma_{g,g',x,l} = \frac{\int_{E\in E_g}\int_{E'\in E_{g'}} \sigma_{x,l}(E,E')\phi_l(E)dE'\,dE}{\int_{E\in E_g} \phi_l(E)dE}, \tag{8.2}$$

where g, g', x, l, $\sigma_x(E)$, $\phi_l(E)$, E_g, $E_{g'}$, and E are incident energy group index, outgoing energy group index, reaction type, Legendre order of angular flux moment, l-th order angular flux moment, energy range for energy group g, energy range for energy group g', and incident energy, respectively.

In an ACE file, angular distributions of emitted neutrons are given for cross-sections having secondary neutron(s), *i.e.*, double differential cross sections are given. However, Legendre moments are necessary for multi-group cross-sections since direct utilization of double differential cross sections is not popular in subsequent neutron transport analyses. The Legendre components of

cross-sections are given by:

$$\sigma_{x,l}(E,E') = \frac{\int_{-1}^{1} \sigma_x(E,E',\mu)P_l(\mu)d\mu}{\int_{-1}^{1} P_l(\mu)d\mu}, \tag{8.3}$$

where $\sigma_x(E,E',\mu)$, μ, and $P_l(\mu)$ are the double differential cross-section of incident energy E, outgoing energy E', scattering angle μ, scattering angle (direction cosine), l-th Legendre polynomial.

8.3.2 Considered Reaction Type (MT)

All types of cross-sections for neutrons in an ACE file are automatically considered in FRENDY and their multi-group cross sections are generated.

In an ACE file, MT=4 (total inelastic scattering) may not exist even if inelastic scattering cross-sections (MT=51-91) exist. FRENDY automatically sums up independent inelastic scattering cross-sections (MT=51-91) and edits the multi-group cross sections for MT=4. It should be noted that MT=4 and MT=51-91 are redundant. Therefore, the summation of MT=4 and MT=51-91 provide incorrect (double) inelastic scattering cross-sections. In subsequent analyses, MT=4 can be used instead of MT=51-91 to avoid summing up. Similar treatments are carried out for MT=18, 103-107 as shown in Table 8.3.1.

A special MT number, MT=-1 is considered in FRENDY, which represents the current (P_1 flux) weighted total cross-section.

Table 8.3.1 Automatically generated MTs in FRENDY

Automatically generated MT number if not exist in an ACE file	Summed MT numbers
4 (inelastic)	51-91
18 (fission)	19, 20, 21, 38
103 (n,p)	600-649
104 (n,d)	650-699
105 (n,t)	700-749
106 (n, ^{3}He)	750-799
107 (n, α)	800-849

8.3.3 Ultra-Fine Group Spectrum Calculation

8.3.3.1 Overview

In FRENDY, two different ultra-fine group neutron spectra can be used to collapse point-wise cross sections in an ACE file. The first one is the neutron spectrum with the narrow resonance (NR) approximation and the second one is that obtained by an ultra-fine group slowing down calculation

in a homogeneous medium.

8.3.3.2 Weighting flux by narrow resonance approximation

The weighting flux used in Eq. (8.1) or (8.2) is given by:[8)]

$$\phi_l(E) = \frac{W(E)}{(\Sigma_t(E) + \Sigma_b)^{l+1}}, \tag{8.4}$$

where $\phi(E)$, $W(E)$, $\Sigma_t(E)$, Σ_b, and l are neutron spectrum (scalar flux, P_0 flux), weight, total macroscopic cross-section, macroscopic background cross-section, and order of Legendre moment, respectively. When one nuclide is considered, Eq. (8.4) is equivalent to

$$\phi_l(E) = \frac{W(E)}{(\sigma_t(E) + \sigma_b)^{l+1}}, \tag{8.5}$$

where $\sigma_t(E)$ and σ_b are microscopic total and background cross-sections, respectively. When multiple nuclides are considered as a material in FRENDY, Eq. (8.4) can be written as

$$\phi_l(E) = \frac{W(E)}{\left(\sum_k \sigma_{t,k}(E)N_k + \sigma_b \sum_k N_k\right)^{l+1}}, \tag{8.6}$$

where $\sigma_{t,k}(E)$ and N_k are the total cross-section and number density of nuclide *k*, respectively.

For the weight $W(E)$, 1/*E*, Fission+1/*E*+Maxwell, or user input value (mg_weighting_spectrum_mode or mg_weighting_spectrum_data) can be used. The 1/*E* weight is given by

$$W(E) = \frac{1}{E}, \tag{8.7}$$

where *E* is incident energy.

The fission + 1/*E* + thermal Maxwell spectrum is given by:[13)]

$$W(E) = \sqrt{E}\,\mathrm{e}^{-\frac{E}{T_f}} \left(E \geq E_f\right), \tag{8.8}$$

$$W(E) = \frac{1}{E} \quad \left(E_f > E > E_t\right), \tag{8.9}$$

$$W(E) = E e^{-\frac{E}{T_m B}} \left(E_t \geq E\right), \tag{8.10}$$

where E, T_f, T_m, B, E_f, and E_t are incident energy [eV], fission temperature [eV], Maxwell temperature [K], Boltzmann constant [eV/K], energy boundary between fission and 1/*E* spectra, and energy boundary between 1/*E* and thermal Maxwell spectra, respectively. These spectra are smoothly connected at the boundaries (E_f and E_t). In other words, the weights given by Eqs. (8.8) - (8.10) are normalized so that two different spectra give the same value at the energy boundaries E_f and E_t.

Any weighting spectrum can be provided through user input (mg_weighting_spectrum_mode or mg_weighting_spectrum_data). The pointwise weighting spectrum is obtained by the linear

interpolation of user input provided at the discrete energy points. The weighting spectra above the highest energy and below the lowest energy of user input are assumed to be 1/*E*.

8.3.3.3 Weighting flux by slowing down calculation

The narrow resonance approximation shown in Eq. (8.4) provides a simple and quick estimation of ultra-fine group flux, but its accuracy is not sufficient when the energy width of a resonance peak is larger than the average loss of neutron energy per collision. Such a situation happens for large resonances of heavy nuclides (*e.g.*, ^{238}U) in the lower energy range. To accurately capture the neutron slowing down effect, the neutron slowing down equation for ultra-fine groups should be numerically solved. The slowing down equation in a homogeneous medium assuming isotropic scattering in the center-of-mass system is expressed as[36)]

$$\Sigma_t(E)\phi(E) = S^{fission}(E) + \int_{E'>E} \sum_k \left(N_k \sigma_{s,k}(E')\right) \phi(E') \frac{dE'}{(1-\alpha_k)E'}, \tag{8.11}$$

where E, $\Sigma_t(E)$, $\phi(E)$, $S^{fission}(E)$, N_k, $\sigma_{s,k}(E)$, and α_k are energy at the LAB system, total cross-section, scalar flux, fission source, the number density of *k*-th nuclide, elastic scattering cross-section of *k*-th nuclide, and $\alpha_k = \frac{(A_k-1)^2}{(A_k+1)^2}$ (A_k is the relative mass of *k*-th nuclide to neutron). Note that inelastic scattering is neglected and a fictitious background (moderator) nuclide having a constant scattering cross-section (σ_b) and zero absorption cross-section is considered in the slowing down calculation.

The discretized form of Eq. (8.11) is

$$\Sigma_{t,g}\phi_g = S_g^{fission} + \sum_{g'=1}^{g-1} \sum_k \left(N_k \sigma_{S,k,g'}\right) \phi_{g'} \frac{dE_{g'}}{(1-\alpha_k)E_{g'}} \tag{8.12}$$

where g and $dE_{g'}$ are the index of ultra-fine energy group and energy width of g'-th ultra-fine energy group. Equation (8.12) is efficiently solved using the recurrent formula proposed by Kier.[36)]

8.3.3.4 Combination of NR and ultra-fine group slowing down spectra

The slowing down calculation can provide an appropriate spectrum for the resonance region where neutron slowing down is the main contributor to form the shape of a spectrum. However, in the fast and thermal energy range, fission source and thermal up-scatter play significant roles for a spectrum shape. Therefore, neutron spectra obtained by the NR approximation and the ultra-fine group slowing down calculation are coupled as the weighting flux. The two boundary energies, E_{high} and E_{low} can be specified in input data (in mg_flux_calc_w_eh_e). The default value of E_{high} and E_{low} are 1.0×10^4 and 1.0, respectively. The NR flux is used for $E > E_{high}$ and $E < E_{low}$, while the slowing down flux is used for $E_{high} \geq E \geq E_{low}$. It should be noted that shapes of

NR and slowing down spectra are different thus the weighting spectrum becomes discontinuous at the energy boundary of connection. Therefore, E_{high} and E_{low} are adjusted to multi-group energy boundaries to avoid an impact on multi-group cross-sections. E_{high} is adjusted to the nearest multi-group energy boundary higher than E_{high}. Similarly, E_{low} is adjusted to the nearest multi-group energy boundary lower than E_{low}.

FRENDY edits multi-group P_0 and P_1 fluxes. In the P_0 and P_1 fluxes, the NR flux is used for all energy range to avoid the above discontinuity. In order words, the slowing down calculation result is not used to edit multi-group P_0 and P_1 fluxes even if the ultra-fine group slowing down calculation is carried out. As discussed later, P_0 flux is necessary to compute fission spectra. For this purpose, the multi-group P_0 flux obtained by the NR approximation is used.

8.3.3.5 Consideration of multiple nuclides

Generation of effective multi-group cross-sections is usually carried out considering a nuclide in focus and a background moderator nuclide that is a pure constant scattering material without absorption. However, FRENDY can treat multiple nuclides to directly consider the resonance interference effect among different nuclides in a material. Number densities of multiple nuclides can be specified in the user input data(in mg_number_density). If multiple nuclides are input, the macroscopic total cross-section used for spectrum calculation is calculated as follows:

$$\Sigma_t(E) = \sum_k \sigma_{t,k}(E) N_k + \sigma_b \sum_k N_k. \tag{8.13}$$

Namely, the background cross-section σ_b is multiplied by the total number density of input nuclides. In this case, the background cross-section would correspond to the escape cross-section which represents the heterogeneous effect in the resonance calculation.

8.3.3.6 Background cross-section

The background cross-section is used to consider the self-shielding effect in a homogeneous medium. Very large and small background cross sections correspond to the infinite-dilute and fully self-shielded conditions, respectively. In FENDY, 10^{10} barn is assumed as the background cross-section for the infinite-dilute condition. Any number of background cross-sections can be specified in the user input data (in sigma_zero_data). FRENDY also provides automated background cross section setting capability. The detail will be described in Section 8.3.4.

8.3.3.7 Mass of background nuclide and IR parameter

In the ultra-fine group spectrum calculation, a fictitious nuclide having a constant background cross-section is considered. The background cross-section corresponds to the elastic scattering cross-section. Usually, the relative atomic mass of the background nuclide is assumed to be the same

as that of hydrogen (0.999167). However, for example, oxygen, which is a major nuclide in a fuel pellet, has a heavier atomic mass thus its effect on slowing down is different from that of hydrogen. The intermediate resonance (IR) parameter is commonly used to capture the impact of the different atomic mass of moderator nuclides in a slowing down calculation.[36)]

The typical calculation procedure for the estimation of IR parameters is as follows. We consider calculating the IR parameter of ^{16}O for ^{238}U.

(1) Generate an effective cross-section of ^{238}U using slowing down calculation. The background cross-section of σ_{b0} and default mass (a_0 =0.999167) for the background nuclide are used. The generated microscopic cross-section is σ_0.
(2) Generate an effective cross-section of ^{238}U using slowing down calculation. The background cross-section of σ_{b0} and mass of oxygen (a_1 =15.8575) for the background nuclide are used. The generated microscopic cross-section is σ_1.
(3) Generate an effective cross-section of ^{238}U using slowing down calculation. The background cross-section of σ_{b1} (e.g., $\sigma_{b1} = 1.05 \times \sigma_{b0}$) and default mass ($a_0 = 0.999167$) for the background nuclide are used. The generated microscopic cross-section is σ_2.
(4) The IR parameter is calculated by

$$f_{IR} = 1 + \frac{\sigma_1 - \sigma_0}{\frac{\sigma_2 - \sigma_0}{\frac{\sigma_{b1} - \sigma_{b0}}{\sigma_{b0}}}}. \tag{8.14}$$

The concept behind the above estimation is as follows. By considering the heavier nuclide (*e.g.*, oxygen), average slowing down lethargy becomes small, by which the depression of neutron spectrum at the resonance peak becomes larger. Therefore, the effective cross-section becomes smaller due to the stronger self-shielding effect. This effect can be alternatively modeled by decreasing the background cross-section. The $\frac{\sigma_2-\sigma_0}{\frac{\sigma_{b1}-\sigma_{b0}}{\sigma_{b0}}}$ in Eq. (8.14) represents the variation of effective cross-section per unit variation of background cross-section. Namely, Eq. (8.14) converts variation of the effective cross-section due to the different mass of moderator nuclide to the variation of background cross-section.

8.3.3.8 Resonance up-scattering correction

In the epi-thermal energy range, neutron scattering is usually treated as the asymptotic kernel that appeared in Eq. (8.11), i.e.:

$$K_{as,i}(E \to E') = \begin{cases} \dfrac{1}{(1-\alpha_i)E} & (\alpha_i E \le E' \le E) \\ 0 & (E' < \alpha_i E,\ E' > E) \end{cases}. \tag{8.15}$$

$$\alpha_i = (A_i - 1)^2/(A_i + 1)^2 \tag{8.16}$$

where, A_i is the relative mass of target nuclide i to a neutron. In the asymptotic kernel, transfer probability takes a constant value for $\alpha_i E \le E' \le E$.

However, especially for heavy nuclides, up-scattering due to thermal motion of nucleus cannot be neglected. In such a case, the following scattering kernel is used[60]:

$$K_{ru,i,l}(E \to E') = \frac{1}{\sigma_{s,i,l}(E)} \frac{\beta_i^{\frac{5}{2}}}{4E} \int_0^\infty t\sigma_{s,i}\left(\beta_i \frac{k_B T}{A_i} t^2\right) \exp\left(\frac{E}{k_B T} - \frac{t^2}{A_i}\right) \Psi_l(t) dt, \tag{8.17}$$

$$\beta_i = (A_i + 1)/A_i, \tag{8.18}$$

where, $\sigma_{s,i,l}(E)$ and $\sigma_{s,i}$, are the l-th order total elastic scattering cross section at T K and the total elastic scattering at 0 K of nuclide i at incident energy E. Note that the isotropic scattering in the center-of-mass system is assumed, which is justified for the epi-thermal energy range of heavy nuclide. $\Psi_0(t)$ for isotropic scattering component in Eq. (8.18) is given by:

$$\begin{aligned} \Psi_0(t) = {} & H(t_+ - t)H(t - t_-)[\mathrm{erf}(t + \varepsilon_{min}) - \mathrm{erf}(\varepsilon_{max} - t)] \\ & + H(t - t_+)[\mathrm{erf}(t + \varepsilon_{min}) - \mathrm{erf}(t - \varepsilon_{min})], \end{aligned} \tag{8.19}$$

$$\varepsilon_{min} = \sqrt{\min(E, E')(A_i + 1)/kT}, \tag{8.20}$$

$$\varepsilon_{max} = \sqrt{\max(E, E')(A_i + 1)/kT}, \tag{8.21}$$

$$t_\pm = (\varepsilon_{max} \pm \varepsilon_{min})/2, \tag{8.22}$$

where, H represents the Heaviside function. The general expression of $K_{ru,i,l}(E \to E')$ can be found elsewhere[61, 62]. The actual calculation procedure considering the up-scattering kernel can be found in reference 63.

8.3.4 Automated Setting of Background Cross-Sections

The choice of background cross-sections is important for accurate interpolation of self-shielding factors while minimizing the number of background cross-sections. In FRENDY, the successive halving method, whose concept is similar to the inverted-stack method used in the reconstruction of point-wise resonance cross-sections in NJOY, is used. The outline of the calculation procedures is summarized in Fig. 8.3.1.

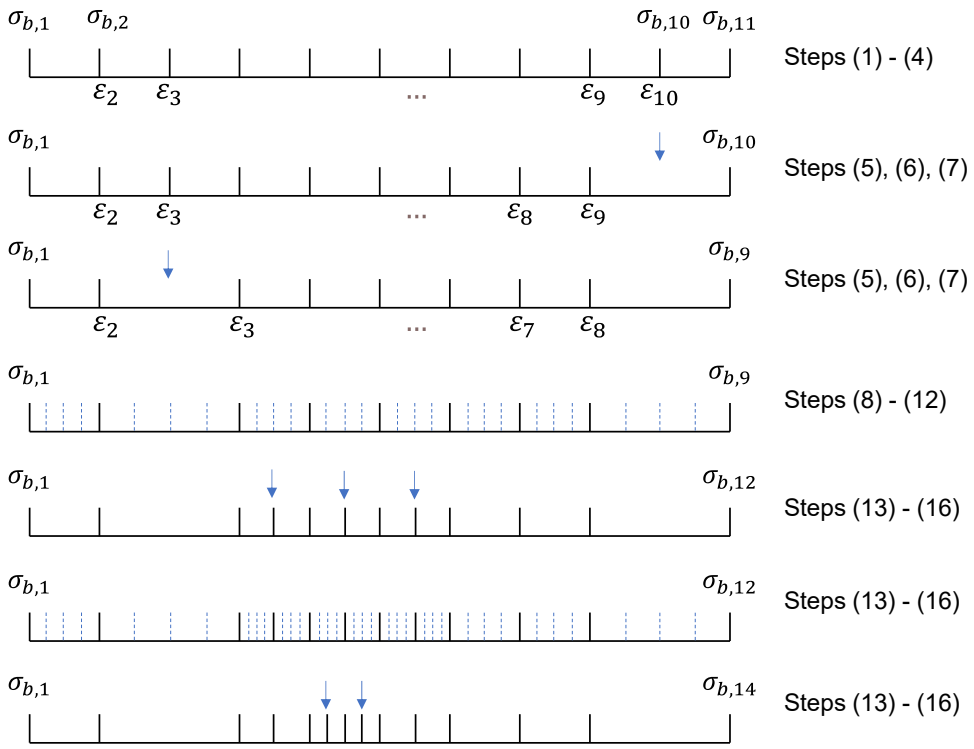

Figure 8.3.1 Calculation flow of adaptive background cross section setting

Firstly, the initial guess of background cross-sections is set in Steps (1) and (2). Secondly, unnecessary background cross-sections are eliminated in Steps (3) – (7). Finally, in Steps (8) – (16), background cross-sections are added until the interpolation error satisfies the error tolerance.

(1) Set minimum and maximum background cross-sections, which correspond to $\sigma_{b,1}$ and $\sigma_{b,11}$ in Fig. 8.3.2. The maximum background cross-section is fixed to 10^{10} barn. The default value of the minimum background cross-section is 10^{-1} barn but can be set by input data (sigma_zero_data) since a fully shielded condition may not be necessary for some nuclides such as fission products due to a small number density in realistic situations.

(2) Divide the range between the minimum and the maximum background cross-sections into 10 equally divided intervals in the logarithmic scale, which gives an initial guess of background cross-sections. Nine background cross-sections are added as the candidates of background cross-section and the total number of background cross sections are 11 including the minimum and the maximum values. Since the initial background cross-sections may include unnecessary points, some of the background cross-sections may be eliminated in the procedures from Steps (3) to (7).

(3) Calculate the interpolation error for each background cross-section except for the minimum and the maximum values. For example, let us consider 2nd background cross-section ($\sigma_{b,2}$ in Fig.

8.3.1). In this case, the self-shielding factor or the reaction rate at the 2nd background cross-section is interpolated using the self-shielding factors or reaction rate at 1st, 3rd, 4th, …, 10th, and 11th background cross-sections. Note that the interpolation method will be described in the next subsection. The interpolation error at k^{th} background cross-section is calculated by

$$\varepsilon_k = \left| \frac{f_k^{int} - f_k^{ref}}{f_k^{ref}} \right|, \tag{8.23}$$

where ε_k, f_k^{int}, and f_k^{ref} are the interpolation error at the kth background cross-section, the interpolated self-shielding factor or reaction rate, and the reference self-shielding factor or reaction rate without interpolation. The reference self-shielding factor or reaction rate is calculated with the ultra-fine group spectrum. The self-shielding factor or reaction rate depends on the energy group and/or type of reactions (typically, total, elastic scattering, fission, and capture). In the present study, the maximum value of ε_k is chosen among the energy groups and/or reactions since uniform background cross-sections are used for all energy groups and reaction types.

(4) Repeat Step (3) for $k = 2, 3, \ldots,$ and $N - 1$ where N is the total number of background cross-sections.

(5) Select the background cross-section point where ε_k takes a minimum value ($\varepsilon_{k,min}$).

(6) If $\varepsilon_{k,min}$ is smaller than the tolerance for interpolation error, eliminate this background cross-section. The tolerance is set by input data.

(7) If ε_k is smaller than the tolerance for interpolation error, return to Step (3). Namely the unnecessary points, where interpolation errors are sufficiently small, are eliminated through the repetition of Steps (3) – (7).

(8) Choose k^{th} interval and set three intermediate points of background cross section considering the logarithmic interpolation for background cross-section:

$$\sigma_{b,k}^{w} \times \sigma_{b,k+1}^{1-w}, \qquad \sigma_{b,k}^{w} \times \sigma_{b,k+1}^{1-w}, \tag{8.24}$$

where $w = \frac{1}{4}, \frac{2}{4}, \frac{3}{4}$. It should be noted that in the conventional inverted stack approach, only the interpolation error at the midpoint is considered. However, during this study, we found that estimation of interpolation error only at the midpoint may not be sufficient since the error may be small at the midpoint due to cancellation. Therefore, three intermediate points are considered.

(9) Evaluate the self-shielding factor or reaction rate at the intermediate points by interpolation.

(10) Evaluate the reference self-shielding factor or reaction rate at the intermediate points using the ultra-fine group spectrum calculation result.

(11) Evaluate the interpolation errors of three intermediate points by Equation (8.23).

(12) Repeat Steps (8) to (11) for all intervals.

(13) Choose an interval that contains the largest interpolation error in Step (12).

(14) Add the midpoint background cross-section (obtained by $\sigma_{b,k}^{1/2} \times \sigma_{b,k+1}^{1/2}$) if the largest interpolation error is larger than the tolerance. The background cross-sections are added as the order of the magnitude of interpolation error, i.e., the interval with maximum interpolation error is considered at first, then the interval with second-to-maximum is considered next, and so on. Note that the midpoint background cross-section is added rather than the background cross-section with maximum interpolation error to construct the uniform background cross-section set.

(15) Terminate the procedure if the total number of background cross sections is larger than or equal to the maximum number of background cross-sections, which is given by input.

(16) Repeat Steps (8) to (15) until all interpolation errors become smaller than the tolerance.

When the reaction rate is used to check convergence, the following equation is used to estimate the reaction rate:

$$rr_{x,k} = \sum_{g \in fast} \sigma_{x,g,k} \phi_g, \tag{8.25}$$

where $rr_{x,k}$, $\sigma_{x,g,k}$, and ϕ_g are the reaction rate (reaction type x, background cross section k), the effective microscopic cross-section (reaction type x, group g, background cross section k), and energy integrated scalar flux (group g). Only the fast group (> 1.0 eV in this study) is considered in Equation (8.25) since the self-shielding factor in the thermal energy region is not usually important. For ϕ_g, those obtained from the infinite-dilute condition are used.

8.3.5 Unresolved Resonance Cross-Sections

8.3.5.1 Calculation of self-shielding factor

In the unresolved resonance region, which may locate the energy range between the fast smooth energy range and the resolved energy range, the probability table may be provided in an ACE file in addition to the point-wise cross-section. Self-shielding factors for microscopic cross-sections are calculated using the probability table of an ACE file in FRENDY. Two options are used in the probability table in an ACE file. When the parameter IFF of the UNR block in an ACE file is 0 (IFF=0), the probability table provides the band cross-sections and the band probabilities. On the other hand, when IFF=1, the self-shielding factors (ratio to the infinite-dilute cross-sections) and the band probabilities are given in the probability table. In the case of IFF=0, the effective cross-sections are once calculated in FRENDY and then they are converted to the self-shielding factor by dividing shelf-shielded effective cross sections by the infinite dilute cross-sections.

The self-shielding factor in the unresolved energy range is multiplied by the point-wise cross-section that is given at the infinite-dilute condition. The “self-shielded” point-wise cross-section is used in the ultra-fine group spectrum calculation (using the NR approximation or the

ultra-fine group slowing down calculation) and successive effective multi-group cross-section calculations.

The effective microscopic cross-section (or self-shielding factor) is calculated by[8,36)]

$$\sigma_x = \frac{\sum_i \frac{w_i \sigma_{x,i}}{\sigma_b + \sigma_{t,i}}}{\sum_i \frac{w_i}{\sigma_b + \sigma_{t,i}}}, \tag{8.26}$$

where σ_x, $\sigma_{x,i}$, σ_b, $\sigma_{t,i}$, and w_i are the effective cross-section of reaction x, the i-th band cross-section of reaction x, background cross-section, i-th band total cross-section, and the band probability (weight). In the case of IFF=0, σ_x is the effective microscopic cross-section while σ_x is the self-shielding factor for IFF=1. In the case of IFF=0, the self-shielding factor is calculated by

$$\frac{\sigma_x}{\sigma_{x,\infty}} = \frac{\frac{\sum_i \frac{w_i \sigma_{x,i}}{\sigma_b + \sigma_{t,i}}}{\sum_i \frac{w_i}{\sigma_b + \sigma_{t,i}}}}{\frac{\sum_i \frac{w_i \sigma_{x,i}}{\sigma_{b,\infty} + \sigma_{t,i}}}{\sum_i \frac{w_i}{\sigma_{b,\infty} + \sigma_{t,i}}}}, \tag{8.27}$$

where $\sigma_{x,\infty}$ and $\sigma_{b,\infty}$ are the infinite-dilute microscopic cross-section and the corresponding background cross-section. It should be noted that the different weights may be used for the total cross-section.

In the case of IFF=0, $\sigma_{t,i}$ is given by a factor to the infinite dilute total cross-section. Therefore, an infinite dilute cross-section is necessary for Eq. (8.26) or (8.27). In FRENDY, the point-wise cross-section given in the ACE file is used as the infinite-dilute cross-sections. It should be noted that the point-wise cross-section, which corresponds to infinite-dilute condition, may be different from the average cross-section obtained by the ladder calculation (random sampling of unresolved resonance cross-section) in the ACE file. Therefore, the self-shielding factor obtained by the multi-group neutron cross-section file would be slightly different from those in the ACE file.

8.3.5.2 P_0 and P_1 flux weighted total cross-section

In the Boltzmann transport equation, the total cross-section is multiplied by the angular flux. Therefore, the point-wise total cross-section should be theoretically collapsed by the angular flux. However, this approach is not favorable since the total cross-section becomes angular dependent and common transport codes cannot handle the angular dependence of the total cross-section. Instead, the total cross-section can be collapsed by the neutron current, which corresponds to the P_1 component of Legendre expansion of angular flux. This approach is theoretically justified since the total cross-section is multiplied by the P_1 moment (P_1 flux) of angular flux in the P_1 transport theory. In the probability table expression, the P_1 flux weighted total cross-section is given by

$$\frac{\sigma_x}{\sigma_{x,\infty}} = \frac{\dfrac{\sum_i \dfrac{w_i \sigma_{x,i}}{\sigma_b + \sigma_{t,i}}}{\sum_i \dfrac{w_i}{\sigma_b + \sigma_{t,i}}}}{\dfrac{\sum_i \dfrac{w_i \sigma_{x,i}}{\sigma_{b,\infty} + \sigma_{t,i}}}{\sum_i \dfrac{w_i}{\sigma_{b,\infty} + \sigma_{t,i}}}}, \tag{8.28}$$

where l is the order of Legendre moment and l=1 for P_1 flux.

8.3.5.3 Treatment of ILF and IOA

In the UNR block in the ACE file, there are two flags except for IFF. The ILF is the inelastic competition flag and the IOA is the other absorption flag. In FRENDY, these flags are not currently used in the processing.

8.3.5.4 Definition of infinite-dilute total cross-section

The probability table in the ACE file is generated by a random sampling method that constructs artificial resonance ladders in the unresolved resonance region. The infinite dilute total cross sections are computed in this processing and used to calculate band cross-sections and probabilities. Since the resonance ladders are generated by the average statistical property of resonances in the unresolved resonance region, some inconsistency may exist between the smooth cross-section in the unresolved resonance region.

The smooth cross-section corresponds to the infinite-dilute cross-section. The infinite-dilute total cross-section can be also calculated by the results of the random sampling. These two infinite-dilute cross-sections are slightly different since these two values are obtained by different routes. In FRENDY, the smooth (point-wise) cross-sections are used as the infinite-dilute cross-sections while that obtained by the random sampling is used in the ACE file generation. Therefore, the self-shielded cross-sections (the Bondarenko cross-sections) generated by the probability table in the ACE file are somewhat different from the multi-group neutron cross-section, especially in highly self-shielded conditions using small background cross-sections. In the continuous energy Monte Carlo calculation code, the smooth cross-sections are used as the infinite dilute-cross sections when IFF=1. In this context, the processing results of FRENDY would be consistent with the treatment in the continuous energy Monte Carlo calculation code.

8.3.6 Cross-Sections with Emitting Neutrons

8.3.6.1 Overview

For the reactions with emitting neutrons, angular and/or energy distributions are provided in an ACE file. As shown in Table 8.3.2, FRENDY handles the elastic scattering and LAW=3, 4, 7, 9, 11, 44, 61, 66 in the DLW block of an ACE file. The angular and/or energy distributions are read and

calculated as follows. For LAW=4, 7, 9, 11, and 66, the angular and the outgoing energy distributions are independently defined. For other cases, the angular and the energy distributions are dependent on each other.

Table 8.3.2 Available LAW number in FRENDY

LAW	Angular distribution	Energy distribution
(Elastic scattering, MT=2)	AND block	Analytically calculated from angular distribution
3 (Inelastic scattering, MT=51-90)	AND block	Analytically calculated from angular distribution
4, 7, 9, 11, 66 (Fission, (n, 2n) reactions, etc.)	AND block	DLW block
44, 61 (Continuum inelastic scattering, MT=91)	DLW block	DLW block

8.3.6.2 Elastic scattering

In the elastic scattering (MT=2), the kinematics based on the two-body scattering is used. In an ACE file, only angular distribution at the incident energy is given in the AND block. The outgoing energy distribution is not provided for elastic scattering since the outgoing energy is analytically calculated by the kinematics.

The multi-group elastic scattering cross-section is calculated by

$$\sigma_{s,l,g\to g'} = \frac{\int_{E\in g}\phi_l(E)\int_{E'\in g'}\sigma_s\left(E,E',\mu(E,E')\right)P_l\left(\mu(E,E')\right)dE'\,dE}{\int_{E\in g}\phi_l(E)dE}, \tag{8.29}$$

where E, E', $\sigma_{s,l,g\to g'}$, $\phi_l(E)$, $\sigma_s(E,E',\mu)$, and $P_l(\mu)$ are the incident energy (LAB), outgoing energy (LAB), multi-group scattering cross-section (l-th order anisotropic), l-th order angular flux moment (P_l flux), scattering cross-section from E to E', scattering angle μ, and l-th order Legendre polynomial $P_l(\mu)$. Note the scattering angle is a function of E and E'.

The angular distribution is given by the center-of-mass (CM) or the laboratory (LAB) system. Since a neutron transport calculation is carried out in the LAB system, the coordinate conversion is necessary when the angular distribution is given in the CM system. The scattering angle (direction cosine) is converted from the CM system to the LAB system as follows:[8)]

$$\mu_{LAB} = \frac{1 + A\mu_{CM}}{\sqrt{1 + A^2 + 2A\mu_{CM}}}, \tag{8.30}$$

where μ_{LAB}, μ_{CM}, and A are the direction cosine of scattering angle in the LAB and CM systems,

the relative atomic mass of target nuclide, respectively. The denominator of Eq. (8.30) becomes zero when $A = 1$ and $\mu_{CM} = -1$. To avoid zero division, the following relation is used when $1 + A^2 + 2A\mu_{CM} < 10^{-10}$.

$$\mu_{LAB} = \frac{1 + \mu_{CM}}{2}, \tag{8.31}$$

Integration in Eq. (8.29) is the triple integration of incident energy, outgoing energy, and direction cosine. In FRENDY, the integration is carried out for the outgoing energy at specific incident energy then averaging on incident energy is carried out. Since the direction cosine is represented as a function of the incident and outgoing energies, the following relation is used.

$$\sigma_{s,l,E\to g'} = \int_{E'\in g'} \sigma_s\big(E, E', \mu(E,E')\big) P_l\big(\mu(E,E')\big) dE', \tag{8.32}$$

where g' indicates the energy range of the outgoing energy group.

The integration of Eq. (8.32) is carried out by:

$$\sigma_{s,l,E\to g'} = \int_{E'\in g'} \sigma_s\big(E, E', \mu(E,E')\big) P_l\big(\mu(E,E')\big) \frac{1}{\frac{d\mu(E,E')}{dE'}} d\mu. \tag{8.33}$$

The actual numerical calculation procedures to calculate multi-group elastic scattering cross-section from the incident energy *E* to outgoing energy group *g'* are as follows.

(1) Choose incident energy *E*, where *E* is specified in the LAB system.

(2) Calculate the maximum and minimum outgoing energy in the LAB system by

$$\begin{aligned} E'_{max} &= E, \\ E'_{min} &= \alpha E, \end{aligned} \tag{8.34}$$

where $\alpha = \frac{(1-A)^2}{(1+A)^2}$ and *A* is the relative mass of the target nuclide to neutron.

(3) Choose energy integration range considering energy group boundary of group *g'* as

$$E'_{upper} = \begin{cases} E'_{max} & \left(E_{g',upper} \geq E'_{max}\right) \\ E_{g',upper} & \left(E_{g',upper} < E'_{max}\right) \end{cases}, \tag{8.35}$$

$$E'_{lower} = \begin{cases} E'_{min} & \left(E_{g',lower} < E'_{min}\right) \\ E_{g',lower} & \left(E_{g',lower} \geq E'_{min}\right) \end{cases}, \tag{8.36}$$

where $E_{g',upper}$, $E_{g',lower}$, E'_{upper}, and E'_{lower} are the upper and the lower energy boundaries of *g'*-th energy group, the upper and the lower energy boundaries of integration, respectively. Note that the integration is not carried out when:

$$\begin{aligned} E'_{upper} &< E_{g',lower}, \\ E'_{lower} &> E_{g',upper}, \end{aligned} \tag{8.37}$$

since the outgoing energy range does not overlap the energy range of *g'*-the energy group. In this

case, $\sigma_{s,l,E\to g'} = 0$.

(4) Divide the energy range E'_{upper}~E'_{lower} into MAX_EOUT_DIV_ELASTIC intervals where MAX_EOUT_DIV_ELASTIC is set to be 64 in FRENDY. If the number of angular distribution points in the table (the AND block in an ACE file) is larger than MAX_EOUT_DIV_ELASTIC, the number of angular distribution points in the AND block is used instead of MAX_EOUT_DIV_ELASTIC.

(5) Scattering angle of a neutron is increased as the outgoing energy decreases when A > 1.0. Therefore, direction cosine for E'_{min} is $\mu_{LAB} = -1$. However, in the case of hydrogen (A < 1.0), the scattering angle increased as the outgoing energy decreases but the scattering angle takes the maximum value, and then the scattering angle decreases as the outgoing energy decreases. In the case of hydrogen, direction cosine for E'_{min} is $\mu_{LAB} = 1$. It means that a minimum μ_{LAB} exists only for hydrogen, which corresponds to

$$\mu_{CM,min} = -A. \tag{8.38}$$

Equation (8.38) can be obtained by

$$\frac{d\mu_{LAB}}{d\mu_{CM}} = \frac{d}{d\mu_{CM}}\left(\frac{1 + A\mu_{CM}}{\sqrt{1 + A^2 + 2A\mu_{CM}}}\right) = \frac{A^3 + A^2\mu_{CM}}{(1 + A^2 + 2A\mu_{CM})^{\frac{3}{2}}} = 0\,, \tag{8.39}$$

Therefore, the outgoing energy corresponding to $\mu_{CM,min}$ is added to the outgoing energy boundary listed in Eqs. (8.35) and (8.36). The outgoing energy corresponding to $\mu_{CM,min}$ is calculated using Eq. (8.39).

(6) The upper and lower boundaries and the average energy of the divided energy range are calculated by

$$\begin{aligned} E'_{i,upper} &= \exp\left\{\frac{\left(\log\left(E'_{upper}\right) - \log\left(E'_{lower}\right)\right)}{n} \times (i+1) + \log\left(E'_{lower}\right)\right\}, \\ E'_{i,lower} &= \exp\left\{\frac{\left(\log\left(E'_{upper}\right) - \log\left(E'_{lower}\right)\right)}{n} \times i + \log\left(E'_{lower}\right)\right\}, \\ E'_{average,i} &= \sqrt{E'_{i,upper} \times E'_{i,lower}}\,, \end{aligned} \tag{8.40}$$

where n is the number of divisions and $0 \le i \le n-1$.

(7) Calculate scattering angle (direction cosine) for $E'_{i,upper}$, $E'_{i,lower}$, and $E'_{average,i}$ by

$$\begin{aligned} \alpha &= \frac{(1-A)^2}{(1+A)^2}, \\ \mu'_{CM} &= \frac{\left(2 \times \frac{E'}{E} - (1+\alpha)\right)}{(1-\alpha)}, \end{aligned} \tag{8.41}$$

$$\mu_{CM} = \begin{cases} -1 \left(\mu'_{CM} < -1\right) \\ \mu'_{CM} \left(-1 \le \mu'_{CM} \le 1\right). \\ 1 \left(\mu'_{CM} > 1\right) \end{cases}$$

Three different direction cosines $\mu_{CM,i,upper}$ $\mu_{CM,i,lower}$, $\mu_{CM,i,average}$ corresponding to $E'_{i,upper}$, $E'_{i,lower}$, and $E'_{average,i}$ are calculated.

(8) Convert μ_{CM} to μ_{LAB} by Eq. (8.30). The direction cosines in the LAB system, $\mu_{LAB,i,upper}$ $\mu_{LAB,i,lower}$, and $\mu_{LAB,i,average}$ are obtained.

(9) Convert the probability density of angular distribution in the CM system to the LAB system as

$$pdf_{LAB,i} = pdf_{CM,i} \times \frac{\left(A^2 + 2A\mu_{LAB,i,average} + 1\right)^{\frac{3}{2}}}{A^2\left(A + \mu_{LAB,i,average}\right)}, \tag{8.42}$$

$pdf_{LAB,i}$ and $pdf_{CM,i}$ are the probability densities of angular distribution in the LAB and CM systems, respectively. For the probability density at $\mu_{CM,i,average}$ is used for $pdf_{CM,i}$.

(10) If the probability density for angular distribution is given in the LAB system, Step (9) is skipped.

(11) Numerical integration is carried out using

$$\sigma_{s,l,E\to g'} = \sum_{i=0}^{n-1} pdf_{LAB,i} \times P_l\left(\mu_{LAB,i,average}\right) \times \left(\mu_{LAB,i,upper} - \mu_{LAB,i,lower}\right), \tag{8.43}$$

(12) Finally, the multi-group scattering cross-section is calculated by

$$\sigma_{s,l,g\to g'} = \frac{\int_{E\in E_g} \sigma_{s,l,E\to g'}\phi_l(E)dE}{\int_{E\in E_g} \phi_l(E)dE} \approx \frac{\sum_i \sigma_{s,l,E_i\to g'}\phi_l(E_i)\Delta E_i}{\sum_i \phi_l(E_i)\Delta E_i}, \tag{8.44}$$

Equation (8.44) is numerically integrated. The following energy grid is also considered in numerical integration for accurate calculation:

-multi-group energy group boundary,

-incident energy whose outgoing energy with $\mu_{CM} = -1$ is a multi-group boundary.

ΔE_i in Eq. (8.44) is set assuming the lethargy width of 0.001.

8.3.6.3 Inelastic scattering (LAW=3: level scattering)

For law=3, the probability density function for angular distribution in the CM system is given in an ACE file while the outgoing energy is calculated by

$$E_C^{out} = \left(\frac{A}{A+1}\right)^2 \times \left(E_L^{in} - \left(\frac{A+1}{A}\right)|Q|\right), \tag{8.45}$$

where

E_C^{out}: outgoing energy of a neutron in the CM system,

E_L^{in}: incident energy of a neutron in the LAB system,

A: relative atomic mass of target nuclide to a neutron,

$|Q|$: Q-value of inelastic scattering where $Q < 0$. The values of $\left(\frac{A}{A+1}\right)^2$ and $\left(\frac{A+1}{A}\right)|Q|$ are given in the DLW block of an ACE file.

The outgoing energy in the LAB system is given by

$$E_L^{out} = E_C^{out} + \frac{E_L^{in} + 2\mu_C(A+1)\sqrt{E_L^{in}E_C^{out}}}{(A+1)^2}, \tag{8.46}$$

μ_C: direction cosine in the CM system.

When the incident and outgoing energies are given in the LAB system, direction cosines in the CM and LAB systems are calculated by

$$\mu_C = \frac{(A+1)^2 E_L^{out} - E_L^{in}(1+R^2)}{2RE_L^{in}}, \tag{8.47}$$

$$\mu_L = \frac{1 + R\mu_C}{\sqrt{1 + R^2 + 2R\mu_C}}, \tag{8.48}$$

$$R = A\sqrt{1 - \frac{(A+1)(-Q)}{AE_L^{in}}}. \tag{8.49}$$

When the probability density for direction cosine is given in the LAB system, the Legendre coefficient is calculated by

$$p_{L,l,g'}(E_L^{in}) = \int_{+\mu_{L,g',lower}}^{+\mu_{L,g',upper}} p_L(E_L^{in}, \mu_L) P_l(\mu_L) d\mu_L, \tag{8.50}$$

where

$p_{L,l,g'}(E_L^{in})$: Legendre coefficient for incident energy E_L^{in} and outgoing energy for g',

$p_L(E_L^{in}, \mu_L)$: probability density in the LAB system.

$\mu_{L,g',upper}$: the upper value of direction cosine in the LAB system corresponding outgoing energy group g',

$\mu_{L,g',lower}$: the lower value of direction cosine in the LAB system corresponding outgoing energy group g'.

$\mu_{L,g',upper}$ and $\mu_{L,g',lower}$ are calculated using Eqs. (8.47) to (8.49) using $E_L^{out,g',upper}$ and $E_L^{out,g',lower}$, which correspond to the upper and lower outgoing energy for energy group g' in the LAB system. When the probability density for direction cosine is given in the CM system, the Legendre coefficient is calculated by

$$p_{L,l,g'}(E_L^{in}) = \int_{+\mu_{L,g',lower}}^{+\mu_{L,g',upper}} p_C(E_L^{in}, \mu_C)\, J(E_L^{in}, \mu_C)\, P_l(\mu_L) d\mu_L, \tag{8.51}$$

where $p_C(E_L^{in}, \mu_C)$ and $J(E_L^{in}, \mu_C)$ is the probability density in the CM system and the Jacobian,

respectively. The Jacobian is necessary since $p_L(E_L^{in}, \mu_C)$ is given per unit direction cosine in the CM system and is given by

$$J(E_L^{in}, \mu_C) = \frac{d\mu_C}{d\mu_L} = \frac{(1 + R^2 + 2R\mu_C)^{\frac{3}{2}}}{R^2(R + \mu_C)}, \tag{8.52}$$

The numerical integration for Eq. (8.50) or (8.51) is carried out as follows.

(1) Set the incident energy in the LAB system, E_L^{in}.

(2) Calculate maximum ($E_L^{out,upper}$) and minimum ($E_L^{out,lower}$) outgoing energies in the LAB system using Eqs. (8.45) and (8.46), and $\mu_C = \pm 1$. Note that $\mu_C = 1$ and $\mu_C = -1$ correspond to the maximum and the minimum outgoing energies, respectively.

(3) Set outgoing energy group g' whose energy group boundaries are $E_L^{out,g',upper}$ and $E_L^{out,g',lower}$.

(4) If $E_L^{out,g',lower} < E_L^{out,upper} < E_L^{out,g',upper}$, set $E_L^{out,g',upper}$ to be $E_L^{out,upper}$.

(5) If $E_L^{out,g',lower} < E_L^{out,lower} < E_L^{out,g',upper}$, set $E_L^{out,g',lower}$ to be $E_L^{out,lower}$.

(6) The energy range between $E_L^{out,g',upper}$ and $E_L^{out,g',lower}$ is subdivided into MAX_EOUT_DIV_ELASTIC intervals where MAX_EOUT_DIV_ELASTIC is set to be 64 in FRENDY. If the number of angular distribution points in the table (the AND block in an ACE file) is larger than MAX_EOUT_DIV_ELASTIC, the number of angular distribution points in the AND block is used instead of MAX_EOUT_DIV_ELASTIC.

(7) The values of $\mu_{L,g',upper}$ and $\mu_{L,g',lower}$ are calculated using Eqs. (8.47) and (8.48) using the subdivided energy range obtained in Step (6).

(8) The Jacobian *J* is calculated by Eq. (8.52) when the probability density function for angular distribution is given the CM system. Note that average μ_C of the energy interval is used.

(9) Interpolate the probability density function $p_L(E_L^{in}, \mu_L)$ or $p_C(E_L^{in}, \mu_C)$ in the ACE file. Note that average μ_C or μ_L of the energy interval is used.

(10) Perform numerical integration of Eq. (8.50) or (8.51). The simple trapezoidal rule is used in FRENDY as follows:

$$p_{L,l,g'}(E_L^{in}) = \sum_i p_L(E_L^{in}, \mu_{L,i})\, P_l(\mu_{L,i}) \Delta\mu_{L,i}, \tag{8.53}$$

$$p_{L,l,g'}(E_L^{in}) = \sum_i p_C(E_L^{in}, \mu_{C,i})\, J(E_L^{in}, \mu_{C,i})\, P_l(\mu_{L,i}) \Delta\mu_{L,i}, \tag{8.54}$$

where

$\mu_{C,i}$: average direction cosine in the CM system of *i*-th outgoing energy interval,

$\mu_{L,i}$: average direction cosine in the LAB system of *i*-th outgoing energy interval,

$\Delta\mu_{L,i}$: width of direction cosine in the LAB system of *i*-th outgoing energy interval.

(11) Finally, the multi-group scattering cross section is calculated by

$$\sigma_{s,l,g\to g'} = \frac{\int_{E\in E_g} \sigma_s(E_L^{in}) p_{L,l,g'}(E_L^{in}) \phi_l(E_L^{in}) dE_L^{in}}{\int_{E\in E_g} \phi_l(E_L^{in}) dE_L^{in}} \approx \frac{\sum_i \sigma_s(E_{L,i}^{in}) p_{L,l,g'}(E_{L,i}^{in}) \phi_l(E_{L,i}^{in}) \Delta E_{L,i}^{in}}{\sum_i \phi_l(E_{L,i}^{in}) \Delta E_{L,i}^{in}}. \quad (8.55)$$

Equation (8.55) is numerically integrated. The following energy grid is also considered in numerical integration for accurate calculation:

-multi-group energy group boundary,

-incident energy whose outgoing energy with $\mu_{CM} = -1$ is a multi-group boundary.

$\Delta E_{L,i}^{in}$ in Eq. (8.55) is set assuming the lethargy width of 0.001.

8.3.6.4 Inelastic scattering (LAW=44, 61: Kalbach-87 etc.)

For LAW=44 or 61, the probability density function for angular distribution is given as a table of the incident energy, outgoing energy, and scattering angle (direction cosine). When the probability density function is given in the LAB system, the Legendre coefficients for the inelastic scattering can be obtained by

$$p_{L,l}(E_L^{in}, E_L^{out}) = \int_{-1}^{+1} p_L(E_L^{in}, E_L^{out}, \mu_L) P_l(\mu_L) d\mu_L, \quad (8.56)$$

where

$p_{L,l}(E_L^{in}, E_L^{out})$: Legendre coefficient,

$p_L(E_L^{in}, E_L^{out}, \mu_L)$: probability density in the LAB system,

E_L^{in}: incident energy in the LAB system,

E_L^{out}: outgoing energy in the LAB system,

μ_L: direction cosine in the LAB system,

$P_l(\mu_L)$: Legendre polynomial of the *l*-th order.

The integration of Eq. (8.56) is numerically carried out using the trapezoidal rule and sufficiently fine discretization on μ_L. The number of intervals for angle integration is the maximum of 20 and the number of angle points in the DLW block for inelastic scattering.

On the contrary, more complicated calculations are necessary when the probability density function is given in the CM system. In this case, the Legendre coefficients $p_{L,l}(E_L^{in}, E_L^{out})$ in the LAB system are obtained by

$$p_{L,l}(E_L^{in}, E_L^{out}) = \int_{\mu_L^{min}}^{+1} p_C(E_L^{in}, E_C^{out}, \mu_C)\, J\, P_l(\mu_L) d\mu_L, \quad (8.57)$$

where

$p_C(E_L^{in}, E_C^{out}, \mu_C)$: probability density distribution in the CM system,

E_C^{out}: outgoing energy in the CM system,

μ_C: direction cosine in the CM system,

$J = \frac{dE_C^{out}}{dE_L^{out}} \frac{d\mu_C}{d\mu_L}$: Jacobian.

It should be noted that E_L^{in} and E_L^{out} are fixed in the integration of Eq. (8.57). Note also that the Jacobian J is necessary since the probability density function $p_C\left(E_L^{in}, E_C^{out}, \mu_C\right)$ is given per unit E_C^{out} per unit μ_C while integration is carried out with μ_L, and $p_{L,l}\left(E_L^{in}, E_L^{out}\right)$ is given per unit E_L^{out}.

In the calculation of $p_{L,l}\left(E_L^{in}, E_L^{out}\right)$, the following relations are used.

$$J = \sqrt{\frac{E_L^{out}}{E_C^{out}}} = \frac{1}{\sqrt{1 + c^2 - 2c\mu_L}}, \tag{8.58}$$

$$c = \frac{1}{A+1}\sqrt{\frac{E_L^{in}}{E_L^{out}}} = \frac{1}{A+1}\frac{v_L^{in}}{v_L^{out}} = \frac{v_L^{in}}{A+1}\frac{1}{v_L^{out}} = v_{cm}\frac{1}{v_L^{out}} = \frac{v_{cm}}{v_L^{out}}, \tag{8.59}$$

$$\mu_C = J(\mu_L - c), \tag{8.60}$$

$$\mu_L^{min} = \frac{1}{2c}\left(1 + c^2 - \frac{E_C^{out,max}}{E_L^{out}}\right), \tag{8.61}$$

$$E_L^{out,max} = E_L^{in}\left(\sqrt{\frac{E_C^{out,max}}{E_L^{in}}} + \frac{1}{A+1}\right)^2, \tag{8.62}$$

where

E_C^{out}: outgoing energy of a neutron in the CM system,

E_L^{out}: outgoing energy of a neutron in the LAB system,

E_L^{in}: incident energy of a neutron in the LAB system,

μ_L: scattering cosine direction in the LAB system,

μ_C: scattering cosine direction in the CM system,

A: relative atomic mass.

Detail calculation procedures are as follows.

(1) Set the incident energy E_L^{in}.

(2) Set $E_C^{out,max}$ from the maximum value of the energy grid in an ACE file for inelastic scattering.

(3) Set $E_L^{out,max}$ from Eq. (8.62).

(4) Set outgoing energy group g'. Energy group boundaries in the LAB system are $E_L^{out,g',upper}$ and $E_L^{out,g',lower}$.

(5) If $E_L^{out,g',lower} < E_L^{out,max} < E_L^{out,g',upper}$, set $E_L^{out,g',upper}$ to be $E_L^{out,max}$.

(6) Sufficiently subdivide the energy range between $E_L^{out,g',upper}$ and $E_L^{out,g',lower}$. The lethargy width of 0.01 is used for subdivision. To avoid too finer or coarser subdivisions, the number of sub-divisions in energy group g' is limited to between 5 and 100.

(7) Calculate μ_L^{min} using Eq. (8.61).

(8) Sufficiently subdivide direction cosine from $+1$ to μ_L^{min}. The number of intervals for angle integration is the maximum of 20 and the number of angle points in the DLW block for inelastic scattering.

(9) Calculate J using Eq. (8.58).

(10) Calculate μ_C using Eq. (8.60).

(11) Calculate E_C^{out} using Eq. (8.58) and the value of J obtained in Step (9).

(12) Interpolate the probability density $p_C\left(E_L^{in}, E_C^{out}, \mu_C\right)$ using the results of Steps (10) and (11).

(13) Perform numerical integration of Eq. (8.57) to obtain $p_{L,l,g'}\left(E_L^{in}\right)$.

(14) Finally, the multi-group scattering cross-section is calculated by

$$\sigma_{s,l,g\to g'} = \frac{\int_{E\in E_g} \sigma_s\left(E_L^{in}\right) p_{L,l,g'}\left(E_L^{in}\right) \phi_l\left(E_L^{in}\right) dE_L^{in}}{\int_{E\in E_g} \phi_l\left(E_L^{in}\right) dE_L^{in}} \approx \frac{\sum_i \sigma_s\left(E_{L,i}^{in}\right) p_{L,l,g'}\left(E_{L,i}^{in}\right) \phi_l\left(E_{L,i}^{in}\right) \Delta E_{L,i}^{in}}{\sum_i \phi_l\left(E_{L,i}^{in}\right) \Delta E_{L,i}^{in}}. \tag{8.63}$$

Equation (8.63) is numerically integrated. The following energy grid is also considered in numerical integration for accurate calculation:

-multi-group energy group boundary,

-incident energy whose outgoing energy with $\mu_{CM} = -1$ is a multi-group boundary.

$\Delta E_{L,i}^{in}$ in Eq. (8.63) is set assuming the lethargy width of 0.001.

8.3.6.5 Other reactions (LAW=4: continuous tabular distribution)

The outgoing energy distribution is given in a tabulated form for each incident energy grid. The table is interpolated based on the option specified by INTT (1/2 = histogram/linear-linear). The incident and outgoing energies are specified in the laboratory system.

8.3.6.6 Other reactions (LAW=7: simple Maxwellian fission spectrum)

The outgoing energy distribution is given by[13)]

$$f(E\to E') = \frac{\sqrt{E'}}{I} \exp\left(-\frac{E'}{\theta(E)}\right), 0 \le E' \le (E-U), \tag{8.64}$$

where

I: normalization factor to make $\int_0^{E-U} f(E\to E')dE' = 1$,

$\theta(E)$: effective temperature as a function of incident energy,

U: a constant to define the upper limit of outgoing energy.

By integrating Eq. (8.64), the multi-group expression is obtained.

$$f(E \to g') = \int_{E_{g'l}}^{E_{g'u}} f(E \to E')dE' = \int_0^{E_{g'u}} f(E \to E')dE' - \int_0^{E_{g'l}} f(E \to E')dE'$$
$$= \frac{1}{I}\left(h(E_{g'u}) - h(E_{g'l})\right), \tag{8.65}$$
$$h(E') = -\theta(E)\sqrt{E'}\exp\left(-\frac{E'}{\theta(E)}\right) + \frac{\sqrt{\pi}}{2}\theta(E)^{\frac{3}{2}}\operatorname{erf}\left(\sqrt{\frac{E'}{\theta(E)}}\right),$$

where $E_{g'u}$ and $E_{g'l}$ show the upper and lower energy boundary of g'-th group.

The incident and outgoing energies are specified in the laboratory system. The analytical form of the normalization factor I is given in the ENDF-6 format manual, but I is numerically obtained as follows in FRENDY:

$$I = \sum_{g'} f(E \to g'). \tag{8.66}$$

Finally, the multi-group transfer probability is calculated by

$$f(g \to g') = \frac{\int_{E_{gl}}^{E_{gu}} \sigma_x(E)\phi_0(E)f(E \to g')dE}{\int_{E_{gl}}^{E_{gu}} \sigma_x(E)\phi_0(E)dE}, \tag{8.67}$$

where

E_{gu}, E_{gl}: upper and lower energy boundary of group g, the highest value of E_{gu} is U,

$f(g \to g')$: group to group transfer probability,

$\sigma_x(E)$: microscopic reaction cross-section of type x,

$\phi_0(E)$: scalar flux.

In the case of the fission spectrum, $\nu(E)\sigma_f(E)$ is used for $\sigma_x(E)$. Numerical integration of Eq. (8.67) is carried out assuming the lethargy width of dE to be 0.001.

8.3.6.7 Other reactions (LAW=9: evaporation spectrum)

The outgoing energy distribution is given by[13)]

$$f(E \to E') = \frac{E'}{I}\exp\left(-\frac{E'}{\theta(E)}\right), 0 \le E' \le (E - U), \tag{8.68}$$

where

I: normalization factor so that $\int_0^{E-U} f(E \to E')dE' = 1$,

$\theta(E)$: effective temperature as a function of incident energy,

U: a constant to define the upper limit of outgoing energy.

By integrating Eq. (8.67), the multi-group expression is obtained.

$$f(E \to g') = \int_{E_{g'l}}^{E_{g'u}} f(E \to E')dE' = \int_0^{E_{g'u}} f(E \to E')dE' - \int_0^{E_{g'l}} f(E \to E')dE'$$
$$= \frac{1}{I}\left(h\left(E_{g'u}\right) - h\left(E_{g'l}\right)\right), \tag{8.69}$$
$$h(E') = \theta(E)\left(\theta(E) - \exp\left(-\frac{E'}{\theta(E)}\right)\left(E' + \theta(E)\right)\right).$$

The incident and outgoing energies are specified in the laboratory system. The normalization factor *I* is obtained by the same procedure shown in LAW=4. The multi-group transfer probabilities are obtained as well.

8.3.6.8 Other reactions (LAW=11: energy-dependent Watt spectrum)

The outgoing energy distribution is given by[13)]

$$f(E \to E') = \frac{\exp\left(-\frac{E'}{a}\right)}{I}\sinh\left(\sqrt{bE'}\right), 0 \le E' \le (E - U), \tag{8.70}$$

where

I: normalization factor so that $\int_0^{E-U} f(E \to E')dE' = 1$,

a, b: parameters as a function of incident energy,

U: a constant to define the upper limit of outgoing energy.

By integrating Eq. (8.68), the multi-group expression is obtained.

$$f(E \to g') = \int_{E_{g'l}}^{E_{g'u}} f(E \to E')dE' = \int_0^{E_{g'u}} f(E \to E')dE' - \int_0^{E_{g'l}} f(E \to E')dE'$$
$$= \frac{1}{I}\left(h\left(E_{g'u}\right) - h\left(E_{g'l}\right)\right),$$
$$h(E') = \frac{\sqrt{a^3 b\pi}}{4}\exp\left(\frac{ab}{4}\right)\left(-\operatorname{erf}\left(\frac{a\sqrt{b} - 2\sqrt{E'}}{2\sqrt{a}}\right) + \operatorname{erf}\left(\frac{a\sqrt{b} + 2\sqrt{E'}}{2\sqrt{a}}\right)\right) \tag{8.71}$$
$$- a\exp\left(-\frac{E'}{a}\right)\sinh\left(\sqrt{bE'}\right).$$

The incident and outgoing energies are specified in the laboratory system. The normalization factor *I* is obtained by the same procedure shown in LAW=4. The multi-group transfer probabilities are obtained as well.

8.3.6.9 Other reactions (*LAW=66: n-body phase-space distribution*)

The outgoing energy distribution is given by[13)]

$$f(E_C \to E'_C, \mu_C) = C_n\sqrt{E'_C}(E_C^{max} - E'_C),$$
$$C_3 = \frac{4}{\pi(E_C^{max})^2}, \tag{8.72}$$

$$C_4 = \frac{105}{32(E_C^{max})^{\frac{7}{2}}},$$

$$C_5 = \frac{256}{14\pi(E_C^{max})^5},$$

where

n: number of bodies in phase space, defined in an ACE file,

E_C^{max}: maximum possible outgoing energy in the CM system,

E_C: incident energy in the CM system,

E_C': outgoing energy in the CM system,

μ_C: scattering angle (cosine direction) in the CM system.

Since multi-group cross sections are calculated in the LAB system, the following relation is used in FRENDY:

$$f(E_L \to E_L', \mu_L) = C_n\sqrt{E_L'}\left(E_C^{max} - \left(E_L^* + E_L' - \mu_L\sqrt{E_L^* E_L'}\right)\right)^{\left(\frac{3n}{2}\right)-4},$$
$$E_L^* = \frac{E_L}{(A+1)^2}, \tag{8.73}$$

where

E_L: incident energy in the LAB system,

E_L': outgoing energy in the LAB system,

μ_L: scattering angle (cosine direction) in the LAB system.

The multi-group expression is given by

$$f_l(E \to g') = \int_{E_{g'l}}^{E_{g'u}} \int_{-1}^{1} f(E_L \to E_L', \mu_L) P_l(\mu_L) d\mu_L \, dE_L', \tag{8.74}$$

where

$E_{g'u}$: upper energy boundary of g'-th energy group,

$E_{g'l}$: lower energy boundary of g'-th energy group.

The normalization of $f_l(E \to g')$ and evaluation of the multi-group transfer probabilities are carried out by the same procedure shown in LAW=4.

8.3.7 Thermal Cross-Sections

8.3.7.1 Incoherent inelastic (free gas model)

The thermal incoherent inelastic scattering for free gas (unbounded atom) is given by

$$\sigma^{inc,inela}(E, E', \mu) = \frac{\sigma_b}{2kT}\sqrt{\frac{E'}{E}}\frac{1}{\sqrt{4\pi\alpha}}\exp\left(-\frac{(\alpha+\beta)^2}{4\alpha}\right), \tag{8.75}$$

$$\alpha = \frac{E' + E - 2\mu\sqrt{EE'}}{AkT},$$

$$\beta = \frac{E' - E}{kT},$$

where

$\sigma_b = \sigma_{free}\frac{(A+1)^2}{A^2}$: the incoherent inelastic scattering cross-section for the bounded state,

σ_{free}: elastic scattering cross-section for unbounded (free) state obtained by pointwise elastic scattering cross-section,

A: relative mass of a nucleus to a neutron,

k: Boltzmann constant [eV/K],

T: Temperature [K],

E: incident energy in the LAB system,

E': outgoing energy in the LAB system,

μ: scattering cosine angle in the LAB system.

The Legendre moments of $\sigma^{inc}(E, E', \mu)$ can be calculated by

$$\sigma_l^{inc,inela}(E, E') = \int_{-1}^{1} \sigma^{inc}(E, E', \mu) P_l(\mu) d\mu, \tag{8.76}$$

where

$P_l(\mu)$: Legendre polynomial of *l*-th order.

Behavior of $\sigma^{inc}(E, E', \mu)P_l(\mu)$ can be very steep for μ when E and E' are close to each other and α can be zero for particular μ. Therefore, conventional numerical integration using the trapezoidal rule requires very fine division on μ therefore longer computation time is necessary. In NJOY, Eq. (8.76) is numerically integrated by the adaptive integration using successive halving of integration intervals. The accuracy of numerical integration is controlled by a tolerance that is given by a user. Note that the minimum value of α is defined in NJOY (10^{-6}) to avoid the numerical issue.

In FRENDY, the following formula is used instead of Eqs. (8.75) and (8.76):[64]

$$\sigma_l^{inc,inela}(E, E') = \int_{\sqrt{a-b}}^{\sqrt{a+b}} \frac{2c}{b} \exp\left(-\frac{1}{4}\left(u + \frac{\beta}{u}\right)^2\right) P_l\left(\frac{a - u^2}{b}\right) du,$$
$$a = \frac{E' + E}{AkT}, \tag{8.77}$$

$$b = \frac{2\sqrt{EE'}}{AkT},$$

$$c = \frac{\sigma_b}{4kT}\frac{1}{\sqrt{4\pi}}\sqrt{\frac{E'}{E}},$$

$$u^2 = \alpha.$$

It should be noted that $P_l\left(\frac{a-u^2}{b}\right)$ in Eq. (8.77) in the above reference seems to be incorrect.

Behavior of $\frac{2c}{b}\exp\left(-\frac{1}{4}\left(u+\frac{\beta}{u}\right)^2\right)$ is generally smoother than that of Eq. (8.75) thus the accuracy of numerical integration would be higher. The following figures show behaviors of Eq. (8.75) and integrand of Eq. (8.77) within the integration range, for E=0.01 [eV], E'=0.00999 [eV], A=230, T=600 [K], σ_b=1.0.

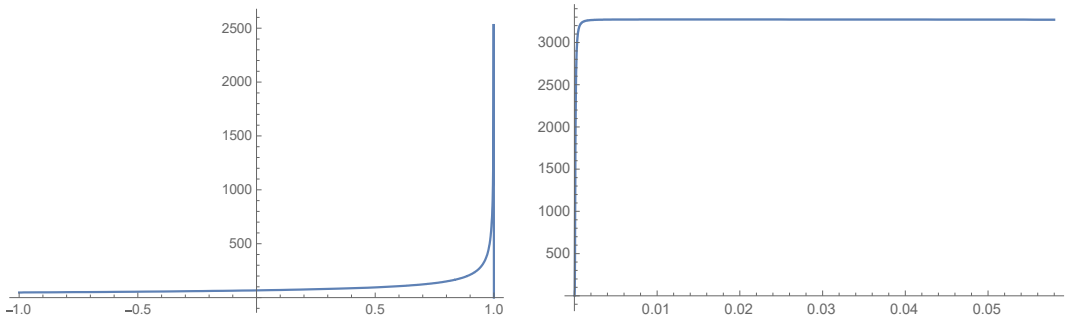

Eq. (8.75) Integrand of Eq. (8.77)

Figure 8.3.2 Example of pseudo resonance structure generation for the ladder method

The adaptive numerical integration is carried out in FRENDY to obtain $\sigma_l^{inc}(E,E')$ using Eq. (8.77) as follows.

(1) The integration range $[\sqrt{a-b},\sqrt{a+b}]$ is initially divided into 32 equivalent intervals.

(2) Estimate $f(u) = \frac{2c}{b}\exp\left(-\frac{1}{4}\left(u+\frac{\beta}{u}\right)^2\right)P_l\left(\frac{a-u^2}{b}\right)$ for $u = u_l, \frac{u_u+u_l}{2}, u_u$ where u_l and u_u are upper and lower bounds of the interval.

(3) Estimate $\varepsilon = \left|\frac{\left(\left(\frac{f(u_l)+f(u_u)}{2}\right)-f\left(\frac{u_u+u_l}{2}\right)\right)}{f\left(\frac{u_u+u_l}{2}\right)}\right|$ that indicates error due to linear interpolation of $f(u)$ for the integration range.

(4) If ε is larger than the tolerance (default:10^{-2}), the current interval is divided into two regions and

goes to Step (2).

(5) If ε is smaller than the tolerance, the integration value for the current interval is estimated by the Simpson formula as

$$\Delta\sigma_l^{inc,inela}(E,E') = \left(f(u_l) + 4f\left(\frac{u_u+u_l}{2}\right) + f(u_u)\right)\frac{u_u-u_l}{6}\Delta u. \tag{8.78}$$

(6) $\sigma_l^{inc}(E,E')$ is obtained by

$$\sigma_l^{inc,inela}(E,E') = \sum \Delta\sigma_l^{inc}(E,E'). \tag{8.79}$$

To obtain the multi-group cross-section, integration on energy is carried out as follows:

$$\sigma_{l,g\to g'}^{inc,inela} = \frac{\int_{E_g^{lower}}^{E_g^{upper}} \phi_l(E) \int_{E_{g'}^{lower}}^{E_{g'}^{upper}} \sigma_l^{inc,inela}(E,E')dE'\,dE}{\int_{E_g^{lower}}^{E_g^{upper}} \phi_l(E)dE} \tag{8.80}$$

$$= \frac{\sum_{E_i\in g} \Delta E_i\, \phi_l(E_i) \sum_{E_j\in g'} \sigma_l^{inc,inela}(E_i,E'_j)\Delta E'_j}{\sum_{E_i\in g} \Delta E_i\, \phi_l(E_i)},$$

where

ΔE_i: i-th energy interval for numerical integration,

E_i: i-th energy grid point,

$\phi_l(E_i)$: weighting flux.

The lethargy width of ΔE_i is set to 0.001. That of $\Delta E'_j$ is set to 0.001 when $g' = g$ and 0.005 when $g' \neq g$ since the variation of $\sigma_l^{inc,inela}(E,E')$ is steep when $E \approx E'$. The identical numerical integration scheme is used for other thermal cross-section treatments. The neutron spectra obtained for the infinite-dilute condition is used for $\phi_l(E)$. In this case, $\phi_l(E)$ is equivalent to $W(E)$ in Eq. (8.4).

To reduce the numerical integration error of Eq. (8.80), the analytical solution for $\sigma_0^{inc,inela}(E,E')$ is used. The analytical solution for the P_0 component of Eq. (8.77) is given as follows:[64)]

$$\sigma_{0,ana}^{inc,inela}(E,E') = \frac{\sigma_f}{E}\frac{\eta^2}{2}\left[\exp\left(\frac{E}{kT}-\frac{E'}{kT}\right)\left\{\mathrm{erf}\left(\eta\sqrt{\frac{E}{kT}}-\rho\sqrt{\frac{E'}{kT}}\right)\right.\right.$$

$$\left.\pm\,\mathrm{erf}\left(\eta\sqrt{\frac{E}{kT}}+\rho\sqrt{\frac{E'}{kT}}\right)\right\} \tag{8.81}$$

$$\left.+\left\{\mathrm{erf}\left(\eta\sqrt{\frac{E'}{kT}}-\rho\sqrt{\frac{E}{kT}}\right)\mp\mathrm{erf}\left(\eta\sqrt{\frac{E'}{kT}}+\rho\sqrt{\frac{E}{kT}}\right)\right\}\right],$$

where erf is the error function, $\eta = \frac{A+1}{2\sqrt{A}}$, $\rho = \frac{A-1}{2\sqrt{A}}$, and upper/lower signs correspond to $E < E'$ or $E' < E$, respectively.

Direct utilization of Eq. (8.80) in numerical calculation results in severe numerical round-off error. Therefore, the following relations are used in the actual implementation of the numerical calculation of $\mathrm{erf}(x) + \mathrm{erf}(y)$ or $\mathrm{erf}(x) - \mathrm{erf}(y)$.

$$\begin{aligned} & x \times y > 0,\ \mathrm{erf}(x) + \mathrm{erf}(y), \\ x \times y < 0,\ \mathrm{erf}(x) + \mathrm{erf}(y) &= \mathrm{erf}(x) - \mathrm{erf}(-y) = 1 - \mathrm{erfc}(x) - (1 - \mathrm{erfc}(-y)) \\ &= \mathrm{erfc}(-y) - \mathrm{erfc}(x), \end{aligned} \tag{8.82}$$

$$\begin{aligned} \sigma_{0,ana}^{inc,inela}(E,E') = \frac{\sigma_f}{E}\frac{\eta^2}{2} & x \times y > 0, \mathrm{erf}(x) - \mathrm{erf}(y) = 1 - \mathrm{erfc}(x) - (1 - \mathrm{erfc}(y)) \\ &= \mathrm{erfc}(y) - \mathrm{erfc}(x), \\ & x \times y < 0, \mathrm{erf}(x) - \mathrm{erf}(y), \end{aligned} \tag{8.83}$$

where $\mathrm{erfc}(x) \equiv 1 - \mathrm{erf}(x)$ is the complementary error function and is an intrinsic function is provided in C++.

Once $\sigma_0^{inc,inela}(E,E')$ is obtained, then $\sigma_{0,g\to g',ana}^{inc,inela}$ is calculated by

$$\begin{aligned} \sigma_{0,g\to g',ana}^{inc,inela} &= \frac{\int_{E_g^{lower}}^{E_g^{upper}} w(E) \int_{E_{g'}^{lower}}^{E_{g'}^{upper}} \sigma_{0,ana}^{inc,inela}(E,E')dE'\,dE}{\int_{E_g^{lower}}^{E_g^{upper}} w(E)dE} \\ &= \frac{\sum_{E_i \in g} \Delta E_i\, w(E_i) \sum_{E_j \in g'} \sigma_{0,ana}^{inc,inela}(E,E')\Delta E'_j}{\sum_{E_i \in g} \Delta E_i\, w(E_i)}. \end{aligned} \tag{8.84}$$

The adaptive numerical integration for Eq. (8.77) is used but $\varepsilon = 0.001$ is used to obtain accurate results.

Finally, $\sigma_{l,g\to g'}^{inc,inela}$ are normalized as

$$\hat{\sigma}_{l,g\to g'}^{inc,inela} = \sigma_{l,g\to g'}^{inc,inela} \frac{\sigma_{0,g\to g',ana}^{inc,inela}}{\sigma_{0,g\to g'}^{inc,inela}}. \tag{8.85}$$

The analytical solution for the higher Legendre components can be obtained by the analytical integration of Eq. (8.85). Thus analytical solution may be used in Eq. (8.80). However, numerical instability is observed due to severe numerical round-off error. Therefore, normalization using only P_0 component is carried out in FRENDY.

8.3.7.2 Incoherent inelastic (SCT approximation)

When the energy transfer is large in the thermal energy range, the short time collision (SCT) approximation can be used instead of the free gas approximation:[65)]

$$\sigma^{inc,inela}(E,E',\mu)=\frac{\sigma_b}{2kT}\sqrt{\frac{E'}{E}}\frac{1}{\sqrt{4\pi\alpha}}\sqrt{\frac{T}{T_{eff}}}\exp\left(-\frac{(\alpha-|\beta|)^2}{4\alpha}\frac{T}{T_{eff}}-\frac{\beta+|\beta|}{2}\right), \tag{8.86}$$

where T and T_{eff} are temperature and the effective temperature in [K]. The effective temperatures are taken from the NJOY2016 values, which come from ENDF-B/III, ENDF/B-VIII, or JENDL-5.

Equation (8.86) is formulated as follows to be consistent with the calculation of free gas:

$$\begin{aligned}
&\sigma^{inc,inela}(E,E',\mu)\\
&=\frac{\sigma_b}{2kT}\sqrt{\frac{E'}{E}}\frac{1}{\sqrt{4\pi\alpha}}\sqrt{\frac{T}{T_{eff}}}\exp\left(-\frac{(\alpha+\beta)^2}{4\alpha}+\frac{(\alpha+\beta)^2}{4\alpha}\right.\\
&\left.-\frac{(\alpha-|\beta|)^2}{4\alpha}\frac{T}{T_{eff}}-\frac{\beta+|\beta|}{2}\right)\\
&=\frac{\sigma_b}{2kT}\sqrt{\frac{E'}{E}}\frac{1}{\sqrt{4\pi\alpha}}\sqrt{\frac{T}{T_{eff}}}\exp\left(-\frac{(\alpha+\beta)^2}{4\alpha}\right.\\
&\left.+\left(1-\frac{T}{T_{eff}}\right)\frac{(\alpha-|\beta|)^2}{4\alpha}\right)\\
&=\frac{\sigma_b}{2kT}\sqrt{\frac{E'}{E}}\frac{1}{\sqrt{4\pi\alpha}}\exp\left(-\frac{(\alpha+\beta)^2}{4\alpha}\right)\\
&\times\sqrt{\frac{T}{T_{eff}}}\exp\left(-\frac{(\alpha+\beta)^2}{4\alpha}+\left(1-\frac{T}{T_{eff}}\right)\frac{(\alpha-|\beta|)^2}{4\alpha}\right).
\end{aligned} \tag{8.87}$$

Equation (8.87) further converted to

$$\begin{aligned}
\sigma_l^{inc,inela}(E,E')=&\int_{\sqrt{a-b}}^{\sqrt{a+b}}\frac{2c}{b}\exp\left(-\frac{1}{4}\left(u+\frac{\beta}{u}\right)^2\right)\\
&\times\sqrt{\frac{T}{T_{eff}}}\exp\left(\frac{1}{4}\left(1-\frac{T}{T_{eff}}\right)\left(u-\frac{|\beta|}{u}\right)^2\right)P_l\left(\frac{a-u^2}{b}\right)du.
\end{aligned} \tag{8.88}$$

The difference between Eqs. (8.69) and (8.80) is the following factor in the integrand:

$$\sqrt{\frac{T}{T_{eff}}}\exp\left(\frac{1}{4}\left(1-\frac{T}{T_{eff}}\right)\left(u-\frac{|\beta|}{u}\right)^2\right). \tag{8.89}$$

Namely, the identical numerical integration procedures can be used for the free gas and SCT except for the factor shown in Eq. (8.89).

8.3.7.3 Incoherent inelastic (S(α,β) data in an ACE file)

The $S(\alpha,\beta)$ data except for the free gas model and the SCT approximation are stored in the thermal scattering block of a thermal ACE file. The following data are given in the case of incoherent inelastic scattering:

•Cross sections for incident energy grid points. (ITIE block),

•Energy/angle distribution table for each incident energy grid point (ITXE block).

In the ITXE block, scattering angle distribution is described in the discrete cosines of scattering angle providing equal probability in each bin. All energies and angles are represented in the LAB system. Therefore, the Legendre components are calculated by

$$\sigma_l^{inc,inela}(E,E') = \sum_{i=1}^{N_\mu} \sigma^{inc,inela}(E,E') \frac{1}{N_\mu} P_l(\mu_i)\,, \tag{8.90}$$

where

$\sigma^{inc}(E,E')$: incoherent inelastic scattering cross-section given in ITIE block and incident and outgoing energies are given by the LAB system,

N_μ: number of equiprobable cosine bins,

μ_i: direction cosine of i-th bin in the LAB system.

To describe the energy transfer probability, one of the following three options are used in an ACE file:

(1) Equally distributed energy grid points (ifeng=0 in ACE file, iwt=1 in ACER),

(2) Skewed distribution of energy grid points (ifeng=1 in ACE file, iwt=0 in ACER),

(3) Continuous distribution energy grid points (ifeng=2 in ACE file, iwt=2 in ACER).

In option (1), outgoing energy is divided into intervals having an equal probability for outgoing energy. Then the average energy preserving average outgoing energy for each energy interval is calculated. The average energy is used as the outgoing energy grid point. In option (2), the skewed weight is used rather than the equal weight in option (1). The first and the last energy intervals have a relative weight of 1, the second and the second-to-last have a relative weight of 4, and the rest of the energy intervals have a relative weight of 10. The setting of average energy for each interval is the same for option (1). Finally, in option (3), many outgoing energy grid points and associate cumulative outgoing probabilities are tabulated.

Since outgoing energy grid points for options (1) and (2) may be too coarse, utilization of ACE files with these options is not recommended. Option (3) is highly recommended to obtain accurate thermal scattering cross-sections. However, options (1) and (2) may be adopted in an ACE file since option (3) can be handled by MCNP version 6 or later and the default input data of ACER in

NJOY2016 is option (2).

To obtain a multi-group scattering cross-section, energy grid points should be further sub-divided since energy grid points and multi-group energy structures are inconsistent. Therefore, a probability density distribution within the outgoing energy range defined in an ACE file is necessary for options (1) and (2). The discretization error becomes large when the probability distribution within an outgoing energy interval is assumed to be constant in options (1) and (2). The larger discretization error results in the unphysical shape of the neutron spectrum in the thermal energy region. Therefore, the probability distribution within an outgoing energy interval is assumed as follows to reduce the discretization error of energy grid points.

$$\sigma^{inc,inela}(E,E') = \begin{cases} \sigma^{inc,inela}(E) f_i \exp\left(-\dfrac{E'}{kT}\right), E < E' \\ \sigma^{inc,inela}(E) f_i \operatorname{erf}\left(\sqrt{\dfrac{E'}{kT}}\right), E > E' \end{cases} \tag{8.91}$$

where f_i is the normalization factor defined by

$$f_i = \begin{cases} \dfrac{w_i}{\int_{E_{i,l}}^{E_{i,u}} \exp\left(-\dfrac{E'}{kT}\right) dE'}, E < E' \\ \dfrac{w_i}{\int_{E_{i,l}}^{E_{i,u}} \operatorname{erf}\left(\sqrt{\dfrac{E'}{kT}}\right) dE'}, E > E' \end{cases} \tag{8.92}$$

w_i:weight for i-th energy interval, which is specified by iwt,
$E_{i,l}$: lower energy boundary of *i*-th outgoing energy interval,
$E_{i,u}$: upper energy boundary of *i*-th outgoing energy interval.

The outgoing energy intervals are not explicitly specified in a thermal ACE file since only outgoing energy grids are specified. Therefore, the outgoing energy intervals are assumed as follows in FRENDY:

$$\frac{E_{i+\frac{1}{2}} - E_i}{E_{i+1} - E_{i+\frac{1}{2}}} = \frac{w_i}{w_{i+1}}, \tag{8.93}$$

where
E_i: energy grid point for *i*-th interval,
$E_{i+\frac{1}{2}}$: boundary between *i*-th and (*i*+1)-th interval.

Note that the upper boundary for the highest interval is set to be thermal cut-off energy and the lower boundary for the lowest interval is set to be the lowest energy boundary of the multi-group structure.

8.3.7.4 Coherent elastic

No energy loss occurs in the coherent elastic scattering. The coherent elastic scattering only gives a self-scattering component since the incident and outgoing energies are identical. The coherent elastic scattering cross-section is written as

$$\sigma^{coh,ela}(E,\mu) = \sum_{i\in(\mu_i\geq -1)} \frac{b_i}{E}\delta(\mu-\mu_i), \qquad \mu_i = 1-2\frac{E_i}{E}\ , \tag{8.94}$$

where

b_i: size of step, defined later,

E_i: the energy of *i*-th Bragg edge.

The step size b_i can be calculated by the following relation, which is obtained by the angular integration of Eq. (8.94):

$$E\sigma^{coh,ela}(E) = \sum_{i\in(\mu_i\geq -1)} b_i, \tag{8.95}$$

In the ACE file, the coherent elastic scattering cross-section is given as follows:

$$\sigma^{coh,ela}(E) = \frac{P(i)}{E}\ , E_{ela}(i) \leq E < E_{ela}(i+1), \qquad \sigma^{coh,ela}(E) = 0, E < E_{ela}(1), \qquad \sigma^{coh,ela}(E) = \frac{P(N_{ela})}{E}, E_{ela}(N_{ela}) < E\ , \tag{8.96}$$

where

$P(i)$: constant given in an ACE file for the interval between *i*-th and (*i*+1)-th Bragg edges,

$E_{ela}(i)$: energy of *i*-th Bragg edge,

N_{ela}: total number of Bragg edges.

Once b_i is obtained, the Legendre components of the coherent elastic scattering cross-section are obtained by

$$\sigma_l^{coh,ela}(E) = \int_{-1}^{1}\sigma^{coh,ela}(E,\mu)d\mu = \sum_{i\in(\mu_i\geq -1)}\int_{-1}^{1}\frac{b_i}{E}P_l(\mu_i)\delta(\mu-\mu_i)d\mu = \sum_{i\in(\mu_i\geq -1)}\frac{b_i}{E}P_l(\mu_i). \tag{8.97}$$

8.3.7.5 Incoherent elastic

No energy loss occurs in the incoherent elastic scattering. The incoherent elastic scattering only gives a self-scattering component since the incident and outgoing energies are identical. In an ACE file, the discrete cosine directions having equally scattering probability are given. Therefore, the

Legendre component of an incoherent elastic scattering cross section is written as

$$\sigma_l^{incoh,ela}(E) = \sigma^{incoh,ela}(E)\frac{1}{N}\sum_{i=1}^{N} P_l(\mu_i)\,, \tag{8.98}$$

where

N: total number of discrete cosine directions,

μ_i: the i-th discrete cosine direction given in an ACE file.

The incoherent elastic scattering, $\sigma^{incoh,ela}(E)$, is tabulated as a function of incident energy in an ACE file.

8.3.8 Fission Spectrum, Nu-value, and Fission Cross-Section

8.3.8.1 Fission spectrum

In an ACE file, energy distributions for prompt and delayed neutrons are given in the DLW block. The fission spectrum for delayed neutron is calculated by

$$\chi_{D,i}(g \to g') = \frac{\int_{E\in g} \nu_{D,i}(E)\sigma_f(E)\phi(E)\int_{E'\in g'} f_{Di}(E \to E')dE'\,dE}{\int_{E\in g} \nu_{D,i}(E)\sigma_f(E)\phi(E)dE}, \tag{8.99}$$

$$\nu_{D,i}(E) = \nu_D(E)g_i(E),$$

where

$\chi_{D,i}(g \to g')$: delayed neutron spectrum for delayed group i, from group g to g',

$\nu_D(E)$: delayed neutron nu-value,

$\nu_{D,i}(E)$: delayed neutron nu-value for delayed group i,

$g_i(E)$: fraction of neutron for delayed group i,

$\sigma_f(E)$: fission cross-section,

$\phi(E)$: neutron spectrum (scalar flux),

$f_{Di}(E \to E')$: energy distribution of delayed neutron group i, from incident energy E to outgoing energy E', where $\int f_{Di}(E \to E')dE' = 1$.

The total delayed neutron spectrum is calculated by

$$\chi_D(g \to g') = \frac{\sum_i \int_{E\in g} \nu_{D,i}(E)\sigma_f(E)\phi(E)\int_{E'\in g'} f_i(E \to E')dE'\,dE}{\sum_i \int_{E\in g} \nu_{D,i}(E)\sigma_f(E)\phi(E)dE}. \tag{8.100}$$

The fission spectrum for prompt neutrons is calculated by

$$\chi_P(g \to g') = \frac{\int_{E\in g} \nu_P(E)\sigma_f(E)\phi(E)\int_{E'\in g'} f_P(E \to E')dE'\,dE}{\int_{E\in g} \nu_P(E)\sigma_f(E)\phi(E)dE}, \tag{8.101}$$

where

$\nu_P(E)$: prompt neutron nu-value,

$f_P(E \to E')$: energy distribution of prompt neutron, from incident energy E to outgoing energy E', where $\int f_P(E \to E')dE' = 1$.

Finally, the fission spectrum for total (both prompt and delayed) neutrons are calculated by

$$\chi(g \to g') = \frac{\begin{array}{c}\int_{E\in g} \nu_P(E)\sigma_f(E)\phi(E) \int_{E'\in g'} f_P(E \to E')dE'\, dE \\ +\sum_i \int_{E\in g} \nu_{D,i}(E)\sigma_f(E)\phi(E) \int_{E'\in g'} f_i(E \to E')dE'\, dE\end{array}}{\int_{E\in g} \nu_P(E)\sigma_f(E)\phi(E)dE + \sum_i \int_{E\in g} \nu_{D,i}(E)\sigma_f(E)\phi(E)dE}. \tag{8.102}$$

Equation (8.102) is usually used for steady-state calculations.

8.3.8.2 Nu-values

The total and/or delayed nu-values are given in an ACE file. In FRENDY, the prompt nu-values are not used even if they are given in the ACE file. The prompt nu-value is calculated by subtracting the delayed nu-value from the total nu-value. Any number of delayed neutron groups can be used in FRENDY. These values are calculated by

$$\begin{aligned} \nu_T(g) &= \frac{\int_{E\in g} \nu_T(E)\sigma_f(E)\phi(E)dE}{\int_{E\in g} \sigma_f(E)\phi(E)dE}, \\ \nu_D(g) &= \frac{\int_{E\in g} \nu_D(E)\sigma_f(E)\phi(E)dE}{\int_{E\in g} \sigma_f(E)\phi(E)dE}, \\ \nu_P(g) &= \nu_T(g) - \nu_D(g). \end{aligned} \tag{8.103}$$

where

$\nu_T(g)$: total nu-value for group g,

$\nu_D(g)$: delayed nu-value for group g,

$\nu_P(g)$: prompt nu-value for group g.

8.3.8.3 Delayed neutron constants

The delayed neutron fraction of each group is calculated by

$$r_{D,i} = \frac{\int_{E\in g} \nu_{D,i}(E)\sigma_f(E)\phi(E)dE}{\sum_i \int_{E\in g} \nu_{D,i}(E)\sigma_f(E)\phi(E)dE}, \tag{8.104}$$

where

$r_{D,i}$: delayed neutron fraction of group i, normalized as $\sum_i r_{D,i} = 1$.

8.3.9 Output Format

8.3.9.1 KRAM cross-section format

The KRAM format was used in the KRAM code, which is a MOC transport solver.[58] The cross-sections generated in the KRAM format is especially suitable for ordinary transport calculations since various cross-sections are processed to be consistent with common transport solvers as follows:

$$\sigma_{t,g} = \sigma_{1,g}, \tag{8.105}$$

$$\sigma_{f,g} = \sigma_{18,g}, \tag{8.106}$$

$$\nu_g = \frac{\sum_{g'} \sigma_{18,g\to g'}}{\sigma_{18,g}} + \nu_{D,g}, \tag{8.107}$$

$$\sigma_{a,g} = \sigma_{18,g} + \sum_{i=102}^{117} \sigma_{i,g} + \left(1 - n_{5,g}\right)\sigma_{5,g} - \left(\sigma_{16,g} + \sigma_{24,g} + \sigma_{30,g} + \sigma_{41,g}\right), \tag{8.108}$$

$$\sigma_{s,g\to g'} = \sum_{\substack{i=2,5,16,17,24,\\ 25,30,37,41,42}} \sigma_{i,g\to g'} + \sum_{j=51}^{91} \sigma_{j,g\to g'}, \tag{8.109}$$

$$\chi_g = \frac{\left(\sum_{g'} \sigma_{18,g'\to g}\phi_{g'} + \chi_{D,g}\sum_{g'} \nu_{D,g'}\sigma_{18,g'}\phi_{g'}\right)}{\left(\sum_g \sum_{g'} \sigma_{18,g'\to g}\phi_{g'} + \sum_{g'} \nu_{D,g'}\sigma_{18,g'}\phi_{g'}\right)}, \tag{8.110}$$

where $\sigma_{i,g}$, $\sigma_{i,g\to g'}$, $n_{5,g}$, subscript D show 1D microscopic cross-section for MT=*i*, the 2D microscopic cross-section for MT=*i* from energy group *g* to *g'*, the number of released neutron for *g*-th energy group for MT=5, and delayed neutron parameters, respectively. Other notations are common ones in lattice physics computation. It should be noted the following relations are used to calculate MT=18, 103-107 when MT=18, 103-107 do not exist but the following reactions exist.

$$\sigma_{18,g} = \sum_{i=19,20,21,38} \sigma_{i,g}, \tag{8.111}$$

$$\sigma_{103,g} = \sum_{i=600}^{649} \sigma_{i,g}, \tag{8.112}$$

$$\sigma_{104,g} = \sum_{i=650}^{699} \sigma_{i,g}, \tag{8.113}$$

$$\sigma_{105,g} = \sum_{i=700}^{749} \sigma_{i,g}, \tag{8.114}$$

$$\sigma_{106,g} = \sum_{i=750}^{799} \sigma_{i,g}, \tag{8.115}$$

$$\sigma_{107,g} = \sum_{i=800}^{849} \sigma_{i,g}. \tag{8.116}$$

8.3.9.2 MATXS

The MATXS is a versatile cross-section format for multi-group cross-sections. The FRENDY code can output the generated multi-group cross sections in the MATXS format. The output cross-sections are chosen to be consistent with GROUPR/MATXSR in NJOY code. It means that part of the edited cross-sections in FRENDY are not used in the cross-section in the MATXS format. For example, though self-shielded cross sections are generated for all reactions with energy transfer in FRENDY, only the elastic scattering and fission matrix cross-sections are output as the self-shielded cross sections in the MATXS format.

All reaction types having 1D cross-section are output in the MATXS file. In addition to the cross-section, the following quantities are also output:

- P_0 multi-group flux,
- P_1 multi-group flux (current),
- Average direction cosine (mu-bar) (MT=251),
- Lethargy width (MT=258),
- Group averaged inverse velocity (MT=259).

The group averaged inverse velocity, the lethargy width, and the mu-bar are calculated by

$$\frac{1}{v_g} = \frac{\int_{E\in g} \frac{1}{v(E)} \phi(E) dE}{\int_{E\in g} \phi(E) dE}, \tag{8.117}$$

$$\Delta u_g = ln\left(\frac{E_{g,upper}}{E_{g,lower}}\right), \tag{8.118}$$

$$\bar{\mu} = \frac{\Sigma_{s1,g}}{\Sigma_{s0,g}} = \frac{\sum_{g'} \Sigma_{s1,g\to g'}}{\sum_{g'} \Sigma_{s0,g\to g'}}. \tag{8.119}$$

All 1D cross-sections are output for the infinite-dilute condition while the following cross-sections and parameters are output for shielded conditions:

- P_0 multi-group flux,
- P_1 multi-group flux (current),
- P_0 weighted total cross-section,
- P_1 weighted total cross-section,
- Elastic scattering,
- Fission cross-sections (MT=18, or 19, 20, 21, 38), if exist,
- Capture cross-section (MT=102),
- Inelastic scattering (MT=51).

All 2D cross-sections with energy transfer are output in the infinite-dilute condition. For the shielded conditions, only the elastic scattering and fission matrix cross-sections are output in the MATXS cross-section file.

In MATXS format, all shielded cross-sections are stored as the difference from those of the infinite-dilute cross-sections. However, P_0 and P_1 multi-group fluxes in the shielded conditions are stored as-is instead of the difference from those of the infinite-dilute conditions.

8.3.9.3 Full MATXS

The ordinally MATXS file is consistent with NJOY2016. However, as described in the previous section, limited reactions are output for shielded conditions. In FRENDY, another option to output all shielded cross-sections exist (FullMATXS option). In this option, all 1D/2D shielded cross-sections are output in the MATXS file include anisotropic scattering. In this option, the size of a MATXS file may become large.

8.3.9.4 GENDF

The GENDF format is used as the output file of the GROUPR module of NJOY. It is also used as an interface file format among several modules, such as DTFR, CCCCR, MATXSR, POWR, and WIMSR. In FRENDY, the GENDF output in text (ASCII) format is implemented. The GENDF format utilizes a similar format with that of ENDF.

The major structure of the GENDF format is as follows:

- General information, background cross-section, energy group structure (MF=1, MT=451),
- One-dimensional cross-sections, nu-value, flux (MF=3),
- Decay constant of the delayed neutron, delayed neutron spectrum if exist (MF=5),
- Two-dimensional cross-sections (MF=6).

The following points are the important to read the GENDF file.

- The floating-point number is expressed as the dedicated format of ENDF (*e.g.*, 9223500+4 instead of 9.22350e+4).
- The maximum and minimum value of the floating-point number is consistent with those in the ENDF format.
- Prompt fission spectrum can be obtained by the fission matrix (MT=18) in MF=6.
- Delayed neutron fraction is considered in the delayed neutron spectrum. Namely, the delayed neutron spectrum in the GENDF file is defined as the normalized delayed neutron spectrum multiplied by delayed neutron fraction. Therefore, the sum of the delayed neutron spectrum is identical to the delayed neutron fraction.
- Energy group index is numbered from lower to higher energy. Namely, the lowest energy group is

the 1st energy in GENDF.

8.3.9.5 Full GENDF

In FRENDY, a GENDF file consistent with that of NJOY2016 is generated in the default. However, limited reactions are output for shielded conditions in NJOY2016. Therefore, the FullGENDF option is available in FRENDY. In this option, all 1D/2D shielded cross-sections are output in the GENDF file include anisotropic scattering. The size of the GENDF file will be larger.

9 Modification of ENDF file

Users may need the modification of the ENDF-6 formatted file if they want to add or replace the other data in the evaluated nuclear data file, *e.g.*, the covariance data is not found in the original nuclear data file or users want to investigate the impact of the neutronics calculation on the difference of evaluated nuclear data file in each reaction type. However, the modification of the ENDF-6 formatted file is difficult for beginners. FRENDY prepares the ENDF modification tool to easily modify the ENDF-6 formatted file.

As shown in Fig. 9.1, the ENDF modification tool removes the specified MF/MT data in the original evaluated nuclear data file and adds and replaces the specified MF/MT data from the other evaluated nuclear data file. The functions of “add” and “replace” commands are the same. If a user selects the “replace” command and the specified MF/MT data is not found in the original file, this tool just adds the specified MF/MT data from the other evaluate nuclear data file. If a user selects the “add” command and the specified MF/MT data is found in the original file, this tool replaces the specified MF/MT data.

Note that the modified evaluated nuclear data file must be checked carefully since this tool does not check the new file. The MF=3 data is related to MF=4, 5, 6, 9, 10, and 33 data. If the user modifies MF=3 data, this modification may affect MF=4, 5, 6, 9, 10, and 33 data. This tool can replace the specified MF/MT data from not only the identical nuclide but also the other nuclide. This tool does not check the material number and automatically modifies the material number when the difference nuclide data is merged. The user must check if the input file is correct or not.

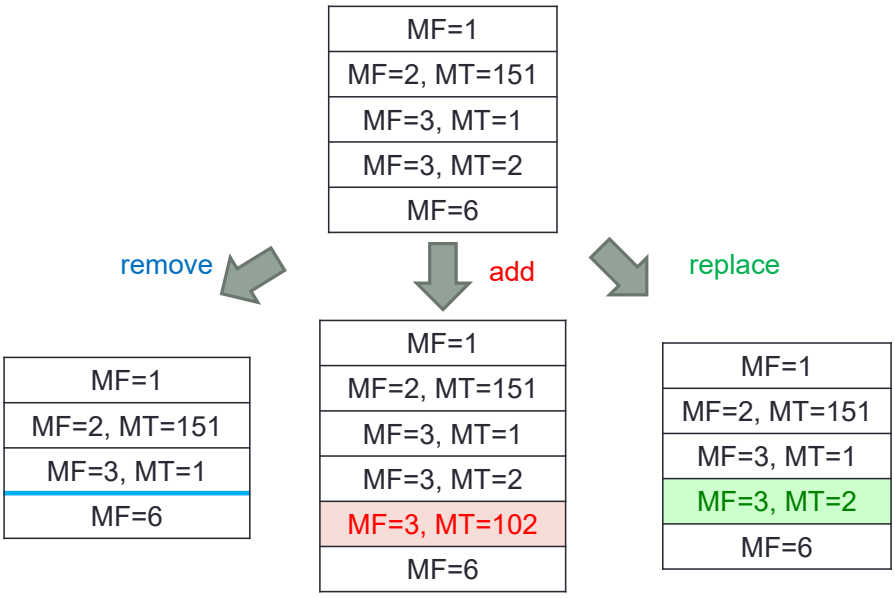

Figure 9.1 Example of ENDF modification tool

The ENDF modification tool has another function. This tool linearizes the TAB1 data in the ENDF-6 formatted file. Though some data processing codes linearize some data, *e.g.*, the cross section data in MF=3, the other data, e.g., the angular and the second energy distribution data in MF=4-6 do not linearize. These codes do not check the interpolation law and the interpolation law is considered the linear-linear or represented by the first interpolation law. In such cases, the processing results of these processing codes are not correct. The linearization of these data before the processing is one of the better ways to correctly process the nuclear data file.

The ENDF modification tool linearizes the TAB1 data in the specified MF or MF/MT data with a simple input file. This tool linearizes the TAB1 data when it reads the specified MF or MF/MT data. This function will help to process the evaluated nuclear data file.

The linearization process is identical to the linearization of the cross section which is described in Section 2.2.1. The default tolerance value for the linearization is 1.0E-3. The users can modify the tolerance value by the input parameter. The detail of the input parameter of this function and sample inputs are described in Section 10.8.

10 Input Instructions

10.1 Input Format

FRENDY accepts two types of input formats:

- FRENDY original input format,
- NJOY[7] compatible format.

The original input format requires only the processing mode name and evaluated nuclear data file name at the minimum. FRENDY has default values in the source code for nuclear data processing. Users can give the parameters in the input file if they want to change the parameters. The original input format is simple and does not require expert knowledge of nuclear data processing.

FRENDY can also treat the input files for NJOY Many users process the evaluated nuclear data file with NJOY. FRENDY interprets the input as the NJOY compatible format when the first parameter is the NJOY module name, *e.g.*, MODER and RECONR. The available module is MODER, RECONR, BROADR, PURR, UNRESR, THERMR, ACER, GROUPR, and MATXSR. Note that the UNRESR module is not prepared in FRENDY. FRENDY calculates the effective self-shielded cross-sections using the probability table method even if the user selects the UNRESR module. Users can easily use FRENDY without changing the input files for NJOY. They can therefore replace NJOY modules with FRENDY ones as they need. In addition, the modules of FRENDY and NJOY can be used in combination. For example, users can generate the multi-group cross-section data library using the GROUPR module of NJOY with the PENDF file generated by FRENDY.

10.2 FRENDY Original Input Format

In the conventional processing code including NJOY and PREPRO[9], users must select the running modules and prepare the input parameters for these modules to generate the cross-section data library. FRENDY automatically generates the cross-section data library with the recommended processing flow as shown in Fig. 10.2.1 when users select an appropriate processing mode at least. They do not need to worry about what modules are required to generate the cross-section data library when they use FRENDY original input format. FRENDY also prepares the skip option to manually select the modules to be executed. Using this option, users can skip some modules in the recommended processing flow.

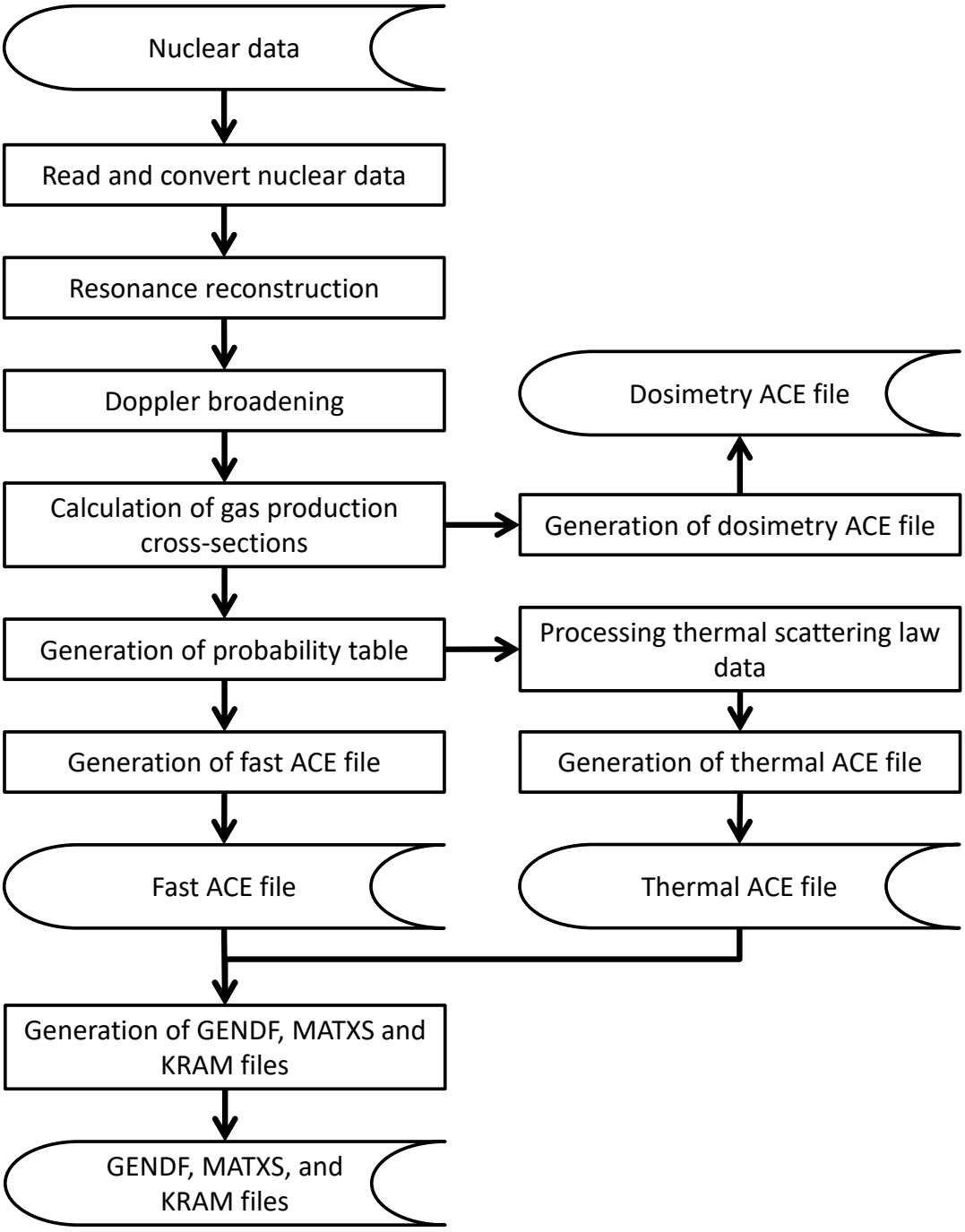

Figure 10.2.1 Processing flow to generate ACE, GENDF, MATXS, and KRAM files

10.2.1 Processing Mode

The order of the input data is free except for the first parameter. Users must set the processing mode as the first parameter. The available processing modes are listed in Table 10.2.1. The representation of the ACE file processing mode is identical to NJOY.

The neutron-induced data and the thermal scattering law data are available to generate the

multi-group cross-section file. The multi-group cross-section generation mode is not divided by the processing type since the FRENDY checks the input parameter and judges which type of data is processed.

FRENDY generates the multi-group cross-section file from the ACE file. The input file format is not only the ENDF-6 formatted file but also the ACE formatted file. The start file format does not set in the processing mode. The start file format is set in the input parameter “mg_start_file_mode”.

Table 10.2.1 Available processing mode

Processing mode name	Description
ace_file_generation_fast_mode ace_fast_mode ace_fast ace_file_generation_normal_mode ace_normal_mode ace_normal	Generation of the particle incident ACE file.
ace_file_generation_thermal_scattering_mode ace_file_generation_thermal_scatter_mode ace_therm_mode ace_therm ace_file_generation_tsl_mode ace_tsl_mode ace_tsl	Generation of the ACE file of the thermal scattering law data.
ace_file_generation_dosimetry_mode ace_dosi_mode ace_dosi	Generation of the ACE file of the dosimetry data.
mg_generation_neutron_mode mg_neutron_mode mg_neutron mg_mode mg	Generation of the neutron-induced multi-group XS file.
endf_file_modification_mode endf_file_modify_mode endf_mod_mode modify_endf_file_mode mod_endf_file_mode mod_endf_mode	Modification of ENDF-6 formatted file. The explanation of the input format is shown in Section 10.7.

10.2.2 Input Parameters

10.2.2.1 General information

The input data except the processing mode consists of “parameter name” and “parameter value”. Users need to set the parameters if they want to modify the default values. FRENDY original input format accepts comment lines. The C++ style comments are available, *i.e.*, “//” for a single line comment and “/* … */” for multi-line comments. FRENDY can read four types of data, *i.e.*, integer, real, string, and text, and the vector data of integer and real. The available types are as follows:

integer : integer number, *e.g.*, -2, -1, 0, 1, 2,
real : real number, *e.g.*, -1.0, 0.0, 1.0, 1.0E-1, 1.0E+1, 1.0D-1, 1.0D+1, 1.0-1, 1.0+1,
string : character data without space, *e.g.*, nuclide_name, calculation-type,
text : multiple lines character data.

Users have to set the vector data in a bracket when they want to set the vector data of integer and real value. If users want to set three values, *i.e.*, 1.0, 2.0, and 3.0, users write as follows:

(1.0 2.0 3.0).

Since FRENDY can read data specified in multiple lines, the following input style is also acceptable

```
(       1.0
        2.0
        3.0         ),
```

or

```
(
        1.0
        2.0
        3.0
                    ).
```

If users want to set the text data, they need to enclose single or double quotation marks. The text data allows multiple lines as follows:

“92-U-238 from JENDL-4.0

Processed with FRENDY
Processed day: 2017/10/13”

or

‘92-U-238 from JENDL-4.0
Processed with FRENDY
Processed day: 2017/10/13’

If users want to use double quotation marks in the comment line, single quotation marks are used to enclose the text data as follows:

‘This is the comment line for the PENDF file.
Users can use the “double quotation marks” when the comment line is enclosed by the single quotation marks.’

If users want to use single quotation marks in the comment line, double quotation marks are used to enclose the text data as follows:

“This is the comment line for the PENDF file.
Users can use the ‘single quotation marks’ when the comment line is enclosed by the double quotation marks.”

10.2.2.2 Input parameter name and recommended value for common utilities

nucl_file_name

Data type: string
Default value: This parameter must be required for the processing.
Explanation of this parameter: ENDF file name
Sample of this parameter

nucl_file_name (U235.dat)

pendf_label_data

Data type: string
Default value: none
Explanation of this parameter: Label for new PENDF tape (Max. 66 words)
Sample of this parameter

pendf_label_data (“PENDF file of U235 from JENDL-4.0”)

comment_data

Data type: list(string)

Default value: none

Explanation of this parameter: Comment line for the PENDF file.

FRENDY recognizes the comment line that is enclosed by double or single quotation.

If the user wants to use the double/single quotation in the comment line, please use the single/double quotation to enclose the comment.

Sample of this parameter

comment_data

("This is the comment line for the PENDF file.

User can use the 'single quotation mark' when the comment line is enclosed by the double quotation.")

error

Data type: real

Default value: 1.00×10^{-3}

Explanation of this parameter: Tolerance value for linearization.

Sample of this parameter

error 1.0E-3

error_max

Data type: real

Default value: error×10.0

Explanation of this parameter: Maximum tolerance value for linearization.

Sample of this parameter

error_max 1.0E-2

error_integral

Data type: real

Default value: error/20000.0

Explanation of this parameter: Maximum integral error for linearization.

Sample of this parameter

error_integral 5.0E-8

add_grid_data

Data type: list(real)

Default value: none

Explanation of this parameter: Additional energy grid [eV].

Sample of this parameter

add_grid_data (0.625 1.000 1.0E+6)

temp or temperature

Data type: real

Default value: 293.6 [K]

Explanation of this parameter: Temperature [K].

Sample of this parameter

temp 300.0

max_broading_ene

Data type: real

Default value: 1.00×10^{6} [eV]

Explanation of this parameter: Maximum energy for the Doppler broadening [eV].

If the upper limit of the resolved resonance energy E_h is smaller than max_broading_ene, the maximum energy for the Doppler broadening is modified to E_h.

Sample of this parameter

max_broadning_ene 1.0E+6

probability_bin_no

Data type: integer

Default value: 20

Explanation of this parameter: Number of probability table bins

Sample of this parameter

probability_bin_no 20

ladder_no

Data type: integer

Default value: 100

Explanation of this parameter: Number of resonance ladders for generating the probability table.

Sample of this parameter

ladder_no 100

sigma_zero_data

Data type: list(real)

Default value: 1.0×10^{10}, 1.0×10^{6}, 1.0×10^{5}, 10000.0, 1000.0, 100.0, 35.0, 10.0, 1.0, 0.1 [barns]

Explanation of this parameter

σ0 values for the Bondarenko-type self-shielded cross-section in the unresolved resonance region [barns]. Maximum σ0 is considered as the σinf value.

The multi-group cross-section generation function can automatically set the background cross-section. The input format for the automatic setting of the background cross-section is as follows:

sigma_zero_data (auto err N_{max} σ_{min} Target INT)

where,

err: Tolerance value.

N_{max}: Maximum number of the background cross-section.

σ_{min}: Minimum background cross-section [barns]

Target: Target of interpolation. (factor or rr)

INT: Interpolation method (cubic or linear)

rr: Interpolation error is estimated for reaction rate

linear: linear interpolation

cubic: monotone cubic interpolation.

Note that the background cross-section of PURR uses the recommended value when the user selects the automatic setting of the background cross-section.

If the upper limit of the resolved resonance energy E_h is smaller than max_broading_ene, the maximum energy for the Doppler broadening is modified to E_h.

Sample of this parameter

sigma_zero_data(1.0E10 1.0E6 1.0E5 10000.0 1000.0 100.0 35.0 10.0 1.0 0.1)

sigma_zero_data(auto 0.1 50 1.0e-10 rr linear)

ene_grid_no_par_ladder or ene_grid_par_ladder or ene _no_par_ladder

Data type: integer

Default value: 10000

Explanation of this parameter: Sampling energy grid number for each ladder number.

Sample of this parameter

ene_grid_no_par_ladder 10000

random_seed

Data type: integer

Default value: 12345

Explanation of this parameter: Random number seed for probability table generation.

Sample of this parameter

random_seed 11111

err_p_table or err_p_tab or err_ptab

Data type: real

Default value: 1.0E-2

Explanation of this parameter: Tolerance value for probability table generation.

If this parameter is used, the ladder_no parameter is disabled.

Sample of this parameter

err_p_table 0.01

ace_file_name

Data type: string

Default value: “nucl_file_name”.ace

Explanation of this parameter: ACE file name.

Sample of this parameter

ace_file_name U235.ace

ace_dir_file_name or ace_dir or mcnp_dir_file_name or mcnp_dir

Data type: string

Default value: "nucl_file_name".ace.dir

Explanation of this parameter: MCNP directory information for the ACE file

When the ace_file_name is set, the default value is "ace_file_name".ace.dir.

Sample of this parameter

ace_dir_file_name U235.xsdir

suffix_id

Data type: real

Default value: .00

Explanation of this parameter: The suffix ID for the ACE file.

Sample of this parameter

suffix_id 0.50

ace_label_data

Data type: string

Default value: none

Explanation of this parameter: Label for the ACE file. (Max. 70 words)

Sample of this parameter

ace_label_data "PENDF file of U235 from JENDL-4.0"

iz_aw_data

Data type: list(real)

Default value: none

Explanation of this parameter: The list of (iz, aw) pairs for the ACE file. (iz=1000.0×Z+A, aw=mass)

Sample of this parameter

iz_aw_data (92235.0 2.330250E+2)

cumulative_angle_distribution_format

Data type: string or integer

Default value: string = yes, integer = 1

Explanation of this parameter: Calculation option of whether new cumulative angular distributions for ACE file generation are used or not.

Available value is use, yes, no, default, 0, and 1 (0=no, 1=use/yes).

where

use, yes, default, 1: Use the new cumulative angular distribution.

no, 0: Do not use the new cumulative angular distribution.

Sample of this parameter

cumulative_angle_distribution_format yes

10.2.2.3 Input parameter name and recommended value which are used only for thermal scattering law data

nucl_file_name_tsl

Data type: string

Default value: This parameter must be required for the processing.

Explanation of this parameter: ENDF file name for thermal scattering law data.

Sample of this parameter

nucl_file_name_tsl (HinH2O.txt)

equi_probable_angle_no

Data type: integer

Default value: 10

Explanation of this parameter: Number of equiprobable angles for thermal scattering law data.

Sample of this parameter

equi_probable_angle_no 10

principal_atom_no

Data type: integer

Default value: FRENDY automatically set from the ENDF file.

Explanation of this parameter: Number of principal atoms for thermal scattering law data.

Sample of this parameter

principal_atom_no 1

atom_type_no

Data type: integer

Default value: FRENDY automatically set from the ENDF file.

Explanation of this parameter: Number of atom types in the mixed moderator.

Sample of this parameter

atom_type_no 1

inelastic_reaction_type_no

Data type: integer

Default value: 221

Explanation of this parameter: Reaction type (MT) number for the inelastic reaction.

Sample of this parameter

inelastic_reaction_type_no 1

max_thermal_ene

Data type: real

Default value: max(10.0, temp/300.0)

Explanation of this parameter: Maximum energy for thermal treatment.

Sample of this parameter

max_thermal_ene 10.0

thermal_za_id_name

Data type: string

Default value: ZA value of the ENDF file.

Explanation of this parameter: ZA ID name for the thermal ACE file (ZA=1000.0×Z+A, Max. 6 words).

Sample of this parameter

thermal_za_id_name lwtr

moderator_za_data

Data type: integer

Default value: none

Explanation of this parameter: Moderator component ZA value.

Sample of this parameter

moderator_za_data 1001

10.2.2.4 Input parameter name and recommended value which are used only for multi-group cross-section generation

mg_tsl_data_type

Data type: list (string)

Default value: This parameter must be required for the processing of the TSL data.

Explanation of this parameter: The S(α,β) type for the MATXS file.

The S(α,β) type used in FRENDY is shown in Table 10.2.2. The S(α,β) type has no impact on the GENDF file. Please set “free” when the user only generates the GENDF file.

Sample of this parameter

mg_tsl_data_type (hh2o)

mg_tsl_data_type (free)

Table 10.2.2 S(α,β) type name list and corresponding material name

Material name	S(α,β) type	Material name	S(α,β) type
Al	al	H in YH_2	hyh2
Be	be	H in ZrH	hzrh
Be in BeO	bebeo	Liquid Methane (CH_4)	lch4
Benzene	benz	N in UN	nun
C in SiC	csic	O in BeO	obeo
$C_5O_2H_8$	c5o2h8	O in D_2O	od2o
D in D_2O	dd2o	O in ICE (H_2O)	oice
Ortho-D	dortho	O in UO_2	ouo2
Para-D	dpara	Polyethylene (CH_2)	poly
Fe	fe	Solid Methane (CH_4)	sch4
Graphite	graph	Si in SIC	sisic
H in H_2O	hh2o	U in UN	uun
H in Ice (H_2O)	hice	U in UO_2	uuo2
Ortho-H	hortho	Y in YH_2	yyh2
Para-H	hpara	Zr in ZrH	zrzrh

mg_file_name

Data type: string

Default value: input file name

Explanation of this parameter: Multi-group XS file name.

The output file name is as follows:

"mg_file_name"_"mg_file_mode"_"ZAID of the ACE file".mg

Sample of this parameter

mg_file_name “U235”

mg_edit_mode or mg_edit_option or mg_edit_xs

Data type: list(string)

Default value: GENDF

Explanation of this parameter: Output format and output data of the multi-group cross-section generation.

The available output format and output data are as follows:

MATXS, SimpleMATXS, GENDF, FullMATXS, SimpleGENDF, FullGENDF, KRAMXS, 1DXS, 2DXS, NuChi, MGFlux, MGCurrent, UFG, UFG1DXS, and RUC.

where

MATXS: Microscopic cross-sections in MATXS format, consistent with NJOY2016.
SimpleMATXS: Microscopic cross-sections in MATXS format, consistent with NJOY99.
FullMATXS: Microscopic cross-sections in MATXS format without truncation of shielded cross-sections. Output file size may be large.
GENDF: Microscopic cross-sections in GENDF format consistent with NJOY2016.
SimpleGENDF: microscopic cross-sections in GENDF format, consistent with NJOY99.
FullGENDF: microscopic cross-sections in GENDF format without truncation of shielded cross-sections. Output file size may be large.
KRAMXS: microscopic cross-sections in KRAM format.

1DXS: One-dimensional cross-sections such as total, fission, radiative capture.
2DXS: Two-dimensional cross-sections such as elastic scattering, inelastic scattering, (n,2n) reaction.
NuChi: Nu-value and fission spectrum.
MGFlux: Multi-group flux (group integrated values).
MGCurrent: Multi-group current (group integrated values).
UFG: Ultra-fine group spectrum, total cross-sections, the slowing down source, total source.
UFG1DXS: One-dimensional ultra-fine group cross-sections such as total, fission, radiative capture.
RUC: The 0 K scattering cross section data. This data is used for the input file of the resonance upscattering resonance up-scattering correction (reso_upscat).

The user can select the specified MT number when 1DXS, 2DXS, and UFG1DXS options are selected as follows:

"1DXS 1, 2, 4, -50"

The minus value for MT means all MT numbers between the previous MT number.

Sample of this parameter

mg_edit_mode “U235”

mg_start_file_mode

Data type: string

Default value: ENDF

Explanation of this parameter: Format of the start file.

FRENDY generates the multi-group cross-section file from the ENDF-6 formatted file and the ACE file. The user selects which data is used to generate the multi-group cross-section file.

The available value is ENDF and ACE.

ENDF: A multi-group cross-section file is generated from the ENDF-6 formatted file.

ACE: A multi-group cross-section file is generated from the ACE file.

Sample of this parameter

mg_start_file_mode ENDF

mg_label_data

Data type: string

Default value: ENDF

Explanation of this parameter: The label of the multi-group cross-section file.

The label is output on the first line of the GENDF file.

Sample of this parameter

mg_label_data "Multi-group XS file of U235"

legendre_order

Data type: integer

Default value: 3

Explanation of this parameter: Maximum Legendre order (P_L order)

Sample of this parameter

legendre_order 3

max_thermal_ene_e_out

Data type: real

Default value: max_thermal_ene

Explanation of this parameter: Maximum energy of the thermal treatment for the outgoing particle energy [eV].

Sample of this parameter

max_thermal_ene_e_out 10.0

mg_weighting_spectrum_mode

Data type: string

Default value: 1/E

Explanation of this parameter: Weighting spectrum.

The available output format and output data are 1/E and Fission+1/E+Maxwell.

1/E: 1/E spectrum for the whole energy range.

Fission+1/E+Maxwell: Fission for fast energy range, 1/E for intermediate energy range,

Maxwell for the thermal energy range.

The other parameters are required to use "Fission+1/E+Maxwell" option as follows:

mg_weighting_spectrum(Fission+1/E+Maxwell E_h E_l T_{fis} E_1 E_2)

where

E_h: Highest energy [eV],

E_l: Lowest energy [eV],

T_{fis}: Fission temperature [eV],

E_1: Energy boundary between fission and 1/E spectra [eV],

E_2: Energy boundary between 1/E and Maxwell spectra [eV].

The sample of "Fission+1/E+Maxwell" is as follows:

mg_weighting_spectrum(Fission+1/E+Maxwell 2.0e+7 1.0e-5 1.6e+6 1.0e+6 0.625)

The default value of E_h, E_l, T_{fis}, E_1, and E_2 are 2.0e+7, 1.0e-5, 1.6e+6, 1.0e+6, and 0.0. When E_2 is 0.0, E_2 is automatically set by this program.

Sample of this parameter

mg_weighting_spectrum_mode “1/E”

mg_weighting_spectrum_data or **mg_weighting_spectrum**

Data type: list (real)

Default value: none

Explanation of this parameter: Weighting spectrum. The user can manually set the weight spectrum.

The format of the weight spectrum is similar to the TAB1 record in the ENDF-6 format as follows:

mg_weighting_spectrum_data(E_1 W_1 E_2 W_2 … E_{i-1} W_{i-1} E_i W_i)

where

E_i is the i^{th} value of energy [eV],

W_i is the i^{th} value of weight.

NJOY's weight spectrum, *i.e.*, the “iwt” number of the GROUPR module and the weighted spectrum name shown in Table 10.2.3, is also available. The input format to select the NJOY's weight spectrum is as follows:

mg_weighting_spectrum_data(iwtXX)

where XX is the “iwt” number (iwt02 ~ iwt12).

Sample of this parameter

mg_weighting_spectrum_data (1.0E-5 1.0 2.0E7 1.0)

mg_weighting_spectrum_data (iwt06)

mg_weighting_spectrum_data (epri-cell-lwr)

Table 10.2.3 Weighted spectrum name list and corresponding "iwt" number

iwt	Weighting spectrum name
2	constant
3	1/e
4	fission+1/e+maxwell
5	epri-cell-lwr
	epri-cell
	epri
9	claw-weight-function
10	claw-with-t-dependent
	claw-with-t-depend
	claw-with-t
	claw-t
11	vitamine-e
	vit-e
	ornl-5505
12	vitamine-e-with-t-dependent
	vitamine-e-with-t-depend
	vitamine-e-with-t
	vit-e-with-t-dependent
	vit-e-with-t-depend
	vit-e-with-t

mg_weighting_spectrum_data_int or **mg_weighting_spectrum_int**

Data type: list (integer)

Default value: 2 (linear-linear)

Explanation of this parameter: Interpolation method of the weight spectrum.

The format of the weight spectrum is similar to the TAB1 record in the ENDF-6 format as follows:

mg_weighting_spectrum_data_int(NBT_1 INT_1 NBT_2 INT_2 … NBT_{i-1} INT_{i-1} NBT_i INT_i)

where

NBT_i is the value of n separating the i^{th} and $(i+1)^{th}$ interpolation range,

INT_i is the interpolation scheme identification number used in the i^{th} range.

The available interpolation scheme is 1 (const), 2 (linear-linear), 3 (linear-log), 4 (log-liner), and 5 (log-log).

Sample of this parameter

mg_weighting_spectrum_data_int (2 1) //NBT=2, INT=1 (const)

mg_structure or mg_structure_neutron

Data type: list (real)

Default value: XMAS 172-group structure

Explanation of this parameter: Energy group structure.

The user can manually set the energy group structure [eV].

NJOY's energy group structure, *i.e.*, the "ign" number of the GROUPR module and the energy group structure name shown in Table 10.2.4, is also available. The input format to select the NJOY's energy group structure is as follows:

mg_structure(ignXX)

where XX is the ign number (ign02 ~ ign34, ign101).

The energy group structure can be automatically set by the user input.

The input format for the automatic setting of the energy group structure is as follows:

mg_structure (auto E_1 N_1 O_1 E_2 N_2 O_2 ... E_{i-1} N_{i-1} O_{i-1} E_i N_i O_i E_{i+1})

where

E_i: Energy boundary i [eV],

N_i: Number of divisions,

O_i: Option for divisions.

The available option for divisions O_i is as follows:

EL: Divide the energy range by equi-lethargy width,

EE: Divide the energy range by equi-energy width.

Sample of this parameter

```
mg_structure ( ign18 ) //XMAS 172-group structure
mg_structure ( 1.0E-5  0.625  2.0E+7 ) //2-group structure
mg_structure ( auto
               2.0e+07  3200   EL
               100.0    1      EL
               1.0e-5 )
```

Table 10.2.4 Energy group structure name list and corresponding "ign" number

ign	Energy group structure name	ign	Energy group structure name	ign	Energy group structure name
2	csewg-239	13	lanl-80	22	xmas-lwpc-172
	csewg	14	eurlib-100		xmas-lwpc
3	lanl-30		eurlib	23	vit-j-lwpc-175
4	anl-27	15	sand-iia-640		vit-j-lwpc
	anl		sand-iia	24	shem-cea-281
5	rrd-50		sand-640		shem-cea
	rrd	16	vitamin-e-174	25	shem-epm-295
6	gam-i-68		vitamin-e	26	shem-cea-epm-361
	gam-i		vitamin-174		shem-cea-epm
	gam-68		vit-e-174	27	shem-epm-315
7	gam-ii-100		vit-e	28	rahab-aecl-89
	gam-ii		vit-174		rahab-aecl
	gam-100	17	vitamin-j-175	28	rahab
8	laser-thermos-35		vitamin-j	29	ccfe-660
	laser-thermos		vitamin-175		ccfe
	laser		vit-j-175	30	ukaea-1025
	laser-35		vit-j	31	ukaea-1067
9	epri-cpm-69		vit-175	32	ukaea-1102
	epri-cpm	18	xmas-nea-lanl-172	33	ukaea-142
	epri		xmas-nea-lanl	34	lanl-618
	epri-69		xmas-lanl	101	vitamin-b6-199
10	lanl-187		xmas-nea		vitamin-199
11	lanl-70	19	ecco-33		vit-b6-199
12	sand-ii-620	20	ecco-1968		vit-199
	sand-ii	21	tripoli-315		
	sand-620		tripoli		

mg_structure_g or **mg_structure_gam** or **mg_structure_gamma**

Data type: list (real)

Default value: none

Explanation of this parameter: Photon (gamma) production energy group structure.

The user can manually set the energy group structure [eV].

If the user does not set this parameter, the photon production data generation is skipped.

NJOY's energy group structure, *i.e.*, the “igg” number of the GROUPR module and the energy group structure name shown in Table 10.2.5, is also available. The input format to select the NJOY's energy group structure is as follows:

mg_structure(iggXX)

where XX is the igg number (igg02 ~ igg10).

Table 10.2.5 Energy group structure name list and corresponding “igg” number

igg	Energy group structure name	igg	Energy group structure name
2	csewg-94	9	vitamin-e-38
	csewg		vitamin-e
3	lanl-12		vitamin-38
4	steiner-21		vit-e-38
	steiner		vit-e
5	straker-22		vit-38
	straker	10	vitamin-j-42
6	lanl-48		vitamin-j
7	lanl-24		vitamin-42
8	vitamin-c-36		vit-j-42
	vitamin-c		vit-j
	vitamin-36		vit-42
	vit-c-36		
	vit-c		
	vit-36		

mg_ufg_structure or **mg_ultra_fine_group_structure**

Data type: list (real)

Default value: (2.0e+07 10000 EL
52475.0 56000 EL
9118.8 12000 EL
4307.4 12000 EL
961.12 8000 EL
130.07 12000 EL
0.32242 10000 EL
1.0e-5)

Explanation of this parameter: Energy group structure to generate neutron flux in the ultra-fine group structure.

The format of this parameter is as follows:

mg_ufg_structure(E_1 N_1 O_1 E_2 N_2 O_2 ... E_{i-1} N_{i-1} O_{i-1} E_i N_i O_i E_{i+1})

where

E_i: Energy of i^{th} boundary [eV],

N_i: Number of divisions,

O_i: Option for divisions

The available option for divisions O_i is as follows:

EL: Divide the energy range by equi-lethargy width.

EE: Divide the energy range by equi-energy width.

Sample of this parameter

```
mg_ufg_structure
  (  2.0e+07        10000    EL
     52475.0        56000    EL
     9118.8         12000    EL
     4307.4         12000    EL
     961.12         8000     EL
     130.07         12000    EL
     0.32242        10000    EL
     1.0e-5 )
```

mg_number_density

Data type: list (real)

Default value: 1.0 (use only one nuclide)

Explanation of this parameter: Number density of each nuclide [1/barn/cm].

If the user processes the one nuclide data, this parameter can be skipped.

Sample of this parameter

```
mg_number_density   ( 1.0 )
```

mg_flux_calc_mode

Data type: string

Default value: SLD

Explanation of this parameter: Calculation option at the resonance region.

The available option at the resonance region is as follows:

NR: Use narrow resonance calculation.

SLD: Use ultra-fine group slowing down calculation.

Sample of this parameter

mg_flux_calc_mode SLD

mg_flux_calc_w_eh_el

Data type: list (real)

Default value: W=0.999167, E_h=1.0×10^4, E_l=1.0

Explanation of this parameter: Calculation condition at the resonance region.

The format of this parameter is as follows:

mg_flux_calc_w_eh_el(W E_h E_l)

where

W: Atomic weight (relative to neutron mass) used for the background moderator nuclide,

E_h: Upper energy to use ultra-fine group slowing down spectrum [eV],

E_l: Lower energy to use ultra-fine group slowing down spectrum [eV].

Sample of this parameter

mg_flux_calc_w_eh_el (0.999167 1.0E4 1.0)

mg_thermal_upscatter_treatment or mg_thermal_xs_treatment

Data type: string

Default value: on

Explanation of this parameter: Option for calculation of the thermal scattering using the free gas model.

Available value is use, on, yes, off, no, default, and def

on, yes, default, def: Calculation of the thermal scattering cross-section

off, no: Skip calculation of the thermal scattering cross-section

Sample of this parameter

mg_thermal_upscatter_treatment on

reso_upscat or reso_up_scat or reso_upscat_data or reso_up_scat_data

Data type: list (string)

Default value: none

Explanation of this parameter: The file name list of the 0 K scattering cross section data.

If the user wants to consider the resonance upscattering correction, please use this option. The user has to set the file name of the 0 K scattering cross section data which is generated by the RUC option in mg_edit_option.

Sample of this parameter

reso_upscat (U235_RUC_MT2.mg)

reso_upscat (skip U235_RUC_MT2.mg U238_RUC_MT2.mg)

//Skip means that this nuclide is not considered the resonance upscattering correlation

reso_upscat_mode or **reso_up_scat_mode**

Data type: string

Default value: ALL

Explanation of this parameter: Calculation option for the resonance up-scattering correction.

ALL: Resonance up-scattering correction is considered not only for 1D effective cross sections but also for the elastic scattering matrix.

XS: Resonance up-scattering correction is considered only for 1D effective cross sections. No resonance up-scattering is considered for the elastic scattering matrix.

Sample of this parameter

reso_upscat_mode (ALL)

potential_scat_xs

Data type: list (real)

Default value: none

Explanation of this parameter: Potential scattering cross-section of each nuclide [barns].

If the user does not set this parameter, FRENDY uses the potential scattering cross-sections obtained by JENDL-4.0, ENDF/B-VIII.0, or JEFF-3.3.

Sample of this parameter

potential_scat_xs 1.15825E+01 //Potential scattering XS of U-235[barns]

mg_mat_no or **mg_mat_list** or **mg_mat_no_list**

Data type: list (integer)

Default value: none

Explanation of this parameter: The MAT number of the GENDF file.

This parameter is only required when the ACE file is used as the start format of the multi-group cross-section generation since the ACE file does not have the MAT number.

Sample of this parameter

mg_mat_no (825 9228 9237) //O16, U235, U238

ace_output_option or **ace_edit_option**

Data type: string

Default value: on

Explanation of this parameter: Output ACE file option until the multi-group cross-section generation.

Available value is on, output, edit, off, no, skip, default, def.

on, output, edit, default, def: Output the ACE file.

off, no: Do not output the ACE file.

Sample of this parameter

ace_output_option output

10.2.2.5 Optional input parameter

print_set_data_resonance_reconstruction or **print_set_data_linearize**

Data type: string

Default value: on

Explanation of this parameter: Output input information for the resonance reconstruction.

Available value is on, yes print write output, off, no, skip, default, and def.

on, yes, print, write, output, default, def: Output the input information.

off, no, skip: Do not output the input information.

Sample of this parameter

print_set_data_resonance_reconstruction on

process_resonance_reconstruction or **process_linearize**

Data type: string

Default value: on

Explanation of this parameter: Processing option for the resonance reconstruction.

Available value is on, yes process, run, off, no, skip, default, and def.

on, yes, process run, default, def: Process the resonance reconstruction.

off, no, skip: Do not process the resonance reconstruction.

Sample of this parameter

process_resonance_reconstruction on

write_pendf_resonance_reconstruction or **write_pendf_linearize**

Data type: string

Default value: off

Explanation of this parameter: Output PENDF file option for the resonance reconstruction.

Available value is on, yes, print, write, output, off, no, skip, default, and def.

on, yes, print, write, output: Output the PENDF file of the resonance reconstruction.

on, yes, print, write, output + PENDF file name: Output the PENDF file of the resonance

reconstruction with a specific name.

off, no, skip, default, def: Do not output the PENDF file of the resonance reconstruction.

Sample of this parameter

write_pendf_resonance_reconstruction (on "U235_reso.pendf")

pendf_file_name_resonance_reconstruction or **pendf_file_name_linearize**

Data type: string

Default value: none

Explanation of this parameter: The PENDF file name for the resonance reconstruction.

The write_pendf_linearize parameter is changed from off to on when this parameter is set.

Sample of this parameter

pendf_file_name_resonance_reconstruction ("U235_reso.pendf")

print_set_data_doppler_boroadening or **print_set_data_dop**

Data type: string

Default value: on

Explanation of this parameter: Output input information for the Doppler broadening.

Available value is on, yes print write output, off, no, skip, default, and def.

on, yes, print, write, output, default, def: Output the input information.

off, no, skip: Do not output the input information.

Sample of this parameter

print_set_data_doppler_broadening on

process_doppler_broadening or **process_dop**

Data type: string

Default value: on

Explanation of this parameter: Processing option for the Doppler broadening.

Available value is on, yes process, run, off, no, skip, default, and def.

on, yes, process run, default, def: Process the Doppler broadening.

off, no, skip: Do not process the Doppler broadening.

Sample of this parameter

process_doppler_broadening on

write_pendf_doppler_broadening or **write_pendf_dop**

Data type: string

Default value: off

Explanation of this parameter: Output PENDF file option for the Doppler broadening.

Available value is on, yes, print, write, output, off, no, skip, default, and def.

on, yes, print, write, output: Output the PENDF file of the Doppler broadening.

on, yes, print, write, output + PENDF file name: Output the PENDF file of the Doppler broadening with a specific name.

off, no, skip, default, def: Do not output the PENDF file of the Doppler broadening.

Sample of this parameter

write_pendf_doppler_broadening (on "U235_dop.pendf")

pendf_file_name_doppler_broadening or **pendf_file_name_dop**

Data type: string

Default value: none

Explanation of this parameter: The PENDF file name for the Doppler broadening.

The write_pendf_dop parameter is changed from off to on when this parameter is set.

Sample of this parameter

pendf_file_name_doppler_broadening ("U235_dop.pendf")

print_set_data_gas_production_cross_section or **print_set_data_gas_xs**

Data type: string

Default value: on

Explanation of this parameter: Output input information for the calculation of the gas production cross-section.

Available value is on, yes print write output, off, no, skip, default, and def.

on, yes, print, write, output, default, def: Output the input information.

off, no, skip: Do not output the input information.

Sample of this parameter

print_set_data_gas_production_cross_section on

process_gas_production_cross_section or **process_gas_xs**

Data type: string

Default value: on

Explanation of this parameter: Processing option for the calculation of the gas production cross-section.

Available value is on, yes process, run, off, no, skip, default, and def.

on, yes, process run, default, def: Process the calculation of the gas production cross-section.

off, no, skip: Do not process the calculation of the gas production cross-section.

Sample of this parameter

process_gas_xs on

write_pendf_gas_production_cross_section or write_pendf_gas_xs

Data type: string

Default value: off

Explanation of this parameter: Output PENDF file option for the calculation of the gas production cross-section.

Available value is on, yes, print, write, output, off, no, skip, default, and def.

on, yes, print, write, output: Output the PENDF file of the calculation of the gas production cross-section.

on, yes, print, write, output + PENDF file name: Output the PENDF file of the calculation of the gas production cross-section with a specific name.

off, no, skip, default, def: Do not output the PENDF file of the calculation of the gas production cross-section.

Sample of this parameter

write_pendf_gas_xs (on "U235_gas_xs.pendf")

pendf_file_name_gas_production_cross_section or pendf_file_name_gas_xs

Data type: string

Default value: none

Explanation of this parameter: The PENDF file name for the calculation of the gas production cross-section.

The write_pendf_gas_xs is changed from off to on when this parameter is set.

Sample of this parameter

pendf_file_name_gas_xs ("U235_gas_xs.pendf")

print_set_data_probability_table or print_set_data_prob_table

Data type: string

Default value: on

Explanation of this parameter: Output input information for the probability table generation.

Available value is on, yes print write output, off, no, skip, default, and def.

on, yes, print, write, output, default, def: Output the input information.

off, no, skip: Do not output the input information.

Sample of this parameter

print_set_data_probability_table on

process_probability_table or **process_prob_table**

Data type: string

Default value: on

Explanation of this parameter: Processing option for the probability table generation.

Available value is on, yes process, run, off, no, skip, default, and def.

on, yes, process run, default, def: Process the probability table generation.

off, no, skip: Do not process the probability table generation.

Sample of this parameter

process_probability_table on

write_probability_table or **write_pendf_prob_table**

Data type: string

Default value: off

Explanation of this parameter: Output PENDF file option for the probability table generation.

Available value is on, yes, print, write, output, off, no, skip, default, and def.

on, yes, print, write, output: Output the PENDF file of the probability table generation.

on, yes, print, write, output + PENDF file name: Output the PENDF file of the probability table generation with a specific name.

off, no, skip, default, def: Do not output the PENDF file of the probability table generation.

Sample of this parameter

write_pendf_probability_table (on “U235_ptab.pendf”)

pendf_file_name_probability_table or **pendf_file_name_prob_table**

Data type: string

Default value: none

Explanation of this parameter: The PENDF file name for the probability table generation.

The write_pendf_prob_tablle parameter is changed from off to on when this parameter is set.

Sample of this parameter

pendf_file_name_probability_table (“U235_ptab.pendf”)

print_set_data_thermal_scattering_law or **print_set_data_tsl**

Data type: string

Default value: on

Explanation of this parameter: Output input information for the calculation of the thermal scattering law data.

Available value is on, yes print write output, off, no, skip, default, and def.

on, yes, print, write, output, default, def: Output the input information.

off, no, skip: Do not output the input information.

Sample of this parameter

print_set_data_thermal_scattering_law on

process_thermal_scattering_law or **process_tsl**

Data type: string

Default value: on

Explanation of this parameter: Processing option for the calculation of the thermal scattering law data.

Available value is on, yes process, run, off, no, skip, default, and def.

on, yes, process run, default, def: Process the calculation of the thermal scattering law data.

off, no, skip: Do not process the calculation of the thermal scattering law data.

Sample of this parameter

process_thermal_scattering_law on

write_pendf_thermal_scattering_law or **write_pendf_tsl**

Data type: string

Default value: off

Explanation of this parameter: Output PENDF file option for the calculation of the thermal scattering law data.

Available value is on, yes, print, write, output, off, no, skip, default, and def.

on, yes, print, write, output: Output the PENDF file of the calculation of the thermal scattering law data.

on, yes, print, write, output + PENDF file name: Output the PENDF file of the thermal scattering law data with a specific name.

off, no, skip, default, def: Do not output the PENDF file of the calculation of the thermal scattering law data.

Sample of this parameter

write_pendf_thermal_scattering_law (on "U235_tsl.pendf")

pendf_file_name_thermal_scattering_law or **pendf_file_name_tsl**

Data type: string

Default value: none

Explanation of this parameter: The PENDF file name for the calculation of the thermal scattering law data.

The write_pendf_tsl is changed from off to on when this parameter is set.

Sample of this parameter

pendf_file_name_thermal_scattering_law (“U235_tsl.pendf”)

print_set_data_ace_data_generator or **print_set_data_ace**

Data type: string

Default value: on

Explanation of this parameter: Output input information for the ACE file generation.

Available value is on, yes, print, write, output, off, no, skip, default, and def.

on, yes, print, write, output, default, def: Output the input information.

off, no, skip: Do not output the input information.

Sample of this parameter

print_set_data_ace_data_generator on

process_ace_data_generator or **process_ace**

Data type: string

Default value: on

Explanation of this parameter: Processing option for the ACE file generation.

Available value is on, yes, process, run, off, no, skip, default, and def.

on, yes, process, run, default, def: Process the ACE file generation.

off, no, skip: Do not process the ACE file generation.

Sample of this parameter

process_ace_data_generator on

10.2.2.6 Other input parameter

nan_err_mes_opt or **err_mes_nan_opt** or **err_nan_opt** or **nan_opt**

Data type: string

Default value: runtime_error

Explanation of this parameter: Policy for dealing with NaN (Not a Number) when data is output to ENDF, PENDF, and GENDF file.

Available value is runtime, runtime_error, error, caution, warning, default, and def.

runtime, runtime_error, error, default, def: The process is aborted when the “NaN” value is found.

caution, warning: The process is not aborted and the “NaN” value is converted -99999999.0 when the “NaN” value is found.

Sample of this parameter

nan_err_mes_opt runtime_error

10.2.2.7 Input parameter name and recommended value list

The input parameter name and its recommended value for the FRENDY original input format are listed in Tables 10.2.6 - 10.2.15. Note the parameters and explanation of them are identical to Sections 10.2.2.2 - 10.2.2.5.

The parameters shaded in Tables 10.2.6 - 10.2.14 always need input. In the default option, FRENDY does not output the PENDF file and users do not need to select the modules to be executed. Users have to set the print and process flags as listed in Tables 10.2.8 - 10.2.14 when they want to write the PENDF file or skip the modules. FRENDY can recognize synonymous words. For example, FRENDY prepares “ene_grid_no_per_ladder”, “ene_grid_per_ladder”, and “ene_no_per_ladder” as the parameter name to change the number of ladders to generate the probability table and “on”, “yes”, “print”, “write”, and “output” to write the PENDF file.

Table 10.2.15 shows the optional input parameter. The input parameters in Table 10.2.15 are used for debug and checking the processing results.

Table 10.2.6 Input parameter name and recommended value for common parameter (1/4)

Parameter name	Type	Recommended value	Description
nucl_file_name	string	-	ENDF file name
pendf_label_data	string	none	Label for new PENDF tape (Max. 66 words)
comment_data	list(string)	none	Descriptive comments for PENDF file (MF=1, MT=451) FRENDY recognize the comment line that is enclosed by double or single quotation. If user wants to use double/single quotation in the comment line, please use single/double quotation to enclose the comment line. Ex) "This is the comment line for the PENDF file. User can use the 'single quotation mark' when the comment line is enclosed by the double quotation."
error	real	1.00×10^{-3}	Tolerance value for linearization
error_max	real	error×10.0	Maximum tolerance value for linearization
error_integral	real	error/20000.0	Maximum integral error for linearization
temp or temperature	real	293.6	Temperature [K]

Table 10.2.6 Input parameter name and recommended value for common parameter (2/4)

Parameter name	Type	Recommended value	Description
add_grid_data	list (real)	none	Additional energy grid [eV]
max_broading_ene	real	1.00×10^{6}	Maximum energy for the Doppler broadening [eV]
probability_bin_no	integer	20	Number of probability table bins
ladder_no	integer	100	Number of resonance ladders for generating the probability table
random_seed	integer	12345	Random number seed for probability table generation
err_p_table	real	1.00E-02	Tolerance value for probability table generation. If this parameter is used, the ladder_no parameter is desabled.
ace_file_name	string	"nucl_file_name".ace	ACE file name
suffix_id	real	.00	Suffix ID for ACE file
ace_label_data	string	none	Label for ACE file (Max. 70 words)
iz_aw_data	list (real)	none	list of (iz, aw) pair iz=1000.0×Z+A, aw=mass
ace_dir_file_name, ace_dir, mcnp_dir_file_name, or mcnp_dir	string	"nucl_file_name".ace.dir or "ace_file_name".ace.dir (When the ace_file_name is changed by user)	MCNP directory information for ACE file

Table 10.2.6 Input parameter name and recommended value for common parameter (3/4)

Parameter name	Type	Recommended value	Description
sigma_zero_data	list (real)	1.0×10^{10}, 1.0×10^{6}, 1.0×10^{5}, 10000.0, 1000.0, 100.0, 35.0, 10.0, 1.0, 0.1	σ_0 values for the Bondarenko-type self-shielded cross section in the unresolved resonance region [barns] Maximum σ_0 is considered as the σ_{inf} value. The multi-group cross-section generation function can automatically set the background cross-section. The input format for the automatic setting of the background cross-section is as follows: sigma_zero_data (auto "error" "maximum number of cross-section" "minimum background cross-section [b]" "target of interpolation (factor/rr)" "interporation method (cubic/linear)") factor: Interpolation error is estimated for self-shielding factor rr: Interpolation error is estimated for reaction rate linear: linear interpolation cubic: monotone cubic interpolation The sample of input is as follows: sigma_zero_data(auto 0.1 50 1.0e-10 rr linear) Note that the background cross-section of PURR uses the recommended value when the user selects the automatic setting of background cross-section.

Table 10.2.6 Input parameter name and recommended value for common parameter (4/4)

Parameter name	Type	Recommended value	Description
ene_grid_no_par_ladder, ene_grid_par_ladder, or ene_no_par_ladder	integer	10000	Sampling energy grid number for each ladder number
ace_dir_file_name, ace_dir, mcnp_dir_file_name, or mcnp_dir	string	"nucl_file_name".ace.dir or "ace_file_name".ace.dir (When the ace_file_name is changed by user)	MCNP directory information for ACE file
cumulative_angle_distribution_format	string or integer	string = yes, integer = 1	Calculation option of whether new cumulative angular distributions for ACE file generation are used or not Available value is use, yes, no, default or 0-1 (0=no, 1=use/yes)

Table 10.2.7 Input parameter name and recommended value which are used only for thermal scattering law data

Parameter name	Type	Recommended value	Description
nucl_file_name_tsl	string	-	ENDF file name for thermal scattering law data
equi_probable_angle_no	integer	10	Number of equi-probable angles for thermal scattering law data
principal_atom_no	integer	-	Number of principal atoms for thermal scattering law data (If user doesn't set this parameter, FRENDY automatically set from the ENDF file)
inelastic_reaction_type_no	integer	221	Reaction type (MT) number for inelastic reaction. (MT=221-250 only)
max_thermal_ene	real	max(10.0, temp/300.0)	Maximum energy for thermal treatment
thermal_za_id_name	string	ZA value of ENDF file	ZA ID name for thermal ACE file (ZA=1000.0×Z+A, Max. 6 words)
moderator_za_data	integer	none	Moderator component ZA value
atom_type_no	integer	-	Number of atom types in mixed moderator (If user doesn't set this, FRENDY automatically set from ENDF file name and so on)
weight_option	string or integer	string = tabulated, integer = 2	Weighting option for thermal ACE file Available value is variable, constant, tabulated, default or 0-2 (0=variable, 1=constant, 2=tabulated)

Table 10.2.8 Input parameter name and recommended value which are used only for multi-group cross-section generation (1/9)

Parameter name	Type	Recommended value	Description
mg_tsl_data_type	list (string)	-	S(α,β) type for MATXS file. This parameter must be required when user processes TSL data. S(α,β) type used in FRENDY is shown in Table 10.2.2. S(α,β) type has no impact on GENDF file. Please set “free” when the user only generates GENDF file.
mg_file_name	string	input file name	Multi-group XS file name The output file name is as follows: "*mg_file_name*"_"*mg_file_mode*"_"*ZAID of the ACE file*".mg
mg_start_file_mode	string	ENDF	Format of the start file. FRENDY can generate the multi-group cross-section file from the ENDF-6 formatted file and the ACE file. The available value is ENDF and ACE. ENDF: Multi-group cross-section file is generated from the ENDF-6 formatted file. ACE: Multi-group cross-section file is generated from the ACE file.
mg_label_data	string	-	Label of multi-group cross-section file. The label is output on the first line of the GENDF file.
legendre_order	integer	3	Maximum Legendre order (PL order)
max_thermal_ene_e_out	real	max_thermal_ene	Maximum energy of thermal treatment for outgoing energy [eV]

Table 10.2.8 Input parameter name and recommended value which are used only for multi-group cross-section generation (2/9)

Parameter name	Type	Recommended value	Description
mg_edit_mode, mg_edit_option, or mg_edit_xs	list (string)	GENDF	Output format and output data of the multi-group cross-section generation. The available output format and output data are MATXS, SimpleMATXS, GENDF, FullMATXS, SimpleGENDF, FullGENDF, KRAMXS, 1DXS, 2DXS, NuChi, MGFlux, MGCurrent, UFG, UFG1DXS, and URC. MATXS/GENDF: Microscopic cross sections in MATXS/GENDF format, consistent with NJOY2016. SimpleMATXS/GENDF: MATXS/GENDF format, consistent with NJOY99. FullMATXS/GENDF: MATXS/GENDF format without truncation of shielded cross sections. KRAMXS: microscopic cross sections in KRAM format. 1DXS: One-dimensional cross sections such as total, fission, radiative capture. 2DXS: Two-dimensional cross sections such as elastic scattering, inelastic scattering, (n,2n) reaction. NuChi: Nu-value and fission spectrum. MGFlux: Multi-group flux (group integrated values). MGCurrent: Multi-group current (group integrated values). UFG: Ultra-fine group spectrum, total cross sections, slowing down source, total source. UFG1DXS: One-dimensional ultra-fine group cross sections such as total, fission, radiative capture. RUC: The 0 K scattering cross section data. This data is used for the input file of the resonance upscattering resonance up-scattering correction (reso_upscat). User can select specified MT number when 1DXS, 2DXS, and UFG1DXS options are selected as follows: "1DXS 1, 2, 4, -50" The minus value for MT means all MT number between previous MT number.

Table 10.2.8 Input parameter name and recommended value which are used only for multi-group cross-section generation (3/9)

Parameter name	Type	Recommended value	Description
mg_weighting_spectrum_mode	string	1/E	Weighting spectrum. The available output format and output data are 1/E and Fission+1/E+Maxwell. 1/E: 1/E spectrum for the whole energy range. Fission+1/E+Maxwell: Fission for fast energy range, 1/E for intermediate energy range, Maxwell for the thermal energy range. The other parameters are required to use "Fission+1/E+Maxwell" option as follows: mg_weighting_spectrum(Fission+1/E+Maxwell E_h E_l T_{fis} E_1 E_2) E_h: Highest energy [eV]. E_l: Lowest energy [eV]. T_{fis}: Fission temperature [eV]. E_1: Energy boundary between fission and 1/E spectra [eV]. E_2: Energy boundary between 1/E and Maxwell spectra [eV]. The sample of "Fission+1/E+Maxwell" is as follows: mg_weighting_spectrum(Fission+1/E+Maxwell 2.0e+7 1.0e-5 1.6e+6 1.0e+6 0.625) The above values are used as the default values if the user does not set these parameters.

Table 10.2.8 Input parameter name and recommended value which are used only for multi-group cross-section generation (4/9)

Parameter name	Type	Recommended value	Description
mg_weighting_spectrum_data or mg_weighting_spectrum	list (real)	-	Weight spectrum. The user can manually set the weight spectrum. The format of weight spectrum is similar to the TAB1 record in the ENDF-6 format as follows: mg_weighting_spectrum_data(E1 W1 E2 W2 … Ei-1 Wi-1 Ei Wi) NJOY's weight spectrum, i.e., iwt of the GROUPR module is also available. The input format to select the NJOY's weight spectrum is as follows: mg_weighting_spectrum_data(iwtXX) where XX is the iwt number (iwt02 ~ iwt12).
mg_weighting_spectrum_data_int or mg_weighting_spectrum_int	list (integer)	2 (linear-linear)	Interpolation method of the weight spectrum. The format of weight spectrum is similar to the TAB1 record in the ENDF-6 format as follows: mg_weighting_spectrum_data_int(NBT1 INT1 NBT2 INT2 … NBTi-1 INTi-1 NBTi INTi)

Table 10.2.8 Input parameter name and recommended value which are used only for multi-group cross-section generation (5/9)

Parameter name	Type	Recommended value	Description
mg_structure or mg_structure_neutron	list (real)	XMAS 172-group structure	Energy group structure. The user can manually set the energy group structure [eV]. NJOY's energy group structure, i.e., ign of the GROUPR module is also available. The input format to select the NJOY's energy group structure is as follows: mg_structure(ignXX) where XX is the ign number (ign02 ~ ign34). The energy group structure can be automatically set by the user input. The input format for the automatic setting of the energy group structure is as follows: mg_structure (auto E1 N1 O1 E2 N2 O2 ... Ei-1 Ni-1 Oi-1 Ei Ni Oi Ei+1) Ei: Energy boundary i [eV] Ni: Number of divisions Oi: Option for divisions The available option for divisions is EL and EE. EL: Divide the energy range by equi-lethargy width. EE: Divide the energy range by equi-energy width. The sample of input is as follows: mg_structure (auto 2.0e+07 3200 EL 100.0 1 EL 1.0e-5)

Table 10.2.8 Input parameter name and recommended value which are used only for multi-group cross-section generation (6/9)

Parameter name	Type	Recommended value	Description
mg_structure_g, mg_structure_gam, or mg_structure_gamma	list (real)	none	Photon (gamma) production energy group structure. The user can manually set the energy group structure [eV]. If the user does not set this parameter, the photon production data generation is skipped. NJOY's energy group structure, i.e., igg of the GROUPR module is also available. The input format to select the NJOY's energy group structure is as follows: mg_structure_gam(iggXX) where XX is the igg number (igg02 ~ igg10).
mg_ufg_structure or mg_ultra_fine_group_structure	list (real)	(2.0e+07 10000 EL 52475.0 56000 EL 9118.8 12000 EL 4307.4 12000 EL 961.12 8000 EL 130.07 12000 EL 0.32242 10000 EL 1.0e-5)	Energy group structure to generate neutron flux in the ultra-fine group structure. The format of this parameter is as follows: mg_ufg_structure(E1 N1 O1 E2 N2 O2 ... Ei-1 Ni-1 Oi-1 Ei Ni Oi Ei+1) Ei: Energy boundary i [eV] Ni: Number of divisions Oi: Option for divisions The available option for divisions is EL and EE. EL: Divide the energy range by equi-lethargy width. EE: Divide the energy range by equi-energy width.

Table 10.2.8 Input parameter name and recommended value which are used only for multi-group cross-section generation (7/9)

Parameter name	Type	Recommended value	Description
mg_number_density	list (real)	1.0 (use only one nuclide)	Number density of each nuclide. If the user processes the one nuclide data, this parameter can be skipped.
mg_flux_calc_mode	string	SLD	Calculation option at the resonance region. NR: Use narrow resonance calculation. SLD: Use ultra-fine group slowing down calculation.
mg_flux_calc_w_eh_el	list (real)	0.999167, 1.0×10^{4}, 1.0	Calculation condition at the resonance region. The format of this parameter is as follows: mg_flux_calc_w_eh_el(W Eh El) W: Atomic weight (relative to neutron mass) used for the background moderator nuclide. Eh: Upper energy to use ultra-fine group slowing down spectrum [eV]. El: Lower energy to use ultra-fine group slowing down spectrum [eV].
mg_thermal_upscatter_treatment or mg_thermal_xs_treatment	string	on	Option for calculation of the thermal scattering using the free gas model. <Calculation of the thermal scattering cross-section> on/yes/def/default <Skip calculation of the thermal scattering cross-section> off/no

Table 10.2.8 Input parameter name and recommended value which are used only for multi-group cross-section generation (8/9)

Parameter name	Type	Recommended value	Description
reso_upscat, reso_up_scat, reso_upscat_data, or reso_up_scat_data	list (string)	-	The file name list of the 0 K scattering cross section data. If the user wants to consider the resonance upscattering correction, please use this option. The user has to set the file name of the 0 K scattering cross section data which is generated by the RUC option in mg_edit_option.
reso_upscat_mode or reso_up_scat_mode	string	ALL	Calculation option for the resonance up-scattering correction. ALL: Resonance up-scattering correction is considered not only for 1D effective cross sections but also for the elastic scattering matrix. XS: Resonance up-scattering correction is considered only for 1D effective cross sections. No resonance up-scattering is considered for the elastic scattering matrix.
potential_scat_xs	list (real)	-	Potential scattering cross-section of each nuclide [barns]. If the user does not set this parameter, FRENDY uses the potential scattering cross-sections obtained by JENDL-4.0, ENDF/B-VIII.0, or JEFF-3.3.

Table 10.2.8 Input parameter name and recommended value which are used only for multi-group cross-section generation (9/9)

Parameter name	Type	Recommended value	Description
mg_mat_no, mg_mat_list, or mg_mat_no_list	list(integer)	-	The MAT number of the GENDF file. This parameter is only required when the ACE file is used as the start format of the multi-group cross-section generation since the ACE file does not have the MAT number.
ace_output_option or ace_edit_option	string	on	Output ACE file option until multi-group cross-section generation. <Writing ACE case> on/output/edit/def/default <Skip ACE case> off/no/skip

Table 10.2.9 Input parameter name and recommended value for resonance reconstruction

Parameter name	Type	Recommended value	Description
print_set_data_resonance_reconstruction or print_set_data_linearize	string	on	Output input information for resonance reconstruction <Writing input information> on/yes/print/write/output/default/def <Skip information> off/no/skip
process_resonance_reconstruction or process_linearize	string	on	Processing option for resonance reconstruction <Running resonance reconstruction case> on/yes/process/run/default/def <Skip resonance reconstruction case> off/no/skip
write_pendf_resonance_reconstruction or write_pendf_linearize	string	off	Output PENDF option for resonance reconstruction <Writing PENDF case> on/yes/print/write/output <Writing PENDF case with specific name> on/yes/print/write/output + PENDF file name <Skip PENDF case> off/no/skip/default/def
pendf_file_name_resonance_reconstruction or pendf_file_name_linearize	string	none	PENDF file name for resonance reconstruction When this parameter is set, write_pendf_linearize parameter is automatically changed from off to on.

Table 10.2.10 Input parameter name and recommended value for Doppler broadening

Parameter name	Type	Recommended value	Description
print_set_data_doppler_broadening or print_set_data_dop	string	on	Output input information for Doppler broadening <Writing input case> on/yes/print/write/output/default/def <Skip case> off/no/skip
process_doppler_broadening or process_dop	string	on	Processing option for Doppler broadening <Running Doppler broadening case> on/yes/process/run/default/def <Skip Doppler broadening case> off/no/skip
write_pendf_doppler_broadening or write_pendf_dop	string	off	Output PENDF option for Doppler broadening <Writing PENDF case> on/yes/print/write/output <Writing PENDF case with specific name> on/yes/print/write/output + PENDF file name <Skip PENDF case> off/no/skip/default/def
pendf_file_name_doppler_broadening or pendf_file_name_dop	string	none	PENDF file name for Doppler broadening When this parameter is set, write_pendf_dop parameter is automatically changed from off to on.

Table 10.2.11 Input parameter name and recommended value for gas production cross-section calculation (1/2)

Parameter name	Type	Recommended value	Description
print_set_data_gas_production_cross_section, print_set_data_gas_production_xs, print_set_data_gas_production, print_set_data_gas_prod_xs, print_set_data_gas_xs, or print_set_data_gas	string	on	Output input information for gas production cross section generation <Writing input case> on/yes/print/write/output/default/def <Skip case> off/no/skip
process_gas_production_cross_section, process_gas_production_xs, process_gas_production, process_gas_prod_xs, process_gas_xs, or process_gas	string	on	Processing option for gas production cross section generation <Gas production cross section generation case> on/yes/process/run/default/def <Skip gas production cross section generation case> off/no/skip

Table 10.2.11 Input parameter name and recommended value for gas production cross-section calculation (2/2)

Parameter name	Type	Recommended value	Description
write_pendf_gas_production_cross_section, write_pendf_gas_production_xs, write_pendf_gas_production, write_pendf_gas_prod_xs, write_pendf_gas_xs, or write_pendf_gas	string	off	Output PENDF option for gas production cross section generation <Writing PENDF case> on/yes/print/write/output <Writing PENDF case with specific name> on/yes/print/write/output + PENDF file name <Skip PENDF case> off/no/skip/default/def
pendf_file_name_gas_production_cross_section, pendf_file_name_gas_production_xs, pendf_file_name_gas_production, pendf_file_name_gas_prod_xs, pendf_file_name_gas_xs, or pendf_file_name_gas	string	none	PENDF file name for gas production cross section generation When this parameter is set, write_pendf_gas is automatically changed from off to on.

Table 10.2.12 Input parameter name and recommended value for probability table generation (1/2)

Parameter name	Type	Recommended value	Description
print_set_data_probability_table_generator, print_set_data_probability_table, print_set_data_prob_table_generator, print_set_data_prob_table, or print_set_data_unreso_utils	string	on	Output input information for probability table generation <Writing input case> on/yes/print/write/output/default/def <Skip case> off/no/skip
process_probability_table_generator, process_probability_table, process_prob_table_generator, process_prob_table, or process_unreso_utils	string	on	Processing option for probability table generation <Probability table generation case> on/yes/process/run/default/def <Skip probability table generation case> off/no/skip
write_pendf_probability_table_generator, write_pendf_probability_table, write_pendf_prob_table_generator, write_pendf_prob_table, or write_pendf_unreso_utils	string	off	Output PENDF option for probability table generation <Writing PENDF case> on/yes/print/write/output <Writing PENDF case with specific name> on/yes/print/write/output + PENDF file name <Skip PENDF case> off/no/skip/default/def

Table 10.2.12 Input parameter name and recommended value for probability table generation (2/2)

Parameter name	Type	Recommended value	Description
pendf_file_name_probability_table_generator, pendf_file_name_probability_table, pendf_file_name_prob_table_generator, pendf_file_name_prob_table, or pendf_file_name_unreso_utils	string	none	PENDF file name for probability table generation When this parameter is set, write_pendf_prob_table parameter is automatically changed from off to on.

Table 10.2.13 Input parameter name and recommended value for thermal scattering law data

Parameter name	Type	Recommended value	Description
print_set_data_thermal_scattering_law, print_set_data_thermal_scattering, print_set_data_tsl	string	on	Output input information for processing thermal scattering law data <Writing input case> on/yes/print/write/output/default/def <Skip case> off/no/skip
process_thermal_scattering_law, process_thermal_scattering, process_tsl	string	on	Processing option for thermal scattering law data <Processing thermal scattering law data case> on/yes/process/run/default/def <Skip thermal scattering law data case> off/no/skip
write_pendf_thermal_scattering_law, write_pendf_thermal_scattering, write_pendf_tsl	string	off	Output PENDF option for thermal scattering law data <Writing PENDF case> on/yes/print/write/output <Writing PENDF case with specific name> on/yes/print/write/output + PENDF file name <Skip PENDF case> off/no/skip/default/def
pendf_file_name_thermal_scattering_law, pendf_file_name_thermal_scattering, pendf_file_name_tsl	string	on	PENDF file name for thermal scattering law data When this parameter is set, write_pendf_tsl parameter is automatically changed from off to on.

Table 10.2.14 Input parameter name and recommended value for ACE file generation

Parameter name	Type	Recommended value	Description
print_set_data_ace_data_generator or print_set_data_ace	string	on	Output input information for ACE file generation <Writing input case> on/yes/print/write/output/default/def <Skip case> off/no/skip
process_ace_data_generator or process_ace	string	on	Processing option for ACE file generation <ACE file generation case> on/yes/process/run/default/def <Skip ACE file generation case> off/no/skip

Table 10.2.15 Optional input parameter name and recommended value

Parameter name	Type	Recommended value	Description
nan_err_mes_opt, err_mes_nan_opt, orerr_nan_opt, or nan_opt	string	runtime_error	Policy for dealing with NaN (Not a Number) when data is output to ENDF, PENDF, and GENDF file. <Process is aborted when the “NaN” value is found> runtime/runtime_error/error/default/def <Process is not aborted and the “NaN” value is converted -99999999.0 when the “NaN” value is found > caution/warning

10.2.3 Examples of FRENDY Input Formatted File

The examples of the input files for the FRENDY original input format are shown in Figs. 10.2.2 - 10.2.6. As shown in Fig. 10.2.2, the “parameter name” and “parameter value” do not need to be placed in the same line. Comment lines can be put among the “parameter name” and the “parameter value”. As shown in Fig. 10.2.4, the minimum input parameters are the processing mode and the evaluated nuclear data file name. FRENDY prepares the recommended values for the other parameters as listed in Tables 10.2.5 - 10.2.13.

```
//Input file of FRENDY for continuous-energy neutron data
ace_fast_mode    //processing mode (generate fast ACE file)

  //Nuclear data file name
    nucl_file_name          U235.dat
  /* ace file name */
    ace_file_name           U235.ace
    temp                    296.0   // temperature [K]
    add_grid_data           (0.625   4.0) //Additional energy grid point
    sigima_zero_data    //sigma-infinity is 1.0E10 [b]
      (1.0E10   1.0E06   1.0E05   1.0E04   1.0E03   1.0E02
       3.5E02   1.0E02   1.0E01   1.0E-1)
```

Figure 10.2.2 Example of input file for continuous-energy neutron data

```
//Input file of FRENDY for thermal scattering law data
ace_therm_mode    //process mode (generate thermal ACE file)

  //Nuclear data file name
    nucl_file_name
        H001.dat
  //Nuclear data file name for TSL
    nucl_file_name_tsl
        H_in_H2O.txt
  /* ace file name */
    ace_file_name
        H_in_H2O.ace
    temp    /* temperature */    296.0 //[K]
```

Figure 10.2.3 Example of input file for continuous-energy thermal scattering law data

```
//Input file of FRENDY for continuous-energy neutron data
ace_dosi_mode    //processing mode (generate dosimetry ACE file)

  //Nuclear data file name
    nucl_file_name          U235.dat
```

Figure 10.2.4 Example of input file for continuous-energy dosimetry data

```
//Input file of FRENDY for multi-group neutron-induced data
mg_neutron_mode    //processing mode (generate multi-group XS file)
  //Nuclear data file name
    nucl_file_name          U235.dat
  /* multi-group XS file name */
    mg_file_name            U235
    temp                    296.0    // temperature [K]
  /* Output data type list */
    mg_edit_mode ( GENDF    MATXS )
  /* energy group structure */
    mg_structure ( ign18 ) // XMAS NEA LANL 172 groups
  /* weight spectrum */
    mg_weighting_spectrum ( iwt05 ) // EPRI-CELL LWR
```

Figure 10.2.5 Example of input file for multi-group neutron-induced data

```
//Input file of FRENDY for thermal scattering law data
mg_neutron_mode    //process mode (generate multi-group XS file)
  //Nuclear data file name
    nucl_file_name        H001.dat
    nucl_file_name_tsl    H_in_H2O.txt
  /* multi-group XS file name */
    mg_file_name          H_in_H2O
    temp    /* temperature */    296.0 //[K]
  /* energy group structure */
    mg_structure ( xmas_nea-lanl_172 ) // ign=18
  /* weight spectrum */
    mg_weighting_spectrum ( epri-cell-lwr ) // iwt=5
```

Figure 10.2.6 Example of input file for multi-group thermal scattering law data

10.3 NJOY Compatible Format

The input format of NJOY is explained in the source code and manuals of the NJOY code system[7,8]. Users can consult them for the details of the format. FRENDY can process the evaluated nuclear data file with the input file of the following modules:

MODER, RECONR, BROADR, GASPR, PURR, UNRESR, THERMR, ACER, GROUPR, and MATXSR.

Though FRENDY processes the evaluated nuclear data file using the NJOY compatible format, users should pay attention to the following points.

- FRENDY reads and writes the PENDF file only in the text format.
- FRENDY does not calculate the self-shielding factor in the unresolved resonance region using the deterministic method and the input file of the UNRESR module is automatically converted to that of PURR.
- The “iform” option in the THERMR module and the “ismooth” option in the GROUPR module in NJOY2016 are ignored to treat both NJOY99 and NJOY2016 formats.
- The fast, thermal, and dosimetry ACE file generation functions are only implemented and other functions in ACER are not currently implemented.
- FRENDY cannot generate the MATXS file from the GENDF file. Users must combine the GROUPR and the MATXSR modules to generate MATXS file.
- FRENDY generates multiple MATXS files when the GENDF file or the PENDF file contains the multi-temperature data.

NJOY reads and writes PENDF files in binary format when the input tape number is negative. The PENDF file in the binary format is used to efficiently access the evaluated nuclear data file. It is difficult to perfectly treat the binary file produced by FORTRAN since FRENDY is written in C++. Furthermore, the PENDF file in the binary format is mainly used as a temporary file. FRENDY changes the negative tape number (binary file) to a positive one (text file) when users set a negative tape number.

FRENDY calculates probability tables to treat the self-shielding effect in the unresolved resonance region with the ladder method. NJOY implements the deterministic method to calculate it with the UNRESR module. According to the manual of NJOY, it is not recommended to use the deterministic method[42]. The self-shielding factor generated by the deterministic method sometimes shows inappropriate values, *e.g.*, negative or larger than 1.0. We believe that the calculation time of the ladder method is acceptable on the current computational platforms. Therefore, we do not implement

the deterministic method and FRENDY calculates the self-shielding effect in the unresolved resonance region using the ladder method even if users select the UNRESR module. The input parameters for the ladder method, *e.g.*, the numbers of bins and ladders, are obtained from the recommended value of the FRENDY original input as shown in Table 10.2.2.

The input formats of the THERMR module and the ACER module of NJOY2016 are slightly different from those of NJOY99. Though FRENDY can treat both input formats, the new input parameter prepared in NJOY2016, *i.e.*, the "iform" option in the THERMR module and the "ismooth" option in the GROUPR module are ignored.

As described in Chapter 7, the ACE file generation for the photo-atomic and the photo-nuclear data is not currently implemented. FRENDY terminates with an error message if users select these calculation modes.

FRENDY generates the MATXS file and the GENDF file from the ACE file. FRENDY cannot generate the MATXS file from the GENDF file. FRENDY shows the warning message and terminates the processing when the input of the MATXSR module is only found in the input data.

NJOY outputs one MATXS file even if the multi-temperature data is found in the GENDF file. The multi-temperature MATXS file contains the difference data from the base temperature data. The multi-temperature data has some problems, *e.g*., the number of significant digits is different in each data block. We believe that the multi-temperature MATXS file should be separated in each temperature.

10.4 Sample Input Data for ACE File Generation

10.4.1 Simplest Input Data

10.4.1.1 Fast ACE file generation

The simplest input format to generate the neutron incident ACE file requires only the processing mode name and evaluated nuclear data file name.

```
ace_file_generation_fast_mode                    // Processing mode name
        nucl_file_name          U235.fast.dat    // Nuclear data file name
```

The above input data generates the ACE file at a temperature of 293.6 K named "U235.fast.dat.ace" and the directory information file named "U235.fast.dat.ace.dir". For the other calculation conditions, the default input parameters listed in Tables 10.2.6 - 10.2.14 are used.

10.4.1.2 Thermal ACE file generation

The simplest input format to generate the ACE file of the thermal scattering law data requires only the processing mode name, evaluated nuclear data file name, and thermal scattering law data file

name.

```
ace_file_generation_thermal_scatter_mode          // Processing mode name
        nucl_file_name          H001.dat          // Nuclear data file name
        nucl_file_name_tsl      HinH2O.dat        // Thermal scattering law data
                                                  // file name
```

The above input data generates the ACE file at a temperature of 293.6 K named “HinH2O.dat.ace”, and the directory information file named “HinH2O.dat.ace.dir”. For the other calculation conditions, the default input parameters listed in Tables 10.2.6 - 10.2.14 are used.

10.4.1.3 Dosimetry ACE file generation

The simplest input format to generate the ACE file for the dosimetry data requires only the processing mode name and evaluated nuclear data file name.

```
ace_file_generation_dosimetry_mode          // Processing mode name
        nucl_file_name     U235.dosi.dat    // Nuclear data file name
```

The above input data generates the ACE file at a temperature of 293.6 K named “U235.dosi.dat.ace”, and the directory information file named “U235.dosi.dat.ace.dir”. For the other calculation conditions, the default input parameters listed in Tables 10.2.6 - 10.2.14 are used.

10.4.2 Input Data to Modify Default Input Parameters

As shown in Tables 10.2.6 - 10.2.14, many input parameters are prepared in the FRENDY original format. However, in conventional applications users usually change only 5 parameters, *i.e.*, the temperature, the number of equiprobable angle bins for thermal scattering law data, ACE file name, directory information for the ACE file, and a suffix ID for the ACE file. This section illustrates examples of the input files to change these input parameters.

10.4.2.1 Fast ACE file generation

```
ace_file_generation_fast_mode                     // Processing mode name
        nucl_file_name          U235.fast.dat     // Nuclear data file name
        temp                    600.0             // Temperature [K]
        suffix_id               .50               // Suffix ID for ACE file
        ace_file_name           U235.fast.ace     // ACE file name
        ace_dir_file_name       U235.fast.ace.dir // MCNP directory information
```

The above input data generates the ACE file at a temperature of 600.0 K named “U235.fast.ace”, and the directory information file named “U235.fast.ace.dir”. In this input file, the suffix ID of the ACE file is changed from 0.00 to 0.50.

10.4.2.2 Thermal ACE file generation

```
ace_file_generation_thermal_scatter_mode          // Processing mode name
    nucl_file_name          H001.dat              // Nuclear data file name
    nucl_file_name_tsl      HinH2O.dat            // TSL data name
    temp                    600.0                 // Temperature [K]
    equi_probable_angle_no  30                    // Number of equi-probable angles
    suffix_id               .50                   // Suffix ID for ACE file
    ace_file_name           HinH2O.tsl.ace        // ACE file name
    ace_dir_file_name       HinH2O.tsl.ace.dir
                                                  // MCNP directory information
```

The above input data generates the ACE file at a temperature of 600.0 K named “HinH2O.tsl.ace”, and the directory information file named “HinH2O.tsl.ace.dir”. In this input file, the number of equiprobable angles is changed from 10 to 30 and the suffix ID of the ACE file is changed from 0.00 to 0.50.

10.4.2.3 Dosimetry ACE file generation

```
ace_file_generation_dosimetry_mode          // Processing mode name
    nucl_file_name          U235.dosi.dat   // Nuclear data file name
    temp                    600.0           // Temperature [K]
    suffix_id               .50             // Suffix ID for ACE file
    ace_file_name           U235.dosi.ace   // ACE file name
    ace_dir_file_name       U235.dosi.ace.dir  // MCNP directory information
```

The above input data generates the ACE file at a temperature of 600.0 K named “U235.dosi.ace”, and the directory information file named “U235.dosi.ace.dir”. In this input file, the suffix ID of the ACE file is changed from 0.00 to 0.50.

10.4.3 Input Data to Reproduce NJOY99 Input

This section illustrates how to make FRENDY input files which is identical to NJOY input files. The details of the input parameters of the NJOY input files are explained in References 7 and 8. All

the input parameters in the NJOY input files are explicitly set in the FRENDY input files. The processing conditions, PENDF file name, ACE file name, and so on of the FRENDY input files are identical to those of the NJOY input files.

10.4.3.1 Fast ACE file generation

The following input files are typical for the fast ACE file generation. These input files process the evaluated nuclear data file of ^{238}U at 300.0 K.

< NJOY99 compatible format >

```
reconr                                / command
 20   21                              / input(tape20), output(tape21)
'pendf tape for JENDL-4.0 U-238'      / identifier for PENDF
 9237   3   3                        / mat, ncards, ngrid
 1.00e-03   0.00                      / err, temp
 '92-U-238 from JENDL-4.0' / cards (1)
 'Processed with FRENDY'   / cards (2)
 'Processed day: 2017/10/13' / cards (3)
 0.625   4.0   100.0                  / enode
 0                                    /
broadr                                / command
 20   21   22                        / input(tape20), pendf(tape21), output(tape22)
 9237   1   0   1   0                / mat, temp_no, restart_opt, bootstrap, temp_initial
 1.00E-03   100000                    / err, max_energy
 300.0                                / temp
 0                                    /
gaspr                                 / command
 20   22    23                       / input(tape20), output(tape23)
 0                                    /
purr                                  / command
 20   23   25                        / input(tape20), pendf(tape23), output(tape25)
 9237   1   7   20   100   1         / mat, temp_no, sig0_no, bin_no, ladder_no, print_opt
 300.0                                / temp
 1.0E10   1.0E4   1.0E3   300.0   100.0   30.0   10.0 / sig0
 0                                    /
acer                                  / command
 20   25    0   30   31              / nendf, npend, ngend, nace, ndir
```

```
 1     1     1    0.30                    / iopt(fast), iprint(max), itype, suffix
 'ACE file for JENDL-4 U238'              / descriptive character
 9237    300.0                            / mat, temp
 1    1                                   / newfor(yes), iopp(yes)
 1    1    1                              / thin(1), thin(2), thin(3)
stop                                      /
```

< FRENDY original input format >

```
ace_file_generation_fast_mode          // Processing mode name
        nucl_file_name                 tape20

        pendf_label_data    "pendf tape for JENDL-4.0 U238"
        error                          1.0E-3
        temp                           300.0
        add_grid_data                  (0.625    4.0    100.0)
        max_broadening_ene             100000    // 1 MeV
        sigma_zero_data    (1.0E10    1.0E4    1.0E3    300.0    100.0    30.0    10.0)
        probability_bin_no             20
        ladder_no                      100
        ace_file_name                  tape30
        mcnp_dir_file_name             tape31
        ace_label_data                 "ACE file for JENDL-4 U238"
        suffix_id                      0.30
        comment_data
“92-U-238 from JENDL-4.0
Processed with FRENDY
Processed day: 2017/10/13”

        // Write PENDF file option for RECONR
                write_pendf_resonance_reconstruction  tape21
        // Write PENDF file option for BROADR
                write_pendf_doppler_broadening        tape22
        // Write PENDF file option for GASPR
                write_pendf_gas_prod_xs               tape23
        // Write PENDF file option for PURR
```

```
        write_pendf_prob_table_generator        tape25

// Skip or running RECONR option
        process_resonance_reconstruction        on
// Skip or running BROADR option
        process_doppler_broadening              on
// Skip or running GASPR option
        process_gas_production_cross_section    on
// Skip or running PURR option
        process_probability_table_generator     on
// Skip or running ACER option
        process_ace_data_generator              on
```

10.4.3.2 Thermal ACE file generation

The following input files are typical for the thermal ACE file generation. These input files process the evaluated nuclear data file of ^{9}Be in BeO at 300.0 K.

< NJOY99 compatible format >

```
reconr                              / command
 20   21                            / input(tape20), output(tape21)
'pendf tape for JENDL-4.0 Be-009'   / identifier for PENDF
  425                               / mat
 1.00e-03    0.00                  / err, temp
 0                                 /
broadr                              / command
 20   21   22                      / input(tape20), pendf(tape21), output(tape22)
  425   1   0   1   0               / mat, temp_no, restart_opt, bootstrap, temp_initial
 1.00E-03 100000.0                 / err, max_energy
 400.0                             / temp
 0                                 /
gaspr                               / command
 20   22   23                      / input(tape20), pendf(tape22), output(tape23)
 0                                 /
thermr                              / command
 60   23   25                      / input(tape60), pendf(tape23), output(tape25)
 27   425 10 1 4 1 1 221           / natde, matdp, nbin, ntemp, iinc, icof
```

```
 400.0                                  / temp
 1.00E-2    4.0                         / tolerance, max energy
purr                                    / command
 20    25    26                         / input(tape20), pendf(tape25), output(tape26)
  425    1    7    20    200    1       / mat, temp_no, sig0_no, bin_no, lad_no, print_opt
 400.0                                  / temp
 1.0E10    1.0E4    1.0E3    300.0    100.0    30.0    10.0 / sig0
 0                                      /
acer                                    / command
 20    26     0    30    31             / nendf, npend, ngend, nace, ndir
 2     1      1    0.30                 / iopt(fast), iprint(max), itype, suffix
 'ACE file for JENDL-4 BeinBeO'         / descriptive character
 425    400.0 'bebeo'                   / mat, temp
 4009 8016                              / iza01, iza02
 221    10    222    0    2    4.0    0 / mti, nbint, mte, ielas, nmix, emax, iwt
stop                                    /
```

< FRENDY original input format >

```
ace_file_generation_thermal_scatter_mode        // Processing mode name
        nucl_file_name              tape20
        nucl_file_name_tsl          tape60

        pendf_label_data    "pendf tape for JENDL-4.0 Be-009"
        error                       1.0E-3
        temp                        400.0
        max_broadening_ene          100000.0 // 1 MeV
        sigma_zero_data             (1.0E10    1.0E4    1.0E3    300.0    100.0    30.0    10.0)
        probability_bin_no          20
        ladder_no                   200
        ace_file_name               tape30_frendy
        mcnp_dir_file_name          tape31_frendy
        ace_label_data              "ACE file for JENDL-4 BeinBeO"
        thermal_za_id_name          "bebeo"
        suffix_id                   0.30
```

```
//Thermal scattering law data only
equi_probable_angle_no          10
principal_atom_no               1   //Be
inelastic_reaction_type_no      221
max_thermal_ene                 4.0
thermal_za_id_name              “bebeo”
moderator_za_data               4009
atom_type_no                    2   //Be and O
weight_option                   0   //0 = variable

// Write PENDF file option for RECONR
        write_pendf_resonance_reconstruction        tape21
// Write PENDF file option for BROADR
        write_pendf_doppler_broadening              tape22
// Write PENDF file option for GASPR
        write_pendf_gas_prod_xs                     tape23
// Write PENDF file option for THERMR
        write_pendf_thermal_scattering              tape25
// Write PENDF file option for PURR
        write_pendf_prob_table_generator            tape26

// Skip or running RECONR option
        process_resonance_reconstruction            on
// Skip or running BROADR option
        process_doppler_broadening                  on
// Skip or running GASPR option
        process_gas_production_cross_section        on
// Skip or running THERMR option
        process_thermal_scattering_law              on
// Skip or running PURR option
        process_probability_table_generator         on
// Skip or running ACER option
        process_ace_data_generator                  on
```

10.4.3.3 Dosimetry ACE file generation

The following input files are typical for the dosimetry ACE file generation. These input files

process the evaluated nuclear data file of ^{238}U at 300.0 K.

< NJOY99 compatible format >

```
reconr                              / command
 20   21                            / input(tape20), output(tape21)
'pendf tape for JENDL-4 U238'       / identifier for PENDF
 9237                               / mat
 1.00e-03   0.0                     / err, temp
 0                                  /
broadr                              / command
 20   21   22                       / input(tape20), pendf(tape21), output(tape22)
 9237 1 0   1   0                   / mat, temp_no, restart_opt, bootstrap, temp_initial
 1.00E-03   100000                  / err, max_energy
 300.0                              / temp
 0                                  /
gaspr                               / command
 20   22   23                       / input(tape20), pendf(tape22), output(tape23)
acer                                / command
 20   23    0   30   31             / nendf, npend, ngend, nace, ndir
 3    1     1   0.30               / iopt(fast), iprint(max), itype, suffix
 'ACE file for JENDL-4 U238'        / descriptive character
 9237   300.0                       / mat, temp
stop
```

< FRENDY original input format >

```
ace_file_generation_dosimetry_mode   // Processing mode name
        nucl_file_name               tape20

        pendf_label_data    "pendf tape for JENDL-4.0 U-238"
        error                        1.0E-3
        temp                         300.0
        max_broadening_ene           100000    //1 MeV
        ace_file_name                tape30
        mcnp_dir_file_name           tape31
        ace_label_data               "ACE file for JENDL-4 U238"
```

```
suffix_id                       0.30

// Write PENDF file option for RECONR
        write_pendf_resonance_reconstruction        tape21
// Write PENDF file option for BROADR
        write_pendf_doppler_broadening              tape22
// Write PENDF file option for GASPR
        write_pendf_gas_prod_xs                     tape23

// Skip or running RECONR option
        process_resonance_reconstruction            on
// Skip or running BROADR option
        process_doppler_broadening                  on
// Skip or running GASPR option
        process_gas_production_cross_section        on
// Skip or running ACER option
        process_ace_data_generator                  on
```

10.5 Sample Input Data for Multi-Group Cross-Section Generation

10.5.1 Sample Input Data to Generate Neutron-Induced Multi-Group Cross-Section File

This section shows the sample input file to generate the neutron-induced multi-group cross-section file from the evaluated nuclear data and the ACE files. The input files in this section process ^{1}H and ^{235}U at 300.0 K.

< Input file to process ^{1}H from evaluated nuclear data file >

```
mg_neutron_mode    //Process mode
  mg_edit_option     ( MATXS   GENDF )   //Output format
  nucl_file_name      ( ../lib/H001.dat )      //ENDF file name
  mg_file_name          H001               //Output file name
  temperature           300.0 //[K]

  mg_structure ( xmas_nea-lanl_172 )      // Identical to ign=18 in GROUPR/NJOY
  mg_weighting_spectrum ( 1/e )           // Identical to iwt=3 in GROUPR/NJOY
```

< Input file to process ^{235}U from evaluated nuclear data file >

```
mg_neutron_mode    //Process mode
   nucl_file_name ( ../lib/U235.dat ) //ENDF file name
   mg_file_name    U235                //Output file name
   mg_edit_mode ( SimpleGENDF    SimpleMATXS    GENDF    MATXS
                  "MGFlux" )
         //SimpleGENDF: MATXS format consistent with NJOY99
         //SimpleMATXS: GENDF format consistent with NJOY99
         //GENDF: GENDF format consistent with NJOY2016
         //MATXS: MATXS format consistent with NJOY2016

   mg_structure ( ign18 )                // Identical to ign=18 in GROUPR/NJOY
   mg_structure_gam ( vitamin-j-42 ) // Identical to igg=10 in GROUPR/NJOY
   mg_weighting_spectrum ( iwt04 )    // Identical to iwt=4 in GROUPR/NJOY
   temp                              300.0 //[K]
   legendre_order                    3
```

< Input file to process ^{235}U from evaluated nuclear data file using specified energy group structure and weighting spectrum>

```
mg_neutron_mode                    //Process mode
   nucl_file_name ( ../lib/U235.dat )    //ENDF file name
   mg_file_name    U235                //Output file name
   mg_edit_option ( SimpleGENDF    SimpleMATXS    GENDF    MATXS
                    MGFlux )
         //SimpleGENDF: MATXS format consistent with NJOY99
         //SimpleMATXS: GENDF format consistent with NJOY99
         //GENDF: GENDF format consistent with NJOY2016
         //MATXS: MATXS format consistent with NJOY2016
   temp                              300.0 //[K]
   mg_structure ( 1.0E-5    0.625    5.0E5    1.0E6    2.0E+7 )    //4-groups
   mg_weighting_spectrum ( 1.0E-5    1.0    2.0E+7    1.0 )     //constant
   legendre_order                    3
```

< Input file to process ^{235}U from evaluated nuclear data file for fast reactor>

```
mg_neutron_mode                    //Process mode
  nucl_file_name ( ../lib/U235.dat )  //ENDF file name
  mg_file_name   U235                 //Output file name
  mg_edit_option ( SimpleGENDF   SimpleMATXS   GENDF   MATXS
                   MGFlux )
       //SimpleGENDF: MATXS format consistent with NJOY99
       //SimpleMATXS: GENDF format consistent with NJOY99
       //GENDF: GENDF format consistent with NJOY2016
       //MATXS: MATXS format consistent with NJOY2016
  temp                          300.0 //[K]
  mg_structure ( sand-iia-640 )       // Identical to ign=15 in GROUPR/NJOY
  mg_weighting_spectrum ( iwt08 )  // Identical to iwt=8 in GROUPR/NJOY
  legendre_order                3

  mg_thermal_upscatter_treatment   off   //Thermal scattering XS treatment
  //Thermal scattering cross-section is not required in fast reactor
```

< Input file to process ^{1}H from ACE file >

```
mg_neutron_mode   //Process mode
  mg_edit_option    ( MATXS   GENDF )   //Output format
  ace_file_name     ( ../ace/H001.ace )     //ACE file name
  mg_file_name        H001                  //Output file name
  temperature         300.0 //[K]

  mg_structure ( xmas_nea-lanl_172 )     // Identical to ign=18 in GROUPR/NJOY
  mg_weighting_spectrum ( fission+1/e+maxwell ) // Identical to iwt=4 in GROUPR/NJOY
```

< Input file to process ^{235}U from ACE file >

```
mg_neutron_mode   //Process mode
  ace_file_name ( ../ace/U235.ace ) //ACE file name
  mg_file_name   U235               //Output file name
  mg_edit_mode ( SimpleGENDF   SimpleMATXS   GENDF   MATXS
                 "MGFlux" )
```

```
        //SimpleGENDF: MATXS format consistent with NJOY99
        //SimpleMATXS: GENDF format consistent with NJOY99
        //GENDF: GENDF format consistent with NJOY2016
        //MATXS: MATXS format consistent with NJOY2016

  mg_structure ( ign18 )              // Identical to ign=18 in GROUPR/NJOY
  mg_structure_gam ( igg10 )          // Identical to igg=10 in GROUPR/NJOY
  mg_weighting_spectrum ( iwt04 )     // Identical to iwt=4 in GROUPR/NJOY
  temp                                300.0 //[K]
  legendre_order                      3
```

< Input file to process ^{235}U from ACE file using specified energy group structure and weighting spectrum >

```
mg_neutron_mode                     //Process mode
  ace_file_name ( ../ace/U235.ace ) //ACE file name
  mg_file_name    U235              //Output file name
  mg_edit_option ( SimpleGENDF    SimpleMATXS    GENDF    MATXS )
        //SimpleGENDF: MATXS format consistent with NJOY99
        //SimpleMATXS: GENDF format consistent with NJOY99
        //GENDF: GENDF format consistent with NJOY2016
        //MATXS: MATXS format consistent with NJOY2016
  mg_structure ( 1.0E-5    0.625    5.0E5    1.0E6    2.0E+7 )    //4-groups
  mg_weighting_spectrum ( 1.0E-5    1.0    2.0E+7    1.0 )      //constant
  legendre_order                    3
```

< Input file to process ^{235}U from ACE file for fast reactor>

```
mg_neutron_mode                     //Process mode
  ace_file_name ( ../ace/U235.ace ) //ACE file name
  mg_file_name    U235              //Output file name
  mg_edit_option ( SimpleGENDF    SimpleMATXS    GENDF    MATXS
                   MGFlux )
        //SimpleGENDF: MATXS format consistent with NJOY99
        //SimpleMATXS: GENDF format consistent with NJOY99
        //GENDF: GENDF format consistent with NJOY2016
```

```
//MATXS: MATXS format consistent with NJOY2016

mg_structure ( ign15 )                  // Identical to ign=15 in GROUPR/NJOY
mg_weighting_spectrum ( iwt08 )   // Identical to iwt=8 in GROUPR/NJOY
legendre_order                  3

mg_thermal_upscatter_treatment    off    //Thermal scattering XS treatment
//Thermal scattering cross-section is not required in fast reactor
```

10.5.2 Sample Input Data to Generate Multi-Group Cross-Section File of TSL Data

This section shows the sample input file to generate the multi-group cross-section file of the thermal scattering law data from the evaluated nuclear data and the ACE files. The input files in this section process H in H_2O at 293.6 K and graphite at 293.6 K.

< Input file to process H in H_2O from evaluated nuclear data file >

```
mg_neutron_mode    //Process mode
   mg_edit_option      ( MATXS    GENDF )        //Output format
   nucl_file_name          ( ../lib/H001.dat )          //ENDF file name
   nucl_file_name_tsl    ( ../lib/01_h_in_h2o.txt ) //TSL file name

   mg_file_name             H_in_H2O        //Output file name
   temperature              293.6 //[K]

   mg_structure ( xmas_nea-lanl_172 )       // Identical to ign=18 in GROUPR/NJOY
   mg_weighting_spectrum ( fission+1/e+maxwell ) // Identical to iwt=4 in GROUPR/NJOY
   mg_tsl_data_type              (hh2o)          //This data type is used for MATXS file generation
```

< Input file to process C in Graphite from evaluated nuclear data file >

```
mg_neutron_mode                                 //Process mode
   nucl_file_name          ( ../lib/C012.dat )          //ENDF file name
   nucl_file_name_tsl    ( ../lib/31_graphite.txt )    //TSL file name
   mg_edit_option      ( MATXS    GENDF )        //Output format

   mg_file_name             C_in_Graphite          //Output file name
   temperature              293.6 //[K]
```

```
   mg_structure ( xmas_nea-lanl_172 )       // Identical to ign=18 in GROUPR/NJOY
   mg_weighting_spectrum ( 1/e )            // Identical to iwt=3 in GROUPR/NJOY
   mg_tsl_data_type          (graph)        //This data type is used for MATXS file generation
```

< Input file to process H in H_2O from ACE file >

```
mg_neutron_mode    //Process mode
   mg_edit_option     ( MATXS    GENDF )      //Output format
   ace_file_name          ( ../ace/H001.ace )          //ENDF file name
   ace_file_name_tsl    ( ../ace/01_h_in_h2o.ace ) //TSL file name

   mg_file_name             H_in_H2O        //Output file name
   temperature              293.6 //[K]

   mg_structure ( xmas_nea-lanl_172 )       // Identical to ign=18 in GROUPR/NJOY
   mg_weighting_spectrum ( fission+1/e+maxwell    ) // Identical to iwt=4 in GROUPR/NJOY
   mg_tsl_data_type              (hh2o)         //This data type is used for MATXS file generation
```

< Input file to process C in Graphite from ACE file >

```
mg_neutron_mode                             //Process mode
   ace_file_name        ( ../ace/C012.ace )          //ACE file name
   ace_file_name_tsl    ( ../ace/31_graphite.ace )   //ACE file name (TSL data)
   mg_edit_option       ( MATXS    GENDF )       //Output format

   mg_file_name             C_in_Graphite          //Output file name
   temperature              293.6 //[K]

   mg_structure ( xmas_nea-lanl_172 )       // Identical to ign=18 in GROUPR/NJOY
   mg_weighting_spectrum ( 1/e )            // Identical to iwt=3 in GROUPR/NJOY
   mg_tsl_data_type          (graph)        //This data type is used for MATXS file generation
```

10.5.3 Sample Input Data to Generate Multi-Nuclide Data

FRENDY can process multi-nuclide data, e.g., ^{235}U, ^{238}U, and ^{16}O. This section shows the sample

input file to process such multi-nuclide data. The input files in this section process ^{235}U, ^{238}U, and ^{16}O at 600.0 K and H in H_2O, D in D_2O, and O in H_2O at 293.6 K.

< Input file to process ^{235}U, ^{238}U, and ^{16}O from evaluated nuclear data file >

```
mg_neutron_mode    //Process mode
   nucl_file_name (
         ../lib/O016.dat
         ../lib/U235.dat
         ../lib/U238.dat ) //ENDF file name

   mg_file_name    mix_UO2            //Output file name

   mg_edit_mode (
         SimpleGENDF
         SimpleMATXS
         GENDF
         MATXS
         "1DXS    1, 2, 4, -50"
         "2DXS    1, 2, 4, -50"
         "MGFlux" )
          //SimpleGENDF: MATXS format consistent with NJOY99
          //SimpleMATXS: GENDF format consistent with NJOY99
          //GENDF: GENDF format consistent with NJOY2016
          //MATXS: MATXS format consistent with NJOY2016
          //"1DXS    1, 2, 4, -50": 1D cross-section data (MT=1, 2, 4 – 50)
          //"2DXS    1, 2, 4, -50": 2D cross-section data (MT=1, 2, 4 – 50)
          //MGFlux: Multi group flux data

   mg_structure ( xmas_nea-lanl_172 )       // Identical to ign=18 in GROUPR/NJOY
   mg_structure_gam ( vitamin-j-42 )        // Identical to igg=10 in GROUPR/NJOY
   mg_weighting_spectrum ( fission+1/e+maxwell ) // Identical to iwt=4 in GROUPR/NJOY

   mg_label_data "This data is UO2 data" //This label is output in the GENDF file
   temp                              600.0 //[K]
   legendre_order                    3
                                     //8016.50c     92235.50c    92238.50c
```

```
   mg_number_density            (4.58e-2        7.18e-4         2.22e-2) //[1/barn/cm]
```

< Input file to process H in H_2O, D in D_2O, and O in H_2O from evaluated nuclear data file >

```
mg_neutron_mode    //Process mode
   mg_edit_option      ( MATXS    GENDF )    //Output format

   nucl_file_name (
         ../lib/H001.dat
         ../lib/H002.dat
         ../lib/O016.dat )    //ENDF file name

   nucl_file_name_tsl (
         ../lib/01_h_in_h2o.txt
         ../lib/11_d_in_d2o.txt
         ../lib/02_o_in_h2o.txt )

   mg_file_name               mix_H2O         //Output file name
   temperature                293.6 //[K]
   mg_structure ( xmas_nea-lanl_172 )       // Identical to ign=18 in GROUPR/NJOY
   mg_weighting_spectrum ( fission+1/e+maxwell ) // Identical to iwt=4 in GROUPR/NJOY

                                    //1001        1002          8016
   mg_number_density            (4.68e-2    7.01e-6    2.34e-2 ) //[1/barn/cm]
   mg_tsl_data_type             ( hh2o       dd2o      oh2o      )
```

< Input file to process H in H_2O, D in D_2O, and O-16 from evaluated nuclear data file >

```
mg_neutron_mode    //Process mode
   mg_edit_option      ( MATXS    GENDF )    //Output format

   nucl_file_name ( ../lib/H001.dat    ../lib/H002.dat    ../lib/O016.dat )    //ENDF file name
   nucl_file_name_tsl ( ../lib/01_h_in_h2o.txt    ../lib/11_d_in_d2o.txt    skip )
```

```
  mg_file_name              mix_H2O         //Output file name
  temperature               293.6 //[K]
  mg_structure ( xmas_nea-lanl_172 )       // Identical to ign=18 in GROUPR/NJOY
  mg_weighting_spectrum ( fission+1/e+maxwell ) // Identical to iwt=4 in GROUPR/NJOY

                                  //1001       1002         8016
  mg_number_density           (4.68e-2    7.01e-6    2.34e-2 ) //[1/barn/cm]
  mg_tsl_data_type            ( hh2o       dd2o      free     )
```

< Input file to process ^{235}U, ^{238}U, and ^{16}O from ACE file >

```
mg_neutron_mode    //Process mode
  ace_file_name (
       ../ace/O016.ace
       ../ace/U235.ace
       ../ace/U238.ace ) //ACE file name

  mg_file_name    mix_UO2            //Output file name

  mg_edit_mode (
       SimpleGENDF
       SimpleMATXS
       GENDF
       MATXS
       "1DXS    1, 2, 4, -50"
       "2DXS    1, 2, 4, -50"
       "MGFlux" )
         //SimpleGENDF: MATXS format consistent with NJOY99
         //SimpleMATXS: GENDF format consistent with NJOY99
         //GENDF: GENDF format consistent with NJOY2016
         //MATXS: MATXS format consistent with NJOY2016
         //"1DXS    1, 2, 4, -50": 1D cross-section data (MT=1, 2, 4 – 50)
         //"2DXS    1, 2, 4, -50": 2D cross-section data (MT=1, 2, 4 – 50)
         //MGFlux: Multi group flux data

  mg_structure ( xmas_nea-lanl_172 )       // Identical to ign=18 in GROUPR/NJOY
```

```
  mg_structure_gam ( igg10 )                  // Identical to igg=10 in GROUPR/NJOY
  mg_weighting_spectrum ( fission+1/e+maxwell ) // Identical to iwt=4 in GROUPR/NJOY

  mg_label_data "This data is UO2 data" //This label is output in the GENDF file
  temp                                 600.0 //[K]
  legendre_order                       3
                                       //8016.50c     92235.50c    92238.50c
  mg_number_density                   (4.58e-2         7.18e-4         2.22e-2) //[1/barn/cm]
```

< Input file to process H in H_2O, D in D_2O, and O in H_2O from evaluated nuclear data file >

```
mg_neutron_mode    //Process mode
  mg_edit_option      ( MATXS    GENDF )    //Output format

  ace_file_name (
        ../ace/H001.ace
        ../ace/H002.ace
        ../ace/O016.ace )    //ACE file name

  ace_file_name_tsl (
        ../ace/01_h_in_h2o.ace
        ../ace/11_d_in_d2o.ace
        ../ace/02_o_in_h2o.ace )

  mg_file_name                 mix_H2O         //Output file name
  temperature                  293.6 //[K]
  mg_structure ( xmas_nea-lanl_172 )       // Identical to ign=18 in GROUPR/NJOY
  mg_weighting_spectrum ( fission+1/e+maxwell    ) // Identical to iwt=4 in GROUPR/NJOY

                                       //1001       1002         8016
  mg_number_density                   (4.68e-2    7.01e-6    2.34e-2 ) //[1/barn/cm]
  mg_tsl_data_type                    ( hh2o       dd2o      oh2o      )
```

< Input file to process H in H_2O, D in D_2O, and O-16 from evaluated nuclear data file >

```
mg_neutron_mode    //Process mode
   mg_edit_option      ( MATXS    GENDF )    //Output format

   ace_file_name ( ../ace/H001.ace    ../ace/H002.ace    ../ace/O016.ace ) //ACE file name
   ace_file_name_tsl ( ../ace/01_h_in_h2o.ace    ../ace/11_d_in_d2o.ace    skip )

   mg_file_name              mix_H2O          //Output file name
   temperature               293.6 //[K]
   mg_structure ( xmas_nea-lanl_172 )       // Identical to ign=18 in GROUPR/NJOY
   mg_weighting_spectrum ( fission+1/e+maxwell    ) // Identical to iwt=4 in GROUPR/NJOY

                                 //1001       1002         8016
   mg_number_density             (4.68e-2    7.01e-6    2.34e-2 ) //[1/barn/cm]
   mg_tsl_data_type              ( hh2o       dd2o       free      )
```

10.5.4 Sample Input Data for Automated Setting of Background Cross Sections

This section shows the sample input file to generate the neutron-induced multi-group cross-section file from the evaluated nuclear data and the ACE files. This sample input file automatically set the background cross-sections of multi-group cross-section file. The input files in this section process ^{235}U at 600.0 K.

< Input file to automatically set the background cross section (processing ^{235}U from evaluated nuclear data file) >

```
mg_neutron_mode    //Process mode
   mg_edit_option      ( MATXS    GENDF )    //Output format

   nucl_file_name ( ../lib/U235.dat )    //ENDF file name

   mg_file_name              U-235          //Output file name
   temperature               600.0 //[K]
   mg_structure ( xmas_nea-lanl_172 )       // Identical to ign=18 in GROUPR/NJOY
   mg_weighting_spectrum ( fission+1/e+maxwell ) // Identical to iwt=4 in GROUPR/NJOY

   sigma_zero_data(auto    0.1    50    1.0e-10    rr    linear)
```

```
    //Tolerance = 0.1 (10%)
    //Maximum number of background XS = 50
    //Minimum background XS = 1.0E-10 (barn)
    //Target of interpolation (factor / rr) = reaction rate)
    //Interpolation method (cubic / linear) = linear interpolation
```

< Input file to automatically set the background cross section (processing ^{235}U from ACE file) >

```
mg_neutron_mode    //Process mode
  mg_edit_option     ( MATXS    GENDF )    //Output format

  ace_file_name ( ../ace/U235.ace )    //ENDF file name

  mg_file_name              U-235         //Output file name
  temperature               600.0 //[K]
  mg_structure ( xmas_nea-lanl_172 )       // Identical to ign=18 in GROUPR/NJOY
  mg_weighting_spectrum ( fission+1/e+maxwell ) // Identical to iwt=4 in GROUPR/NJOY

  sigma_zero_data(auto    0.1    50    1.0e-10    rr    linear)
        //Tolerance = 0.1 (10%)
        //Maximum number of background XS = 50
        //Minimum background XS = 1.0E-10 (barn)
        //Target of interpolation (factor / rr) = reaction rate)
        //Interpolation method (cubic / linear) = linear interpolation
```

10.5.5 Sample Input Data for Automatic Setting of Energy Group Structure

This section shows the sample input file to generate the neutron-induced multi-group cross-section file from the evaluated nuclear data and the ACE files. This sample input file automatically set the energy group structure of multi-group cross-section file. The input files in this section process ^{235}U at 300.0 K.

< Input file to process ^{235}U from evaluated nuclear data file >

```
mg_neutron_mode                    //Process mode
  nucl_file_name ( ../lib/U235.dat )    //ENDF file name
  mg_file_name    U235               //Output file name
  mg_edit_option ( GENDF    MATXS )
```

```
   temp                                300.0 //[K]
   mg_structure ( auto    2.0E+7    100    EL
                          1.0E+2    100    EL
                          1.0E-5 )
            // 2.0E+7 eV – 1.0E+2 eV: Divide 100 energy groups by equi-lethagy width
            // 1.0E+2 eV – 1.0E-5 eV: Divide 100 energy groups by equi-lethagy width
            //EL: Divide by equi-lethagy width, EE: Divide by equi-energy width
   mg_weighting_spectrum ( iwt03 )    // Identical to iwt=3 in GROUPR/NJOY
```

< Input file to process ^{235}U from ACE file >

```
mg_neutron_mode                    //Process mode
   ace_file_name ( ../ace/U235.ace ) //ACE file name
   mg_file_name    U235               //Output file name
   mg_edit_option ( GENDF    MATXS )
   temp                                300.0 //[K]
   mg_structure ( auto    2.0E+7    100    EL
                          1.0E+2    100    EL
                          1.0E-5 )
            // 2.0E+7 eV – 1.0E+2 eV: Divide 100 energy groups by equi-lethagy width
            // 1.0E+2 eV – 1.0E-5 eV: Divide 100 energy groups by equi-lethagy width
            //EL: Divide by equi-lethagy width, EE: Divide by equi-energy width
   mg_weighting_spectrum ( iwt03 )    // Identical to iwt=3 in GROUPR/NJOY
```

10.5.6 Sample Input Data for Resonance Up-Scattering Correction

FRENDY can consider the resonance up-scattering correction. This section shows the sample input file to use this function. The input files in this section process ^{16}O, ^{235}U, and ^{238}U at 600.0 K. The resonance up-scattering correction of ^{16}O is not considered. The scattering cross section data at 0 K is required to consider the resonance up-scattering correction. This section shows two types of input data *i.e.*, generation of the scattering cross section data at 0 K and generation of the multi-group cross section data considering the resonance up-scattering correction.

< Input file to generate scattering cross section data at 0 K (processing ^{235}U from evaluated nuclear data file) >

```
mg_neutron_mode    //Process mode
```

```
   mg_edit_option     ( GENDF    RUC )    //Output format
   nucl_file_name ( ../lib/U235.dat )         //ENDF file name

   mg_file_name              U235_RUC      //Output file name
   temperature               0.0 //[K]
   mg_structure ( xmas_nea-lanl_172 )       // Identical to ign=18 in GROUPR/NJOY
   mg_weighting_spectrum ( fission+1/e+maxwell    ) // Identical to iwt=4 in GROUPR/NJOY
```

< Input file to generate scattering cross section data at 0 K (processing ^{238}U from evaluated nuclear data file) >

```
mg_neutron_mode    //Process mode
   mg_edit_option     ( GENDF    RUC )    //Output format
   nucl_file_name ( ../lib/U238.dat )         //ENDF file name

   mg_file_name              U238_RUC      //Output file name
   temperature               0.0 //[K]
   mg_structure ( xmas_nea-lanl_172 )       // Identical to ign=18 in GROUPR/NJOY
   mg_weighting_spectrum ( fission+1/e+maxwell    ) // Identical to iwt=4 in GROUPR/NJOY
```

< Input file to generate multi-group cross section considering resonance up-scattering correction (processing ^{16}O, ^{235}U, and ^{238}U from evaluated nuclear data file) >

```
mg_neutron_mode    //Process mode
   mg_edit_option     ( GENDF    MATXS )    //Output format
   nucl_file_name ( ../lib/O016.dat    ../lib/U235.dat    ../lib/U238.dat )    //ENDF file name

   mg_file_name              mix_UO2_with_RUC      //Output file name
   temperature               600.0 //[K]
   mg_structure ( xmas_nea-lanl_172 )       // Identical to ign=18 in GROUPR/NJOY
   mg_weighting_spectrum ( fission+1/e+maxwell    ) // Identical to iwt=4 in GROUPR/NJOY

                             //8016.50c      92235.50c    92238.50c
   mg_number_density    (4.58e-2          7.18e-4          2.22e-2)    //[1/barn/cm]
   reso_upscat    ( skip    U235_RUC_92235.00c_MT2.mg    U238_RUC_92238.00c_MT2.mg )
```

10.6 Input Instruction of ACE File Perturbation Tools

The ACE file perturbation tool contains two tools as follows:

tools/make_perturbation_factor/make_perturation_factor.exe

tools/perturation_ace_file/perturbation_ace_file.exe

The input format of both tools is explained in this section. The installation of these tools is found in the readme file of these tools (tools/README_tools).

10.6.1 Input Instruction of make_perturbation_factor

This tool is the uncertainty analysis tool using the Random Sampling method for the ACE file. This tool generates perturbation factor from the relative covariance matrix of cross-section and outputs the input data of the “perturbation_ace_file.exe”. Note that the license of this tool is not the 2-clause BSD license. The make_perturation_factor.exe uses the Eigen library. The license of this tool is the MP2L license since the Eigen library is open-source software under the MP2L license.

The tool requires the following input data. In the input file, these terms are required and the user has to enclose by "<>" to set the data of each term.

(1) Sample size (int): <sample_size> *sample_no*

The first parameter is the number of random samplings. The number of random samplings is identical to the number of output files.

(2) Random seed (int): <seed> *seed_val*

The second parameter is the initial random seed.

(3) File name of covariance matrix (string): <relative_covariance> *cov_file_name*

The third parameter is the name of the covaiance matrix file.

(4) Energy grid of covariance matrix [MeV] (real): <energy_grid > (E_1 E_2 E_3 … E_{g-1} E_g)

The fourth parameter is the energy group structure. The number of energy grids of the input file must be identical to that of the covariance matrix. The energy group structure is enclosed by the bracket “()”.

(5) Nuclide name of the covariance matrix (string): <nuclide > ($Nucl_1$ $Nucl_2$ … $Nucl_{i-1}$ $Nucl_i$)

The fifth parameter is the energy group structure. The nuclide name is used as the directory name which stores the output files. If the covariance matrix uses the multiple nuclides, the nuclide name is enclosed by the bracket “()”.

(6) Reaction type (MT) of covariance matrix (int): <reaction > (MT$_1$ MT_2 MT_3 ... MT_{i-1} MT_i)

The sixth parameter is the reaction type number. If the covariance matrix uses the multiple reaction type, the reaction type is enclosed by the bracket "()".

10.6.2 Sample Input of make_perturbation_factor

The sample input file of this tool is as follows:

< Generation of 100 sampling data from U-235 using cov_matrix.csv >

```
<sample_size>          100
<seed>                 20190504
<relative_covariance>  cov_matrix.csv
<energy_grid>          (1.0E-11  6.8E-7  2.0E1)
<nuclide>              (U235)
<reaction>             (2  18  102)
```

In this case, the sample number is 100, the initial random seed is 20190504, the covariance file name is "cov_matrix.csv", energy grid number is 2, the energy grid boundary is 1.0E-11 MeV, 6.8E-7 MeV, and 20MeV, the nuclide name is U235, and reaction type (MT number) is MT=2, 18, and 102, respectively.

< Generation of 200 sampling data from U-235 and U-238 using cov_matrix.csv >

```
<sample_size>          200
<seed>                 1
<relative_covariance>  cov_matrix.csv
<energy_grid>          (1.0E-11  6.8E-7  2.0E1)
<nuclide>              (U235  U238)
<reaction>             (2  18  102)  (4  16)
```

In this case, the sample number is 200, the initial random seed is1, the covariance file name is "cov_matrix.csv", energy grid number is 2, the energy grid boundary is 1.0E-11 MeV, 6.8E-7 MeV, and 20MeV, the nuclide name is U235 and U238, and reaction type (MT number) is MT=2, 18, and 102 for U235 and MT=4 and 16 for U238, respectively.

10.6.3 Input Instruction of perturbation_ace_file

This tool generates the perturbed ACE file when the user sets the ACE file name, reaction type, energy region, and amount of perturbation. This tool can use the output file of the "make_perturbation_factor" tool.

The perturbation tool perturbs the cross-section, the number of neutrons per fission (ν_{total}, ν_{delay}, and ν_{prompt}), and fission spectrum line by line. The input format of this tool is as follows:

"*MT number*" E_{max} E_{min} f

or

"*MT number*" E_{min} E_{max} f

where E_{max} is the maximum energy of perturbation [MeV], E_{min} is the minimum energy of perturbation [MeV], and f is the amount of perturbation, respectively. Note that the above data must be set in one line. The number of the perturbed data files is identical to the number of lines. The available reaction type (MT number) is all reaction cross-section type, ν_{total} (MT=452), ν_{delay} (MT=455), ν_{prompt} (MT=456), and fission spectrum (MT=1018).

For example, if the user wants to modify elastic scattering cross-section (MT=2) from 1.0E-11 MeV to 1.0E-10 MeV and fission cross-section (MT=18) from 1.0E-6 eV to 1.0E-5 eV, the perturbation data file is as follows:

```
 2   1.0E-10   1.0E-11   1.1
18   1.0E-5    1.0E-6    0.9
```

or

```
 2   1.0E-11   1.0E-10   1.1
18   1.0E-6    1.0E-5    0.9
```

The execution command of the perturbation tools is as follows:

./perturbation_ace_file.exe "*ACE file name*" "*input file list*"

The perturbation tools developed for the uncertainty analysis tool using the Random Sampling method. The input file list is required to run this tool and the input file name is written in the input file list to perturb a lot of ACE files simultaneously.

This tool is developed to use the output file of "make_perturbation_factor" as the perturbation data file. The input file name must be "AAA_nnnn", where "AAA" is the file name and "nnnn" is 4 numbers. For example, if there are three perturbation data files and the target nuclide is U-235, the

input file list is as follows:

inp/U235_0001
inp/U235_0020
inp/U235_0300

The perturbation tool reads "U235_0001", "U235_0020", and "U235_0300" files in "inp" directory and output three perturbed ACE files. The perturbed ACE file name is automatically set using 4 numbers in the perturbation data file name (the "nnnn" part in the input file name). In this case, the perturbed ACE file name is ace_file.ace_0001, ace_file.ace_0020, and ace_file.ace_0300 when the original ACE file name is "ace_file.ace_0001".

10.7 Input Instruction of ENDF Modification Tool

This tool is involved in the executable of FRENDY. The execution method is identical to the processing of the nuclear data file.

The user must set the processing mode as the first parameter. The processing mode to modify the ENDF-6 formatted file is as follows:

“endf_file_modification_mode”, “endf_file_modify_mode”, “endf_mod_mode”, or
“mod_endf_mode”

The modification tool performs the modifications line by line. If the user wants to remove specified MF/MT data, the user sets the following command:

remove MF “*MF number*” MT “*MT number*” “*Original file name*” “*Modified file name*”
remove MF “*MF number*” “*Original file name*” “*Modified file name*”
remove MT “*MT number*” “*Original file name*” “*Modified file name*”

If the user selects both MF and MT numbers, specified MF/MT data is removed from the original file. If the user only selects the MF number, specified MF data is removed. If the user only selects the MT number, specified MT data in all MF data are removed.

If the user wants to replace the specified MF/MT data, the user sets the following command:

replace MF “*MF number*” MT “*MT number*” “*Original file name*” “*Replaced file name*”
“*Modified file name*”
replace MF “*MF number*” “*Original file name*” “*Replaced file name*” “*Modified file name*”

replace MT "*MT number*" "*Original file name*" "*Replaced file name*" "*Modified file name*"

The modification tool removes the specified MF/MT data in the original file and copies the specified MF/MT data in the replaced file. The specified MF/MT data in the replaced file is copied even if the original file does not contain the specified MF/MT data

If the user wants to add the specified MF/MT data, the user sets the following command:

add MF "*MF number*" MT "*MT number*" "*Original file name*" "*Replaced file name*" "*Modified file name*"
add MF "*MF number*" "*Original file name*" "*Replaced file name*" "*Modified file name*"
add MT "*MT number*" "*Original file name*" "*Replaced file name*" "*Modified file name*"

The modification tool copies the specified MF/MT data in the replaced file. The specified MF/MT data is replaced if the original file contains the specified MF/MT data.

If the user wants to linearize the specified MF/MT data, the user sets the following command:

linearize MF "*MF number*" MT "*MT number*" "*Original file name*" "*Modified file name*"
linearize MF "*MF number*" "*Original file name*" "*Modified file name*"

The linearization of the data is only available for the specified MF or MF/MT data.

10.8 Sample Input of ENDF Modification Tool

When the user wants to remove MT=19 from "./j40/Pu239.dat", replace the MF=2 data with "./b80/n-094_Pu_239.endf", and add the MF=35/MT=18 data in "./f33/94-Pu-239g.jeff33", the sample input of modification tools is as follows. Note that after "//" is the comment.

endf_file_modification_mode ***//processing mode***
remove MT 19 ./j40/Pu239.dat ./Pu239_mod01.dat
replace MF 2 ./Pu239_mod01.dat ./b80/n-094_Pu_239.endf ./Pu239_mod02.dat
add MF 35 MT 18 ./Pu239_mod02.dat ./f33/94-Pu-239g.jeff33 ./Pu239_mod03.dat

In this sample input, the modified file name is "./Pu239_mod03.dat". As shown in the sample input file, the user has to modify the original input file name in each line if the user wants to make multiple modifications.

When the user wants to linearize MF=4, 5, and 6 data of "./j40/Pu239.dat", the sample input of modification tools is as follows.

endf_file_modification_mode ***//processing mode***

linearize MF 4 ./j40/Pu239.dat ./Pu239_mod01.dat
linearize MF 5 ./Pu239_mod01.dat ./Pu239_mod02.dat
linearize MF 6 ./Pu239_mod02.dat ./Pu239_mod03.dat

In this sample input, the modified file name is "./Pu239_mod03.dat".

This program can linearize some evaluated nuclear data files in one input file. When the user wants to linearize MF=4 and MF=5/MT=18 of "./j40/U235.dat", "./j40/U238.dat", and "./j40/Pu239.dat", the sample input of modification tools is as follows.

endf_file_modification_mode ***//processing mode***

linearize MF 4 ./j40/U235.dat ./U235_mod01.dat
linearize MF 5 MT 18 ./U235_mod01.dat ./U235_mod02.dat
linearize MF 4 ./j40/U238.dat ./U238_mod01.dat
linearize MF 5 MT 18 ./U238_mod01.dat ./U238_mod02.dat
linearize MF 4 ./j40/Pu239.dat ./Pu239_mod01.dat
linearize MF 5 MT 18 ./Pu239_mod01.dat ./Pu239_mod02.dat

In this sample input, the modified file name is "./U235_mod02.dat", "./U238_mod02.dat", and "./Pu239_mod02.dat", respectively.

The user can also set the tolerance of the linearization. The default tolerance value is 1.0E-3, *i.e.*, 0.1%. When the user wants to linearize a small tolerance value, the sample input is as follows:

endf_file_modification_mode ***//processing mode***

tolerance 1.0E-4
linearize MF 4 ./j40/U235.dat ./U235_mod01.dat
linearize MF 5 MT 18 ./U235_mod01.dat ./U235_mod02.dat

In this sample input, the tolerance value is changed from 1.0E-3 to 1.0E-4.

11 Installation of FRENDY

This chapter describes how to install FRENDY on Linux, UNIX, or macOS platforms.

1. A disk space of about 1.2 Gbytes is required to make the executables from the program sources and run all test programs and sample files. A disk space of about 210 Mbytes is required if users make only the executables from the program sources.
2. A C++ compiler, the Boost library, and the LAPACK library are required to compile source programs. The compilation has been confirmed for an Intel compiler (ICC) version 13.1.3 and a GNU compiler (GCC) version 4.4.7 with the Boost library version 1.60.0 and the LAPACK library[66] version 3.8.0.
3. Since FRENDY stores all nuclear data on memory, a large memory size is required. More than 1 Gbytes is recommended to run FRENDY.

11.1 Directory Structure

The directory structure is shown in Fig. 11.1.1. The “frendy” directory contains the source files. The “sample” directory contains the input files for the test calculations to generate the fast and thermal ACE files. The “test” directory contains source files to run the Boost.Test library.

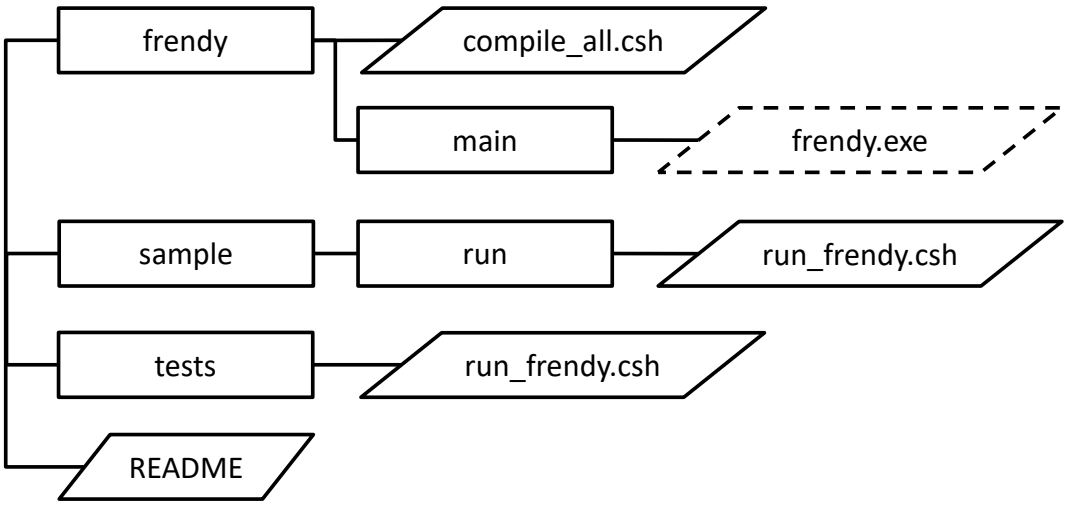

Figure 11.1.1 Directory structure of FRENDY

11.2 How to Install FRENDY on Linux, UNIX, or macOS Platforms

A shell script of “compile_all.csh” is included in the “frendy” directory to compile FRENDY source codes. The users run only this shell script or issue the “make” command in “frendy/main” directory. If the compiler successfully builds the executable file of FRENDY, the following message

is written on the display.

Completed to make FRENDY

The executable file named “frendy.exe” is generated in “frendy/main” directory.

FRENDY has the NJOY mode which processes the evaluated nuclear data file with the NJOY calculation method. The differences between the NJOY mode and the original mode are as follows:

1. The NJOY mode calculates the unresolved resonance cross-section using cross-section formulas on the fixed energy grid points and other energy grid points are calculated by the interpolation method. The fixed energy grid points are 1.00×10^n, 1.25×10^n, 1.50×10^n, 1.70×10^n, 2.00×10^n, 2.50×10^n, 3.00×10^n, 3.50×10^n, 4.00×10^n, 5.00×10^n, 6.00×10^n, 7.20×10^n, and 8.50×10^n. This difference has an impact on resonance reconstruction.
2. The calculation method of the complex error function which is defined in Eq. (2.3.41) is different. The complex error function is used to calculate the Doppler broadened cross-sections with the Single-Level Breit-Wigner representation. This difference has an impact on resonance reconstruction and probability table generation.
3. The calculation method of the cross-sections at 0 eV is different. The cross-section at 0 eV is required to calculate the Doppler broadened cross-sections at the low energy region. The NJOY mode assumes that the cross-section obeys the 1/v law. This approximation is appropriate for many reactions. However, the elastic scattering cross-sections do not obey the 1/v law since the elastic scattering cross-section is constant due to the potential scattering cross-section at the low-energy region. In such a case, the linear-linear interpolation is appropriate. The NJOY mode uses the 1/v law to reproduce the NJOY results. This difference affects the Doppler broadened elastic scattering cross-sections at the low-energy region.
4. The NJOY mode uses the fixed incident neutron energy grid to calculate the incoherent inelastic scattering cross-section. The number of energy grid points is 117 from 1.0×10^{-5} to 10 eV to calculate the incoherent inelastic scattering cross-section and secondary energy and angular distributions. The incoherent inelastic scattering cross-section at the other energy grid points is interpolated using the fifth-order Lagrange interpolation and secondary energy and angular distributions are not calculated. This difference affects some materials, *e.g.*, H in ZrH, for which the incoherent inelastic scattering cross-section oscillates.
5. The NJOY mode uses discrete random numbers to calculate the chi-squared random numbers with k degrees of freedom $R_{\chi^2}(k)$. This difference has an impact on the probability table

generation.

Users run “compile_all.csh” or “make” command in “frendy/main_njoy_mode” directory if they want to compile with this calculation mode. The executable file named “frendy_njoy_mode.exe” is generated in “frendy/main_njoy_mode” directory.

11.3 How to Execute FRENDY

The execution command is

frendy.exe “input file name”

The input file name is set as a command-line argument.

11.4 Test Calculation with Samples

The sample input files are located in the “sample/input” directory. The sample input files which are listed in this manual in Sec. 10 are used as the sample calculations. All nuclides and thermal scattering law data are copied from JENDL-4.0. The “run_all.csh” shell script in the “sample/run” directory automatically runs all the sample input files.

11.5 Test Programs for Boost Test Library

For quality assurance, the test programs are included to verify the capabilities. The Boost test library[20] is used for the test programs. Using the Boost test library, comparison of the calculation results and confirmation of the run-time errors are easily done.

The source files for Boost test library are contained in the “test” directory. Users must run the “run_all_class.csh” shell script in the “test” directory if they want to compile and run all the test programs. The source file name and the directory structure correspond to those of FRENDY sources in the “frendy” directory. Users must recompile and run the test programs when they modify the source files.

The test programs start with the following message

Running *X* test cases...

where *X* is the number of test cases. If the test programs are successfully finished, the following message is written on the display

***** No errors detected**

If the test programs find errors, the following message is written on the display

***** *Y* failures detected in test suite "Master Test Suite"**

where *Y* is the number of errors.

11.6 How to Install FRENDY on Visual Studio 2019

This section shows the installation of FRENDY using Visual Studio 2019. The author strongly recommends using the Windows Subsystem for Linux to compile FRENDY since the installation of FRENDY using Visual Studio 2019 is difficult. The installation of FRENDY using Windows Subsystem for Linux is explained in “FRENDY installation” on the web page of the FRENDY training course: https://rpg.jaea.go.jp/main/en/program_frendy/index.html.

11.6.1 Installation of Boost Library

Installation of the Boost library is required before the compilation of FRENDY. The installation of the Boost library is as follows:

1. Go to the web page of the Boost library: https://www.boost.org/doc/
2. Click “Getting Started”.
3. Click “Next: Getting Started on Microsoft Windows”.
4. Download the latest version of the Boost library.
5. Unzip the downloaded file.
6. Open the x64 native tools command prompt for VS2019. (Windows menu -> Visual Studio 2019 -> x64 Native Tools Command Prompt for VS2019)
7. Move to the unzipped Boost directory.
8. Run “bootstrap”.
9. Run “.¥b2”

11.6.2 Installation of CLAPACK Library

Installation of the CLAPACK library is required before the compilation of FRENDY. The CLAPACK library is only used to treat the resonance parameter written in the R-matrix limited formula. The user can skip this process if the user doesn’t need to treat this resonance parameter.

The installation of the CLAPACK library is as follows:

1. Go to the web page of the CLAPACK library: https://icl.cs.utk.edu/lapack-for-windows/clapack/

2. Download the CLAPACK library from the following web page:
   https://icl.cs.utk.edu/lapack-for-windows/clapack/clapack-3.2.1-CMAKE.tgz
3. Decompress the CLAPACK library.
4. Install the CLAPACK library.
5. Run installed CMake and select the source code directory of the CLAPACK library and the new directory to build.
6. Select Visual Studio 2019.
7. Click the “Finish” button.
8. Select the compiled directory and click the “Configure” button.
9. Click the “Generate” button.
10. Click the “Open Project” button and open the window of Visual Studio 2019.
11. Select “ALL_BUILD” in the solution explorer and run debug and release.
12. Select “INSTALL” in the solution explorer and run debug and release.

11.6.3 Installation of FRENDY

The installation of FRENDY is as follows:

1. Download the “msdirent.h” file instead of the “dirent.h” file from the following web page:
   http://svn.apache.org/repos/asf/avro/trunk/lang/c/tests/msdirent.h
2. Copy the “msdirent.h” file to the “frendy¥VisualStudio” directory.
3. Generate a project of FRENDY with “Continue without code”.
4. Click File -> New -> Project From Existing Code.
5. Input source directory of FRENDY.
6. Select “Console Application Project”.
7. Click the “Finish” button.
8. Remove main.cpp, main_frendy_njooy_mode.cpp, and main_frrendy.cpp.
9. Open property of this project. (Project -> Property).
10. Add include directory of the Boost library, the CLAPACK library and FRENDY.
11. Add additional dependency file as follows:
    For release : lapack.lib;blas.lib;libf2c.lib;
    For debug : lapackd.lib;blasd.lib;libf2cd.lib;
12. Compile FRENDY using release mode.

11.6.4 Running FRENDY with bat Files

The users can run FRENDY using the following two bat files:

(1) run.bat

```
set INPNAME=inp_JENDL-4_U235
call run_frendy.bat
```

(2) run_frendy.bat

```
set EXE=frendy.exe
rem set EXE= frendy.exe
set INP_DIR=..¥input
set LIB_DIR=..¥lib

set OUT_DIR=out
set PEN_DIR=pendf
set ACE_DIR =ace

mkdir %OUT_DIR%
mkdir %PEN_DIR%
mkdir %ACE_DIR_FAST%
mkdir %ACE_DIR_THERM%

set DIR_DATA=xsdir_list
set LOG=log

rem del %DIR_DATA%
rem del %LOG%

set INP=%INP_DIR%¥%INPNAME%.dat
set LIB=%LIB_DIR%¥%LIBNAME%.dat
set LIBK=%LIB_DIR%¥%TSKNAME%.txt

copy %LIB%    tape20
if exist %LIBK%    copy %LIBK% tape23

echo %LIBNAME%
echo %LIB%
echo %LIBK%
echo %LIBNAME%    >> %LOG%
```

```
echo ""                         >> %LOG%
%EXE%    %INP%      >> %LOG%
echo ""                 >> %LOG%
echo "============================================================" >> %LOG%
echo ""                 >> %LOG%

copy    output    %OUT_DIR%¥frendy_output_%LIBNAME%%TSKNAME%.dat
copy    tape25    %PEN_DIR%¥frendy_result_%LIBNAME%%TSKNAME%.dat
copy    tape30    %ACE_DIR %¥frendy_acer_%LIBNAME%%TSKNAME%.dat
type    tape31    >> %DIR_DATA%

del output
del tape20
del tape21
del tape22
del tape23
del tape25
del tape30
del tape31

rem rmdir /s /q %OUT_DIR%
rem rmdir /s /q %PEN_DIR%
rem rmdir /s /q %ACE_DIR_FAST%
rem rmdir /s /q %ACE_DIR_THERM%
```

Acknowledgements

The authors especially wish to thank Prof. Go Chiba of Hokkaido University, Prof. Tomohiro Endo of Nagoya University, and Masayuki Tojo and Michitaka Ono of Global Nuclear Fuel-Japan Co., Ltd. for their contribution to verifying and improving the FRENDY functions. The authors also wish to thank Dr. Kenji Yokoyama, Mr. Tomoyuki Jin, Mr. Ryoichi Kondo, Dr. Yosuke Iwamoto, Dr. Chikara Konno, Dr. Kenya Suyama, Dr. Teruhiko Kugo, and Dr. Tokio Fukahori of JAEA and members of the nuclear data processing working group of the JENDL committee for their helpful suggestions and continuous encouragement. This study could not be completed without their help.

References

1) K. Shibata, O. Iwamoto, T. Nakagawa, N. Iwamoto, A. Ichihara, S.Chiba, K. Furutaka, N. Otuka, T. Ohsawa, T. Murata, H. Matsunobu, A. Zukeran, S. Kamada, J. Katakura, "JENDL-4.0: A New Library for Nuclear Science and Engineering", *J. Nucl. Sci. Technol.*, 48(1), pp.1-30 (2011).

2) Y. Nagaya, K. Okumura, T. Mori, M. Nakagawa, "MVP/GMVP II: General Purpose Monte Carlo Codes for Neutron and Photon Transport Calculations based on Continuous Energy and Multigroup Methods", *JAERI 1348* (2004) 388p.

3) K. Yokoyama, T. Jin, Y. Hirai, T. Hazama, "Development of the Versatile Reactor Analysis Codes System, MARBLE2", *JAEA-Data/Code 2015-009* (2015) 120p. (in Japanese).

4) T. Sato, Y. Iwamoto, S. Hashimoto, T. Ogawa, T. Furuta, S. Abe, T. Kai, P. Tsai, N. Matsuda, H. Iwase, N. Shigyo, L. Sihver, K. Niita, "Features of Particle and Heavy Ion Transport code System (PHITS) version 3.02", *J. Nucl. Sci. Technol.*, 55(6), pp.684-690 (2018).

5) T. Tone, S. Katsuragi, "PROF GROUCH-G; A Processing Code for Group Constants for a Fast Reactor", *JAERI 1192* (1970) 22p.

6) N. Yamano, T. Minami, K. Koyama, Y. Naito, "RADHEAT-V4; A code system to generate multigroup constants and analyze radiation transport for shielding safety evaluation", *JAERI 1316* (1989) 307p.

7) R. E. MacFarlane, D. W. Muir, "The NJOY Nuclear Data Processing System, Version 91", *LA-12740-M*, Los Alamos National Laboratory (1994).

8) A. C. Kahler, Ed., "The NJOY Nuclear Data Processing System, Version 2016", *LA-UR-17-20093*, Los Alamos National Laboratory (2016).

9) D. E. Cullen, "PREPRO 2017, 2017 ENDF/B Pre-processing Codes (ENDF/B-VII of proposed VIII Tested)", *IAEA-NDS-39*, Rev.17, International Atomic Energy Agency (2017).

10) M. B. Chadwick, et. al., "Special Issue on ENDF/B-VII.1 Library", *Nucl. Data Sheets*, 112(12), pp.2887-3152 (2011).

11) A. Koning, C. Dean, U. Fischer, R. Mills, "Validation of the JEFF-3.1 Nuclear Data Library," *JEFF-Report 23* (2013).

12) C. M. Mattoon, B. R. Beck, N. R. Patel, N. C. Summers, G. W. Hedstrom, D. A. Brown, "Generalized Nuclear Data: A New Structure (with Supporting Infrastructure) for Handling Nuclear Data", *Nucl. Data Sheets*, 113,(12), pp.3145-1371 (2012).

13) A. Trkov, M. Herman, D. A. Brown, "ENDF-6 Formats Manual", Report *BNL-203218-2018-INRE* (2018).

14) K. Tada, Y. Nagaya, S. Kunieda, K. Suyama, T. Fukahori, "Development and verification of a new nuclear data processing system FRENDY", *J. Nucl. Sci. Technol.*, 54(7), pp.806-817 (2017).

15) J. Leppänen, M. Pusa, T. Viitanen, V. Valtavirta, T. Kaltiaisenaho, "The Serpent Monte Carlo

Code: Status, Development and Applications in 2013", *Ann. Nucl. Energy*, 82, pp.142-150 (2015).

16) X-5 Monte Carlo Team, "MCNP – A General Monte Carlo N-Particle Transport Code, Version 5", *LA-UR-03-1987* (2003).

17) A. Yamamoto, K. Tada, et al., "Multi-group neutron cross section generation capability for FRENDY nuclear data processing code," *J. Nucl. Sci. Technol.*, **59** (2021).

18) K. Tada, R. Kondo, et al., "Development of ACE file perturbation tool using FRENDY," *J. Nucl Sci. and Technol.* (2022).

19) S. Chacon and B. Straub, "Pro Git SECOND EDITION", Apress, New York (2014).

20) P. Hamill, "Unit Test Frameworks", O' Reilly Media, California (2014).

21) G. Breit, E. Wigner, "Capture of Slow Neutrons", *Phys. Rev.*, 49, pp.519-531 (1936).

22) D. B. Adler, F. T. Adler, "Neutron Cross-sections in Fissile Elements", Proc. Conf. on Breeding Economics and Safety in Large Fast Power Reactors, Argonne, Monograph *ANL-6972* (1963).

23) F. T. Adler, D. B. Adler, "Interpretations of Neutron Cross-sections of the Fissionable Materials for the Resolved Resonance Region", Conf. on Neutron Cross-section Technology, Washington, D. C., *CONF-660303*, 2, pp.873-893 (1966).

24) C. W. Reich, M. S. Moore, "Multilevel Formula for the Fission Process", *Phys. Rev.*, 111(3), pp.929-933 (1958).

25) M. S. Moore, "Fundamentals and Approximations of Multilevel Resonance Theory for Reactor Physics Applications", *Nuclear Theory for Applications*, *IAEA-SMR-43*, pp.31-57 (1980).

26) K. Yagi, "Genshikakubutsurigaku", Asakura-shoten, Tokyo, pp.257-263 (1971) (in Japanese).

27) A. M. Lane, R. G. Thomas, "R-Matrix Theory of Nuclear Reactions", *Rev. Mod. Phys.*, 30(2), pp.257-353 (1958).

28) K. Kobayashi, "Genshirobutsuri", Corona-sha, Tokyo, pp.1-80 (1996) (in Japanese).

29) S. Kunieda, "Status of the R-matrix Code AMUR toward a consistent cross-section evaluation and covariance analysis for the light nuclei", *EPJ Web of Conferences*, 146, pp.12029_1-12029_4 (2017).

30) N. M. Larson, "Updated Users' guide for SAMMY: Multilevel R-Matrix Fits to Neutron Data Using Bayes' Equations", *ORNL/TM-9179/R8*, *ENDF-364/R2*, p.9 (2008).

31) F. H. Frohner, "Applied Neutron Resonance Theory", Nuclear Theory for Applications, *IAEA-SMR-43*, pp.59-95 (1980).

32) H. Henryson II, B. J. Toppel, C. G. Stenberg, "MC2-2: A Code to Calculate Fast Neutron Spectra and Multigroup Cross-sections", *ANL-8144* (1976).

33) C. E. Porter, R. G. Thomas, "Fluctuations of Nuclear Reaction Width", *Phys. Rev.*, 104(2), pp.483-491 (1956).

34) R. N. Hwang, H. Henryson II, "Critical Experimentation of Low-Order Quadratures for

Statistical Integrations", *Trans. Am. Nucl. Soc.*, 22, pp.712-713 (1975).

35) N. M. Steen, G. D. Byrne, E. M. Gelbard, "Gaussian Quadratures for the Integrals", *Math. Comp.*, 23(107), pp.661-671 (1969).

36) R. E. MacFarlane, "Neutron Slowing Down and Thermalization", *Handbook of Nuclear Engineering*, 3, Springer, Berlin (2010).

37) D. E. Cullen, "Program SIGMA1 (version 79-1) Doppler broaden evaluated cross-sections in the evaluated nuclear data file/version B (ENDF/B) format", *UCRL-50400*, 17, Part B, Rev. 2 (1979).

38) D. E. Cullen, "Nuclear Data Preparation", *Handbook of Nuclear Engineering*, 1, pp.282-425, Springer, Berlin (2010).

39) W. Haeck and A. Trkov, "Nuclear Data Processing", *INDC(NDS)-0748* (2018).

40) H. D. Lemmel, C. H. Westcott, "Fission and Absorption g-factors of ^{241}Pu", *J. Nucl. Energy*, 21(5), pp.417-424 (1967).

41) R. Pynn, "neutron scattering A PRIMER", Los Alamos Science Summer 1990 (1990).

42) R. E. MacFarlane, A. C. Kahler, "Methods for Processing ENDF/B-VII with NJOY", *Nucl. Data Sheets*, 111(12), pp.2739-2890, (2010).

43) R. W. Richards, J. L. Thomason, "Small-Angle Neutron Scattering Study of Block Copolymer Morphology", *Macromolecules*, 16(6), pp.982-992 (1983).

44) J. I. M. Damian, J. R. Granada, D. C. Malaspina, "New thermal neutron scattering kernels for light and heavy water based on molecular dynamics simulations", *Phisics Procedia*, 60, pp.300-309 (2014).

45) A. Yamamoto, N. Sugimura, "Improvement on multi-group scattering matrix in thermal energy range generated by NJOY", *Ann. Nucl. Energy*, 33(6), pp.555-559 (2006).

46) R. D. Mosteller and R. C. Little, "Impact of MCNP Unresolved Resonance Probability-Table Treatment on Uranium and Plutonium Benchmarks", *Proc. ICNC'99*, Sep. 20-24, 1999, Versailles, France (1999).

47) L. B. Levitt, "The Probability Method for Treating Unresolved Resonances in Monte Carlo Criticality Calculation", *Trans. Am. Nucl. Soc.*, 14, p.648 (1971).

48) I. I. Bondasrenko, Ed., "Group Constants for Nuclear Reactor Calculations", Consultants Bureau, New York (1970).

49) D. M. Green and T. A. Pitterle, "ETOE, A Program for ENDF/B to MC2 Data Conversion", *APDA-219*, Atomic Power Development Associates, Inc. (1968).

50) J. M. Otter, R. C. Lewis, L. B. Levitt, "U3R A Code to Calculate Unresolved Resonance Cross-section Probability Tables", *AI-AEC-13024*, Atomics International (1972).

51) T. Yotsuji, Probability Distribution Random Number Generating Method for Calculator Simulation, Pleiades Publishing (2010) [in Japanese].

52) G. Marsaglina and W. Tsang, "A Simple method for generating gamma variables", *ACM Trans.*

Math. Softw., 26(3), pp.363-372 (2000).

53) D.M. O'Shea and H.C. Thacher, Jr. "Computation of Resonance Line Shape Function", *Trans. Am. Nucl. Soc.*, 6, pp.36-37 (1963).

54) G.P.M. Poppe and C.M.J. Wijers, "More Efficient Computation of the Complex Error Function", *ACM Trans. Math. Softw.*, 16(1), pp.38-46 (1990).

55) O. Shcherbakov and H. Harada, "Resonance Self-Shielding Corrections for Activation Cross-section Measurements", *J. Nucl. Sci. Technol.*, 39(5), pp.548-553 (2002).

56) P. Martin, G. Donoso, J. Zamudio-Cristi, "A modified asymptotic Pade method. Application to multipole approximation for the plasma dispersion function Z", *J. Math. Phys.*, 21(2), pp.280-285 (1980).

57) K. Tada, "Improvement of Probability Table Generation Using Ladder Method for a New Nuclear Data Processing System FRENDY", *Proc. Physor2018*, Cancun, Mexico, Apr. 22-26, 2018 (2018).

58) D. Knott, "KRAM, a Lattice Physics Code for Modeling the Detailed Depletion of Gadolinia Isotopes in BWR Lattice Designs," Ph.D. Thesis, The Pennsylvania State University (1990).

59) A. Yamamoto, T. Endo, K. Tada, "Adaptive setting of background cross sections for generation of effective multi-group cross sections in FRENDY nuclear data processing code," *J. Nucl. Sci. Technol.*, **59**, pp.1343-1350 (2021).

60) M. Ouisloumen, R. Sanchez, "A Model for Neutron Scattering off Heavy Isotopes that Accounts for Thermal Agitation Effects", *Nucl. Sci. Eng.*, **107**, pp.189-200 (1991).

61) S. Ghrayeb, M. Ouisloumen, A. Ougouag, K. Ivanov, "Deterministic Modeling of Higher Angular Moments of Resonant Neutron Scattering," *Ann. Nucl. Energy*, **38**, pp.2291-2297 (2011).

62) J. Xu, T. Zu, L. Cao, "Development and verification of resonance elastic scattering kernel processing module in nuclear data processing code NECP-Atlas," *Ann. Nucl. Energy*, **110**, pp.301-310 (2019).

63) A. Yamamoto, T. Endo, G. Chiba, K. Tada, "Implementation of Resonance Up-scattering Treatment in FRENDY Nuclear Data Processing System," *Nucl. Sci. Eng.*, (2022).

64) W. Zeng, R. McClarren, "Semi-analytic benchmark for multi-group free-gas Legendre moments and the application of Gauss quadrature in generating thermal scattering Legendre moments," *Ann. Nucl. Energy*, **85**, pp.1131-1140 (2015).

65) T. Sutton, et al, "Comparison of Some Monte Carlo Models for Bound Hydrogen Scattering," *Proc. M&C2009*, May 3-7, Saratoga Springs, USA, (2009).

66) E. Anderson, Z. Bai, C. Bicchof, S. Blackford, J. Demmel, J. Dongarra, J. D. Croz, A. Greenbaum, S. Hammarling, A. McKenney, D. Sorensen, *LAPACK Users' Guide Third Edition*,

Society for Industrial and Applied Mathematics, Philadelphia (1999).